Copy

CA8160 Georgia Institute of Technology 04-OCT-1998 14:07
Office of Contract Administration
OCA PAD AMENDMENT - PROJECT HEADER INFORMATION

Document Header Id #: 37486 ACTIVE
Project #: E-20-W95 Cost share #: E-20-313 Rev #: 5
Center #: 10/24-6-R8701-0A0 Center shr #: 10/22-1-F8701-0A0
OCA file #: Project type: RES

Contract #: 50SBNB5C8781 Mod #: 5 Award type: CONTR
Prime #: Contract entity: GTRC
Contract type: CRNF

CFDA:
PE #:

Project unit: CIVIL ENGR Unit code: 25
Project director(s):
PDPI- GOODNO B CIVIL ENGR (404)894-2227

Sponsor : US DEPT OF COMMERCE/NATL INST OF STDS & TECH
Division Id: 110 / 3418
Award period: 22-SEP-1995 to 31-AUG-1998 (performance) 31-AUG-1998 (reports)

Sponsor amount	New this change	Total to date
Contract value:	10,985.00	142,194.00
Funded:	10,985.00	142,194.00
Cost sharing amount:	0.00	14,000.00

Does subcontracting plan apply? N

Title: DUCTILE CLADDING CONNECTION SYSTEMS FOR SEISMIC DESIGN

PROJECT ADMINISTRATIVE DATA

OCA contact: Brian J. Lindberg (404) 894-4820

Sponsor technical contact:
DR. RILEY CHUNG
U.S. DEPARTMENT OF COMMERCE
NIST
BUILDING 226, ROOM B158

Phone: 3019756062
Fax: GAITHERSBURG MD 20899
Email:

Sponsor issuing office:
JOAN SMITH
NIST
ACQ. & ASST. DIVISION
BUILDING 301, ROOM B117

Phone: 3019756458
Fax: GAITHERSBURG, MD 20899
Email:

Security class (U,C,S,TS): U
Defense priority rating : N/A

ONR resident rep is ACO (Y/N): N
Supplemental sheet: N/A

Equipment title vests with: SPON

Administrative comments -
MODIFICATION NO. 5 EXTENDS PERIOD OF PERFORMANCE THROUGH AUGUST 31, 1998.

Closeout Notice Date 14-OCT-1998

Project Number E-20-W95 Doch Id 37486

Center Number 10/24-6-R8701-0A0

Project Director GOODNO, BARRY

Project Unit CIVIL ENGR

Sponsor US DEPT OF COMMERCE/NATL INST OF STDS & TECH

Division Id 3418

Contract Number 50SBNB5C8781 Contract Entity GTRC

Prime Contract Number

Title DUCTILE CLADDING CONNECTION SYSTEMS FOR SEISMIC DESIGN

Effective Completion Date 31-AUG-1998 (Performance) 31-AUG-1998 (Reports)

Closeout Action:	Y/N	Date Submitted
Final Invoice or Copy of Final Invoice	Y	
Final Report of Inventions and/or Subcontracts	Y	
Government Property Inventory and Related Certificate	Y	
Classified Material Certificate	N	
Release and Assignment	Y	
Other	N	

Comments

Distribution Required:	
Project Director/Principal Investigator	Y
Research Administrative Network	Y
Accounting	Y
Research Security Department	N
Reports Coordinator	Y
Research Property Team	Y
Supply Services Department/Procurement	Y
Georgia Tech Research Corporation	Y
Project File	Y

NOTE: Final Patent Questionnaire sent to PDPI

DUCTILE CLADDING CONNECTION SYSTEMS FOR SEISMIC DESIGN

Barry J. Goodno
School of Civil and Environmental Engineering

James I. Craig
School of Aerospace Engineering

with

Tumay Dogan
Graduate Research Assistant

Peeranan Towashiraporn
Graduate Research Assistant

School of Civil and Environmental Engineering
Georgia Institute of Technology
Atlanta, GA 30332-0355

FINAL REPORT

Submitted to

National Institute of Standards and Technology (NIST)
Structures Division
Building and Fire Research Laboratory

October 1998

Table of Contents

Appendices

Preface

This report documents research performed under contract 50SBNB5C8781 at the Georgia Institute of Technology by the authors and their graduate students. In addition, the report also summarizes in a single volume the authors' continuing research on the use of architectural cladding as a passive damping component in the structural performance of a building. In this respect it combines the results of several previous projects and provides a more comprehensive treatment of the problem. Specifically, this report summarizes early results on the performance of cladding connectors developed by Mr. Christian Moor in a Masters Special Problem Report as well as initial work on the testing of representative cladding connector systems and the optimal design of these connectors in buildings that was developed by Dr. Jean-Paul Pinelli in a Doctoral Thesis. Finally, the report describes in detail how in the present study these preliminary developments have been refined and applied to a practical and contemporary problem involving the "redesign" of an existing 20 story building located in a West Coast seismic zone. It also presents further test results for additional families of energy dissipative, advanced cladding connectors. This latter research was carried out by current graduate students, Mr. Tumay Dogan and Mr. Peeranan Towashiraporn. The contributions of everyone involved in the preparation of this report are gratefully acknowledged.

SUMMARY

Prior analytical and experimental studies by the authors over the past several years have shown that promising levels of seismic response attenuation can be designed into new and existing building structures through use of "advanced" connections for precast cladding systems. This report provides a brief summary of past work then describes analytical and experimental studies of several developmental "advanced" cladding connectors. The connectors were designed to provide ductility and energy dissipation through relative displacements between the structure and the cladding panels. A test fixture designed as part of an earlier doctoral thesis is described along with a summary of the results from a family of flexural connectors developed as part of the same thesis. Tests were performed on flexural and torsional designs as well as on composite laminated neoprene and steel isolating pads enclosed within steel flexures for bearing applications. Nonlinear analytical models developed for the various connector designs were incorporated into existing nonlinear software for time history dynamic analysis of planar structural systems. Optimization of the connector properties for an actual 20 story building application resulted in controlled energy dissipation in the cladding connectors, and reduced demands on the supporting structural framework. Results for this building showed that either up to 41% reduction in peak displacement response could be achieved from the baseline (as-built) configuration by retrofitting advanced cladding connectors, or else as much as a 20.3% reduction in structural weight (in the longitudinal direction) could be achieved for the same baseline response level. This suggests that use of an energy dissipating cladding system could lead to either improved serviceability (reduced drift) or else a savings in structural steel, or some combination of both.

1. Introduction

1.1 Background

The authors have been studying the performance of architectural cladding in buildings for a number of years. These efforts began with early attempts to predict building response to wind loads and subsequently to explain building mode shapes and eigenfrequencies measured in actual field testing. Comprehensive structural analysis of the study building was unable to predict the experimental results unless additional interstory shear stiffness was added to the model to represent the presence of the heavy precast cladding that was used on the building. Closer examination of the cladding system, which was not designed for seismic loads, strongly suggested that the particular bolted connections using wedge inserts in the cladding panels were easily capable of developing the needed additional interstory stiffness to provide agreement between the structural model and the measured modal frequencies. Since architectural cladding is almost always designed to play no structural role (and in fact is usually protected from structural loads), this surprising result led to the initial attempt to describe this problem in more detail and to suggest ways in which it might be used to advantage in building design [Palsson 1982b]. Subsequent research by the authors and other investigators into the role that architectural cladding actually plays in structural systems is described in detail in Section 2 of this report.

Several practitioners [Das 1986, Charney and Harris 1989, Iverson 1989, Spronken 1989] have pointed out the lack of adequate information on which to base a rational design technique for architectural cladding, especially in seismic zones. The conservative design approach, which is widely used today and is recognized in current code provisions, attempts to protect the cladding from structural loads by providing nearly total isolation of the panels from any structural interaction with the building. This is commonly achieved by providing connections to support only the bearing loads and panel alignment while otherwise isolating the panel from other structural interactions with the building. Thus, only the mass of the cladding system will contribute to the seismic response of the building, and any possible structural role is essentially eliminated

The present report suggests that a structural role for the architectural cladding is not unreasonable provided the resulting forces can be limited to reduce the risk of façade damage. More specifically, the suggested structural role is to introduce added passive hysteretic damping into the structural system through ductile deformation of specially designed "advanced" cladding connectors. The cladding system would thus perform in a role not unlike that of other passive response modification (e.g., damping) systems that are gaining favor with structural engineers. The report summarizes an initial effort to develop a performance-based design methodology that can be used to design the advanced connectors in an optimal fashion. The design objective can be to either provide additional seismic protection for a building structure that is otherwise adequately designed, or to provide an acceptable baseline level of performance with a commensurate reduction in the cost (weight) of the conventional building structural system. The first objective might be more suitable for retrofit considerations or to add additional protection to essential facilities, but the second objective is perhaps more appropriate to achieving more cost-effective new designs.

1.2 Objectives of the Reported Work

The objectives of the reported work include:

1. Survey previous research in the use of architectural cladding as a means to implement passive response modification in buildings,
2. Develop a seismic design methodology that is capable of defining optimal properties of advanced connectors for architectural cladding,
3. Identify advanced cladding connection concepts that by various means are able to develop high levels of ductility for inplane racking loads while also performing the normal functions of providing panel alignment and supporting bearing loads,
4. Fabrication at full scale and test several advanced connections designs in a specially designed laboratory fixture to verify predicted behavior and to define representative design parameters;
5. Apply this design methodology with representative advanced connectors to an existing building structure in order to:
   5.1. reduce peak displacement response for the "as-built" building from its baseline value (without advanced cladding) for the design earthquake, and
   5.2. redesign the primary structural system (steel frame members) to achieve the same baseline response with advanced connectors but using reduced structural steel.

1.3 Organization of the Present Investigation

This report provides a brief summary of past work on the potential of energy absorbing cladding systems then describes analytical and experimental studies of several developmental "advanced" cladding connectors. The concept and overall design approach for advanced cladding systems are presented in Chapter 2. The different flexural, torsional and composite connector designs considered to date are discussed in Chapter 3. Several different designs were fabricated and tested in a special laboratory test fixture; sample test results and corresponding analytical models developed on the basis of test data are presented in Chapter 3. To test the validity of the advanced cladding concept, a baseline 20-story building was chosen for detailed evaluation, both with and without the potential benefit of an energy absorbing cladding system. The building, the associated structural model, and the optimized cladding connection system are presented in Chapter 4. The performance of the structure in one orthogonal direction was studied in detail using both nonlinear time history and response spectrum analyses. The structure, which included the optimized cladding system, was redesigned to reduce overall structural steel weight and these results are described in Chapter 4. Finally, overall conclusions of the study and possible directions for follow-on research are presented in Chapter 5.

2. Survey of Previous Approaches

2.1 Architectural Cladding

It is very common in modern buildings to employ heavy precast concrete panels for exterior cladding. The function of these cladding panels is mainly architectural but they also protect the interior from environmental factors. They are classified and designed as nonstructural elements, and are considered as a dead weight that does not contribute any structural function to the building.

Facade design is a fundamental expression of architecture and therefore the design of the cladding panels is governed mainly by aesthetic considerations [Morris 1978]. The panel materials and texture, their contours, the number and location of window openings, and the configuration pattern of the cladding are all powerful means that architects use to define the style of a building [Sands 1986; Arnold 1989]. In addition, cladding panels must satisfy certain practical criteria [Hotz 1982; Hegle 1989]: they must be able to transmit wind forces and their own weight to the main structure; the facade must provide a first line of defense against environmental loadings such as moisture or temperature changes; and the panels must also resist environmental deterioration [Stockbridge 1984]; finally, cladding panels must be easy to manufacture in series, transport, and erect [Meyer and Hatfield 1987]. Das [1986] offers an excellent detailed overview of the complex set of different design criteria that a successful facade design must satisfy. However, in spite of this complexity, and given the assumed non-structural characteristics of the facade panels, structural engineers often leave the choice of cladding and its connections entirely to the architect and precast concrete contractor [Spronken 1989]. In doing so, they overlook important cost and safety issues.

The cost of the facade will vary, among others, with the size and importance of the facility, and with the materials used. It can become a significant part of the total cost of a building, especially in the case of tall buildings with granite or marble facades where it can easily cost as much as 10 to 20% or more of the total cost [Facades 1980]. If, after construction, repairs or replacements are needed because of poor design, the cost of a building facade can become much more than originally anticipated. Finally, it is obvious that cladding failure also entails a possible risk of injury to the public, especially in the event of an earthquake.

In spite of these cost and safety issues, it is only recently that cladding has became a concern to engineers, for various reasons. First, there have been numerous cladding failures [Sutter 1976; Dreger 1989], particularly in the case of earthquakes (see [Goodno, Craig, and Wolf 1987-1989; Fintel 1986] for the Mexico earthquake; [Costes 1992] for the Armenian earthquake). Second, heavy precast cladding has to compete with other materials for facade enclosures, and better engineered designs, which could result in innovative uses, are one way to face the competition [Symposium 1980; Skidmore 1986; Arnold 1987; Cladding Solutions 1988; Priestley 1988; Englekirk 1989; Freeman 1989]. Third, there has been renewed interest in methods for passive and active control to attenuate the dynamic response of buildings [Elsesser 1986; Soong, Masri, and Housner 1991; Goodno, Craig and Calise 1992a; Pinelli 1992; Pinelli et al 1993; Pinelli., Moor, Craig, and Goodno 1996].

It has been well established that attenuation and control of the seismic response of buildings can be achieved through ductile inelastic action of the structural system. This has traditionally been achieved by deliberate design of structural details, such as eccentric bracing, that will

develop well-behaved inelastic action without critical loss of general structural integrity or stability. At the same time there has been widespread interest in the possible application of pre-engineered ductile elements, devices or mechanisms that can augment the ductility of a conventional structural system. While these approaches are generally used to handle severe conditions, similar methods could also be applied to other building subsystems, such as cladding, not traditionally considered to play a structural role.

In fact, studies of building structural and cladding systems coupled with experimental observations of the actual dynamic response of these buildings, have lead to a recognition that, whether by deliberate design or not, cladding systems (particularly heavy precast systems) can measurably affect the structural stiffness and therefore the dynamic response of buildings. Research has also pointed to the potential role that properly designed precast concrete cladding can play in providing ductility and energy dissipation to the overall building structure, especially during strong ground motions. Experimental studies and extensive analytical modeling carried out at Georgia Tech and elsewhere point to the critical role that the cladding connections play in this process.

A cladding panel in a building facade is typically attached at four points, two at the bottom and two at the top. In U.S. practice the bottom connections are usually bearing type connections while the top connections are usually tie-back connections. Although this arrangement has the virtue of simplicity, it may lead to catastrophic failure in the case of failure of the upper connections. For this reason in other countries (e.g., Japan) different arrangements are preferred [Wang 1987].

During an earthquake the behavior of the cladding will be dictated by cyclic interaction between the panels and the supporting primary structure, and typically the connections are simultaneously subjected to three primary effects:

(i) inertia forces generated by the acceleration of the panel, transmitted from the panel to the main structure via shear loading of the connectors;

(ii) horizontal interstory drift resisted by the panels which results in horizontal shear forces in the connections; and,

(iii) gravity load of the panels which is supported by the bearing connections.

While other forces, moments and displacements may be developed, they are generally assumed to be of secondary importance. Conventional connection designs try to cancel the second effect by isolating the panel from the main structure. According to the Precast/ Prestressed Concrete Institute [PCI 1985; 1988], the panels should be designed and detailed to transfer only wind and thermal forces to the supporting frame, with the panel connections resisting these forces in addition to the panel's own weight. Sliding or flexible connections are recommended by PCI to allow movement in the plane of the panel, in this way lessening panel interaction with the supporting frame. Because of this structural separation between panel and frame, the cladding panels are classified and designed as nonstructural elements.

However, sliding connections may be rendered ineffective by poor construction practice and lack of inspection, or by connection deterioration with time, (e.g., rust or corrosion), or by insufficient length of the slot (as was shown in the tests carried out by Wang [1987]). More importantly, studies have shown that the disregard of precast panels attached with conventional connections to carry lateral load or add lateral stiffness is not entirely warranted. Even when designed as isolated non-structural elements, in accordance with existing state-of-the-art

connection design practice, it has been shown that cladding can add significantly to the lateral stiffness [Palsson 1982].

Therefore, it seems promising to explore a different approach. Instead of minimizing, or canceling the structure-panel interaction, why not take advantage of it to dissipate energy, thereby reducing the response of the main structure? The key to this new concept of cladding participation is the development of so-called advanced, or engineered, connections. An *advanced* connection is one which exhibits superior properties of ductility and damping and results in high energy dissipation without failure during moderate or strong earthquakes. These connections must also limit the forces transmitted into/through the panel.

By using advanced cladding connections with structural cladding, significant advantages can be achieved over more conventional designs [Goodno 1986; Thiel et al. 1986; Goodno and Craig 1988; Pinelli 1992]. The energy dissipation can be distributed more evenly over the height of the building, and does not involve (or reduces the involvement of) structural members, therefore preserving structural integrity. Due to the increased damping, the overall response of the building is maintained between acceptable limits, and damage to other nonstructural elements and contents is avoided. It is felt that such an approach will lead to an improved and economically achievable level of safety and performance that is comparable to or even better than more traditional design alternatives.

This report is concerned with the testing and analytical modeling of such connections, and development of appropriate design criteria.

2.1.1 Analytical Studies

A number of researchers have studied the contribution of cladding to structure lateral stiffness. Dubas [1972], and Oppenheim[1973] investigated the effect of cladding on tall structures. They reported an increase in lateral resistance provided by the panels, and the effect of varying panel stiffnesses on the structural response. Henry [1980, 1986] and Stein [1983] studied the effect of cladding on reinforced concrete buildings, for the case of panels connected to the columns. Their studies showed that it is not always conservative to ignore the lateral stiffening effect of cladding, and that the connector should be carefully designed to accommodate large forces. Henry [1989] later proposed a box frame mathematical model to represent the structural aspects of cladding panels. This model provided designers with a tool to allow them to incorporate cladding in structural analysis.

In Canada, Smith and Gaiotti [1989a,Gaiotti and Smith 1992] showed how the interaction between panel and structure contributes to the stiffening of the overall building, even for facades designed according to PCI recommendations. They also developed an analogous spring model to allow for a better visualization of the cladding-structure interaction.

At Georgia Tech, the earliest work in the mid-'70's focused on studies of a local 25-story steel frame structure with heavy cladding. The cladding panels, typical of those in common use in the region, were contoured precast concrete with reinforcing steel and wire mesh. Each panel was connected to the exterior lightweight frame spandrel beams at four attachment points. Typical top connections consisted of an adjustable loop insert bolted to a clip angle which in turn was welded to the frame spandrel beam. The angles had horizontally slotted bolt holes for ease of panel installation and to permit movement to occur without high force levels in the panels and connections. Typical bottom connections, designed to support the weight of the panel, consisted of a shelf angle insert bolted to a clip angle which was welded to the frame spandrel beam. The

insert for the bottom connection was made of ductile iron with a wedge shaped track to accommodate vertical adjustment and to prevent slippage. Gram [1976], following the research of Sherwood [1975], established through analytical modeling coupled with experimental measurements of the actual ambient level dynamic response of the building, that the cladding was contributing 30% or more to the lateral stiffness of the twenty five story primary structure.

Palsson et al. [1982a, 1982b, 1984, 1988] and Goodno et al. [1981, 1984, 1986a] used a tier building model of the actual twenty five story steel frame structure to determine the interaction between exterior precast concrete cladding and the primary frame structure of the building. Linear behavior of the core and exterior frames as well as both composite and non composite floor beam behavior were assumed. No attachment or contact between panels was assumed. The study included several steps. First, an assumed shear stiffness constant, representing the interstory shear stiffness of a row of panels between story levels on each structure face, was adjusted until a match in measured and computed frequencies was obtained. Then a variety of different cladding models, both linear and nonlinear, were used in dynamic response studies of the overall structure model. Localized panel response studies were also performed to determine connection force levels and the influence of connection stiffness on cladding lateral stiffness.

The study confirmed that the exterior facade is a participating structural element despite assumptions to the contrary. Translational frequencies were increased due to cladding interaction by as much as 33% and torsional frequencies by as much as 65% for the composite model. Overall structure response was either increased or decreased by adding cladding lateral stiffness depending upon the frequency content of the earthquake record applied. These findings suggest that failure to include cladding stiffness effects may be unconservative in some cases. Also, linear panel models were generally found to bracket the nonlinear cases in which strong ground motion was assumed to cause partial cladding failure and/or connection slip once allowable interstory drift limits were exceeded. Connection forces and interstory shear stiffness values were found to be significantly affected by the presence of slots in connection angles, oversized bolt holes, and initial friction in connection attachments.

Pinelli [1984], Goodno and Pinelli [1986b], and Goodno and Naman [1986c] reported studies on the influence of cladding systems on the lateral stiffness of low-rise steel buildings. In their investigations they used a program developed by Pless [1982] for the linear analysis of 2D frames with cladding. They were able to show, in a series of step by step linear analyses, how the contribution of non-structural elements, like cladding and infill walls, to lateral stiffness can significantly alter the seismic response of a lowrise building.

The influence of the cladding connections themselves on the cladding-structure interaction problem was investigated by other researchers at Georgia Tech. LeBoeuf [1980] continued studies reported by Will et al. [1979] where finite elements were used to model a precast concrete panel and its clip-angle connections of the same 25-story steel frame structure mentioned above. The effect of connection details on the interstory shear stiffness of the curtain wall was analyzed. A wide range of stiffness values was obtained depending on panel support conditions and connection details.

At Georgia Tech, Meyyappa, Goodno, and Fennell [1988] developed a finite element model of wedge inserts embedded in concrete slabs to study insert behavior under pull-out loads. The effects of bond deterioration between an insert and the surrounding concrete were included in the study. Analytical predictions were found to agree with measured laboratory data for a specimen

which exhibited linear response. However, a nonlinear model for cracked concrete was necessary to describe the nonlinear behavior of other test specimens.

In subsequent analyses, Goodno, Meyyappa, and Nagarajaiah [1988] developed a super-element model of a heavyweight cladding system representative of U.S. practice. The model was intended for use in an overall building model. The model included the precast panel, the clip angle attachments, and the supporting spandrel members from the supporting frame. Only the essential degrees of freedom on the periphery were retained for use in the dynamic analysis of the overall structure. Using back-substitution, the connection and member forces as well as the distortions and stresses in the precast panel were determined at selected locations on the exterior facade at the completion of the lateral force analysis.

Elsewhere, Sack et al. [1981] also investigated the interaction between structural framing and precast concrete curtain walls. The amount of lateral stiffness provided by the panels to the structure was found to vary from negligible to large, depending on the type of connection system. Gjelsvik [1974] carried out elasto-plastic analyses to determine the interaction between precast panels and frame. The collapse mechanism appeared to vary depending on the strength of the bolted connections.

Several researchers have investigated the design and behavior of other nonstructural elements. Sharpe [1972] stated that nonstructural elements extending from floor to floor had to be designed to accommodate interstory displacement if seismic damage was to be avoided. McCue et al. [1975, 1978] showed how the stiffening effect of the cladding could result in a shift of vibration frequencies of the building toward a more critical earthquake ground motion frequency range, resulting in higher seismic response. Glogau [1977] proposed to prevent any unfavorable change in the intended performance of a structure due to the cladding by separating nonstructural components from the main structure. This view ran against Kulka et al. [1975] who contended that it was impossible in practice to accomplish such a separation.

Studies involving large panel structures have been reported. Spencer [1971] investigated the nonlinear dynamic earthquake response of a 20-story prestressed concrete structure with nonstructural interfloor elements. He concluded that the elements helped reduced interstory drift, and that their efficacy depended on the level of yielding and energy dissipation, with non-yielding elements being more effective. Powell and Schricker [1977] studied the ductility demand on joints in large panel structures. The planes of weakness provided by the joint in a large panel shear wall were considered as structural fuses, limiting the stress developed in the panels. They concluded that joints designed to accommodate sliding could effectively reduce seismic induced panel stresses. Becker et al. [1980] reported on research into the seismic behavior of a vertical stack of simple precast concrete panels having only horizontal connections. The only sources of nonlinear inelastic behavior were in the rocking-induced opening of the horizontal joints, and in the horizontal slippage between panels. They concluded that the first of these phenomena controlled the response of the wall through a lengthening of the wall period, and that the coupling of rocking with slippage could lead to stress concentrations in the joint and subsequent failure. At the same time, Mueller and Becker [1980] explored the potential of an aseismic design concept that used the vertical connections in large panel precast concrete walls as primary energy dissipating elements (a concept similar to the proposed role of advanced cladding connections in precast facades in this research). The relationship between the vertical connection characteristics and the structure response was studied, and a criterion for the optimum strength of the energy dissipating elements was established.

At Georgia Tech, El-Gazairly and Goodno [1989; 1990] studied the effect of cladding on the fundamental frequencies, mode shapes and seismic response of a twelve story reinforced concrete frame structure damaged in the 1985 Mexico earthquake. The structure was analyzed as a tier building model in which the lateral stiffness of the frames, shear walls and cladding panels were generated separately and combined, along with an appropriate foundation representation, to form a model for the whole building. Finite elements were used to model the column cladding panels which had cracked at the location of the plate inserts in the panels during the earthquake. Linear springs with stiffnesses of 400, 800, and 1000 kips/inch (70,040; 140,080; and 175,100 kN/m) were employed to represent the panel connections.

Several significant conclusions were made from the El-Gazairly and Goodno study. First, cladding stiffness resulted in an increase of 30% to 49% in the lower frequencies, and maximum reductions of 93% and 94% in translational and rotational floor displacements, respectively. However, forces at column cladding locations, calculated based on interstory drifts, were found to exceed the estimated cladding connection capacity of 10 kips by a substantial amount. While confirming the observed failure in these connections, these force levels also violated the original assumption of linearity in the model and analysis. In subsequent research by these investigators [El-Gazairly et al. 1992; Goodno et al. 1992b], GT-IDARC, a modified version of program IDARC [Young et al. 1987; Kunnath et al. 1989], was used to model the three dimensional nonlinear behavior of the RC frame, attached cladding system, and unreinforced masonry infill walls. The nonlinear analysis was used to evaluate the seismic behavior of the case study building, and to explain observed damage and failure patterns of different building components.

Wolz [1990; 1991a; 1991b] and Hsu [1991] studied the influence of variations in the stiffness and strength of a hysteretic connection on the response of a six story space frame. The building model was created using the computer program DRAIN-2D [Powell 1973], which had to be modified to include the cladding panels and nonlinear cladding connections. These studies were continued by Goodno, Craig, and Hsu [1991], and Goodno, Craig, El-Gazairly, and Hsu [1992b]. The additional stiffness provided by the cladding caused top floor displacement reductions of maximum 74 % and a significantly lower response to the ground motion. The hysteretic damping caused by the cyclic deformations of the connections was sufficient to reduce the frame response without exceeding the assumed connection capacity of 10 kips. Cohen and Powell [1991] carried out similar investigations on energy dissipating cladding-to-frame connections, and their conclusions were similar to Wolz's. These studies suggest that a design criterion for a structure with advanced connections would be best formulated in terms of energy, and this topic is treated in more detail in Section 2.4.

Finally, it must also be pointed out that the study of the cladding-structure interaction has not been confined to seismic loading. A number of studies address as well the problem of wind loading [Kareem 1986, Reed 1987, Smith et al. 1989b]. Raths [1989] not only treats the issue of wind loading but he also provides a good example of conventional current practice in the design of heavy weight cladding.

2.1.2 Experimental Studies

There has been relatively little attention given to testing the structural performance of either cladding panels or cladding connection elements. When testing of these components was done, the objective was almost always to determine the performance of environmental sealing systems or the resistance to wind and thermal inputs. Information on structural performance is usually of

interest only when problems are encountered in the tests. There is a general feeling among practitioners that isolating cladding connections, as presently designed, work properly. As a result, there is only a limited amount of test data available today, and much of it is for structural components that are also employed in other applications.

Various types of concrete anchor systems that are appropriate for cladding applications have been tested and modeled [Burdette et al. 1983; Klingner and Mendonca 1982a,b; Peier 1982; Shaikh et al. 1985; Spencer and Neille 1976; Ueda 1990]. The cited work is typical of a larger body of information on similar anchor systems, but in almost all cases, the testing is designed to yield anchor capacity figures for simple loadings. No specific reference has been made to cladding connections.

Several connectors used in large structural panel construction were also tested experimentally by Osborn et al. [1981]. Both bolted and welded connections were tested, and results showed welded connections to be more suitable for aseismic design and several recommendations for the connection design were issued. Kallros [1987] conducted an experimental investigation of the behavior of connections in thin precast concrete panels under earthquake loading. Several specimens were tested and their behavior under cyclic loading was investigated. Failure in the inelastic range was found to be due either to rebar failure, resulting in small deflections, or to spalling of the concrete, resulting in larger deflections. Connections tied to embedded rebar exhibited better behavior than the ones tied to a wire mesh. It was also found that the yield stress of the rebar had an influence on the fatigue rather than the strength of the connection.

There is, in addition, a growing body of information on the performance of structural precast panels and connections under seismic loading conditions. This work has been driven by the need to answer fundamental questions about the ability of these types of structural systems to resist seismic loads before they can be widely employed for construction in seismically active regions. Some of the findings can be extrapolated to precast cladding. In full panel experiments, Anicic et al. [1980] performed experimental studies on two reinforced concrete facade panels, in which only cyclic loads perpendicular to the plane of the panels were applied. Throughout the studies no difference in behavior could be observed between the panel with an opening and the one without an opening, and it was shown that the panels withstood much higher loads than computed, failing by plastic buckling of the main web reinforcement. Likewise, studies involving large precast panel walls have also been reported. Following the analytical investigations of Becker et al. [1980], Oliva and Shahrooz [1984], and Clough et al. [1989] conducted shaking table tests of wet mortar jointed precast panel walls. They concluded that rocking motion provided the major contribution to the overall displacement if shear slip motion was constrained by shear keys. They showed that rocking motion isolated the wall from ground motion but could lead to instability problems.

There have been almost no experimental studies of cladding panels themselves, a situation that may be due to the complexity of such tests and their relatively high cost compared to component level tests. There are, however, a few valuable exceptions. Uchida et al. [1973], performed vibration tests on a two story, two bay steel frame with precast concrete panels to obtain data on the effect of cladding on the dynamic properties of the structure. The studies, which included both free vibration and forced vibration tests, showed that cladding increased lateral stiffness and damping of the test frame. Sack et al. [1981, 1989] tested a one-story, one-bay steel frame clad with two flat precast concrete panels, which were each connected with two rods at the top and two clip angles at the bottom. The test frame was subjected to inplane

dynamic forcing. The top connectors were found to be highly stressed in horizontal bending and the rods were susceptible to low cycle fatigue when subjected to several earthquake floor motion records.

Wang [1986; 1987] conducted a series of static tests to study the performance of cladding on a full scale test frame. Wall panels as well as column covers attached with a variety of tie back and bearing connections were tested. The study made an interesting comparison between California and Japanese practice, and concluded that although the Japanese design seemed conceptually better, it would be hard to implement in the U.S. due to its complexity. The report stressed the importance of simplicity, ductility, and flexibility in connection design, not only for the tie back connections but also for the bearing connections as well.

Rihal [1988a,b, 1989] conducted cyclic in-plane racking tests of precast concrete cladding panels with bearing connections at the bottom and threaded-rod lateral connections at the top. Relative motion across the connection elements was measured. Results showed that the load-capacity of the threaded rod specimens decreased with increasing length. Results also demonstrated that the in-plane resistance of the panels was controlled by the binding resistance of the threaded-rod lateral connections.

In other types of experimental panel connection studies, Sack et al. [1981, 1989] also studied the stiffness characteristics of certain types of cladding connections and their capacity to withstand low cycle fatigue. The connection tests included rod elements, and mating threaded inserts in concrete fixtures as well as clip angles welded or bolted into concrete attachments. As opposed to typical anchor tests which generally report pull-out capacities, these tests were designed to explore the behavior of connections and anchors under lateral loads representative of cladding applications. Analytical studies of the same connections were carried out in parallel and differences were within 30%.

At Georgia Tech, Meyyappa, Palsson, and Craig [1981] measured the ambient response of a 24 story steel frame office building to determine the effects of lightweight cladding on frequencies and damping of different modes. Response measurements were collected at different stages of construction, and frequencies and damping were found to change as additional cladding was placed on the structure. The frequencies of the second and third mode increased while the fundamental frequencies were not affected during construction. It was also found that cladding has an increasing effect on damping values in general, with the increase for torsional modes being more important. Goodno, Craig, Meyyappa, and Palsson [1983]; and Meyyappa and Craig [1984] were also concerned with demonstrating the validity of the previously described analytical investigations that pointed to the significant increase in lateral stiffness provided by heavy weight cladding. Experimental studies were conducted on the same twenty four story steel frame structure. Both ambient level vibration measurements and forced vibration testing were used to determine overall building natural frequencies, modal damping, and mode shapes for multi-axis bending and torsion modes. Comparisons with the results of numerical analyses confirmed that the heavy precast cladding was contributing to the lateral stiffness of the building, although this effect was not considered in the design of the structure. Parameter estimation methods were used to identify the contribution of this cladding to the interstory shear stiffness in both principal directions, and these results were then used to estimate the contributions of a typical cladding panel to the interstory shear stiffness. These studies revealed that while the identified stiffnesses were well within the capacities of the particular precast panels employed on

the case study building, the governing factor was the connection between the panels and the building structure.

Laboratory tests of the connections employed in the twenty four story building were also conducted [Goodno, Meyyappa, and Nagarajaiah 1988; Meyyappa, Goodno, and Fennell 1988]. These connections are described in the previous section. The tests were accompanied by detailed finite element modeling of the inserts themselves and strain measurements were made at points on the insert for comparison with the computed values. In general, it was found that the overall behavior of these inserts could be predicted by sufficiently detailed models, but that such models were far too complex for routine design purposes. Pull-out tests of the same inserts were also carried out [Keister 1983; Craig et al. 1986]. The method of failure of the inserts was brittle, sudden, and with catastrophic fracture of the concrete. To provide some ductility to the anchor, the authors recommended the use of longer reinforcement for the inserts, and the tying of the inserts to the panel flexural steel.

Leistikow [1988], and Craig, Leistikow, and Fennell [1988], conducted tests of ductile rod push-pull panel connections subjected to inplane shear and pull-out loads. The ductile rods are widely used in West Coast US practice for cladding-structure isolation for inplane motions while providing adequate out-of-plane resistance to seismic and environmental loads. These tests approximated the service conditions that might be encountered in practice. One end of the threaded rod was fixed in a typical ferrule loop insert imbedded into a precast concrete specimen while the other end was attached to an enlarged hole in a clip angle using washers and nuts typical of common practice. Cyclic lateral displacements were applied to 203.2, 228.6, 279.4, and 304.8 mm (8, 9, 11, and 12 inch long), 15.9mm diameter (5/8 inch), threaded A-36 ductile rods to measure the rod stiffness and fatigue life. Pull-out tests were also conducted on the panel insert alone.

A number of experimental observations were made. While the tests provided good elasto-plastic data on the constitutive properties of the rod, they also showed that rod stiffnesses decreased rapidly as the rods approached the elastic limit, and that the rods were susceptible to low-cycle fatigue failure after as few as 20 cycles of loading at displacements within currently allowable interstory drift limits. Slipping of the nut-washer assembly, observed in a number of tests, increased the fatigue life of the ductile rods, but ultimately led to loss of connection integrity. The pull-out load of the loop ferrule insert guaranteed by the manufacturer was found to be conservative, and the tests suggested that a sudden failure of the insert was unlikely. Finally, comparison with linear analytical estimates of clip angle connection stiffness by Palsson [1982] showed that panels with push-pull tie-back connections contribute less than 1/25 the interstory shear stiffness of panels with clip angle tie- back connections.

2.1.3 Actual Implementations of Structural Cladding

There is a significant volume of architectural literature on cladding, but there are few recent examples in the literature of actual cases of structural cladding implementation where cladding was purposely designed to withstand lateral forces. Matthewson and Davey [1979] designed a six story office building in Wanganui, New Zealand with energy absorbing devices. The façade cladding panels included braces with energy dissipating steel inserts (see Figure 2.1). The devices were mild steel sections of the cross bracing used in the panels, which yielded axially at a given force level. The vertical component of the diagonal forces was transferred by panel-column steel plate connections, while inertia loads were applied to the panel top chords by the

floor diaphragms. The panels were part of the lateral force resisting system, and "truss" action of the cross bracing dominated the structural behavior. Frame action became significant only after yielding of the inserts.

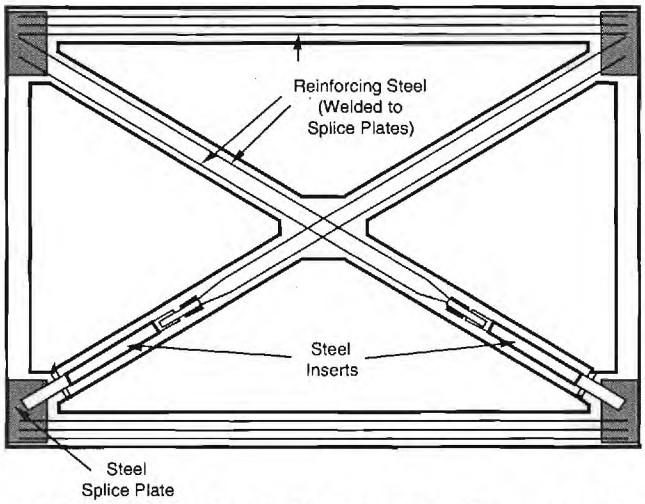

Figure 2.1 Braced Concrete Wall Panel with Steel Inserts. From [Matthewson and Davey 1979]

The design of the building was based on a static space frame analysis. Then nonlinear dynamic time history analyses were conducted using a series of recorded earthquake records. The ductility demand in the steel inserts was below the available level for all the events, and the interstory drift exceeded the maximum admissible value in one case only. For that reason, it was suggested that the building would survive the maximum credible earthquake event with little damage. This building, using precast concrete panels as structural elements, cost approximately twenty-five percent less per square meter than a six story conventional reinforced concrete frame building of similar size and use.

Tomasetti et al. [1986] described the case of a high rise building where thin wall metal facade panels were incorporated in the structural design to provide lateral stiffness against wind loading. The structural use of the panels resulted in drift reduction and in an overall economic design. However, seismic loading was not mentioned, and no energy dissipation was involved in the connections.

2.2 Passive Energy Dissipation

It has long been recognized that providing additional passive energy dissipation (damping) would improve the dynamic response of civil engineering structures such as steel and reinforced concrete frame buildings. One way to provide this extra damping is through the use of special passive energy absorbing devices. Kelly, Skinner, and Heine [1972], and Skinner, Kelly, and Heine [1973, 1975] reported on the development of three special mechanical devices to be incorporated into a structure specifically to passively absorb energy generated by an earthquake (see Figure 2.2):

(a) Rolling- bending thin U-shaped strips;

(b) torsional energy absorbers; and,

(c) flexural energy absorbers.

They are all based on hysteretic damping developed through plastic deformation of mild steel, and they were tested in the laboratory to measure their hysteretic behavior and fatigue life.

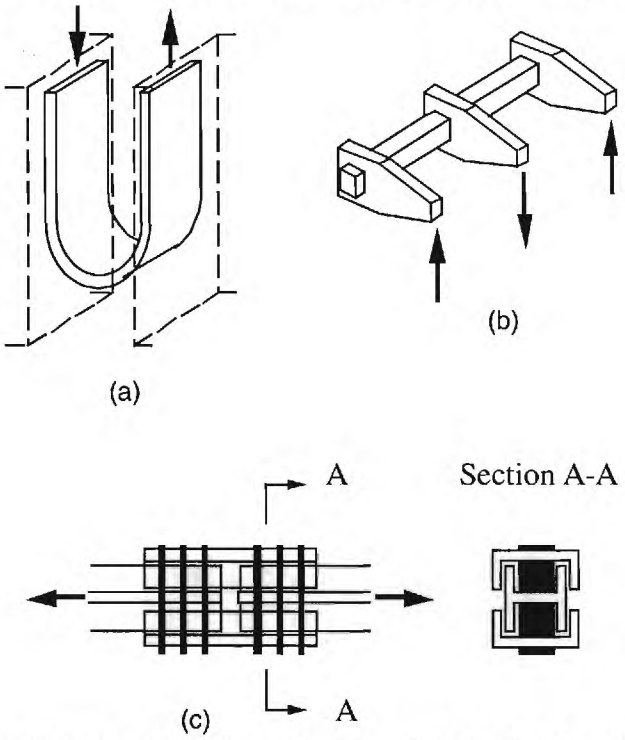

Figure 2.2 Three Types of Energy Absorbing Devices: (a) The U-Bar, (b) the Torsional Bar, and (c) the Flexural Device. From [Kelly et al. 1972]

The U-shaped steel strips (Figure 2.2-a) interact between adjacent surfaces whose relative movement is directed parallel to each other, and therefore were designed for use between flexibly based shear walls. The device makes use of the rolling (bending) of flat strips. The plastic deformation occurs when the strip changes from straight to curved. Different specimens were tested under controlled cyclic displacements. The peak load, dissipated energy and the total number of cycles to failure depended on the thickness, radius and width of the device. In all the tests the shape was fairly well maintained until the failure began. A kink was developed followed by complete transverse fracture. The fact that the U-bar is very flexible in one dimension, but stiff in the other two, could make it suitable for bearing cladding connections.

The torsional bar (Figure 2.2-b) uses a combination of torsion and bending, and therefore was designed for use between surfaces moving away from each other in foundations or shear wall systems. Square and rectangular bars of annealed or unannealed steel were tested in pure torsion and combined torsion and bending. In pure torsion, the failure occurred slowly and in a controlled manner. There was no real fracture of the bar. After longitudinal cracking, the peak torque decreased until almost no energy dissipation could be registered. In combined torsion and bending, depending on the geometry, the cracking was either longitudinal or transverse, followed by a decreasing torque or a rapid collapse, respectively. Both cases showed that the annealed steel was superior in fatigue resistance to the unannealed.

The flexural device (Figure 2.2-c) uses bending of short rectangular beams, and therefore was designed for use in diagonal bracing to provide the energy absorption normally developed in the vicinity of beam-column connections. The test peak load was achieved at around the second

cycle and stayed constant until a transverse crack across one of the beams occurred which was followed by a rapid failure of that beam. The device is not as efficient in energy absorption nor as fatigue resistant as the torsional bar, but it can be easily located and readily be replaced in the event of earthquake damage. Matthewson and Davey [1979] used a similar device in the panels of the building mentioned in Section 2.1.

The test results showed that, if dimensioned to achieve sufficient ductility and to avoid low-cycle fatigue, the energy-absorption capacity of these three devices could significantly augment that of a conventional building structure. The torsional device was the most efficient energy absorber, with lifetimes in the range of 100 to 1000 cycles. Furthermore, Skinner, Beck, and Bycroft [1975], showed that these hysteretic dampers could be combined with base isolation systems, and used for the isolation of bridges, nuclear reactors, and other special structures.

Robinson, and Greenbank [1976] reported their investigation on the use of an extrusion energy absorber which worked by extruding lead back and forth through an orifice. On being extruded the lead recrystallizes immediately, thereby recovering its original mechanical properties before the next extrusion. The energy absorption capacity of the device is limited only by its heat capacity, the melting point of the lead being the upper limit to the operating temperature.

Tyler [1978a] proposed the use of round bars to dissipate energy, in a manner similar to an inelastic coil spring. The idea was to introduce a bow in the bars to allow them to extend as the connected parts would move away from each other. The device is very simple, and its tensile capacity makes it suitable for base isolation systems. At the same time, the desire to utilize to the fullest extent the material present in a dissipator led Tyler to develop the tapered energy dissipator. It is also a flexural device where the taper is shaped so that the material is fully loaded over the whole length of the device. He proposed two types of tapered cantilever beams. The round type (Figure 2.3) provides damping in any arbitrary direction. The taper, which is a cubic curve, reaches over two thirds of the length, leaving some material at the top for attachment.

The plate type (Figure 2.4) can only provide energy dissipation in one direction, but it is cheaper to fabricate. The device has a linearly decreasing width over two thirds of the length while the thickness is kept constant. For both devices, design curves were developed that yield the required length and diameter or width given the maximum strain level, the damping force and the stroke.

Skinner, Heine, and Tyler [1977], Skinner, Tyler, Heine, and Robinson [1980], and Key [1984] reported on the actual use of several of the above mentioned devices, and their seismic performance. The dampers were installed among others in an industrial chimney, in several bridges, and in buildings. In all cases, the analyses showed significant reductions in dynamic structural response.

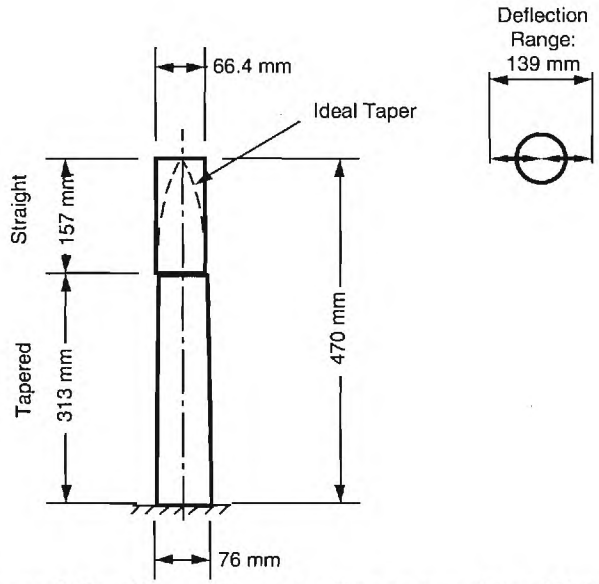

Figure 2.3 Round Tapered Cantilever Damper. Taper over Two Thirds of the Length, then Constant Diameter. From [Tyler 1978b].

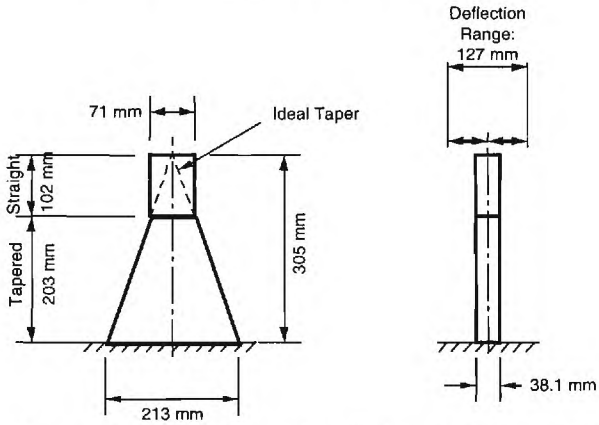

Figure 2.4 Tapered Cantilever Damper, Plate Type with Taper over Two Thirds of the Length, then Constant Width. From Tyler [1978].

The great simplicity of the tapered energy dissipator, not only in terms of its use as a dissipating mechanism but also of its fabrication, makes it very attractive. In the U.S., several investigators continued with additional studies of the device. A main area of application was found in pipe line support. Schneider et al. [1983] report on the development of a tapered X-plate steel device for use as an energy absorbing device in complex spatial piping systems. More recently, a patented energy dissipator from the Bechtel Power Corporation, based on tapered X-plates, has received the attention of a number of researchers. Scholl [1988] described this so-called added damping and stiffness element (or ADAS) and its applications. Bergman, and Goel [1987] carried out a series of cyclic tests to evaluate the properties of ADAS elements, and they pointed out their good fatigue resistance. Alonso [1989] studied in detail the mechanical characteristics of X-plate energy dissipators, and looked for analytical ways to predict their properties. Whittaker et al. [1991], investigated the use of ADAS elements in the retrofit of moment resisting frames. They showed that these energy absorbing devices can successfully

reduce the dynamic response of a moment resisting frame, and they proposed to extend their use to other types of structural systems.

Other types of energy dissipation mechanisms have also been investigated. Mahmoodi [1969] tested viscoelastic dampers, and Zhang, Soong, and Mahmoodi [1989] performed analytical studies on the seismic response performance of the same discrete viscoelastic dampers, located on the main diagonals of a ten story steel frame structure. Sandwiched between a centerplate and two flanges, the viscoelastic material deformed in pure shear, providing energy dissipation in proportion to its volume. Similar dampers have been used effectively in The World Trade Center and Columbia Center for controlling wind-induced motion. Damper stiffness values were calculated based on damper dimensions, and modal damping estimates were made based on the cyclic shear deformation of the viscoelastic material using a relationship between strain and absorbed energy. Frame response with the dampers was at least fifty percent less at each floor level than the response of the bare frame when subject to earthquake excitations.

Bergman and Hanson [1988] conducted laboratory tests of both direct shear seismic dampers, which also utilize viscoelastic material in shear, and steel plate devices, which depend upon yielding of their steel plate elements for energy absorption. Results showed that while all dampers dissipated energy enough to introduce appreciable amounts of damping in building frames, some viscoelastic dampers can be dependent on excitation frequency, shear strain level, and previous shear distortion. The damping and stiffness degradation of the steel plate devices were found to be independent of displacement amplitude. In addition, the hysteretic behavior of these devices was unaffected by the previous cyclic distortion, and the fatigue resistance would be adequate for even the most severe seismic events.

Friction devices to dissipate energy in connection elements were studied by several researchers. Tyler [1977] proposed the use of friction damped PTFE (Teflon) sliding joints between cladding panels, or partitions, and the main structure to reduce earthquake and wind motions. Pall [1980, 1989] developed a patented friction-damped bolted connection to tie precast concrete cladding to a structural frame of concrete or steel. The connection had several configurations and consisted of friction pads between two flat steel plate surfaces which were bolted together through a slotted hole. The connection was designed not to slip under service loads, wind loads, or mild earthquakes. During a major earthquake, however, before the elastic capacity of the structural member or panel was reached, the connection was designed to slip and dissipate seismic energy. Cyclic dynamic laboratory tests of these connections demonstrated that their inelastic performance was described by rectangular hysteresis loops with negligible fade over several cycles of reversal.

Nonlinear dynamic analyses of a ten story, three bay concrete building with cladding were performed. First, the optimum slip level for the connections was determined. Then, results were used to demonstrate the reduction in building response, structural member forces, and floor accelerations achievable by use of the friction-slip connections. Pall's work promoted a reliable interaction between cladding and the supporting frame and pointed to the economic and safety gains available through rational use of cladding-structure connections.

Finally elastomers have been considered for passive energy dissipation, although the relative magnitude of the hysteretic damping is much less than for inelastic ductile materials. Elastomers are more commonly used for isolation purposes such as for building base isolation systems where they are often combined with other ductile materials (e.g., lead plugs) that will provide

most of the energy dissipation. Moor [1992] offers a good summary of the different systems in use. Since the bearings of base isolation systems have to carry the load of a building, they can easily be compared with bearing connections for cladding panels. In fact, Kemeny and Lorant [1989] proposed the use of energy dissipating elastomeric cladding connections. The bolted connection is composed of a steel insert embedded in an elastomer body. At low level of load, when the elastomer is elastic and not yet compacted, the connection has a low stiffness, therefore isolating the cladding from the structure. However, for higher load, when the elastomer becomes compacted between the steel teeth of the insert, these teeth bend elastically and later yield providing delayed strength and stiffness and finally ductility by yielding. This device has never actually been tested on cladding, and its energy dissipation performance remains to be evaluated.

2.3 Advanced Cladding

Although there are many different kinds of connection systems, all are generally composed of three main components as shown in Fig. 2.5

(a) the anchor point, or insert, built into the precast panel, provides the panel anchorage;

(b) the connection body (often a steel angle), or connector, forms the structural connection between the cladding panel and the main structure; and,

(c) the anchor into the building structure (a second insert or an attachment to a steel member).

There is considerable variation in the design of each of the three major components depending upon the function of the connection (bearing or tie-back), the type of connection (welded or bolted), the architectural requirements, and other considerations [PCI 1988].

The connection anchor usually consists of a steel insert embedded in the concrete of the panel or the structure. Unlike the case of load-carrying structural panel connections, the anchorage of architectural cladding connections may be subjected, in addition to possible shear and pull-out, to torsional and bending moments due to the eccentricity of most of the connection designs. An experimental test program [Pinelli et al. 1990] has provided information on the behavior of cladding connection anchors when subjected to these combined shear and bending actions.

The data available from the tests showed that inserts embedded in concrete are not by themselves capable of providing the levels of ductility and damping required from an advanced connection without loss of strength and integrity due to extensive cracking of the concrete surrounding the insert. The conclusion is that in an advanced connection the energy dissipation must occur in the connector body if the integrity of the concrete panels is to be maintained, and the anchor must be kept in the linear elastic range. In other words, only one component in the connection system should yield, and this should be the connection body. The yielding of the connector therefore serves two purposes: it produces the necessary energy dissipation; and it protects the anchors by limiting the load that can be transferred through the connection.

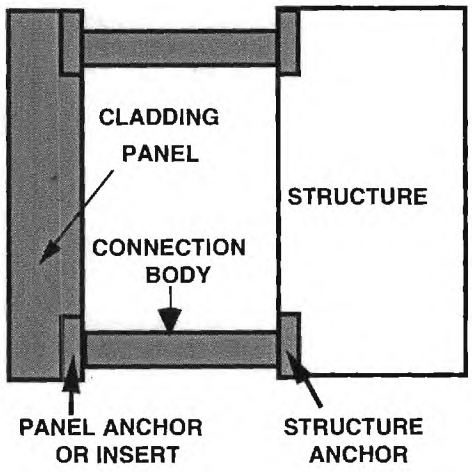

(a) Schematic Diagram

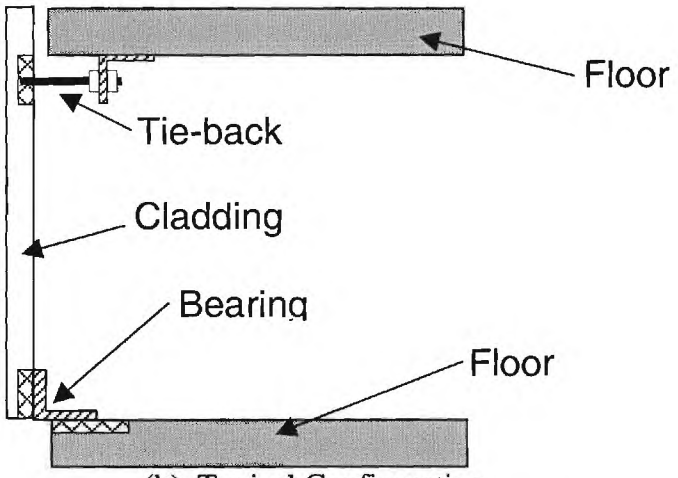

(b) Typical Configuration

Figure 2.5 Schematic Diagram and Typical Configuration of a Cladding System

The connector, then, becomes the focus of attention and must be designed to develop the needed energy dissipation while maintaining the structural integrity needed to insure that the cladding panels remain attached to the building structure. There are an almost unlimited number of devices that could be considered for such an application, although it is perhaps useful to consider the primary applied loads. A cladding connector must be capable of transmitting the following loads (listed in order of importance):

- vertical or gravity load (the weight of the panel)
- normal load (force perpendicular to the vertical plane of the cladding)
- transverse load (force in the plane of the cladding in the horizontal direction)

Load in these cases generally refers to a force, but it may also involve a moment if a "significant" rotational constraint is also present in the connector attachment. Figure 2.6 shows these forces schematically. The vertical or gravity load may be carried by only a few of the cladding connectors used for a given panel while other connectors need not support any gravity

load. This is often selected in order to provide a simpler statically determinate configuration for supporting gravity loads. As a result, connectors capable of supporting gravity loads are usually called "bearing" connectors. Normal loads arise from wind, environmental or seismic forces are usually carried by all kinds of connectors. Transverse loads usually arise from seismic forces or from interstory drift due to seismic or environmental forces. They can also arise due to thermal or weathering expansion or shrinkage.

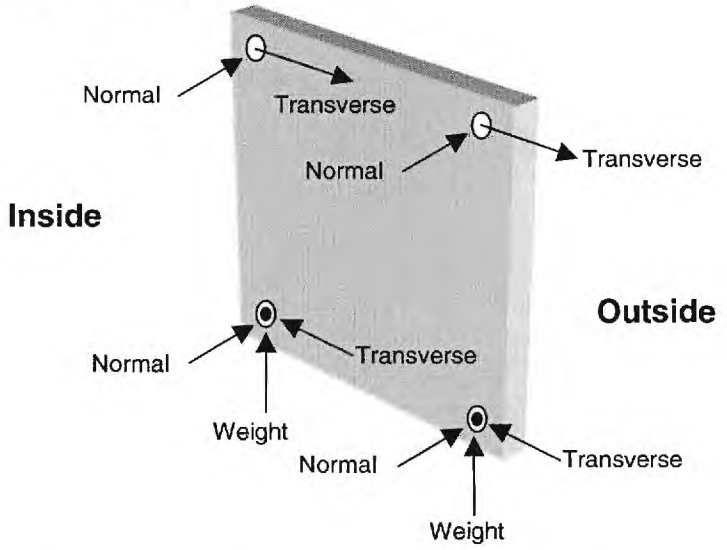

Figure 2.6 Schematic Diagram of Cladding Panel Loads

In general, the accepted design practice is to use bearing connections to support the gravity loads in a statically determinate manner and to support normal loads at each connector (usually in a statically indeterminate fashion). The panel is then isolated from transverse loads by insuring that all but the bearing connectors are very flexible in the transverse direction. This provides resistance to seismic forces but isolates the panels from interstory drift and from environmental forces in the transverse direction. Such cladding connectors are frequently referred to as "tie-back" connectors because their primary role is to tie the panel back to the building structure and maintain the proper vertical alignment of the facade. (Note: while interstory drift can also result in relative displacement between top and bottom of a panel in a direction normal to the cladding plane, this is not normally assumed to give rise to interaction forces in the cladding because the connectors are usually very flexible in bending about a horizontal axis in the cladding plane.)

The advanced connectors as defined in this report are assumed to function in every respect as conventional cladding connectors, BUT they are also allowed to transmit horizontal transverse loads (in the plane of the panel) that arise from interactions between the panel and the supporting structure due to interstory drift. In this respect the advanced connectors will allow the cladding to contribute to the interstory shear resistance of the building and at the same time to dissipate energy as a result of this interaction. Such action will introduce inplane shear forces into the cladding panel, and the panel must be capable of supporting such loads. However, by proper design, the connector can also be configured to limit the maximum level of shear force that can be introduced into the panel, thereby protecting not only the panel but also the panel insert and the building attachment.

There are a number of different ways to develop the desired properties in an advanced connector. Such a connector should provide about the same axial (normal) behavior as a conventional design but it should exhibit a finite stiffness in the transverse direction with a well-defined yield force and a generous and stable hysteresis loop (thereby assuring good hysteretic energy dissipation). The advanced connector should also exhibit good ductility and maintain its structural integrity during repeated cycles of transverse deflection. Of course the connector should also be simple to install and use to align the panel in the building facade.

With these characteristics in mind, Figure 2.7 shows a number of conceptual sketches for an advanced connector. They are based on some of the ideas for structural dampers that have already appeared in the literature (and reviewed in Section 2.2 previously) and they incorporate the constraints particular to a cladding connector. A useful taxonomy for such connectors is to characterize them by the principal kind of structural deformation that they employ. In this case, a suitable classification is:

- simple axial deformation of a prismatic structural member,
- flexural designs that involve transverse beam bending,
- shear designs that employ shear deformation (in beams or other forms),
- torsion designs that utilize torsional deformation of a shaft.

Axial deformation designs are the simplest in concept but they do not inherently make use of structural geometry beyond a simple cross sectional area. Flexural designs have received a great deal of attention due to their simplicity and familiarity. They make use of beam bending action in which the geometry of the beam, including its cross section as well as its taper, can profoundly affect the transverse deformation. Shear designs can utilize shear deformation in a number of ways ranging from simple shear webs to shear deformation in beam bending. Torsional designs are somewhat more complex because the rectilinear interstory drift must be converted into a rotation about the shaft of the torsion member. However, torsion designs, like some shear designs, can often be designed so that the stresses are developed more uniformly throughout the material than is the case for flexural designs. This means that the load transmitting material in the connector can be more effectively utilized to develop hysteretic energy dissipation.

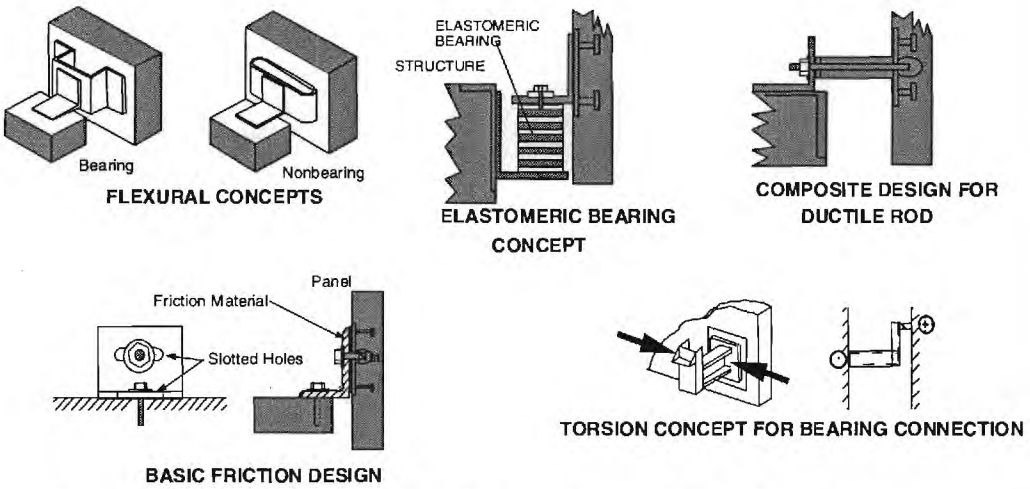

Figure 2.7 Conceptual Designs for an Advanced Cladding Connector

Most of the conceptual designs in Figure 2.7 can make use of common mild structural steel which exhibits most of the desirable qualities (good ductility, stable hysteretic behavior, well-defined yield behavior) noted earlier. However, other materials such as lead could be used for their hysteretic behavior although other structural materials would be required to carry the other structural loads and to provide the needed structural integrity. An interesting concept involves the use of composite materials in conjunction with the primary structural material. The layered neoprene bearing pad is a common composite design that has potential for bearing type connectors. Typically, these kinds of components are employed as bearing pads (e.g., in bridges) where they can support very high compression loads across the bearing while accommodating almost effortless transverse deformation. These designs have also received much attention for use in base isolation applications where other materials, such as lead, are used to provide energy dissipation.

Some of these conceptual examples have been studied in previous tests. A series of simple flexural designs for advanced cladding connection bodies was designed and tested by Pinelli, et al [1996]. The specimens utilized inelastic flexural deformation to provide energy dissipation. Similar energy absorbing steel devices have been reported in the literature for several purposes, among others for energy dissipating bracing connections [Whittaker et al. 1991). All of them take advantage of the fact that mild steel can provide high stiffness in the elastic range as well as absorb energy with moderate strain hardening when deformed beyond the elastic limit. In addition to its good material qualities, steel is relatively easy to fabricate in a variety of shapes, and the stiffness and damping properties of the devices can be improved with judicious choice of geometries. Steel is also economical, and widely used in construction, and therefore it is a material trusted by practitioners.

Details for the particular flexural connector design developed by Pinelli are shown in Figure 2.8. It is fabricated from a section of square structural tube cut away to create two narrow flexural elements whose widths are tapered to initiate plastification over the greatest part of material in the beams. The two tapered beams in flexure have a smaller maximum width through the cut-away than the fixed untapered elements, to ensure that they will deform with double curvature. Complete detailing of the connection would be necessary for a practical design. The connector could be placed between a panel and the supporting structure through a bolted attachment.

More recently, tests described in Section 3 have been carried out on connector designs that might be suitable for advanced bearing connectors [Blanchet, Craig, Goodno 1998]. In this case, neoprene-steel laminated bearing pads were combined with tapered flexures to achieve ductility in the transverse direction while supporting bearing loads. In other work [Khan 1997], a conceptual design for a torsion connector element was developed and a preliminary test article was fabricated and tested.

2.4 Advanced Cladding Design Approach

The design of an advanced cladding system requires the specification of connector properties that will result in increased seismic performance of the building structure. The performance criterion can be any one of a number of choices depending upon what the overall design objectives might be. The study of the influence of hysteretic energy dissipation in the cladding connection on the response of a building suggests that a design criterion would be best formulated in terms of energy dissipation. But the dissipator (cladding connector) also adds

stiffness to the system, because of the bracing effect of the cladding, and therefore it changes the dynamic characteristics of the structure. In addition, the energy dissipated in the connectors is not a given fixed property. It depends on the magnitude of the yield strength of the connection, and it is a function of the excitation, which in turn depends on the modified dynamic characteristics of the structural system. The key here is to find the optimal balance of stiffness and yield strength to be added to the system by the cladding connector dissipators that will result in a maximum energy dissipation, and a reduced response.

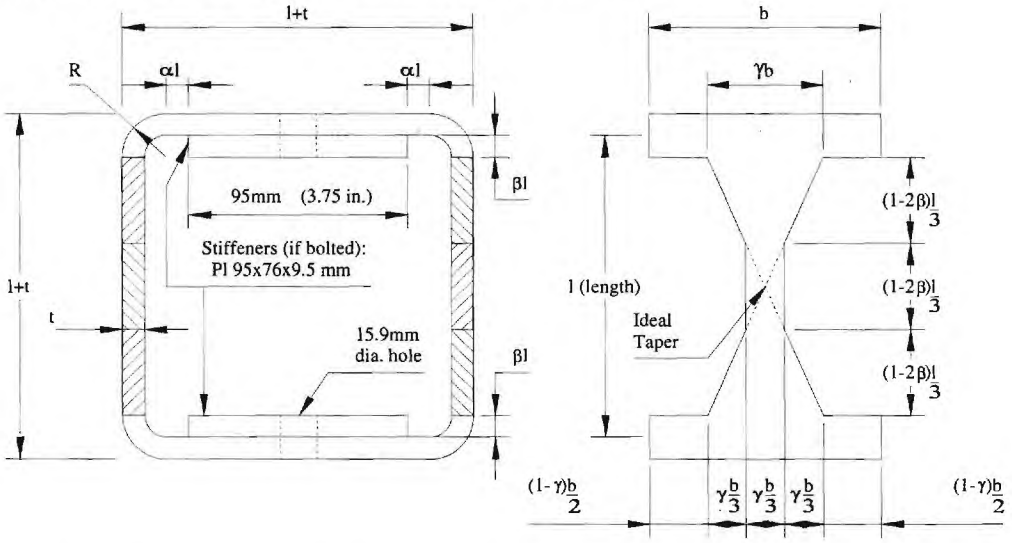

Figure 2.8 Advanced Cladding Structural Tube Tapered Flexural Connector

2.4.1 Design Criterion

An energy-based design aims at resisting, or balancing the energy input to the structure by the excitation (i.e. an earthquake) with the energy the structure is capable of absorbing. If the equation of motion is integrated with respect to the relative displacement from the time the ground motion excitation starts, the resulting "relative" energy equation is (Uang and Bertero 1990):

$$E_i = E_k + E_s + E_d + E_h \qquad (1)$$

where:

E_i = the relative energy input by the earthquake;

E_k = the relative kinetic energy;

E_s = the recoverable elastic strain energy;

E_d = the viscous damping energy; and,

E_h = the irrecoverable hysteretic energy.

For a structure to resist an earthquake excitation in an economical and feasible way, part of the energy must be dissipated through viscous or hysteretic damping. However, hysteretic damping is often associated with yielding and damage to the structural members, formation of plastic hinges, and possibly collapse of the structure. Alternatively, many of the so-called energy dissipators developed in recent years aim at concentrating the dissipation, either viscous or

hysteretic, away from the structural members, in a few pre-engineered elements. This is exactly the idea behind the advanced cladding connections.

In order to identify the best possible design for an advanced connection, the following criterion is adopted [Pinelli, Moor, Craig, Goodno 1996]:

the best connection design will be the one that provides the highest ratio E_C/E_i,

where E_C is the total hysteretic energy dissipated in all the connections on the facade, and E_i is the relative energy input to the structure at the end of the motion.

At the same time, several constraints must also be satisfied:

- the ductility demand on any of the connections should not exceed an allowable value defined for each particular energy dissipator (e.g. from laboratory tests);
- the connection should be able to satisfy the minimum code requirement regarding strength (e.g. Uniform Building Code 1997, Section 1633.2.4.2); and,
- the forces induced in the panel by the connections should not exceed the panel capacity.

The E_C/E_i criterion takes the fullest advantage of the energy dissipation property of the connections. At the same time, energy is a variable that globally characterizes the damage potential of the earthquake for the entire structure, and does so more effectively than a displacement or interstory drift at a specific point. Pinelli, Moor, Craig and Goodno [1996] showed that satisfaction of this design criterion will ensure that little hysteretic energy is dissipated in the structural members, and that the overall seismic response of the building is reduced.

A critical issue in the design of energy dissipators is the definition of ductility. The traditional definition of ductility, as the ratio of maximum displacement to yield displacement, provides only limited information to designers in the case of systems subjected to random vibrations with varying amplitudes. It overlooks important parameters like the number of cyclic reversals and the energy dissipated by the system. Here, a more comprehensive definition of ductility due to McCabe and Hall [1989] has been adopted.

The total ductility of a system, μ, is divided in two parts; an elastic ductility μ_e, varying from 0 to 1 which corresponds to the elastic behavior of the system; and a plastic ductility μ_p, starting from 0 at the yield point. Consequently, once a system has yielded, $\mu = 1 + \mu_p$.

McCabe and Hall assumed that the damage suffered by an elasto-plastic structural steel system during an earthquake is similar to a low cycle fatigue phenomenon. Based on their work, it is possible to predict an equivalent monotonic ductility, μ_p, for a system subjected to an arbitrary cyclic loading. This equivalent monotonic plastic ductility, or ductility demand, is the maximum plastic ductility that the system should exhibit in a monotonic loading test in order to dissipate the same amount of energy as that obtained during the cyclic loading. The equivalent monotonic plastic ductility demand on the system can be evaluated in terms of energy, and load reversals, as:

$$\mu_p = \frac{H_t}{f_y u_y (2N_f)^{0.4}} \qquad (2)$$

where H_t is the total hysteretic energy dissipated in the system during N_f load reversals; and f_y and u_y are the yield load and yield displacement of the system.

2.4.2 Optimization

The design criterion as stated above is, in fact, a classical constrained optimization problem. The objective function to be optimized (or maximized in this case) is the ratio of energies E_c/E_i. The objective function will be a function of what are called "decision variables" which are the design variables to be determined that appear directly in the objective function. The design constraints noted above can be expressed in terms of the decision variables, and these can be conveniently expressed in a standardized form, c(i)<0, where for the present problem:

1. $c(1) = \mu_p - 30$ if the maximum allowable connector ductility demand is chosen to be 30;
2. $c(2) = f_{min} - f_y$ where f_y is the connector yield force and f_{min} is the value of the minimum force requirement specified according to section 2337 (b)4.B. of the Uniform Building Code (1991) [or 1997 UBC, Sec. 1633.2.4.2(4)]; and,
3. $c(3) = f_y - f_{max}$ where f_{max} is the upper bound placed on f_y to avoid damaging the cladding panels.

It is assumed that all the constraints c(i) are satisfied as long as they remain negative.

It should be noted that for c(1), the ductility demand, μ_p, represents an equivalent monotonic plastic ductility as defined by equation (2), and not the actual maximum ductility that the connector would exhibit during the loading history. Accordingly, this latter ductility will be substantially lower than μ_p.

For purely practical reasons, additional constraints should also be added. In general it is unlikely that a given set of connector design properties can be uniquely related to a particular connector geometry, that is, more than a single geometric configuration could yield the same design properties. As a result, it may be necessary that the advanced connector also satisfy practical criteria related to constructability such as:

- the total length of the connector should be constrained for manufacturing and installation requirements, and to accommodate typical spacing between the cladding panel and the structure;
- certain material thicknesses in the connector must be maintained within practical limits.

These can be added in a manner similar to the other constraints noted above.

In addition, it is often necessary when applying numerical optimization to add what are usually referred to as side constraints on the decision variables. For example, in the present case it is impossible to have negative values for either the maximum connector force or the initial linear stiffness, even though this may not cause problems for the mathematical models themselves. Rather than define these requirements as constraints, they are typically added as what are called side constraints.

2.4.3 Design Models

In order to apply the above design criterion to a particular building application, it is necessary to start with a suitable model for design purposes. Before discussing the precise nature of the particular model to be used, it may be illustrative to consider the role of models in design. From

a purely analytical perspective it is always a very desirable goal to develop a model that provides the highest degree of fidelity. That is, the model should represent as much physics as possible in the real system so that all significant behavior is incorporated into the model. However, this grand goal all too often results in large, complex and ultimately unwieldy models that are impractical for design purposes. In design studies it is often necessary to assess the performance of a range of design variations, and if a great deal of time and (computational) effort are required, it may not be practical to employ such a detailed model.

What is needed, instead, is a "design model" that provides a reasonable level of fidelity but yet is computationally tractable. Such a model frequently omits inclusion of certain "details" of the actual behavior which, while they may be important issues later when addressing details of the design, are nonetheless relatively unimportant in the conceptual stages of design. These "details" may be extremely important for other more detailed aspects of the design involving, for example, matters such as localized stresses. Finite element models provide a useful example to consider. One would be unlikely to attempt to carry out a conceptual design for a structural system by using a highly detailed finite element model involving a large number of very accurate, high-order elements. For one, such a model generally requires very detailed geometric and material information that is not normally available or even defined at an early conceptual stage of design. In such cases, a much simpler model, perhaps not even involving finite element analysis, might be more practical and useful.

Of course, an obvious problem exists with this situation. At some point, the design model must be converted (or evolve) into a detailed model suitable for more extensive analysis purposes. As a result, the design model must be fully consistent with more detailed models.

One further point needs to be made in connection with the present work. In this case the application of a new technology to an existing building is being considered so that it is actually possible to develop quite realistic and detailed structural models for the building. And based on previous research on connector models [Pinelli 1992] it is also possible to develop very detailed and accurate models for certain advanced connector designs. However, the need for a suitable design model still exists because both of these detailed models are computationally unwieldy for design purposes. On the one hand, while details of the building structure are readily available, it is impractical to synthesize equivalent levels of detail for a connector concept. And at the same time, the resulting analytical models are far too time-consuming to use to study many different configurations.

2.4.4 Nominal Model

The above definition of a design model leads logically to the concurrent definition of what is called a "nominal model." A nominal model is defined as the highest fidelity model for the system being designed, and it is the model that most accurately and completely represents the behavior (e.g., performance) of the system. Typically, the nominal model will be a much more complex computational model compared to the design model, and it will require considerably more computational effort to execute. On the other hand, the nominal model will be capable of describing almost all of the detailed behavior of the system. Development of the nominal model may begin at any point in the design cycle, but it may not reach full maturity until very late in the design process when all of the system configuration information is available.

2.4.5 Connector Design Model

An analytical model for a cladding connector should be capable of representing all aspects of the measured behavior of the connector under all service conditions. Such models could be constructed from purely physics-based reasoning or they could be based entirely on the measured behavior of a number of test articles. The first type of model may require considerable physical reasoning and detailed mathematical formulations, while the latter kind of model could be based on a purely geometric representation of the measured behavior (often called "curve-fit" models). Both have been successfully used to describe mechanical systems. Pinelli [1992] provides a useful discussion of both approaches.

A design model for a cladding connector must necessarily involve a relatively small number of design variables in order to be practical. In the present study, a cladding connector adds energy dissipation through hysteretic action. The hysteretic action is based on structural deformation so that a force is needed to activate this and a structural stiffness is added to the structural system. One of the simplest structural hysteresis models is based on an assumed elastic-perfectly plastic material behavior. In this case an initial stiffness and a yield force could be used to describe the material. As a result the minimum practical number of design variables needed to describe such a device would then be two, e.g., a stiffness and a yield force. Of course, additional design variables such as strain hardening or the Bauschinger effect could be added to provide more realistic behavior, but for purely design purposes, these details are of little importance.

In the present study, the cladding connector design model was assumed to be based on an elastic-perfectly plastic material model. Even though this may be appropriate for mild, ductile steel, the geometric configuration of a particular connector could introduce other effects (such as loss of bilinearity or addition of strain hardening). Nonetheless, a simple piecewise linear elastic-perfectly plastic model is assumed as a design model for the connector. The resulting design variables are taken to be the initial linear stiffness and the yield force. Equivalently, one could also choose the yield force and the yield displacement to describe the same connector design. Figure 2.9 illustrates a typical connector design model.

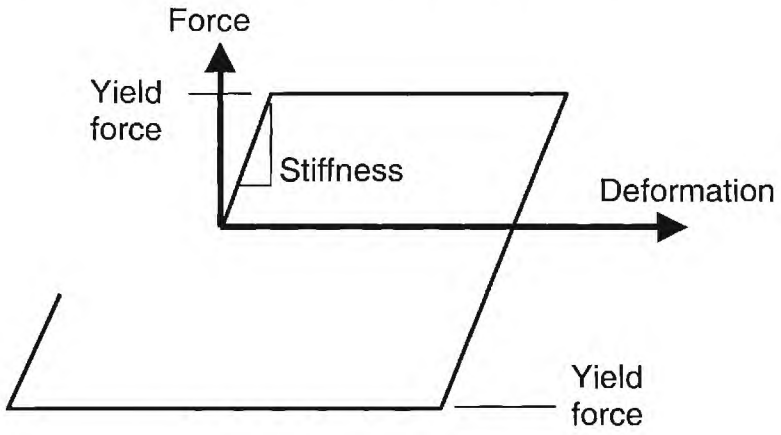

Figure 2.9 Representative Cladding Connector Design Model

For such a design model, the decision variables in the optimization problem will be the connector design model variables for each of the individual panels in the building. In practice, this could amount to hundreds of decision variables and the result could quickly become computationally impractical. On the other hand, it is unlikely that different connector properties, even if computed, could be manufactured for each individual connector or panel. Rather, it is more likely that a given set of connectors would be used for a particular set of cladding panels. In this case, only as few as a half-dozen or so different connector sizes might be employed so that the number of decision variables might be less than 30 in number – a very practical figure given contemporary computational capabilities.

2.4.5 Building Design Model

The building design model necessarily represents a compromise between the precise definition inherent in a full 3D finite element model and the computational efficiency of a much simpler (e.g., 2D) structural model. For the cladding design studies, it was assumed that a 2D model (e.g., a model representing behavior in one vertical plane of symmetry of the building) would be sufficient for the class of problems to be considered. However, given the presence of energy dissipation devices in the structure and the possible hysteretic, inelastic behavior of structural members, it was necessary to utilize a nonlinear structural model. The analysis software selected for these studies is DRAIN-2dx [Prakash, Powell, Campbell 1993] although an earlier version, DRAIN-2d, which was extensively modified at Georgia Tech, was used in earlier studies by the authors. DRAIN-2dx is a well known 2D nonlinear dynamic finite element analysis program that is the result of computational research carried out by Graham Powell and his students at the University of California Berkeley over the past two decades or more. The code is available in source form and can be customized by the addition of user-developed elements and user-specific data handling routines. DRAIN-2dx is even more useful when coupled with a commercial pre/post-processing program called Nonlin-Pro [Charney 1997].

A suitable building design model for DRAIN-2dx is basically a 2D-frame structure to represent the structural behavior of the study building in one of the principal directions. Since DRAIN-2dx is only a 2D code, it is therefore not possible to study structures with significant asymmetry or for which coupled bending-torsion effects are a factor (these effects are not important for the doubly-symmetric study building chosen as part of this investigation; however, extended versions of this software, DRAIN-3dx and DRAIN-BUILDING, are available from NISEE to account for these 3D effects if needed). DRAIN-2dx has suitable element models to represent linear and practical nonlinear behavior of steel beams and columns (with more limited ability to handle reinforced concrete). Building mass is represented in DRAIN-2dx using a lumped-model approach.

The cladding panels can be represented in DRAIN-2dx by either a shear panel type of element or by a rigid truss of similar overall dimension. The shear panel element is more useful if the panel shear stiffness is relatively low (compared to the cladding connectors), but a panel constructed from an X-braced rectangular frame is computationally simpler and quite suitable if the panel is assumed to be much stiffer in shear than the connectors. Figure 2.10 shows a schematic diagram of a typical building design model with cladding panel modeled using braced-frames. This particular model is actually for a ¼ scale building model that has been tested extensively on the NCEER shake table [Reinhorn, et. al.1989]. The cladding panels are assumed to be connected at one end (typically the lower end) to corresponding nodes in the structural frame to simulate rigid bearing connections. The advanced cladding connectors are then affixed

at the upper corners of the panel. These connectors are represented in the design model by connector design models similar to those described in the previous section. Such connectors can involve elastic-perfectly plastic behavior in the horizontal direction only, or they can also include vertical and rotational components. In DRAIN-2dx, these connector design models are implemented using the bilinear spring element available in the standard version (Type 04 element).

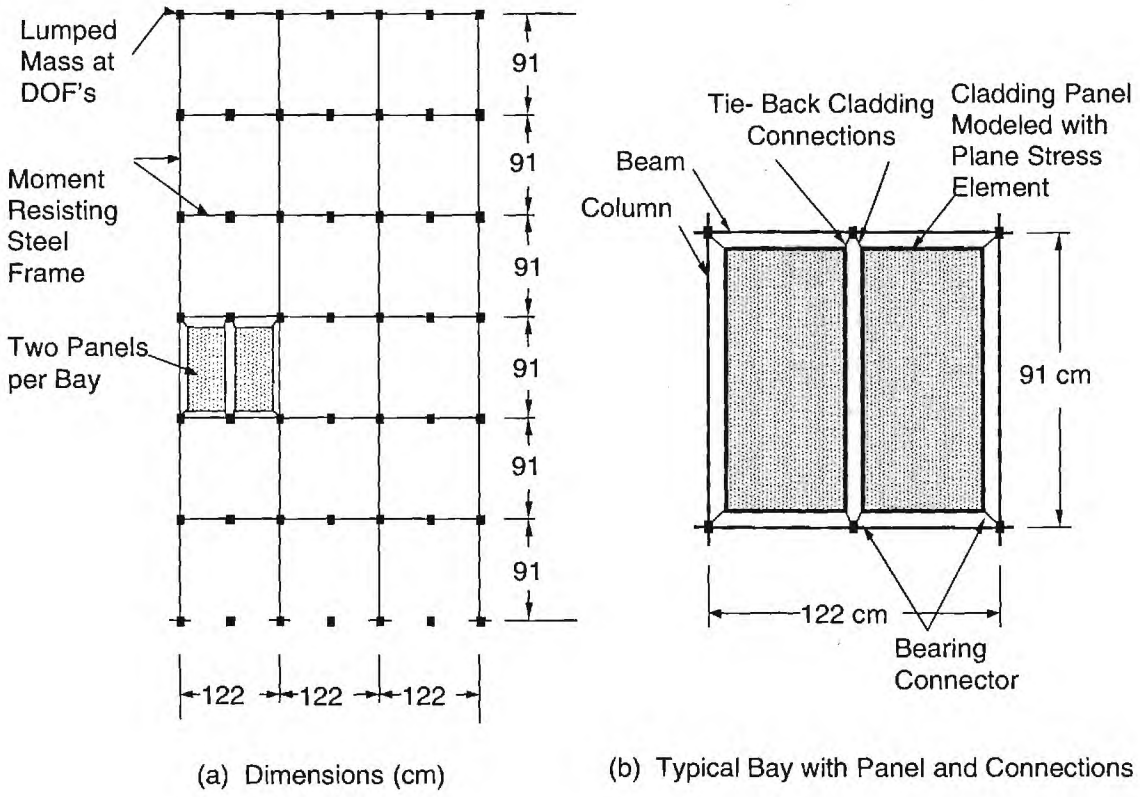

Figure 2.10 Building Design Model

The building design model as described above typically includes several hundred degrees of freedom and requires on the order of 10 minutes of execution time for a dynamic response computation over a 45 second earthquake record using a 300 MHz Pentium CPU with 128 Mb of memory. As such it is marginally useful for design purposes that require frequent response computations (such as those involving numerical optimization). For more than this level of complexity, it is necessary to develop a simplified model involving either consolidation of the frame members (e.g., reduction in number of bays) or condensation of unnecessary degrees of freedom (this cannot be readily accomplished in DRAIN-2dx at this point).

2.4.6 Numerical Optimization

The advanced cladding design process next involves the specification of the properties of the advanced cladding connectors that is needed to achieve the best level of seismic performance achievable. As noted in Section 2.4.1, for the cladding design model presented above, the necessary properties are the initial elastic stiffness and the yield force. In addition upper/lower

bounds must also be specified as side constraints. Finally, the maximum dynamic ductility must also be specified to insure the structural integrity of the advanced connectors.

The numerical optimization problem was then solved using the commercially available optimization code called DOT [Vanderplaats 1993]. DOT is capable of either unconstrained or constrained optimization. For the former either the Broydon-Fletcher or Fletcher-Reeves methods can be selected and for the former DOT employs the Modified Method of Feasible Directions. Sequential Linear Programming and Sequential Quadratic Programming methods are also available. DOT is provided in source format and the objective function (the function being minimized or maximized) must be computed using a user-developed procedure. Constraints must be expressed either as simple side constraints on the decision variables or else as inequality constraints. For example, if it is desired to maximize the volume of a cardboard box for a given amount, A, of cardboard, the following definitions might be made:

- Decision Variables: length, width, height
- Objective Function (volume): length*width*height
- Constraint: $0 \geq A - 2*(\text{length}+\text{width})*\text{height}$
- Side Constraints: length ≥ 0; width ≥ 0; height ≥ 0

For the advanced cladding design problem, the appropriate definitions for numerical optimization were specified as:

- Decision Variables: connector stiffness, k_c, and connector yield, f_c
- Objective Function: (Energy Dissipated in Advanced Connectors)/(Input Energy)
- Constraints:
  Ductility: $c(1) = \mu_p - 30$ (e.g., max dynamic ductility = 30)
  Yield: $c(2) = f_{min} - f_y$ where f_y is the connector force and f_{min} is the minimum value
  Yield: $c(3) = f_y - f_{max}$ where f_{max} is the upper bound placed on f_y to avoid damage.
- Side Constraints: Decision Variables must be positive.

The decision variables are the stiffness, k, and yield load, f_y, for each of the energy dissipative connectors in the system. Thus, the total number of decision variables varies with the number of different advanced connectors used on the facade. This could amount to a very large (and unwieldy) number of decision variables, but if nominally identical connectors are used for all the advanced connections, then a minimum of only two decision variables are needed. On the other hand, better performance might be possible with some variation in connector properties, either across the building or vertically (more likely) so it may also be useful to group the advanced connectors into two or more groups. In this case the number of decision variables would be 2*Ng where Ng = number of groups, and the constraints would be increased as well.

The Objective Function involves the computation of energy dissipation in the advanced connectors and the total energy input into the structure by the design earthquake. These variables must be determined using DRAIN-2dx to compute the dynamic response for a given design earthquake. In addition, the dynamic ductility (Equ. 2) must also be computed. The standard release of DRAIN-2dx is not capable of computing all of these variables, so it was necessary to modify the original source code to provide this capability. The results were added to the standard DRAIN-2dx output files, although a cleaner solution would have been to output these variables into the user-defined output files that are incorporated into the design of DRAIN-

2dx. This was not done in the present case due to the more involved coding required. The Appendix provides listings of those DRAIN-2dx routines that were modified for this purpose.

All of the analysis and numerical optimization coding were implemented on Pentium class PC's running Windows NT. The codes were either available in executable forms or else source code was compiled and linked using Digital Visual Fortran 5 from within the Microsoft Developer Studio environment. Appropriate pre- and post-processing scripts and codes were used to integrate all of the analysis and design modules together.

2.4.7 Sample Results

Given a baseline structural design including advanced cladding connectors and a suitable design model implemented in DRAIN-2dx, the design objective is to determine the properties of the cladding connectors that will provide the best level of building performance for a given design earthquake. As noted above the decision variables are the connector design properties:

- initial elastic stiffness, and
- yield force

subject to constraint on the connector maximum dynamic ductility. (Other practical constraints related to constructability of the connectors were not considered in the present cases.)

The measure of performance (objective function) to be maximized is the dimensionless ratio of energy dissipated in the connectors to the total seismic energy input to the building during the earthquake. There are other choices for a performance measure. For example, a more practical and obvious measure is the peak displacement of the building, but the RMS displacement over all floors could also be used. The peak displacement for the design with advanced connectors when compared to the similar peak displacement for the conventional (isolating) cladding connectors provides a ready measure of how well the advanced connectors work, and this measure is used to provide a general measure of performance.

Figure 2.11 provides a summary of an optimal design using the 1952 Kern County (S48E Santa Barbara courthouse) earthquake for a sample case of a reduced-scale 6 story building used for testing purposes at NCEER in the mid-'80's [Pinelli, Moor, Craig, Goodno 1996]. This figure shows the optimal cladding parameters as determined from numerical optimization, and it also shows contours for the objective function to better illustrate how the location (solid ball) is defined. Constraint contours (dashed lines) are shown as well and it is clear that the optimal solution is on the constraint (ductility demand = 50 in this example) at the highest value of the objective function.

Figure 2.11 was prepared from a grid of data obtained from numerous individual computations of the objective and constraint functions. Normally, this would be too time-consuming for practical purposes, but it is provided in this research effort to better understand how the optimal solution is constructed. The figure also shows example constraint lines that might be used to define a practical connector by constraining the physical dimensions (size). In this case a practical design must lie within the "V" shaped region (defined by the hollow ball).

Figure 2.12 shows the peak interstory drifts (as a dimensionless fraction of story height) computed using DRAIN-2dx for the design earthquake. The "optimal connectors" are connectors providing the best optimal solution while the "tapered connectors" are constrained by practical manufacturing considerations. The "conventional connections" are the conventional, tie-back connectors that effectively isolate the cladding panels from the structural system.

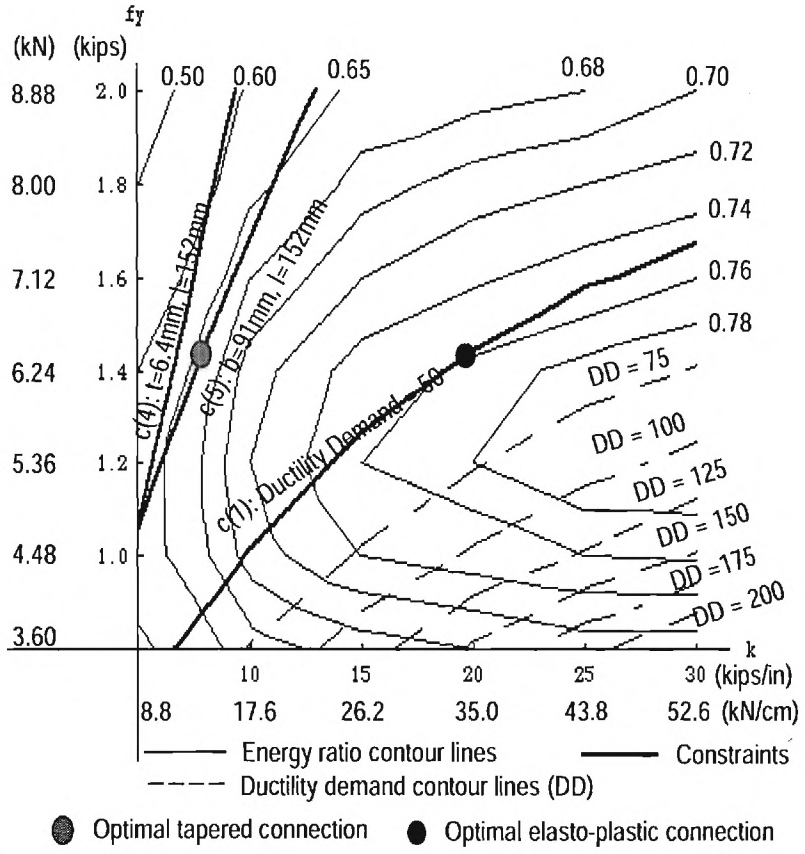

Figure 2.11 Optimal Cladding Connector Design (from Pinelli, Craig, Goodno 1995)

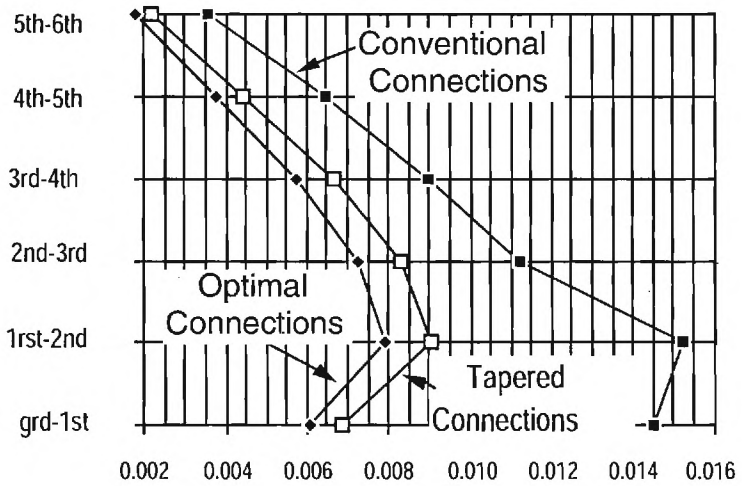

Figure 2.12 Peak Interstory Drift Envelopes (from Pinelli, Craig, Goodno 1995)

The preliminary results shown above illustrate the basic advanced cladding connection design process as developed in earlier research by the authors. The drift and time history results illustrate the potential improvement in building seismic design that might be obtained from this approach. From the figures it is clear that displacement response reductions on the order of 20-50% are reasonable. On the other hand, the corresponding reductions in member forces are not obvious from these results.

The overall building seismic design process may have two different objectives, among others, as follows:

- use advanced cladding connectors to provide an extra measure of performance and consequent improvement in margin of safety for a design that meets code provisions, or
- instead, use advanced cladding connectors to allow a reduction in basic structural steel while not exceeding seismic response levels appropriate to a conventional structure.

The first objective is readily demonstrated by the results presented above, and this kind of approach is most appropriate to basic retrofit situations or to retrofit situations where the existing structure does not meet current code specifications. In this case the advanced cladding connections may overcome the deficiencies in structural performance. On the other hand, the second objective may be more appropriate to a new design in which case the advanced cladding connections can be employed to absorb seismic energy and therefore allow a reduction in the required structural member sizes. The corresponding reduction in structural weight can be translated into equivalent cost-savings for the building. In this case, the advanced cladding system may directly allow the design of a more cost-effective building. It is this latter point of view that will be explored in more detail in the present report.

3. Experimental Study of Advanced Connector Concepts

Advanced cladding connectors capable of developing significant levels of energy dissipation have been under study by the authors for a number of years. This section of the present report summarizes in a comprehensive manner much of this prior research which otherwise has been published in different formats. This section extends this prior research to propose and examine the behavior of two new designs for advanced cladding connectors.

The primary objectives of this research were to develop prototypes to prove the feasibility of the advanced connection concept, and to generate sufficient experimental data regarding energy dissipation behavior to use in later computer simulations of entire building-cladding systems. Complete detailing of the connections is certainly the final goal and would be necessary for a practical design. The proposed design concepts can certainly be improved to meet practitioner requirements.

3.1 Advanced Connector Concepts

Advanced connector concepts were introduced in Section 2 and several basic categories of energy dissipators where identified. More detailed consideration of some of the most promising approaches are presented in the following section.

3.1.1 Friction Mechanism

A friction mechanism is the basis for a number of proposed connection designs [Tyler 1977, Pall 1980, and Palsson 1982b]. A recent potential candidate for friction damped cladding connections is the slotted bolted connection developed by Grigorian, Yang, and Popov [1987].

Great quantities of energy can be dissipated through friction since the inelastic performance is described by rectangular hysteresis loops with negligible fade over several cycles of reversal. However, the reliability of friction induced mechanisms has yet to be proven. Since there is no slippage during normal operation, corrosion may increase the friction and change the properties or destroy the mechanism. Also, as in conventional tie-back connections, an insufficient length of the slot could reduce the effectiveness of the friction mechanism

3.1.2 Composite Material Mechanism

The connector itself could be a composite system manufactured with different materials selected for strength and ductility, in a manner similar to that in which elastomers are being used in a variety of base isolation systems. Kemeny, and Lorant [1989] proposed the use of energy dissipating elastomeric cladding connections which had the particularity of providing zero initial stiffness for low levels of excitation. A design for an advanced bearing connector constructed using composite materials will be considered in the present report.

3.1.3 Plastic Deformation Mechanism

Many energy dissipating devices based on the inelastic deformation of steel take advantage of the fact that mild steel can reliably provide high stiffness in the elastic range as well as absorb energy with moderate strain hardening when deformed beyond the elastic limit. In addition, steel is relatively easy to manufacture in different shapes, and the stiffness and damping properties of

the devices can be improved with judicious choice of geometries. Steel is also economical, and widely used in construction, and therefore it is a material trusted by practitioners.

Plastic deformation can be initiated by a number of structural mechanisms including: axial, flexure, shear, or torsion loading of a structural member. While some of the mechanisms are more complex than others, each one has certain advantages and disadvantages. Some of the more promising concepts for an advanced cladding connector are noted below.

A promising flexural concept, shown in Figure 3.1, is inspired by the research reported by Kelly., Skinner., and Heine [1972]. In this case, the connector is a ductile closed loop made of mild steel with semi-circular ends. The flexural action in the rolling and unrolling of the loop ends will provide the energy dissipation during a moderate or strong earthquake. The advantage of the loop is its symmetry which makes it suitable for cyclic loading. Also, in a loop, the strain depends on the ratio of thickness to radius and is independent of the displacement.

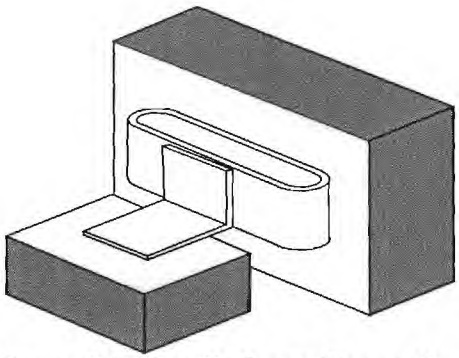

Figure 3.1 Ductile Loop Connection

The above figure shows but one of a large number of different concepts for flexural deformation, and these are quite popular because the understanding of simple beam bending (flexure) is a basic component of structural engineering and great confidence in put in this knowledge. A very promising flexural design for an advanced cladding connector will be described in a later section of this report.

Torsion is an attractive plastic deformation mechanism for steel connections. Torsional devices have some advantages: they have better energy absorption qualities because the uniform distribution of the torsional moment results in a better use of the material; and they exhibit progressive ductile failure distributed over the length of the device. However, the attachment is somewhat complicated if trying to achieve pure torsion in a device between surfaces moving parallel to each other, although the design can be simplified if torsion and bending are combined. In spite of these obstacles, a novel torsion configuration for a cladding connector will be described in this report and preliminary results will be presented.

Each of these examples is but one of a number of different concepts for an advanced cladding connector. As noted in Section 2, there are a number of basic mechanical approaches and an almost unlimited number of different concepts based on these. In general, conventional connectors can be categorized by the kinds of loads that they support and in this case the primary classification is into either bearing or nonbearing designs, the latter often referred to as "tie-back" connectors because their primary function is to maintain a panel in the façade plane and otherwise to provide no structural capability in the lateral direction. For advanced cladding

connectors, the same classification is appropriate with a key provision: all of the connectors will also be capable of supporting significant lateral (horizontal, inplane) loads and exhibiting hysteretic energy dissipation for deformation in this direction. Otherwise, bearing connections will be assumed to support gravity loads with minimal deformation and tie-back connectors will be very stiff normal to the façade but may or may not exhibit stiffness and dissipation in the vertical direction. Note that since most bearing connections are quite stiff vertically, there is relatively little interest in the vertical behavior of a tie-back connector so long as it does not interfere with other connector actions.

In this section four different concepts for advanced cladding connectors will be described and preliminary experimental testing to ascertain general behavior will be presented. The concepts consist of the following:

1. Tapered flexural tie-back connector,
2. Composite bearing connector,
3. Composite bearing connector with tapered flexures, and
4. Torsion tie-back connector.

The first concept was actually developed in prior research by the authors and is being included in the present report for completeness. The third design is a variant of the second and includes tapered flexures to provide significant energy dissipation for lateral motion. Finally, the fourth concept is a novel approach that has only been evaluated conceptually at this point. Together, these different concepts form the beginnings of a handbook of cladding connector designs that might be considered for practical applications or for commercial products. In either case, additional testing will be required to verify some of the design parameters.

3.2 Experimental Facility

3.2.1 Test Apparatus

A laboratory testing machine especially conceived for the study of cladding connections was developed in earlier work by the authors and it is described in detail in [Pinelli 1992; Pinelli, Moor, Craig, Goodno 1992, 1996]. The primary objective behind the development of the test apparatus was the simulation of the behavior of an advanced cladding connection subjected to interstory drift, and any useful machine for testing advanced connections must have:

- the ability to isolate and monitor the behavior of the connector element;
- the ability to reproduce the actual service loads and deformations to which a connector is subjected during an earthquake; and,
- the ability to accommodate testing of a variety of connector damping mechanisms with different conditions of fixity for the connector ends.

In order to be able to achieve these objectives, the machine must be capable of applying a number of specific kinds of loads to a connector. For purposes of description, it will be assumed that the connector is arranged in the machine in the same orientation as it would have when used to support a vertical cladding façade. In this case the loads and constraints are:

- horizontal (shear) force or displacement,
- connector moment fixity at both ends in both lateral directions,
- shear release in vertical direction,

- axial release (normal to vertical façade plane), and
- optionally, gravity load (vertical shear)

A number of different concepts were examined for such a test apparatus and some were quite novel but not practical [Pinelli 1992]. The design chosen provides the desired end fixities along with shear and axial releases using large precision roller bearings. The horizontal force or displacement across the connector are created using servohydraulic actuators and the gravity load, if needed, is applied using lead weights. An overall schematic of the test fixture is shown in Figure 3.2a, and a detailed schematic showing the kinematics of the fixture is shown in Figure 3.2b. Figure 3.3 shows a conventional 3-view drawing. The test fixture is composed of the following major components:

- the building anchor consisting of a thick vertical steel plate affixed to a rigid steel box supported on massive roundway bearings; the box can slide back and forth horizontally to provide full constraint release in the axial direction (normal to cladding façade plane);
- the panel anchor consisting of a rigidly framed square steel plate facing the building anchor; it is mounted to the support frame using 4 long rods with swivel ends so that for any motion the panel anchor will remain parallel to the building anchor (e.g., it can move parallel to itself in the horizontal and vertical directions);
- horizontal (shear) load system consisting of two hydraulic actuators with total force capacity of +/- 67 kN (15 kips); the actuators are mounted horizontally in the façade plane and are attached to the edge of the panel anchor; the lower and main actuator is a double stroke actuator with a stroke of 15.24 cm (6 in), a piston of 33.74 cm^2 (5.23 in^2), and it develops the primary shear loads or displacements; the upper actuator is a single stroke actuator that prevents the panel anchor from rotating in its own plane ; both actuators are coupled with 89 kN (20 kips) capacity load cells; and,
- two smaller hand-operated hydraulic actuators that lift the required lead weights to apply a gravity load in the case of bearing connections; the weights are 24 kg (50 lb) lead blocks stacked on a wheeled cart.

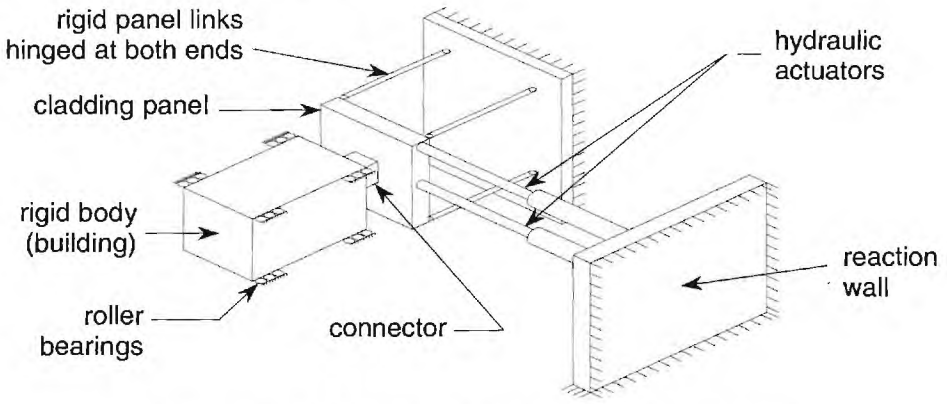

(a) Overall Schematic of Connection Test Fixture

Figure 3.2 Schematic Diagrams of Connection Test Fixture

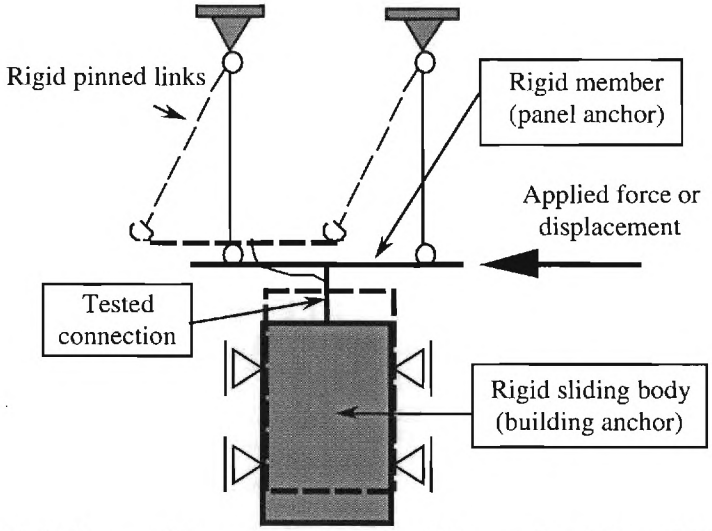

(b) Detailed Fixture Schematic Showing Kinematics (viewed from above)

Figure 3.2 Schematic Diagrams of Connection Test Fixture-(continued)

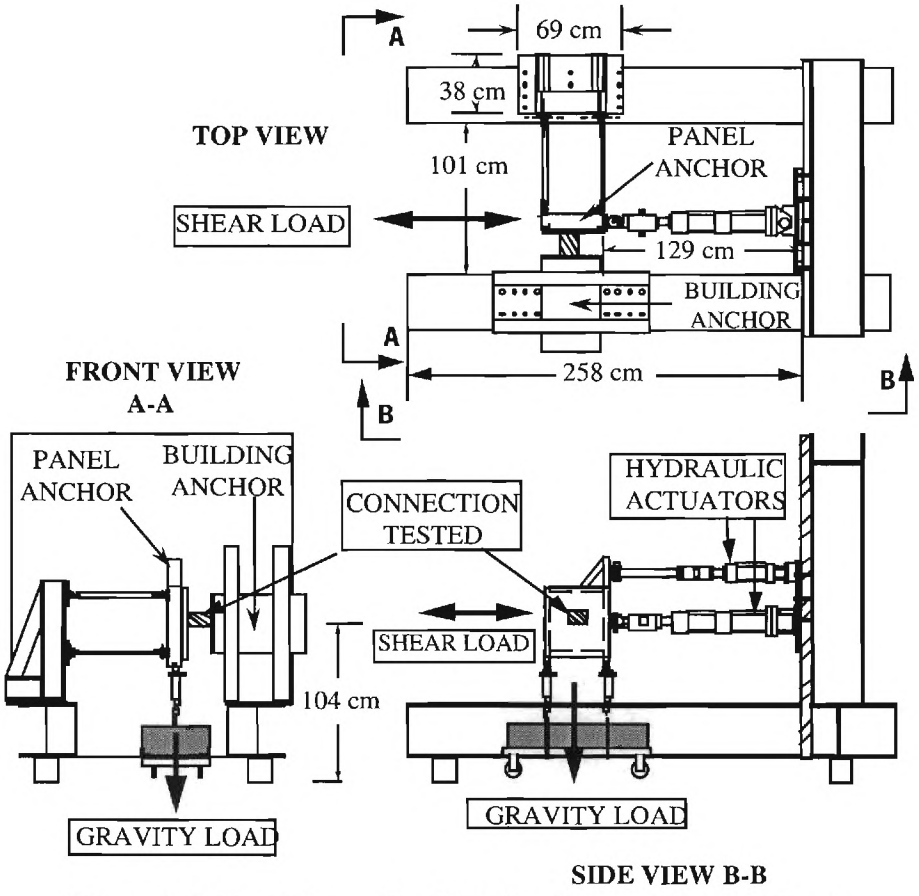

Figure 3.3 Test Fixture for Cladding Connections (3-View).

3.2.2 Data Acquisition

The control of the test machine and the behavior of the connector under test can be controlled and monitored by an instrumentation system that consists of an analog servohydraulic control system and a PC-based data acquisition system. Much of the simplicity of the test machine is provided by its inherent mechanical design so that the required instrumentation system is reduced to applied load measurement and measurement of the relative displacement across the connector under test. The applied loads are measured directly by the load cells affixed to the servohydraulic actuators. The displacement measurement system consists of a total of eight (8) linear variable differential transformers (LVDT's) arranged in a redundant array to measure displacement of the panel anchor in all possible degrees of freedom relative to the building anchor. The LVDT's are mounted to an aluminum frame affixed to the building anchor and are oriented to that the measure the relative inplane (vertical & horizontal) movement as well as the axial movement. Four LVDT's are used to redundantly measure the relative axial displacement between the panel and building anchors at the four corners of these plates. From these measurements is possible to compute the net axial displacement and the relative rotation about both the vertical and horizontal inplane axes (which should be negligible if the bearing systems function correctly). Figure 3.4 shows the schematic of this system and a more detailed description is provided in [Pinelli 1992].

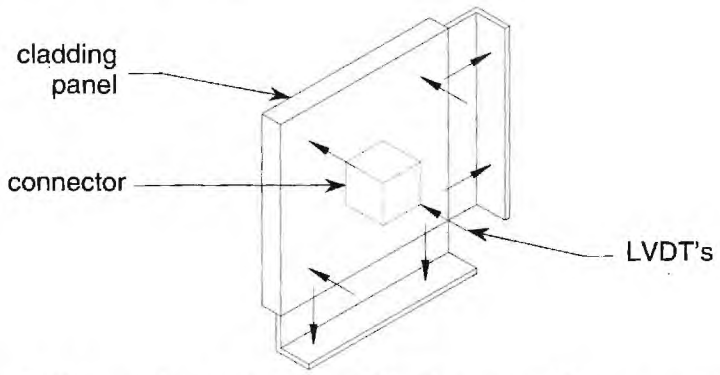

Figure 3.4 Schematic of Connector Displacement Measurement System

The servohydraulic controllers consist of two MTS 406 series analog proportional/derivative (PD) closed loop controllers. To maintain alignment of the panel anchor during testing, the controllers are operated in displacement mode and are carefully adjusted to cause the actuators to track each other's displacement exactly. The applied load is therefore a dependent variable and is recorded along with the displacements.

The data acquisition system is a PC-based design constructed around a laboratory grade integrating digital voltmeter, a reed relay input scanner, and appropriate signal conditioning. The use of this particular voltmeter, which operates with 6 digit resolution and microvolt sensitivity, means that minimal signal conditioning is required for either LVDT or strain gage channels. However, the performance is achieved at the expense of speed and the present system is limited to about 5 samples/second. Programming is done in TurboPascal using a simple test executive and a library of instrument custom procedures developed in the lab.

3.2.3 Testing Procedure

For an advanced cladding connection, the energy dissipation mechanism is triggered by the interstory drift during an earthquake, and for the present connector designs, damping results from a hysteretic process. In view of the relatively small inertia of the connector and the fact that the energy dissipation mechanisms being investigated are assumed to be mainly hysteretic, it was decided that the tests could be quasi-static with the ability to apply cyclic displacements of varying amplitude. Cycles of increasing displacement are applied in small step increments. At each step, displacements and forces are recorded, and the corresponding hysteresis cycles, shear force versus transverse displacement, are plotted. Alternatively, some specimens can be tested in fatigue by applying a number of cycles of equal amplitude until the specimens fail. For any cases, a gravity load can be applied using the lead weights.

The objective of the tests may include the following:

- evaluate the stiffness, ductility and energy dissipation characteristics of each of the connectors (these are usually the primary objectives);
- evaluate the influence of different attachment schemes (bolted and welded) on the properties of the connectors;
- investigate the fatigue behavior of the connectors; and,
- investigate the influence of a vertical (gravity) load on the lateral behavior of the connectors.

By appropriate configuration of the test machine and the data acquisition system one or more of these objectives may be achieved in a testing program. The following sections describe results from a series of tests of 3 different kinds of advanced connectors.

3.3 Flexural Connector

3.3.1 Concept

As noted previously, the flexural connector concept is perhaps the most easily understood, both in terms of geometric configurations as well as analytical models (beam bending). In this case the required energy dissipation is produced as a result of hysteretic action associated with inelastic deformation of the flexural element(s).

Keeping in mind that manufacturing, maintenance, and reliability are as important as good performance, a series of simple flexural designs for advanced cladding connectors were developed. This particular design was developed by the authors and a former doctoral student, and it is included in this report for completeness. The results presented below appear in detailed form in the dissertation [Pinelli 1992] and in abbreviated form in subsequent publications [Pinelli, Moor, Craig, Goodno 1992, 1996]. Details of the connector design are illustrated in Figure 3.5. The connector is fabricated from a section of square structural tube, cut away as shown to create two narrow flexural elements whose widths are tapered to initiate plastification over a greater portion of material. The dimensionless parameters shown in Figure 3.5 are properties of individual families of these connectors fabricated from material of different thickness to obtain different design parameters.

When the tapered elements deform laterally in bending with a double curvature, plastification will occur at all cross sections along the taper, since both the height of the beam and the bending moment vary linearly. The results will be "fat", almost rectangular hysteresis

loops that reflect the high energy dissipation resulting from the plastification. In order to get the necessary double curvature (so that the variation in height and moment coincide), it is crucial that the beam's ends be fixed. This fixity is achieved through the cut-away between the supporting untapered elements and the tapered beams, which ensures that the rotational stiffness of the support is higher than the beam's.

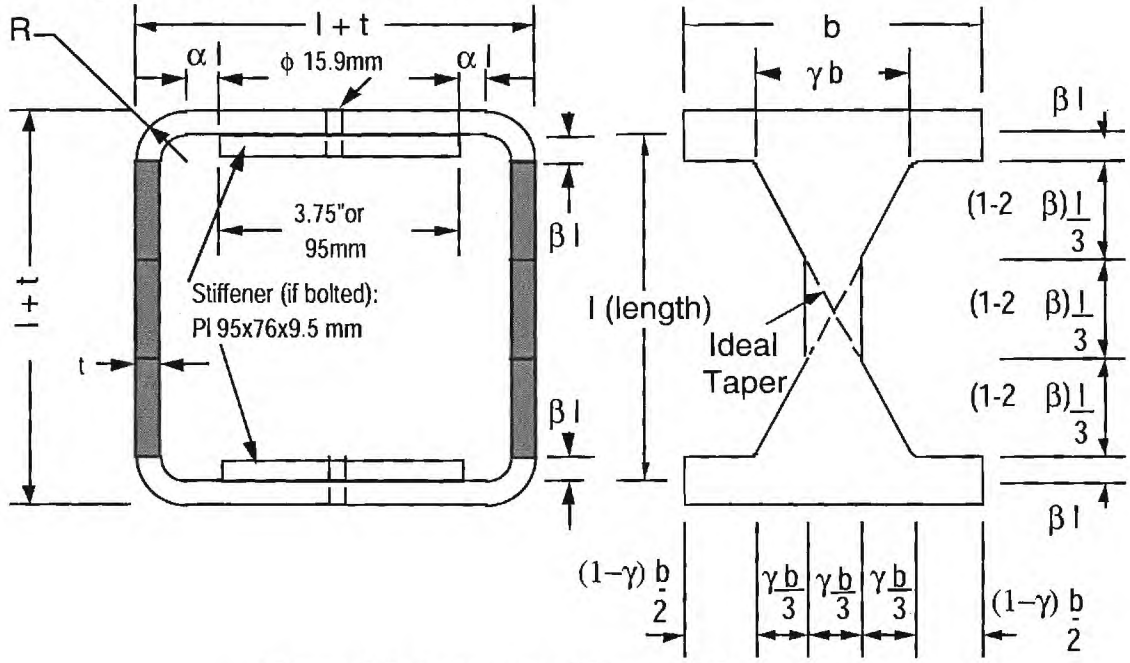

Figure 3.5 Geometry of Tapered Flexural Connection

The connector could be placed between a panel and the supporting structure through a bolted attachment (where the compression forces are minimized through a vertical slot), as shown in Figure 3.6. The attachment is composed of two parts: a flexible part, which is the advanced tapered connector itself; and a stiff part which provides a rotational restraint to avoid lateral buckling of the beams of the connector. The stiff part could be any device. The arrangement proposed here is a square tube welded on top of a steel base plate. The height of the resulting box can be adjusted during installation through a leveling bolt. Once the panel is installed, the box is welded between two steel angles, one on each side. An alternative to the above would be a welded attachment where the tapered tube would be directly welded to the anchor plate and square tube.

Several tubes with different thicknesses were tested. Figure 3.5 and Table 3.1 give the geometric description of each of them. All the specimens were cut out from 15.2 cm x 15.2 cm (6 in x 6 in) hot rolled square tubes. In all the cases, the central portion of the beams was cut straight to avoid any geometric discontinuity. The material was ASTM A500 grade B steel with a yield stress $\sigma_y = 31.7$ kN/cm^2 (46 ksi) in all cases.

Three parameters, α, β, γ, determine the geometry of a tapered connection. They are defined in Figure 3.5. The variable α represents the portion of the length of the support face of the tube which is straight and not fixed. It is dependent on the type of fixation, and the closer to a situation of total fixity at the flexure ends, the smaller is α. The variables ß represents the portion of the length of the beam with full height b (the length itself is computed from center to

center of opposite faces). The variables γ is the ratio between the maximum height of the tube and the height of the taper. Both ß and γ are dependent on the geometric dimensions and vary with each connector.

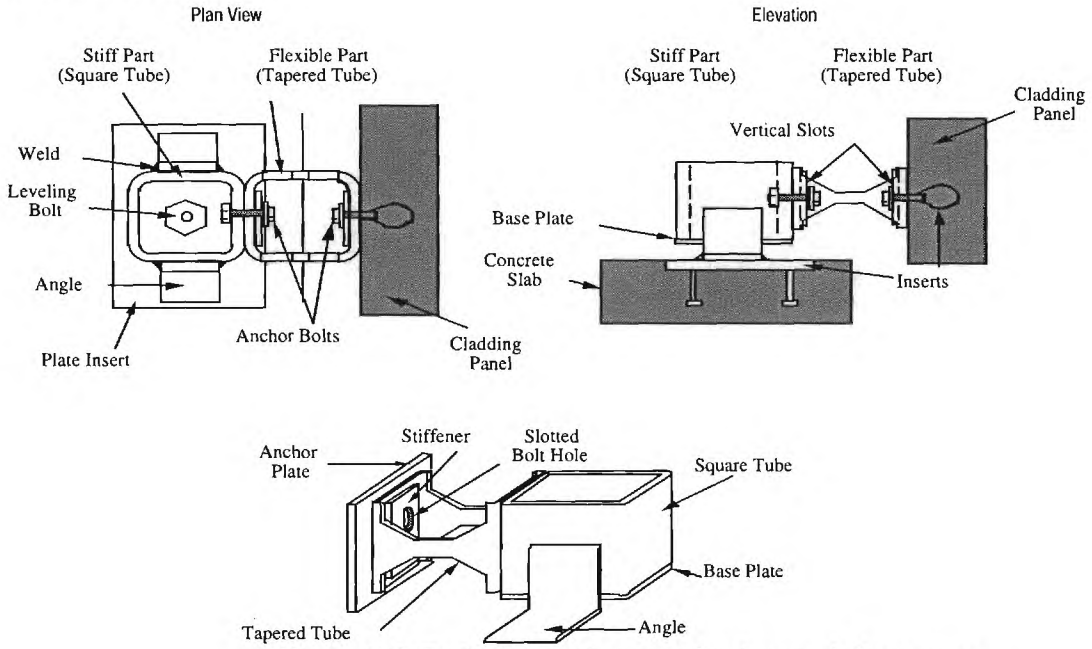

Figure 3.6 Bolted Attachment of Advanced Connector

Table 3.1 Dimensions of Connector Specimens (1 in = 25.4mm)

Specimen Name	TT375	TB375, TF375 TW375	TT500	TB250
Tube Dimension	15.2x15.2x9.5 6x6x0.375	15.2x15.2x9.5 6x6x0.375	15.2x15.2x12.7 6x6x0.500	15.2x15.2x6.4 6x6x0.250
Attachment	welded	bolted	welded	bolted
l (in l mm)	5.625 l 142.9	5.625 l 142.9	5.500 l 139.7	5.750 l 146.
R (in l mm)	0.75 l 19.1	0.75 l 19.1	1.00 l 25.4	0.50 l 12.7
b (in l mm)	4.50 l 114.3	4.50 l 114.3	4.00 l 101.6	4.50 l 114.3
a	0.044	0.067	0.000	0.109
b	0.100	0.100	0.136	0.065
g	0.533	0.533	0.525	0.533

3.3.2 Test Results

From the force-displacement relationships measured in the tests, several properties regarding forces, stiffnesses, displacement and ductility were evaluated. These are summarized in Figure 3.7 and Table 3.2.

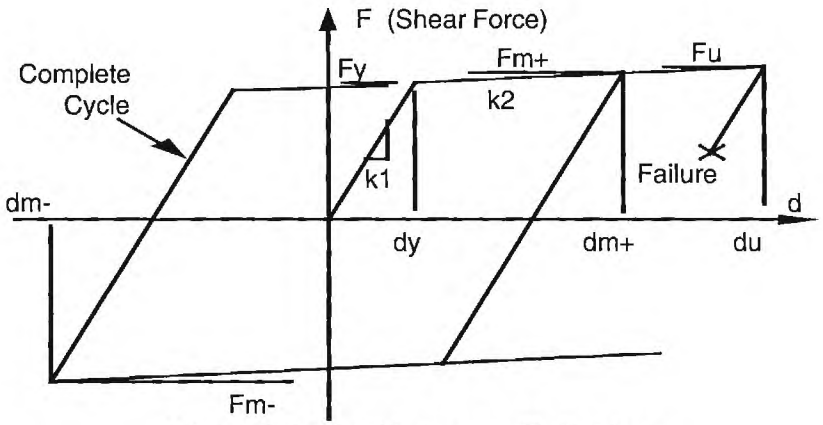

Figure 3.7 Test Parameter Definitions

Both conventional and plastic ductilities were quantified. The conventional ductility, μ, is defined as the ratio of the actual displacement to the yield displacement of the first cycle. The equivalent plastic monotonic ductility is the maximum plastic ductility that the system should exhibit in a monotonic loading test in order to dissipate the same amount of energy than during the cyclic loading. The equivalent monotonic plastic ductility demand on the system can be evaluated in terms of energy, and load reversals, as:

$$\mu_p = \frac{H_t}{F_y d_y (2N_f)^{0.4}} \tag{3}$$

where H_t is the total hysteretic energy dissipated in the system during N_f load reversals. This definition of ductility, derived from McCabe and Hall [1989], has the advantage of taking into account the characteristics of the cyclic loading. The corresponding values of μ_p are much higher than those of μ.

Table 3.2 Test Results for the Tapered Flexure Specimens

Specimen	TT375	TT500	TB375	TB250	Comments (see Figure 3.7)
k_1 (kN/cm)	36.8	82.3	33.3	8.9	elastic stiffness
k_2 (kN/cm)	1.4	2.6	1.3	0.5	Post-yield stiffness
k_1 / k_2	26	31	25	20	
F_y (kN)	17.8	33.8	16.5	6.2	yield force
F_u (kN)	29.4	43.2	27.6	11.6	ultimate force
F_u / F_y	1.65	1.28	1.68	1.86	
F_{m+} (kN)	27.1	42.3	27.6	10.7	maximum positive force in a cycle
F_{m-} (kN)	29.4	43.2	27.1	11.6	maximum negative force in a cycle
d_y (cm)	0.5	0.4	0.5	0.7	yield displacement
d_u (cm)	7.0	4.0	7.1	7.4	ultimate displacement
$\mu = d_u/d_y$	14.4	9.8	14.3	10.6	conventional ductility
d_{m+} (cm)	7.0	3.7	7.1	7.4	max. positive displacement in a cycle
d_{m-} (cm)	6.8	4.0	6.7	6.9	max. negative displacement in a cycle
H_t (kJ)	35.0	63.6	53.5 49.3*	23.1	maximum energy dissipated in test
μ_p	67	72	84 80*	80	equivalent plastic monotonic ductility

* values for TF375

TT375 Test.

The specimen was tested with cycles of increasing displacement amplitude. At the 21st cycle, the test machine maximum permissible displacement was applied, deforming the specimen 70 mm After three more cycles at the same amplitude, it broke in the middle of the tapered part of one web. The test was continued with one web only and the specimen completely failed shortly thereafter due to the combination of torsion and flexure on the remaining web. The hysteresis loop from the experiment is shown in Figure 3.8, and the results are presented in Table 3.2.

The hysteresis loop showed an increasing stiffness for displacements above 5.7 cm, which was a consequence of the large deformation. At this level of displacement, the shear force was no longer transmitted by pure bending but by bending and membrane action, which stiffened the device. Because of the increase in stiffness, the ultimate force exceeded the yield force by 65 %, but the round corners at the supports still remained elastic and the weld intact. At the extreme displacement of 7.0 cm, the two end plates moved about 2.5 cm closer to each other.

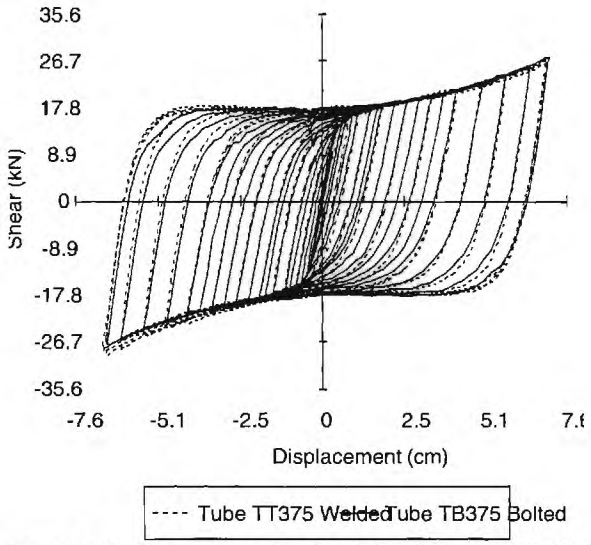

Figure 3.8 Test Results for TB375a and TT375

TB375a Test

TB375 was attached to the end plates with a single 15.9 mm diameter bolt on each side which replaced the weld of the previous specimen. A 95x76x9.5 mm washer stiffened the straight faces of the tube (see Figure 3.5), to insure the end fixity of the tapered beams.

Three identical specimens were produced and tested in different ways. The first specimen, TB375a, was subjected to 21 cycles with increasing amplitude up to 7.1 cm, in a way similar to TT375. No damage was observed during the test. Then the maximum displacement was held constant at 2.5 cm for each cycle which corresponded to a strain of 3.5 %. The specimen failed

after an additional 24 cycles due to fatigue. There was no significant difference between TB375a and TT375 (see Figure 3.8 and Table 3.2).

TF375b Test

The second bolted specimen, TF375b, was tested for fatigue only. The hysteresis loops were stable (Figure 3.9), showing no stiffness degradation until the first web broke. It is notable that with only one web, the tube could still provide stiffness and energy dissipation for 9 more cycles, in a very ductile manner.

TW375 Test

The third specimen , TW375, was tested as a bearing connection carrying gravity (vertical) load in addition to being subjected to the horizontal displacement. The maximum displacement was kept constant at 2.5 cm, and the gravity load was increased with each cycle. After 11 cycles of progressively increasing gravity load, the maximum gravity load of 10.1 kN was added and no cracks were visible. Neither stiffness nor ultimate force were affected by the vertical load and the hysteresis loop was almost the same as that from the test without gravity load (Figure 3.10), although the total vertical displacement between end plates increased to 3.0 cm . At this point, the specimen was tested further for fatigue with the gravity load maintained at 10.1 kN and with a cycle amplitude of 2.5cm displacement. After 19 additional cycles a crack appeared and the specimen failed after a total of 37 cycles. The hysteresis loops were stable with no stiffness degradation. The gravity load did not affect the lateral behavior.

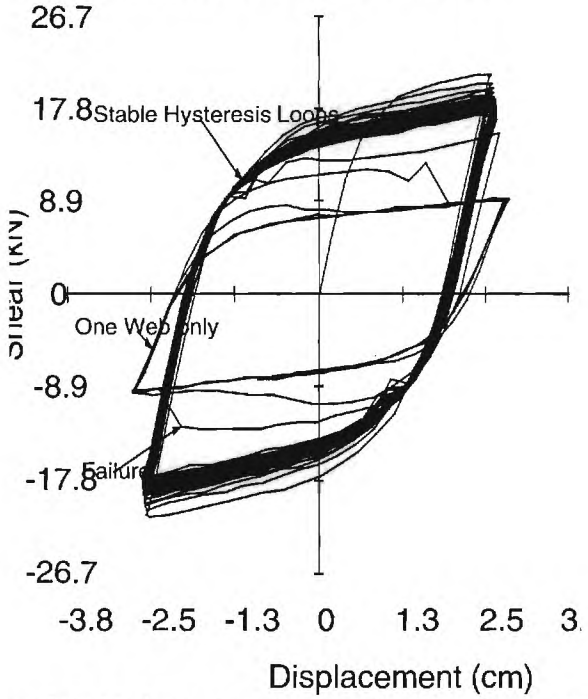

Figure 3.9 Fatigue Test Results for Specimen TF375

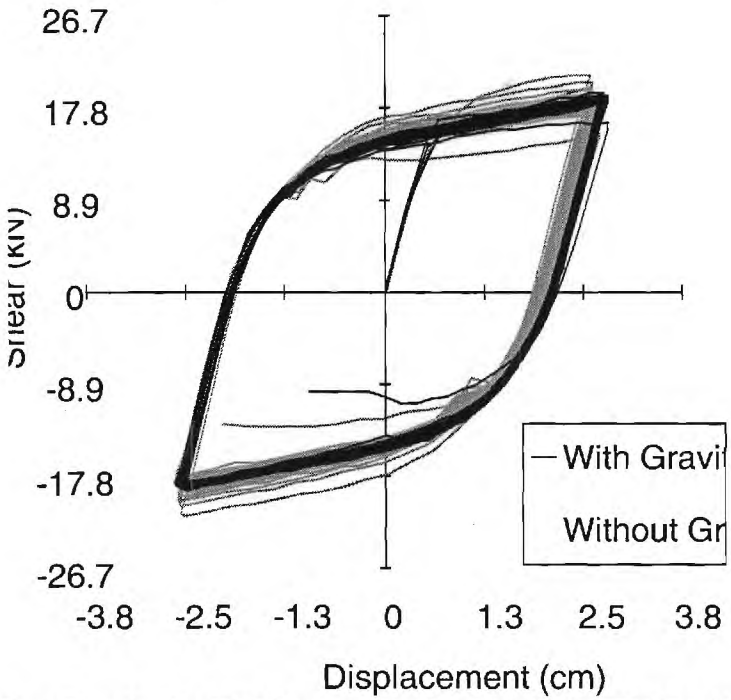

Figure 3.10 Test Results for TF375 (No Gravity Load) vs. TW375 (Gravity Load)

TT500 Test

A 1.3 cm (0.5 in) thick tube was tested to examine the influence of the wall thickness. The specimen was first tested for 10 cycles with increasing amplitude and showed a behavior similar to the TT375. The results are shown in Figure 3.11 and in Table 3.2. The maximum displacement was limited to 3.8 cm in order to get a maximum strain similar to the TT375 case (9.4 % strain). A fatigue test was then performed with a displacement of 3.0 cm (7.5 % strain). The specimen broke after 16 cycles at the transition between the taper and the center part. The hysteresis loops were stable (Figure 3.12) with almost no stiffness degradation or strength deterioration.

TT500 showed the same positive characteristics as TT375. The specimen was deformed in double curvature and the attachment zone remained elastic. The weld was also sufficient for the thicker specimen and showed no weakness during the test. The lifetime was low with only 26 cycles, because of the high strain (7.5 % vs. 3.5% for TF375) during the fatigue test.

TB250 Test

Specimen TB250 with a flexure thickness of 0.63mm (0.25 in) was first tested for 20 cycles of increasing amplitude up to a maximum displacement of 7.4 cm (4.4 % strain), as shown in Figure 3.13. A fatigue test was then performed at 3.5 % strain (5.8 cm displacement), which lasted 9 cycles until failure (Figure 3.14). The total lifetime of the specimen was then 29 cycles. This is considerably less than the lifetime of TB375 (45 cycles), which was tested in an identically manner. Apparently the cracks that occurred in the tapered beams had a shorter way to grow from the surface to the center, reducing the lifetime. The elastic stiffness and the ultimate force may be too low for a practical cladding connection.

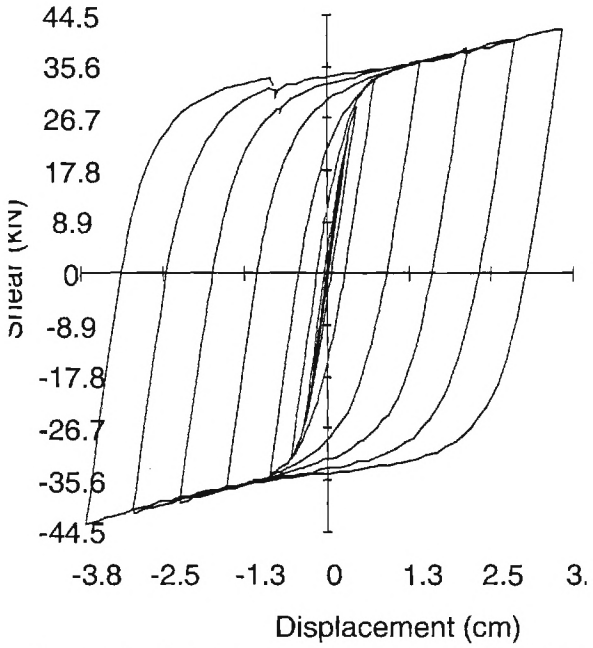

Figure 3.10 Initial Test Results for TT500

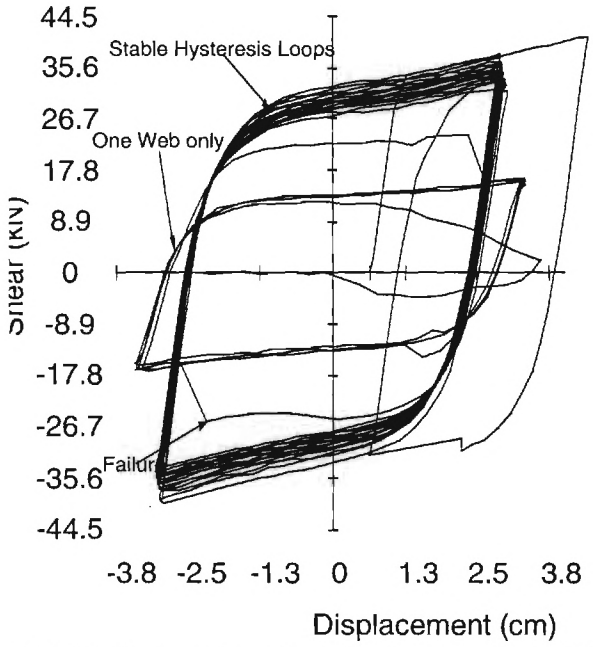

Figure 3.12 Fatigue Test Results for Specimen TT500

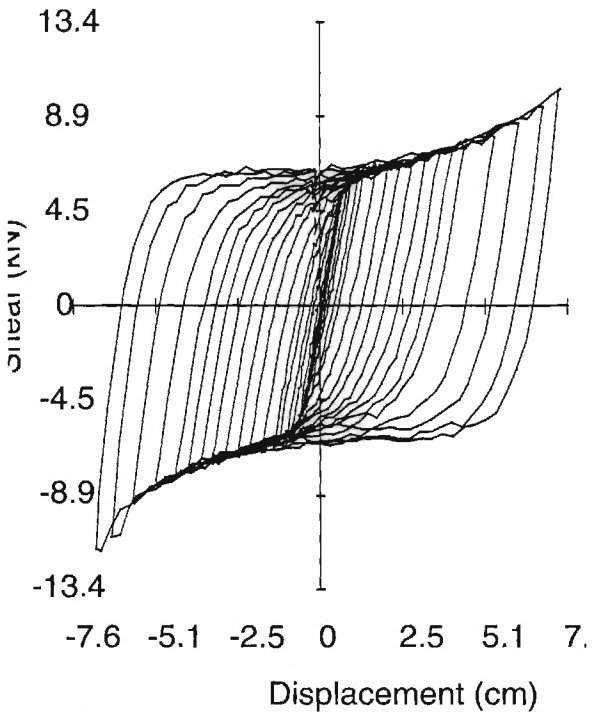

Figure 3.13 Initial Test Results for Specimen TB250

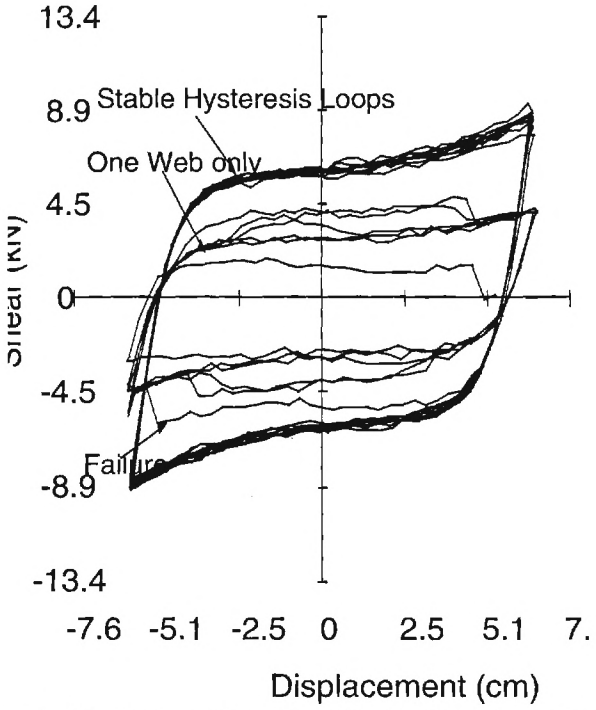

Figure 3.14 Fatigue Test Results for Specimen TB250

Test Conclusions

The tapered flexure advanced connections performed very well in the tests, and the following notes summarize the observations.

1. In all the cases, the connectors exhibited an advantageous hysteretic behavior, with fat, stable loops, with no apparent stiffness degradation or strength deterioration. The plastic deformation was distributed uniformly over the beams thanks to the taper, resulting in large admissible displacements and a maximum ductility of 14 (see Figures 3.8 and 3.13). Higher ductility values could have been obtained since the maximum displacement of the specimens for monotonic failure was beyond the range of the test machine (±7.6cm). The ductility in this case is defined as the maximum displacement divided by the yield displacement.
2. The specimens had good low cycle fatigue behavior, and sustained a large number of cyclic reversals without failure (see Figures 3.9, 3.10, 3.12). This is in accordance with similar results obtained by Tyler [1978], Bergman and Goel [1987], and Whittaker et al [1991] in fatigue tests of tapered steel specimens. For maximum strain not exceeding 3.5% the maximum number of cycles was close to 40. In an actual building, the allowable story drift should result in even lower strains, and hence longer lifetime. In almost all cases, the fracture occurred at the transition between the taper and the center straight part, probably due to stress concentrations at the kick in the steel shape. This suggests that a more elaborate manufacturing with round corners at the transition zones will translate in a higher number of cycles before failure.
3. Whether the specimen is bolted or welded has no influence on its behavior (see Figure 3.8). The fact that the connector can be bolted to the insert with a single bolt (like many conventional connectors), without any drawback in performance, makes it very attractive from an installation and maintenance point of view.
4. In previous test reports on tapered specimens [Tyler 1978, Whittaker, et al 1991], the key issue has always been the provision of a sufficiently fixed condition for the ends of the tapered beams. The design presented here provides a simple and effective solution through the use of a reduced width of the flexural elements.
5. The failure of each tapered specimen was shown to be very ductile. The failure always initiated in one of the two tapered beams through some progressive cracking. After failure of one beam, the remaining beam provided an additional reserve of strength and ductility for a few extra cycles (see Figures 3.9, 3.10, 3.12 and 3.14).
6. The specimen can sustain vertical loads without losing its energy dissipation capabilities (see Figure 3.10). This result indicates that the specimen should be able to perform adequately in the presence of combined high vertical and horizontal accelerations like the ones observed in the 1994 Northridge earthquake, although the presence of a vertical slot in the bolted connection (see Figure 3.5) should minimize the influence of the vertical loading. More testing involving cyclic loading in both directions should be done to verify this point. The result also shows that some of these tapered designs could be used for combined bearing and energy dissipating connections.

This last point requires some additional comments. On the basis of safety concerns, one could question the merit of combining gravity load support with energy dissipation. However, the key point is the fact that vertical loads do not necessarily adversely affect the lateral behavior and energy dissipation of the tapered connector. The behavior of advanced bearing connectors will be discussed in the next section.

3.4 Composite Bearing Connector

3.4.1 Concept

The objective of this design is to develop a load-bearing connector that provides panel alignment and maintains high levels of ductility in the lateral direction while supporting the panel weight. This is a complex issue because it requires high levels of stiffness in two directions and lower levels of hysteretic stiffness in an orthogonal direction. In order to achieve this result while preserving the relative simplicity required to qualify as a good cladding connection, it was decided to combine two simple concepts into a single unit.

The first task is to provide sufficient load-bearing capacity. Elastomeric neoprene bearing pads laminated with steel plates, which are typically used in bridge applications, serve this purpose very well. They are very rigid in the direction of bearing, but they are capable of sustaining large displacements perpendicular to the bearing load. The steel laminates prevent the elastomeric material from bulging under large compressive forces.). The shear stiffness is not a function of these steel plates and depends only on the elastomeric material and the pad dimensions. The size and spacing of these laminates can be specified using established design methods [Lee 1971].

The next requirement is to provide ductile behavior in the horizontal direction. It is difficult to provide this ductile behavior while maintaining the simplicity of the connector. The added element(s) must act in parallel with the elastomer but remain isolated so that the two parts do not interfere with each other. The next section describes four of the options considered.

3.4.2 Bearing Connection Candidates

Ductile Inserts

Rods of lead or another ductile material could be inserted into cylindrical voids in the elastomeric pad. While the pad deformed elastically, the rods would reach their yield point and decrease the overall stiffness of the unit, providing ductility, energy dissipation, and favorable hysteretic behavior. Figure 5 is a schematic of this concept.

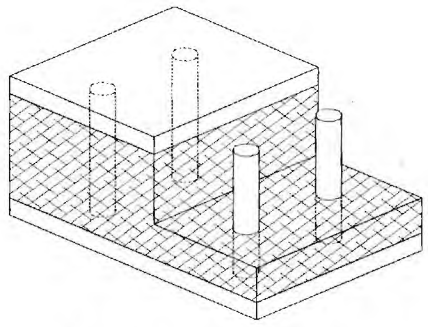

Figure 3.15 Elastomer with Ductile Inserts.

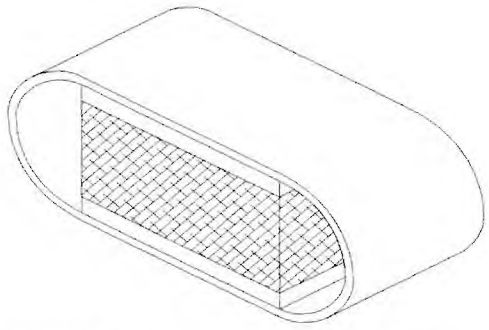

Figure 3.16 Elastomer with Ductile Loop.

Ductile Loop

Similar to a concept studied in New Zealand [Kelly et al 1972], a loop made of ductile steel with flat sides and semicircular ends could be wrapped around the outside of the bearing pad. The rolling action of the curved ends of the loop as it is deformed would provide the required ductility due to flexure in the steel. The symmetry of this section makes it suitable for cyclic loading. The geometry of the loop also provides that the strain in the material depends on the ratio of plate thickness to radius and not the displacement. Figure 3.16 illustrates this concept.

Double Taper Flexure

The mild steel double tapered flexure concept used in the previous tests could be extended to work in the current application. As shown in Figure 3.17, a mechanism could be fabricated to fit around the perimeter of the bearing pad such that the imposed deformations would force the taper into double curvature. The effectiveness of this geometry was proven in the previous study, but there is a slight difference in this case that makes it more complex. The presence of the elastomeric material introduces a displacement constraint axial to the flexures and this can lead to higher than expected axial forces in the flexures (causing premature failure). In the flexure test studies, there was no such constraint, and in fact, there was significant axial deformation along the axis of the flexures. The single tapered flexure below overcomes these problems.

Single Taper Flexure

A singly tapered flexural section of mild steel could be configured as shown in Figure 3.18. The concept is the same as the double taper, but releasing the axial restraint would alleviate the problem of tension in the steel. Releasing the rotation at the thin end of the taper would allow the section to act as a simple cantilever. This would force the tapered section into single curvature; hence, the single taper geometry would maximize the amount of steel that would yield.

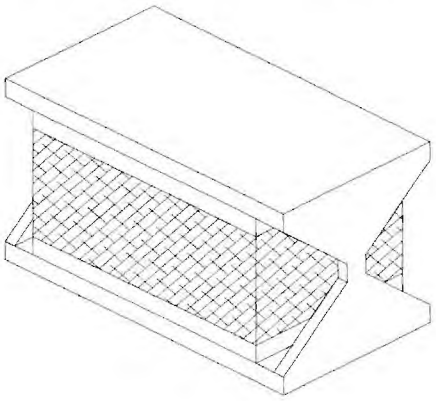

Figure 3.17. Elastomer with Double Taper.

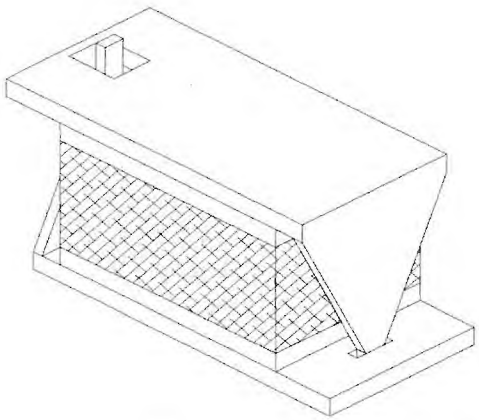

Figure 3.18. Elastomer with Single Taper.

3.4.3 Test Specimen Design

The single taper option was chosen for the current investigation. The design of the test connector was broken into two parts. First, the elastomeric pad was designed using standard procedures for the design of bridge bearing pads [Lee 1971]. Figure 3.19 shows the final elastomeric pad dimensions and specifications. The steel plates bonded to the top and bottom of the pad provide a means of positive connection between the panel and the structure.

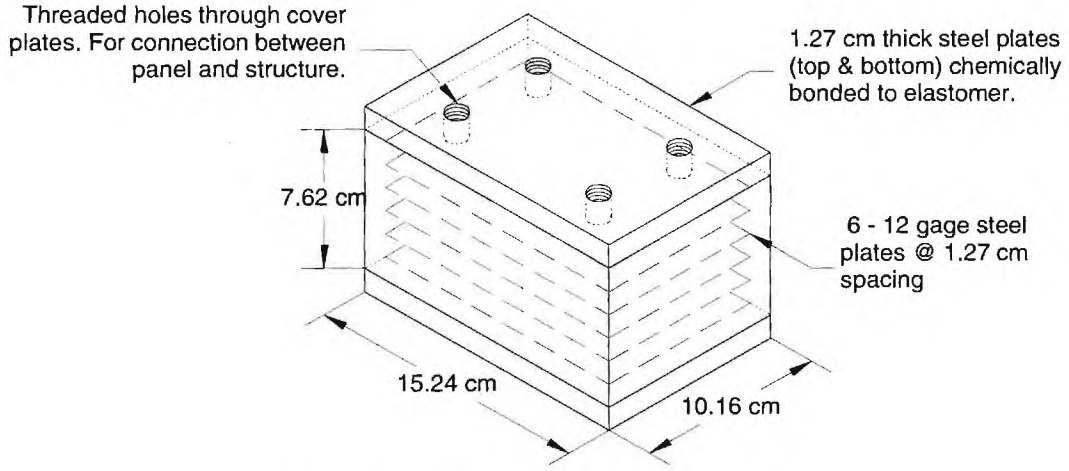

Figure 3.19 Elastomeric Pad, Final Design.

Next, the steel taper was designed. The design was based on an elastic, mechanics of materials model utilizing the parameters shown in Figure 3.20. (A simplified version of this model, intended for practical design purposes, is presented in the Design Considerations section below.) The objective was to achieve uniform stress along the length of the taper for any given elastic displacement. This would maximize the amount of material that would yield, and therefore maximize the energy dissipated by the connector. Final dimensions for the taper are given in Table 3.3. Note that symmetry permits the use of two tapered plates, one on each side of the pad, which allows for a greater amount of material yielding.

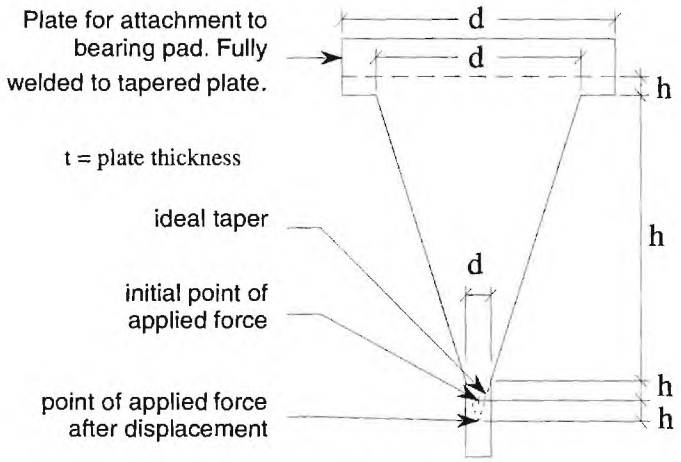

Figure 3.20. Tapered Flexure Parameters.

Table 3.3 Test Specimen Parameters

Dimension	Test Specimen
t	0.635 cm
d_0	10.16 cm
d_1	7.62 cm
d_2	0.9525 cm
h_0	0.635 cm
h_1	8.5725 cm
h_2	0.9525 cm
h_3	Varies with displacement

3.4.4 Test Objectives and Description

The test objective was to acquire data for the individual parts of the connector and so the tests were conducted in two steps. The first step was to test the bearing pad alone and the second step involved testing the composite pad and tapered flexure assembly. Finally, by a comparison of the results, the behavior of the tapered flexures could be inferred and compared to analytical beam models, which could then be transformed into design models.

The bearing pad was tested first. Tests were conducted both with and without constant applied vertical loads to simulate bearing loads. Direct shear was applied across the elastomer at different loading rates, and the amplitude and numbers of cycles were varied for each test. This provided data on the effect of gravity (bearing) loads, different loading rates and amplitudes, and numbers of cycles on the shear stiffness of the elastomer.

The composite connector (Figure 3.18; Table 3.3) was then tested. The initial tests were conducted with increasing displacement amplitudes for each cycle. This was done to determine the elastic limit of the connector along with its inelastic behavioral characteristics. Subsequent tests were conducted over repeated cycles of fixed amplitude to determine the low cycle fatigue behavior of the connector.

Figure 3.21 below shows a photo of a composite connector located in the test fixture and ready for cyclic loading either with our without applied bearing loads. The photo was taken looking between the building surface on the right and the cladding panel surface on the left, and it shows the composite connector viewed from its end with the tapered flexure visible in the center.

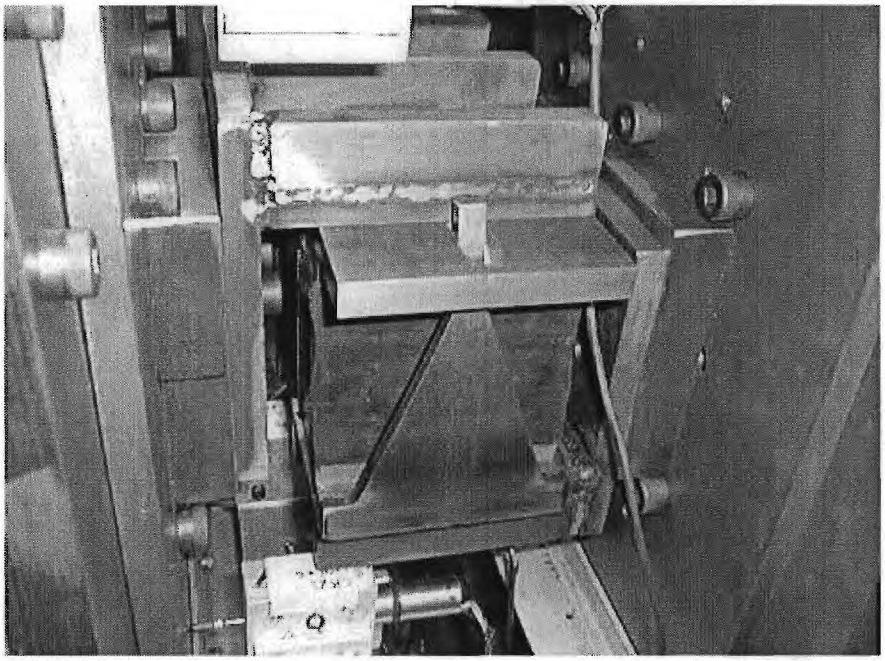

Figure 3.21 Photo of Composite Bearing Connector in Test Fixture

3.4.5 Test Results

Bearing Pad

The bearing pad alone was tested several times as described above. Data acquired from these tests revealed that the shear stiffness of the elastomer is independent of the gravity (bearing) load, loading rate, and amplitude and number of cycles. All of the tests showed that the bearing pad remains elastic and has a shear stiffness of approximately 1.5 kN/cm, or roughly 0.2 kN/cm per centimeter of elastomer thickness. Figure 3.21 shows the force-displacement plots generated from two of the tests with different bearing loads.

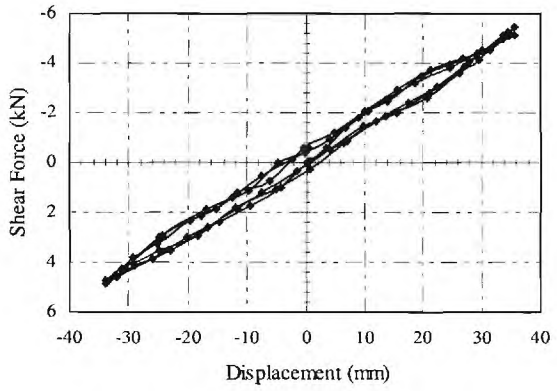

(a) with 5.5 kN bearing load.

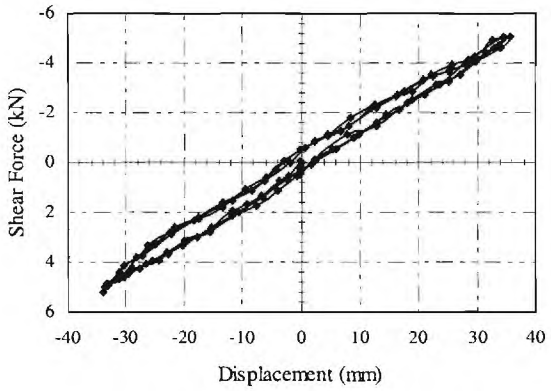

(b) with 1.1 kN bearing load.

Figure 3.21 Elastomeric Bearing Pad Results

Composite Specimen

Testing of the composite connector under a 5.5 kN bearing load produced the force-displacement plots presented in Figure 3.22. Note that hysteresis is now prevalent due to the addition of the tapered flexures and that the low cycle fatigue behavior of this specimen is excellent. Over 40 cycles were applied to the connector, and no sign of cracking or imminent failure was visible.

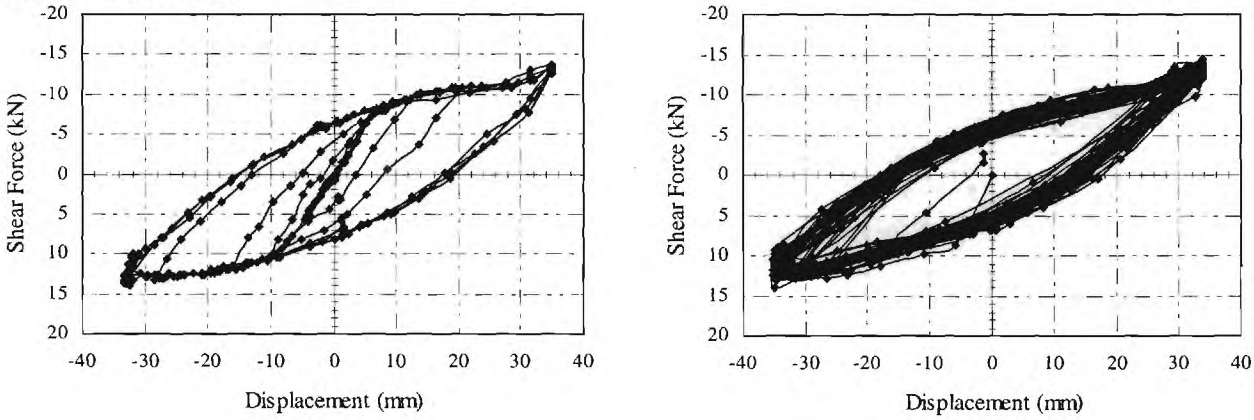

(a) Initial testing

(b) Low-cycle fatigue tests

Figure 3.22 Composite Specimen Test Results

Taper Properties

Subtracting the elastic stiffness of the bearing pad from the hysteresis loops generated by the composite connector produced the force-displacement plots in Figure 3.23. These plots are useful for determining the energy dissipation characteristics of the tapered flexures. They can be compared to analytical models of the flexures to validate potential design models for the advanced connectors.

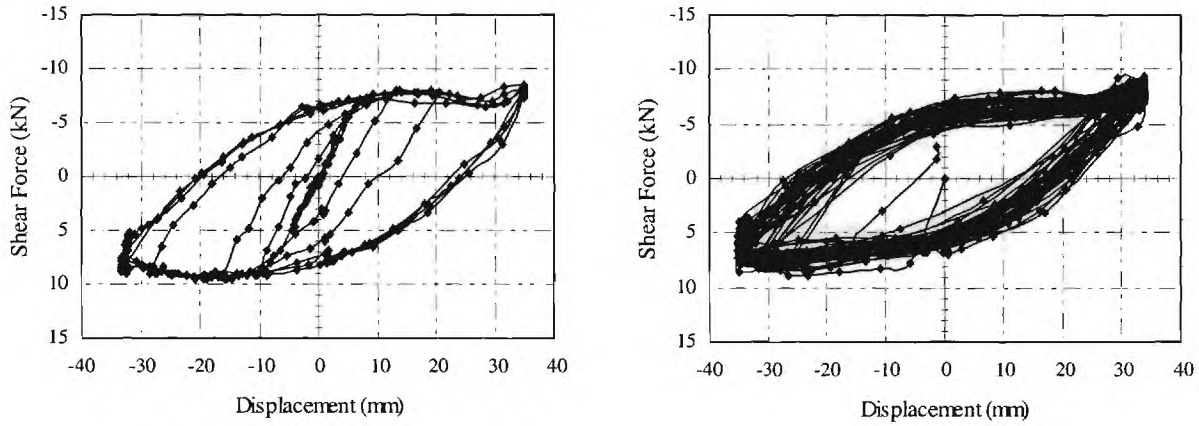

(a) Tapered flexure alone – initial tests

(b) Tapered Flexure – low cycle fatigue properties.

Figure 3.23 Test Results for Tapered Flexure Alone

3.4.6 Design Considerations

Figure 3.24 illustrates a simplified model of an ideal tapered flexure. Since the both the bending moment and the bending rigidity increase linearly along the beam from its tip, it follows that constant bending stress is achieved along the length of the flexure for a any tip load, P, in the elastic range of the material. This value of constant stress can be determined from simple beam theory as shown in Equation 2 where S_b is the bending stress, and the dimensions are shown in Figure 3.24.

$$S_b = 6PL/bt^2 \quad (4)$$

It can also be shown that the tip displacement for the tapered flexure depends only on the applied load, P, and the overall dimensions of the taper. This relationship is given in Equation 3 where d is the tip displacement, E is Young's Modulus of the material, and the geometric dimensions are shown in Figure 3.24.

$$d = 6PL^3/Ebt^3 \quad (5)$$

Based on this formulation, the initial elastic stiffness of the tapered flexure (k_e) can be written using Equation 5 as:

$$k_e = P/d = Ebt^3/6L^3 \quad (6)$$

If the material is assumed to be elastic-perfectly plastic (no strain hardening), then the uniaxial yield stress can be defined as, s_y, and the maximum tip load at which this occurs is given from Equation 4 as:

$$P_y = s_y\, bt^2/6L \quad (7)$$

and the tip displacement at which this occurs, d_y, is given from Equation 5 as:

$$d_y = s_y\, t^2/EL \quad (8)$$

Finally, after substituting the appropriate material and geometric values into the equations above, a theoretical force-displacement plot can be derived. For the specimen used in the study, the appropriate values are: b= 7.62cm (3 in.), L= 10.16cm (4 in.), t= 0.635cm (0.25 in.), E= 20,000 kN/cm^2 (29,000,000 lb./in.^{2}). Cold-rolled, high strength steel was used in these tests, so an elastic limit of 45 kN/cm^2 (65,000 lb./in.^{2}) was assumed. Figure 3.25 shows the theoretical force-displacement plot derived from this simplified model. Note that the force, P, in this plot is doubled to account for the presence of two tapered flexures in the composite connector.

By comparing the ideal force-displacement plot in Figure 3.25 to the hysteresis loops in Figure 3.23, it can be seen that the computed behavior is a good approximation to the behavior of the actual test specimen. The elastic stiffness is nearly identical in both cases, and the assumption of elastic-perfectly-plastic behavior appears to be reasonable. The yield point on the ideal curve is somewhat lower than the yield point on the test curve, but this is likely due to an error in the estimation of the yield stress of 45 kN/cm^2 (65,000 lb./in.^{2}) assumed for in the material. The reasonable correlation between this simple beam model and the actual behavior suggests that it should be straightforward to development design charts and equations based on simplified analytical models of these advanced load-bearing connectors.

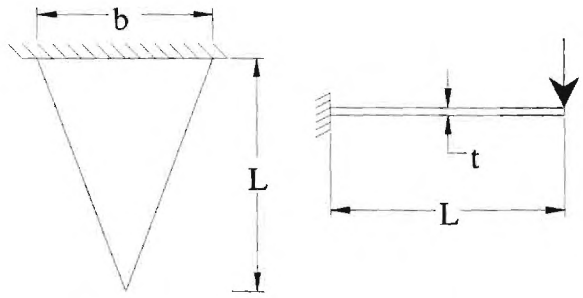

Figure 3.24 Geometry for Tapered Flexure.

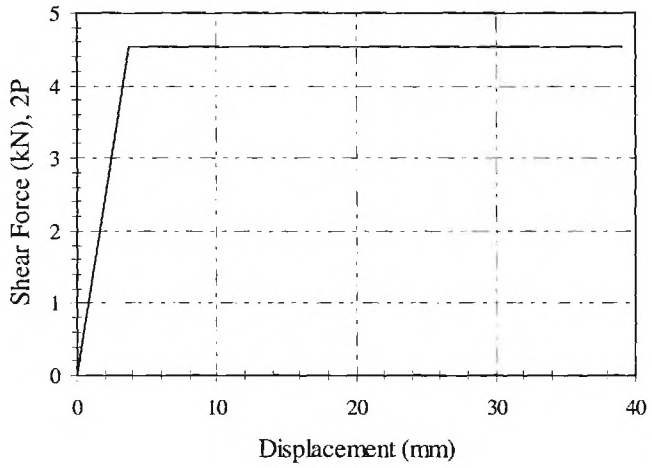

Figure 3.25. Theoretical Force-Displacement Curve for Tapered Flexure.

3.5 Torsion Connection

As noted in Section 2, torsion of a prismatic bar presents a number of desirable characteristics for an advanced cladding connector, but it is also plagued by difficult problems involved with the conversion of the rectilinear interstory drift into proportional rotation to activate a torsion device. The desirable characteristics include:

- development of plastic deformation throughout all the material in a hollow prismatic member (e.g., effective use of material),
- relative simplicity of boundary conditions for the torsion member to minimize premature failure at these critical locations, and
- generally stable behavior for ductile materials.

On the other hand, the need to create rotational deformation from rectilinear displacement requires:

- a mechanism to handle the kinematic conversion,

- bearings to support the rotational motion of the device, and
- structure to support the torsion reaction at the fixed end of the connector element.

Nonetheless, the present effort focused on development of an advanced connector capable of developing good energy dissipation qualities through torsional deformation in such a way as to achieve good ductile properties and promote plastification of the largest possible fraction of material in order to develop large, stable hysteresis loops. Such a connector should also be capable of sustaining at least 30-50 full-load cycles without any failure.

3.5.1 Design Configuration

After consideration of the fundamental torsion problem, it was determined that a hollow circular shaft under torsion could provide a reasonable solution of this design problem. The shaft twist rate is constant and the plastification begins at the outer radius and moves smoothly to the inner radius as the torque is increased, at which point the entire member is in plastic deformation. Noncircular shafts result in uneven distributions of shear stresses and solid shafts make poor use of material at the axis of revolution.

The geometric configuration presents more of a challenge in order to address the points made previously. The conceptual design shown in Figure 3.26 forms the basis for the work reported here. The torsion device consists of a circular torsion element mounted inside concentric tube and attached to a vertical surface of the building structure. The outer tube supports the torsion element and fixes it at the lower end and provides rotational bearing support at the upper end in this figure. An arm connected to the torsion element is used to convert the interstory drift (left-right in the illustration) into rotation. The arm is attached to the cladding panel (shown in wireframe mode) with a pin and clevis. In this concept, the connection is a nonbearing or tie-back design, and vertical movement can be accommodated by axial movement along the clevis pin. Figure 3.27 shows a variation of this concept with the torsion device oriented horizontally so that it might be attached to the top or underside of a floor slab. In this case the moment arm rotates in the vertical façade plane.

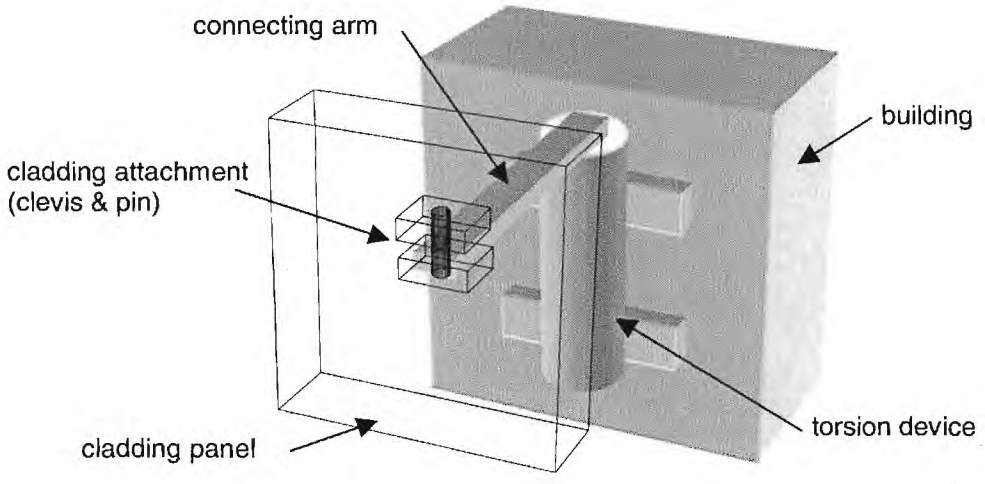

Figure 3.26 Conceptual Mode for Torsion Connector - Vertical

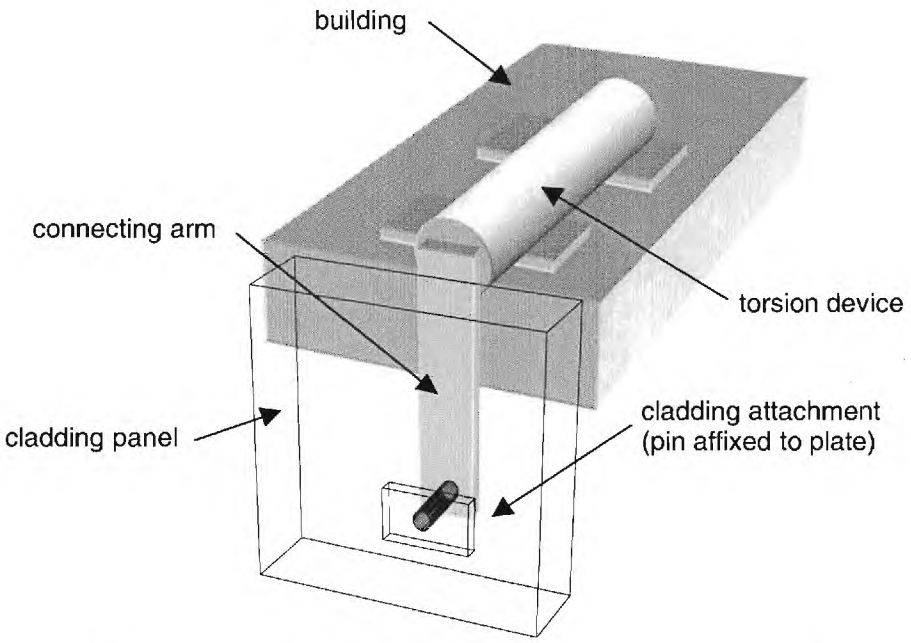

Figure 3.27 Conceptual Mode for Torsion Connector - Horizontal

3.5.2 Design Analysis

Torsion of circular shafts is almost as well understood by structural engineers as beam bending, but it is much less commonly utilized in structural applications. The following basic treatment of the torsion problem is used to identify the basic design parameters for the proposed torsion device. When a circular shaft is subjected to a torque, the shaft will twist and the twist rate, ϕ, is defined as the amount of twisting per unit length of the shaft. The total twist for a given length of shaft is θ, and it follows that the twist rate can be defined as: $\phi = d\theta/dx$ where x is the axial position. Conversely, the total twist can be calculated by direct integration of the above definition of the twist rate. From basic strength of materials it can be shown that the torque in a circular shaft produces a shear stress, τ_{xs}, given by:

$$\tau_{xs} = G\theta r \tag{9}$$

where G is the shear modulus of the material and r is the radial distance from the centerline of the shaft. For pure torsion, no other stresses are significant, and so the primary stress in the shaft is τ_{xs} which increases linearly with r and reaches a maximum at the outer radius of the shaft. It can also be shown from strength of materials that the torque, T, applied to the shaft can be related to the twist rate as:

$$T = GJ\theta \tag{10}$$

where J is the polar area moment of inertia of the circular cross section (GJ is called the torsional rigidity). From geometry, the polar area moment of inertia of a circular cross section of radius, R, is given by:

$$J = \int_A r^2 dA = \frac{\pi^2 R^4}{2}$$

and for a hollow circular cross section with outer and inner radii, R_o and R_i, it follows:

$$J = \frac{\pi^2 \left(R_o^{\ 4} - R_i^{\ 4} \right)}{2} \tag{11}$$

These simple equations provide all the information necessary for design purposes. By using Equations 9 and 10 and eliminating θ, an expression for the shear stress in terms of the applied torque, T, can be written as:

$$\tau_{xs} = \frac{rT}{J} = \frac{2rT}{\pi^2 \left(R_o^{\ 4} - R_i^{\ 4} \right)} \tag{12}$$

This result shows that the torsion stress is constant along the length of a shaft of constant cross section shape and increases linearly with radius. The shear stress acts in a circumferential direction (s direction) on surfaces perpendicular to the axis of the shaft (as well as on the complementary shear surface).

As the torque is increased from zero, the resulting shear stress increases at a proportional rate and reaches the yield value first at the outer surface of the shaft. With further increase in the torque, this point moves to smaller and smaller radii until reaching the inner radius, at which point the entire cross section is at or beyond the yield stress and the shaft is fully plastic. For intermediate conditions there are thus two distinct annular regions: (a) an outer region where stresses are above yielding, and (b) an inner region where stresses are still at elastic levels. The total torque carried by the shaft under this condition is the sum of the torque carried by each section:

$$T = T_{elastic} + T_{plastic}$$

and each contribution can be obtained by integration of the torsion shear stress over the appropriate annular cross section region. The result is an expression:

$$T = \int_{A_e} \tau_{rs} dA + \int_{A_p} \tau_{rs} dA \tag{13}$$

where each integrals are for the elastic (A_e) and plastic (A_p) regions.

In order to evaluate the integrals in Equation 13, it is necessary to be able to express the torsion shear stress in terms of the radius (e.g., the variable of integration). In the inner elastic region, A_e, this is simply Equation 9, but in the plastic region, it is necessary to specify a particular kind of inelastic behavior. The simplest inelastic behavior for a ductile material like mild steel is the elastic-perfectly plastic model assumed earlier for analysis of the flexures and characterized by an initial linearly elastic behavior followed by a constant yield stress for deformation beyond the yield point. For this case, the torsion shear stress, $\tau_{\xi\sigma}$ in the outer plastic region is simply the yield stress, τ_y. Equation 13 then becomes:

$$T = \int_0^{2\pi} \int_{Ri}^{Ry} \tau_y \frac{r}{R_y} r^2 dr d\theta + \int_0^{2\pi} \int_{Ry}^{Ro} \tau_y r^2 dr d\theta$$

where R_y is the radius which defines the boundary between the elastic inner and plastic outer regions of the shaft. The integrals can be readily evaluated to yield the final result:

$$T = \frac{\pi}{2} \tau_y \left(R_y^3 - \frac{R_i^4}{R_y} \right) + \frac{2\pi}{3} \tau_y \left(R_o^3 - R_y^3 \right) \tag{14}$$

which expresses the torque carried by the shaft in terms of the material yield shear stress, the geometry of the shaft, and the radius at which plastic stresses are first reached.

Elastic behavior

Until the yield stress is first reached, the shaft behaves elastically and Equation 12 defines the resulting torsion stress. The resulting total twist angle for the shaft is simply the integral of the twist rate from Equation 10 and for a constant cross section shaft:

Yielding is reached first at the outer radius of the shaft and so setting $R_y=R_o$ in Equation 14 yields:

$$T_y = \frac{\pi}{2}\tau_y\left(R_o^3 - \frac{R_i^4}{R_o}\right) \tag{15}$$

where T_y is the torque at which yielding is first reached.

Intermediate behavior

For the intermediate conditions where only an inner annular portion of the cross section is still elastic and the outer area is plastic, the behavior can best be described by the equation for the torque ratio, T/T_y, where T_y is the torque required to initiate yielding as defined above:

$$\frac{T}{T_y} = \frac{4}{3}\left[1 - \frac{1}{4}\left(\frac{R_y}{R_o}\right)^3 - \frac{3}{4}\left(\frac{R_i}{R_o}\right)^4 \Big/ \left(\frac{R_y}{R_o}\right)\right] \tag{16}$$

This expression is awkward to interpret because it depends on the value of R_y which defines the boundary between the elastic and plastic regions. It can be shown from a simple analysis of the shear deformation (which is unaffected by the inelastic behavior) that:

$$\frac{R_y}{R_o} = 1 \Big/ \left(\frac{\phi}{\phi_y}\right)$$

where ϕ is the twist angle of the shaft and ϕ_y is the twist at the initiation of yielding on the cross section. Using this in Equation 16 yields a more useful expression for the torque in terms of the twist:

$$\frac{T}{T_y} = \frac{4}{3}\left[1 - \frac{1}{4}\Big/\left(\frac{\phi}{\phi_y}\right)^3 - \frac{3}{4}\left(\frac{R_i}{R_o}\right)^4\left(\frac{\phi}{\phi_y}\right)\right] \tag{17}$$

Equation 17 is shown in Figure 3.28 below for several different values of the shaft thickness ratio, R_i/R_o, which defines the shape of the shaft cross section. As expected the progressive development of plastic deformation across the cross section as the torque is increased beyond the yield point rounds off the sharp elastoplastic yield point assumed for the material. Furthermore, as the thickness ratio is increased from 0 (solid shaft) towards the limit of 1 (thin wall tube), the curves will shrink towards a sharp yield at $T/T_y=1$ as expected (all the material in the thin wall yields at once and there is no progressive plastic development). Figure 3.28 shows, however, that a thick-walled shaft will develop upwards of 30% strength beyond the yield torque as the twist approaches 2x the yield value.

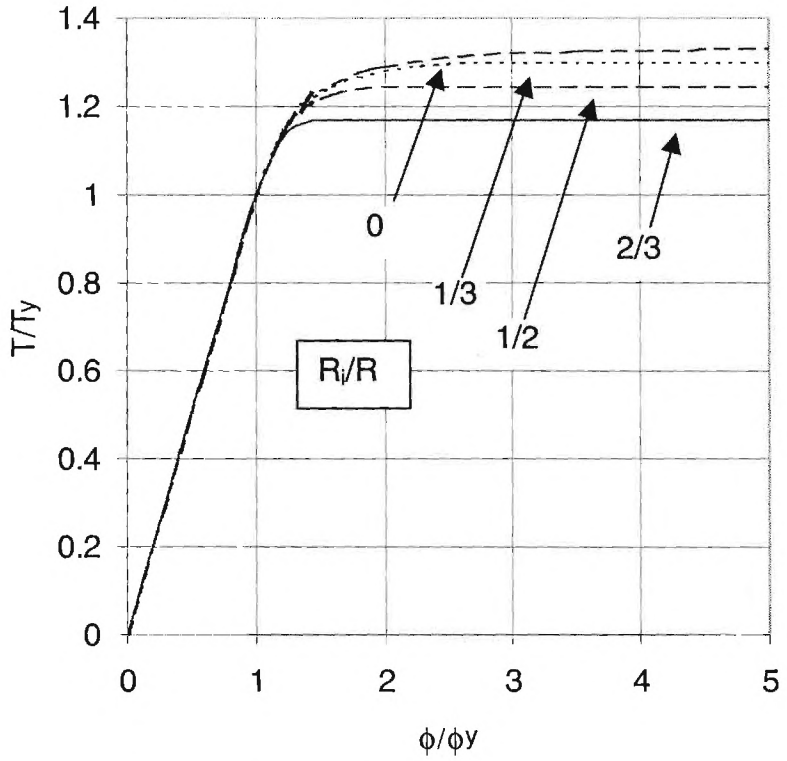

Figure 3.28 Torque versus Twist for Hollow Circular Shafts

Fully plastic behavior

The other extreme is the situation in which the cross section is fully plastic and there is no longer any elastic behavior present. This occurs when $R_y=R_i$ in Equation 14:

$$T_p = \frac{2\pi}{3}\tau_y (R_o^3 - R_i^3) \tag{18}$$

This defines the maximum torque that the shaft can carry. Attempting to apply greater torque will cause an arbitrarily large rotation with no further increase in the reaction torque provided by the shaft. The result is similar to a plastic hinge for a structural frame. The margin beyond the yield torque can be expressed from these results as:

$$\frac{T_p}{T_y} = \frac{4}{3}\frac{1-\left(\frac{R_i}{R_o}\right)^3}{1-\left(\frac{R_i}{R_o}\right)^4} \tag{19}$$

where the maximum value of 4/3 is developed for a solid shaft ($R_i/R_o=0$).

3.5.3 Connector Design

Using the above design equations, a conceptual design for an advanced torsion connector in the geometric configuration shown in Figure 3.26 was undertaken. As a baseline, the following connector properties were used:

- Material: A-36 steel (G=11,500 ksi, τ_y=20.5 ksi)
- Connector yield force = 1,000-2,000 lbs
- Yield Displacement = 0.5-1.0 inches
- Fully Plastic Displacement = 1.0-1.5 inches

On this basis, the baseline connector dimension were chosen to be :

- R_o = 0.625 inches
- R_i = 0.375 inches
- L = 5.25 inches
- H = 4.65 inches (connector moment arm length)

The value of torque required to initiate yielding is given by Equation 15 as:

$$T_y = 6{,}840 \text{ lb-in}$$

for the above design parameters, and this corresponds to a force at the end of the connector moment arm of length H of:

$$F_y = T_y/H = 1{,}471 \text{ lbs}$$

Similarly, the limiting force required to produce complete plasticity in the shaft can be computed from Equation18 as:

$$F_p = T_p/H = 1{,}767 \text{ lbs}$$

The corresponding shaft twist angles can also be calculated as:

$$\phi_y = 1.7 \text{ degrees}$$
$$\phi_p = 2.3 \text{ degrees}$$

and the equivalent lateral displacements at the tip of the connector moment arm will be:

$$d_y = 0.18 \text{ inches}$$
$$d_p = 0.24 \text{ inches}$$

Using these design parameters, the prototype torsion connector shown in Figure 3.29 was developed. The torsion element was turned from thick-walled tube stock, leaving enlarged ends for attachment to the connector housing. The connector housing is a steel tube inside which the torsion element is placed. The housing is fitted with mounting straps (welded to the exterior) for attachment of the connector to the building structure. A 4-tooth spline joint is used to securely fix the connector element one end of the housing tube but yet allow disassembly and/or replacement. The other end of the torsion element is left free to twist inside the housing (which also provides a bearing support for the element).

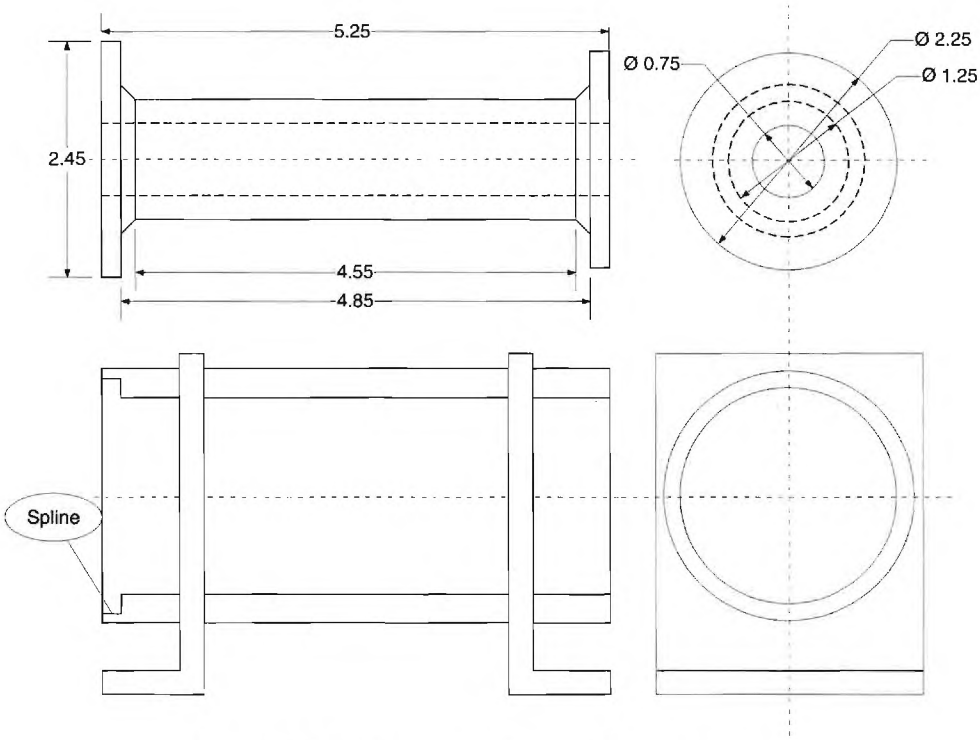

Figure 3.29 Prototype Torsion Connector

Attachment of a moment arm to the torsion element proved to be very difficult to accomplish and proved to be the weak point in this particular design. A number of concepts were considered:

- spline joint,
- pinned connection (using hardened steel shear pins),
- bolted connection.

but most were ruled out for cost or complexity reasons. Only the bolted connection was actually fabricated, but as will be seen later, hysteresis in the bolted joint overwhelmed the behavior of the torsion element.

All design parameter values were checked for appropriate safety factors to make sure that the only inelastic action that would develop would take place within the torsion element as planned.

3.5.4 Testing

The connection test fixture described in Section 3.2 was used to test the prototype torsion connector under the design conditions. The connector was mounted in the configuration shown in Figure 3.26. The connector housing was bolted to the building surface of the test fixture and the connector moment arm was connected to the cladding surface of the fixture using a small pin and clevis assembly. Figure 3.30 shows a photo of the connector in the test fixture.

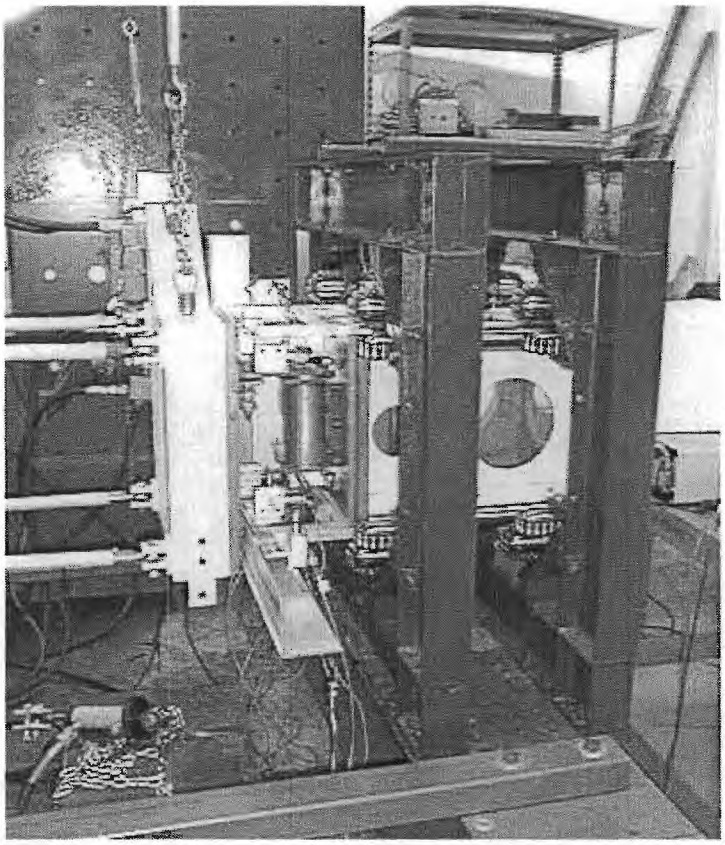

Figure 3.30 Photo of Prototype Torsion Connector in Test Fixture

The prototype connector was subjected to an initial test involving bi-directional loading cycles of increasing displacement amplitude beginning well within the expected linear range of behavior. In such tests, load-deflection plots for successive cycles are examined to determine if characteristic inelastic hysteretic action develops, and this is used to determine the measured yield loads. Testing is then carried out with increasing cyclic amplitude into the plastic range of behavior and the resulting load-deflection cycles are assessed. Finally, depending on the test objectives, other design parameters might be varied (e.g., bearing loads) or a low cycle fatigue test or a monotonic load-to-failure test might be conducted. In the present case, however, these options were not exercised because the initial elastic tests revealed that the connector moment arm was not firmly enough attached to the torsion element and significant slippage and hysteresis was occurring at the bolted joint. Figure 3.31 shows test results when the prototype connector was loaded into the inelastic range. As can be seen, the expected ductile behavior is masked by slippage in the moment connection between the torsion element and the connector moment arm. Unfortunately, due to time and resource limitations, this problem was not corrected and the test program was terminated.

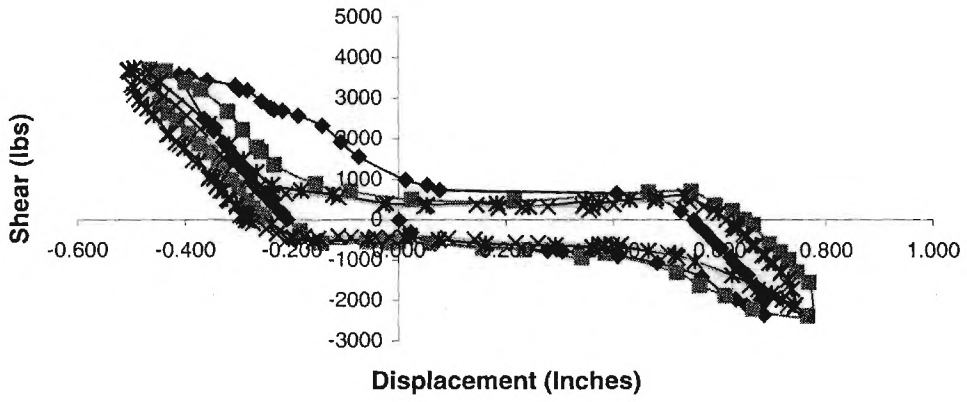

Figure 3.31 Preliminary Test Results for Prototype Torsion Connector

Nonetheless, in spite of problems with some of the prototype torsion connector construction details, it is still felt that this approach offers certain attractive advantages, especially for a prefabricated commercial advanced connector. Changes in the design parameters (e.g., yield force, yield displacement, initial stiffness, etc.) can readily be handled either with changes to the torsion element diameters and length or to the length of the connector moment arm. For example, a standard housing could be fabricated in different lengths to accommodate different length for the torsion element. A much greater variety of torsion element diameters could be manufactured without requiring changes to the housing. Finally, it is a very simple matter to employ different connector moment arm lengths.

4. Building Studies

The application of advanced cladding connectors to practical building design was investigated by careful examination of an actual contemporary building in an active seismic zone and its redesign to incorporate advanced cladding connectors. The advanced connectors would replace the conventional connectors which were designed provide full structural isolation from the building structure. As noted in the Introduction (Section 1), the objective for this building study was to "redesign" the structure to incorporate advanced cladding and then to assess both the improvement in seismic performance (e.g., reduction in forces and displacements) as well as the potential for cost savings through use of reduced structural steel needed to achieve the same level of performance as the original building (if one were to construct a new building).

4.1 Baseline Building

The building that was investigated in this study is located in the West Coast seismic zone. It was originally constructed in the early 80's and is shown in Figure 4.1. The building structure is a 20 story steel frame with A36 steel used for all beams and A50 steel used for all columns. The transverse direction consists of 3 different steel frames linked together: a 3-bay exterior moment resisting frame, a 1-bay braced frame, and a 3-bay braced frame. The longitudinal direction consists of a 13-bay moment resisting frame system. The floor plan of this building is shown schematically in Figure 4.2. The floor decks were constructed with reinforced concrete and had a total thickness of 140 mm ($5^1/_2$ in). Each bay of both transverse and longitudinal frames supports a 115 mm ($4^1/_2$ in) thick precast panel which comprises the exterior facade.

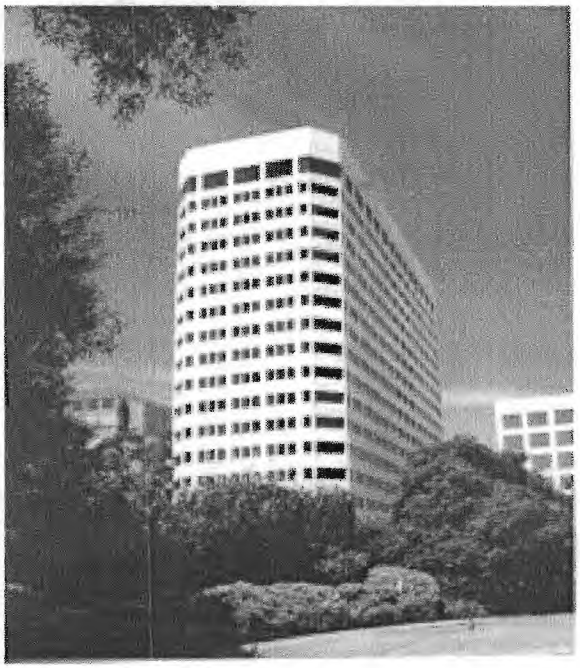

Figure 4.1 : Baseline Building on West Coast of U.S.

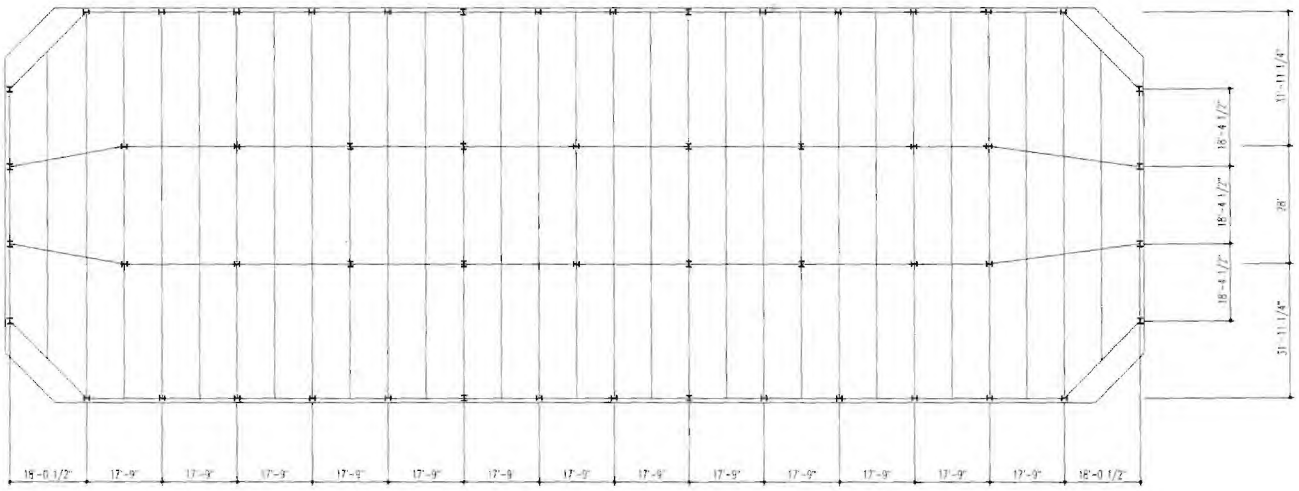

Figure 4.2 : Baseline Building Floor Plan (1 ft = 30.5 cm)

4.2 Structural Model

In order to investigate the behavior and performance of the baseline building and to test the validity of the proposed advanced connections, several types of two dimensional computer models were created. Program DRAIN-2dx, which can perform nonlinear time-history dynamic analysis, was used in analysis of these models. Since DRAIN-2dx is a two dimensional analysis system, it is necessary to model the building structure as a two dimensional assemblage of nonlinear elements connected at nodes. However, due to time and resource limitations in the present study, it has only been possible to study the building in a single direction; a full three-dimensional response was not needed in this case (due the building symmetry, coupled bending-torsion is not a factor - future studies which involve possible application of advanced cladding to unsymmetric structures will require use of either DRAIN-3dx or DRAIN-BUILDING). Due to the greater complexity and the greater cladding area available along the longitudinal sides, only the longitudinal structural direction was chosen for the present study. For design purposes, the first 50 seconds of a synthetic earthquake ground acceleration record appropriate to the Oakland area was provided for these analyses [Freeman, 1998]. The peak ground acceleration of this record is equal to 0.47g. The full ground acceleration record is shown in Figure 4.3.

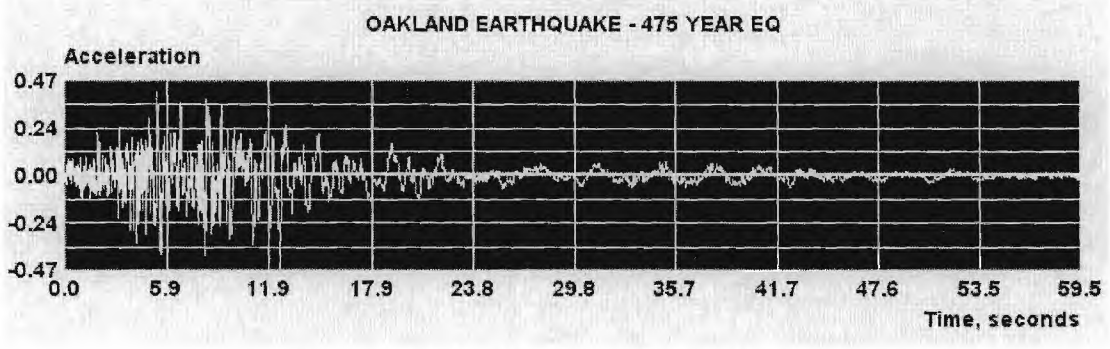

Figure 4.3 : Oakland Ground Acceleration

4.2.1 Nominal Model

The nominal or "as-built" model is a detailed model based on the full twenty story, thirteen bay moment resisting frame with the overall dimensions of 70.33 m (2769 in) wide and 76.34 m (3006 in) high, as shown in Figure 4.4. The model contains 294 nodes, 540 elements, and 840 dynamic degrees of freedom. Tributary masses were lumped at each floor node. The total floor masses are shown in Table 4.1. The properties of beams and columns used for this model were obtained from a structural drawing of an existing building.

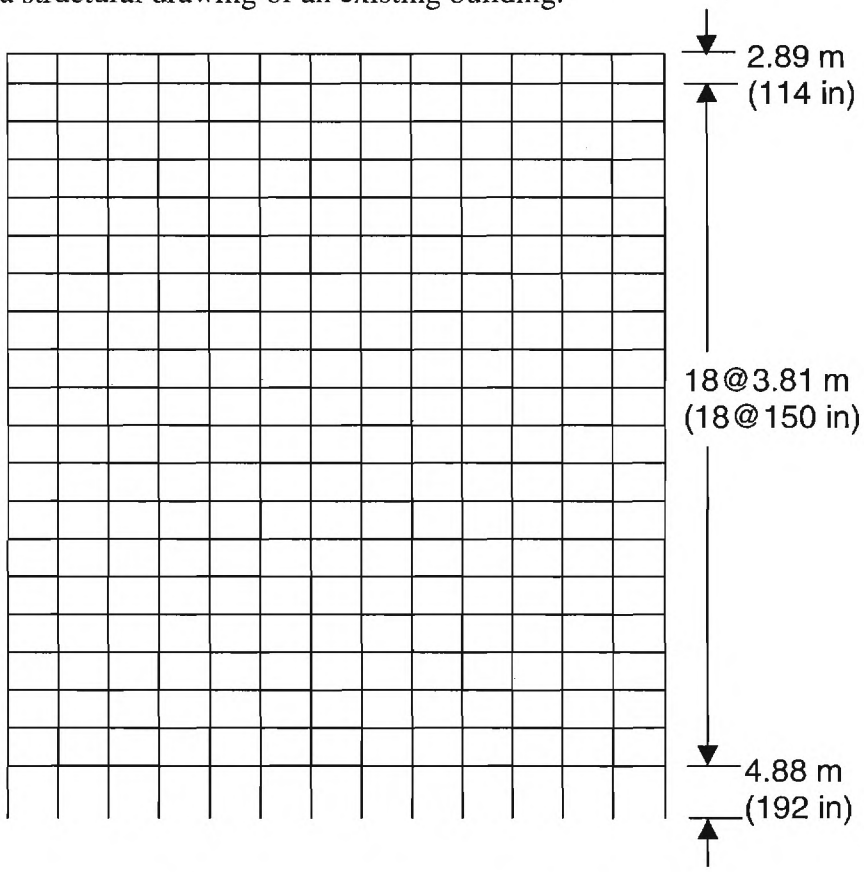

Figure 4.4 : Nominal Model Configuration

For preliminary evaluation of the nominal model and comparison to available design information from the building structural engineers, a modal analysis using DRAIN-2dx (linear stiffness only) gave periods for the first three modes of 3.313, 1.235, and 0.730 seconds, respectively, which are in generally good agreement with the design values. Mode shapes for the first three modes are shown in Figure 4.5.

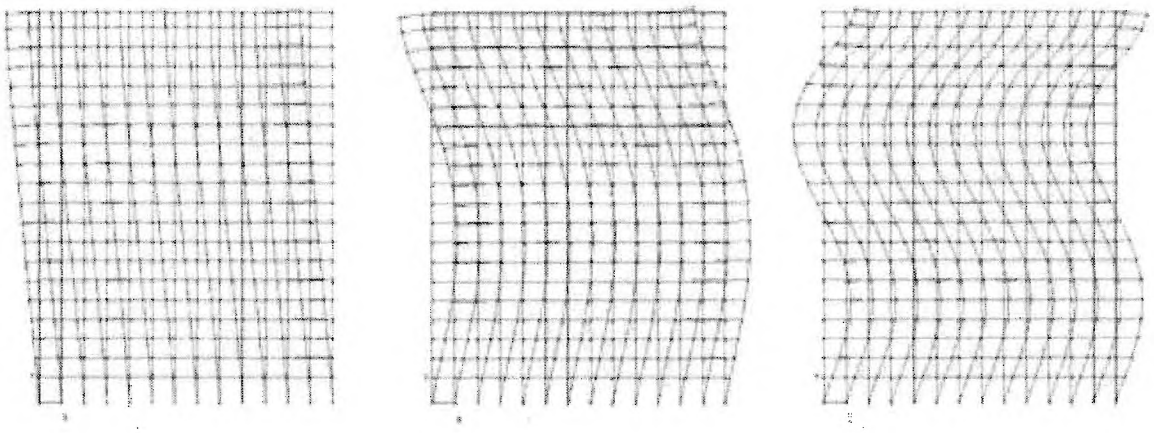

Figure 4.5 : Nominal Model Mode Shapes for the First Three Modes

Table 4.1 : Nominal Model Floor Masses

Floor	Floor Mass (10^3 kg)[a]	Floor Weight (kips)[b]	Floor Mass (kip-sec^2/in)
1	472.7	1042.3	2.69858
2	475.3	1048.0	2.71347
3	474.4	1046.0	2.70830
4	473.0	1043.0	2.70053
5	471.7	1040.0	2.69276
6	470.7	1038.0	2.68758
7	469.4	1035.0	2.67981
8	467.6	1031.0	2.66946
9	466.9	1029.5	2.66557
10	466.2	1028.0	2.66169
11	464.9	1025.0	2.65392
12	453.1	999.0	2.58660
13	451.7	996.0	2.57884
14	450.3	993.0	2.57107
15	448.5	989.0	2.56071
16	446.5	984.5	2.54906
17	445.1	981.5	2.54129
18	444.4	980.0	2.53741
19	435.6	960.5	2.48698
20	395.1	871.3	2.25590

[a] 1 kg = 2.205 lbm
[b] 1 kip = 4.448 kN

For the nominal model, one cladding panel per bay was attached to the baseline model as shown in the Figure 4.6. All openings in the cladding panels were neglected in this model. The panels were assumed to be rigid and modeled using the elastic panel element (element Type 06) for DRAIN-2dx. One fourth of the masses of these panels were lumped at each of the four corner nodes.

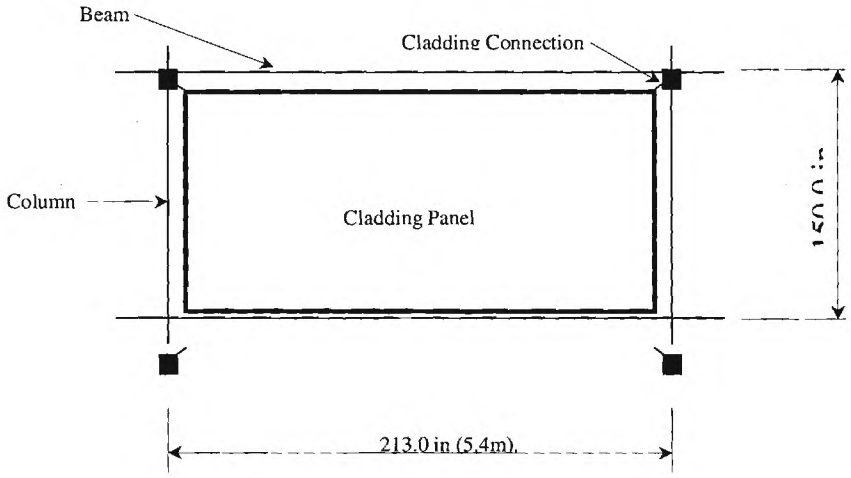

Figure 4.6 : Typical Bay with Cladding Panel and Connections in Nominal Model

The cladding connections were all modeled as simple connection elements (element Type 04) in DRAIN-2dx with elasto-plastic characteristics as shown in Figure 4.7. The use of a perfectly plastic model (no strain hardening) is a simplification that is judged reasonable based on the behavior of advanced cladding connectors observed in the lab tests reported in Section 3. The Type 04 elements are restricted in DRAIN-2dx to the x or y axis orientations only and may have zero length. As illustrated in Figure 4.8, the constitutive behavior can be either elastic (same loading and unloading paths) or inelastic with elastic unloading; strain hardening is included in the element but was not used in the present studies.

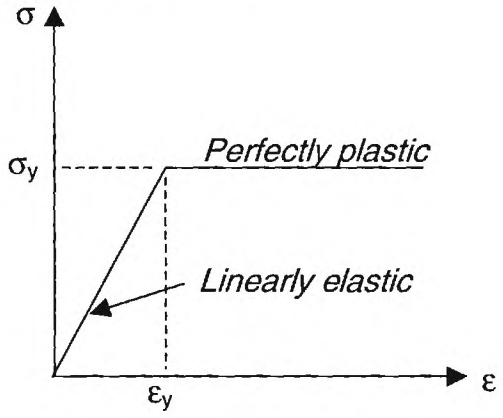

Figure 4.7 : Assumed Elasto-Plastic Characteristic

Each panel node has two cladding connections, one in the x-direction (horizontal) and the other in the y-direction (vertical). For the bearing connections at the bottom panel nodes, the connector elements in both x and y directions were assumed to be very stiff (values of 1,000,000 kips/in (175 GN/m) and 10,000 kips (44.5 MN) were used for the initial stiffness and the yield force, respectively). The elastic code for these bearing connections was set to 1 which is "Unload Elastically" in DRAIN-2dx, shown in Figure 4.8. The strain hardening ratio is equal to zero for the elasto-plastic material as stated previously.

Each node at the top of the panel also has two connections. The vertical tie-back connection stiffness was set to a nearly zero value and, like the bottom bearing connection, was assumed to unload elastically (elasticity code = 1 in DRAIN-2dx). On the other hand, the horizontal tie-back connections were assumed to represent the advanced cladding connectors. As a result, the Type 04 element was assumed to develop hysteresis through inelastic unloading (elasticity code = 0), as shown in Figure 4.8. The initial stiffness and the yield force of these horizontal tie-back connections are the decision variables in the cladding design optimization process.

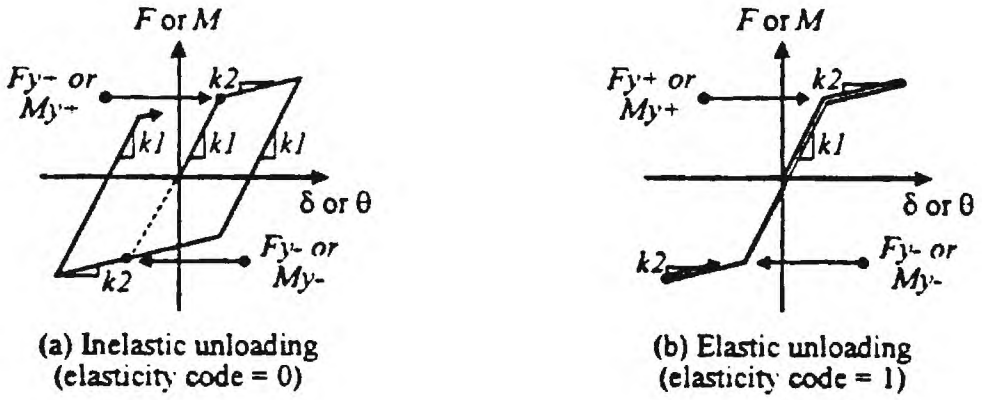

Figure 4.8 : Behavior Options Used in DRAIN-2dx

4.2.2 Design Model

The design model was created for the purpose of simplifying the nominal model to make it computationally tractable for design purposes in the numerical optimization process to obtain the optimal properties of the connections, as will be discussed later. The design model is a twenty story, one bay moment resisting frame with the overall dimensions identical to each bay of the nominal model which is 213 in. (17.75 ft., 5.4 m) wide and 150 in (12.5 ft, 3.8m) high. The design model, similar to the nominal model, has one cladding panel per bay attached to the frame with two connections at each of the four panel nodes. All connection behavior and connection characteristics are similar to those in the nominal model. The total number of nodes, elements, and degrees of freedom in the design model is as follows:

- 42 frame nodes
- 84 cladding panel nodes
- 200 dynamic degrees of freedom
- 60 beam and column elements
- 20 cladding panel elements

- 80 bearing connections elements
- 80 tie-back connections elements

In order to make this design model accurately represent the nominal model, the frame and scaling factors were adjusted so that the basic dynamic behavior, specifically the periods for the first five modes and the top floor displacements, were in good agreement as shown in Table 4.3. The beam and column properties were factored until the periods and the top floor displacement of the unclad design model agreed with the unclad nominal model. The beam and column properties for the one-bay design model are compared to the 13-bay nominal model in Table 4.2.

Table 4.2 : Beams and Columns Properties for the One-Bay Design Model

Floor	Floor Height (in.) (note 1)	Columns		Beams		Mass (kip-sec^2/in) (note 4)
		A (in.^{2}) (note 2)	I (in.^{4}) (note 3)	A (in.^{2}) (note 2)	I (in.^{4}) (note 3)	
1	192.0	8548.8	27410.0	34.2	69020.0	2.7575
2	150.0	7033.0	21470.0	29.1	55860.0	2.7135
3	150.0	7033.0	21470.0	29.1	55860.0	2.7083
4	150.0	6379.1	19060.0	29.1	55860.0	2.7005
5	150.0	6379.1	19060.0	29.1	55860.0	2.6928
6	150.0	5825.3	16810.0	29.1	55860.0	2.6876
7	150.0	5825.3	16810.0	29.1	55860.0	2.6798
8	150.0	5567.9	16300.0	27.7	45780.0	2.6695
9	150.0	5567.9	16300.0	27.7	45780.0	2.6656
10	150.0	5179.2	14820.0	27.7	45780.0	2.6617
11	150.0	5179.2	14820.0	27.7	45780.0	2.6539
12	150.0	4342.0	11890.0	27.7	45780.0	2.5866
13	150.0	4342.0	11890.0	27.7	45780.0	2.5788
14	150.0	3892.2	10591.0	22.4	29400.0	2.5711
15	150.0	3892.2	10591.0	22.4	29400.0	2.5607
16	150.0	3666.0	10094.0	20.1	25620.0	2.5491
17	150.0	3666.0	10094.0	20.1	25620.0	2.5413
18	150.0	2589.6	6466.0	20.1	25620.0	2.5374
19	150.0	2589.6	6466.0	20.1	25620.0	2.5374
20	114.0	2480.4	6213.0	13.0	11802.0	2.4157

Notes:

1. 1 inch = 25.4 mm
2. 1 in^2 = 645 mm^2
3. 1 in^4 = 416.2e3 mm^4
4. 1 kip-sec^2/in = 175.2 x10^3 kg

Since the 13 bays of the nominal model are reduced to only a single bay in the design model, it is necessary to scale up the properties of the tie-back connections in the design model. The factor of 13 was initially used for the yield force and the initial stiffness of those connections based on the ratio of panels in each model, and they were then manually adjusted until the dynamic characteristics of the two models matched. The final values of the scaling factors of 13 and 17.5 for the yield force and initial stiffness, respectively, were obtained and used in the design model.

Table 4.3 : Dynamic Behavior of the Design Model and the Nominal Model Based on 6 sec. of Oakland Ground Acceleration

		Without Cladding Connection		With Cladding Connections	
		Design Model	Nominal Model	Design Model	Nominal Model
Periods (s)	Mode 1	3.302	3.313	2.173	2.176
	Mode 2	1.217	1.235	0.739	0.759
	Mode 3	0.713	0.730	0.416	0.454
	Mode 4	0.507	0.518	0.295	0.323
	Mode 5	0.389	0.398	0.228	0.251
Max Displ (in)[a]		10.70	10.46	9.14	9.00

[a] 1 inch = 25.4 mm

In the development of the scaling factors, reasonable baseline values of yield force (21.3 kN or 4.8 kips) and initial stiffness (14 MN/m or 80 kips/in) were picked for the nominal model, and, in order to reduce computer time, only the first six seconds of the Oakland ground acceleration record was applied to the models. As a result, the tie-back connections in the design model have corresponding baseline values of yield force of 277 kN (62.4 kips) and initial stiffness of 245 MN/m (1400 kips/in). Results from those design and nominal models compared very well, as shown above in Table 4.3, giving confidence to representation of the nominal model by the design model.

4.3 Optimization

The optimal values for the cladding connectors (initial stiffness and yield force) were determined using numerical optimization as described in Section 2.4. In the present study, the DOT program [Vanderplaats 1993] was used in connection with the DRAIN-2dx program for analysis of the building. Using the same approach as described in Section 2.4, the following optimization problem was defined:

Objective Function:	(Energy dissipated in cladding connectors)/(Input seismic energy)
Decision Variables:	Connector initial stiffness
	Connector yield force
Constraint:	Dynamic ductility demand is fixed
Side Constraints:	Maximum & minimum values for decision variables

The DOT program consists of a Fortran primary subroutine and several supporting subroutines. The user must then construct a main program which will set up the optimization program and call the DOT primary subroutine. If this subroutine is able to converge on the optimal solution, it returns an appropriate result and the main program finishes. If the optimal solution has not yet been reached, then the DOT subroutine returns new values of the decision variables and the main program must use these to compute new values for the objective function and the constraint(s). The main program loops back to call DOT once more.

In order to evaluate the objective function, DRAIN-2dx must be run for the one-bay design building model and the design earthquake. The output files produced by DRAIN-2dx must then

be read and the appropriate information extracted to allow computation of the energy terms needed to compute the objective function as defined above. Fortunately, the needed results are a normal part of the available output from DRAIN-2dx. In addition, the Type 04 element used to model the cladding connectors in DRAIN-2dx was modified to compute the dynamic ductility as defined in Equation 1 in Section 2 and to return this result in the output files.

The main numerical optimization program was developed using DEC Visual Fortran (Intel version). DRAIN-2dx was called from the main program using the Windows API library included in Visual Fortran, and several subroutines were used to extract the needed information from the resulting DRAIN-2dx output files. Figure 4.9 describes the process in a schematic diagram. The program listings are included in the Appendix.

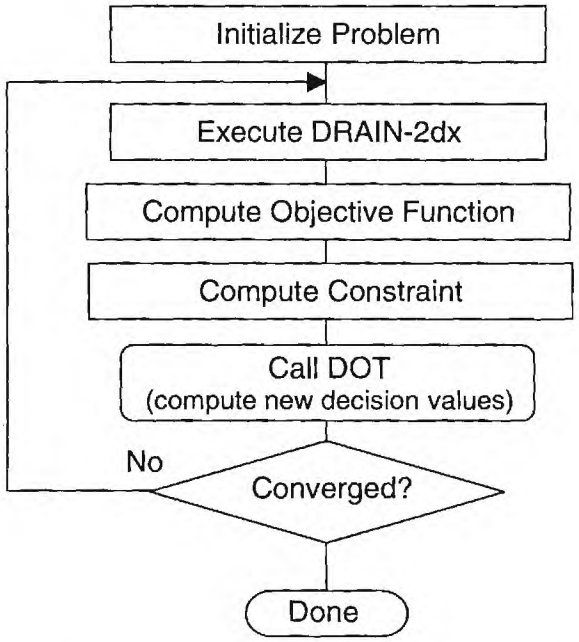

Figure 4.9 Numerical Optimization Program Flowchart

When started from a feasible design point using the initial values for cladding connector stiffness and yield force, the numerical optimization program ran automatically until an optimal solution was obtained (or numerical and computational limits were reached). Typically, this required from 25-35 evaluations of the objective function which required a corresponding number of executions of DRAIN-2dx using the design model and design earthquake. With typical DRAIN-2dx execution times of 1-2 minutes, the full optimal design computation typically took from 25-45 minutes to complete (on a 266 MHz Pentium class personal computer).

The numerical optimization gives only the final outputs which are the parameters and the objective functions at the optimal point, and with intermediate results (if requested), it is then possible to trace how the optimization process was done and how the objective and constraint functions changed as the parameters varied. However, this information still only provides a narrow glimpse of the design space as a whole, and it provides little or no insight into the design

process itself. (This is a familiar and all too common consequence of the use of numerical optimization in design problems.)

As a result, in this study a manual optimization process was used instead.. The objective function (the ratio between the elasto-plastic work in the connections and the external work) was computed using DRAIN-2dx for a range of values of the decision variables that defined the overall design space with reasonable fineness. The result of these calculations was then a grid of values of the objective and constraint (dynamic ductility demand) functions that could be plotted as superposed contour plots. A total of 196 test cases were investigated with the design model subjected to 50 seconds of the synthesized Oakland ground acceleration. The yield force and the initial stiffness of the connections ranged from 178 to 1334 kN (40 to 300 kips) and from 87.4 to 1226 MN/m (500 to 7,000 kips/in), respectively.

Both the contour lines of the energy ratio and of plastic ductility demand are super imposed in Figure 4.10. The contour lines for the energy ratio are shown as solid lines while the contour lines for the plastic ductility demand are shown as dashed lines. The optimal points are indicated by the black cross marks on the plot.

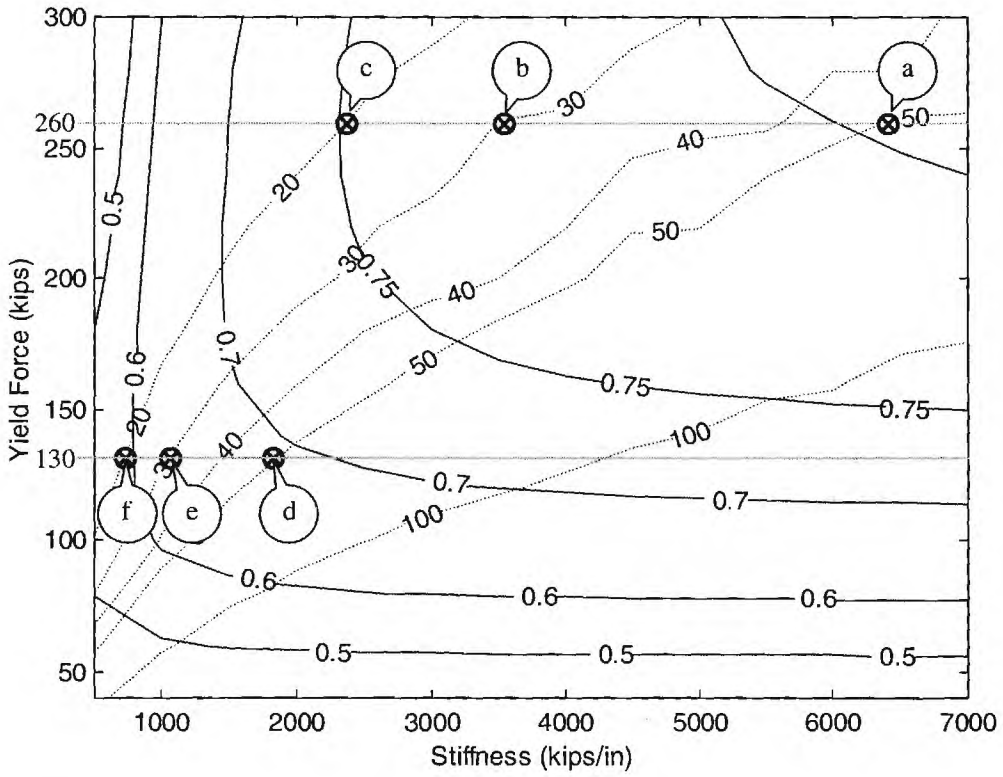

Figure 4.10 : Contour Plots for the Energy Ratio and The Plastic Ductility Demand
(Note: 1 kip = 4.48 kN, 1 kip/inch = 175 kN/m)

Depending on the different design assumptions employed (which involve variations in the assumed maximum force to be transmitted into the panels and the maximum dynamic ductility demand to be allowed), a total of six different optimal combinations of connector yield force and stiffness values were identified in Figure 4.10 (labeled as Cases a-f) and are defined as follows:

Case Description

(a) Yield force of 1156 kN (260 kips) and initial stiffness of 1116 kN/m (6375 kips/in) with the dynamic ductility demand of 50
(b) Yield force of 1156 kN (260 kips) and initial stiffness of 606 kN/m (3460 kips/in) with the maximum dynamic ductility demand of 30
(c) Yield force of 1156 kN (260 kips) and initial stiffness of 420 kN/m (2400 kips/in) with the maximum dynamic ductility demand of 20
(d) Yield force of 578 kN (130 kips) and initial stiffness of 315 kN/m (1800 kips/in) with the maximum dynamic ductility demand of 50
(e) Yield force of 578 kN (130 kips) and initial stiffness of 175 kN/m (1000 kips/in) with the maximum dynamic ductility demand of 30
(f) Yield force of 578 kN (130 kips) and initial stiffness of 105 kN/m (600 kips/in) with the maximum dynamic ductility demand of 20.

The periods of the three lowest modes and the maximum displacement at the top floor were also computed and are shown in Table 4.4 for the six design cases defined above.

Table 4.4 : Behavior of the Design Model with the Optimal Connections

Case	Yield Force (kips)[a]	Stiffness (k/in)[b]	Periods (sec)			Max. Top Disp. (in)[c]
			Mode 1	Mode 2	Mode 3	
a	260	6375	1.481	0.466	0.243	15.16
b	260	3460	1.722	0.565	0.305	16.31
c	260	2400	1.895	0.633	0.348	17.08
d	130	1800	2.042	0.689	0.384	19.87
e	130	1000	2.348	0.807	0.459	20.51
f	130	600	2.596	0.906	0.521	20.92

[a] 1 kip = 4.448 kN
[b] 1 kip/in = 0.17512 MN/m
[c] 1 in = 2.54 cm

4.4 Performance with Advanced Connectors

As shown previously in the contour plots, the optimization process resulted in six different optimal configurations, depending on the assumed design objectives for the advanced connections in the design model (e.g., constraints on dynamic ductility demand and the maximum force allowed to transmitted into the panel). In the subsequent application of these optimal connections to the nominal 13-bay model, the scale factors were applied as follows. The factor of $^1/_{13}$ was applied to the yield force while the factor of $^1/_{17.5}$ was applied to the initial stiffness of the advanced connections, as stated in Section 4.2. Therefore, the optimal advanced connections for the nominal model (e.g., the full model) can be calculated and listed for each case as follows.

Case Description

(a) Yield force of 89 kN (20 kips) and initial stiffness of 63.7 MN/m (364 kips/in) with the maximum dynamic ductility demand of 50

(b) Yield force of 89 kN (20 kips) and initial stiffness of 34.7 MN/m (198 kips/in) with the maximum dynamic ductility demand of 50

(c) Yield force of 89 kN (20 kips) and initial stiffness of 24 MN/m (137 kips/in) with the maximum dynamic ductility demand of 50

(d) Yield force of 44.5 kN (10 kips) and initial stiffness of 18 MN/m(103 kips/in) with the maximum dynamic ductility demand of 50

(e) Yield force of 44.5 kN (10 kips) and initial stiffness of 10 MN/m(57 kips/in) with the maximum dynamic ductility demand of 50

(f) Yield force of 44.5 kN (10 kips) and initial stiffness of 6.0 MN/m (34 kips/in) with the maximum dynamic ductility demand of 50

The behavior of the nominal model with optimal advanced connections, including the periods of the three lowest modes and the maximum top floor displacements, are shown in Table 4.5.

Table 4.5 : Behavior of the Nominal Model with the Optimal Connections

Case	Yield Force (kips)[a]	Stiffness (k/in)[b]	Periods (sec)			Max. Top Disp. (in)[c]
			Mode 1	Mode 2	Mode 3	
a	20	364	1.294	0.436	0.261	13.50(41.4%)*
b	20	198	1.632	0.557	0.333	15.28(33.7%)*
c	20	137	1.852	0.638	0.381	16.48(28.5%)*
d	10	103	2.025	0.702	0.420	19.58(15.1%)*
e	10	57	2.368	0.834	0.498	20.00(13.2%)*
f	10	34	2.626	0.938	0.560	19.90(13.7%)*

[a] 1 kip = 4.448 kN
[b] 1 kip/in = 0.17512 MN/m
[c] 1 in = 25.4 mm
* percent change with respect to baseline (isolated cladding) case

For comparison purposes, the periods of the three lowest modes of the baseline "as-built" model in which the panels and their connections are isolated from the structure (e.g., a zero connector yield force value) are 3.313, 1.235, and 0.730 seconds, respectively. The maximum top floor displacement for this model is 58.5 cm (23.05 inches). In comparison, both the displacement and periods of the structure decrease significantly when the optimal advanced connections are added.

The top floor displacement time-histories were also computed for the optimal connector stiffness and strength values and compared for different values of the dynamic ductility demand. These are shown in Figures 4.11, 4.12, and 4.13 below.

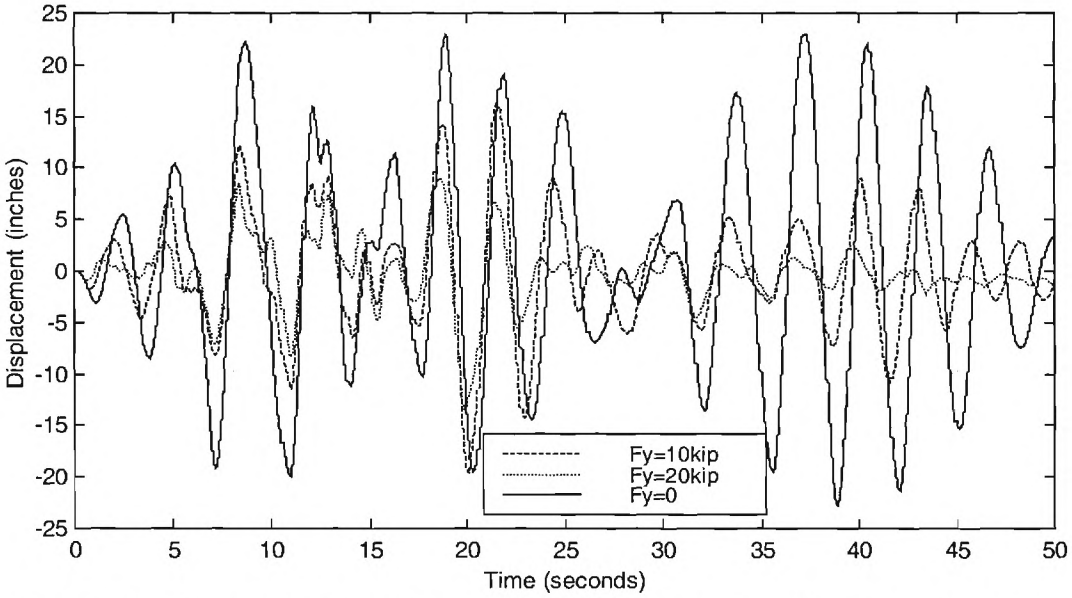

Figure 4.11 : Time-History Top Floor Displacement, Dynamic Ductility Demand = 50

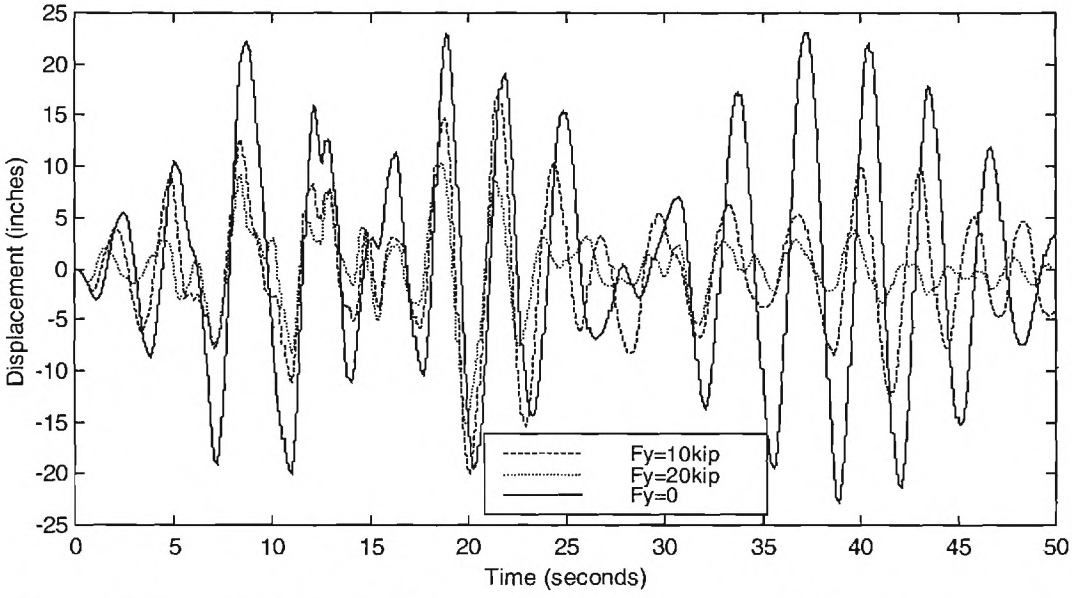

Figure 4.12 : Time-History Top Floor Displacement, Dynamic Ductility Demand = 30

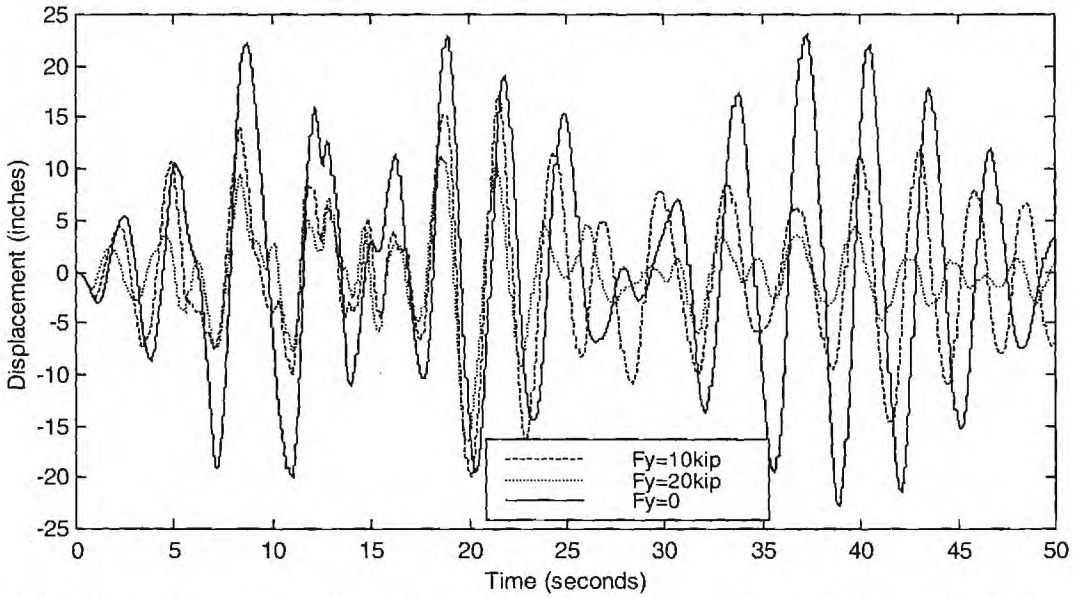

Figure 4.13 : Time-History Top Floor Displacement, Dynamic Ductility Demand = 20

Each of the figures above shows the top floor displacement time-histories for the 13-bay nominal model with an assumed maximum ductility demand and different values for the optimal connector stiffness and yield parameters. The two dashed lines represent the displacements of the nominal model with the optimal advanced connections. The long-dash line is for the model with a yield force constraint of 89 kN (20 kips), while the short-dash lines is for the 44.5 kN (10 kips) yield force constraint. The solid line, which show the largest top floor displacement, is for the nominal model with isolated panels (e.g., yield force constraint is zero) which is also referred to as the "as-built" model.

These results clearly show the effects of using advanced cladding connectors in the building structure. As expected, the presence of these devices results in significant energy dissipation through their interaction between the cladding and the supporting structure (e.g., see objective function values in the contour plot in Figure 4.10). Perhaps more dramatically, the advanced connectors result in a reduction in the peak top floor displacements of up to 41% compared to the "as-built" model. More subtly, the advanced connections system seems to also affect the dynamic characteristics of the building structure in the sense that the eigenvalues are also slightly altered (see the modal periods in Tables 4.4 and 4.5).

4.5 Comparison of Results for DRAIN-2dx and ETABS Models

As an additional check on the results computed using the DRAIN-2dx model presented above, a computer model of the 13 bay moment frame (nominal model) was also developed using the nonlinear dynamic analysis computer program ETABS-PLUS.

Two advanced tie-back connections and two very stiff bearing connections per panel were included as part of the overall steel frame-cladding model. The upper advanced tie-back connections were modeled as link elements of zero length between the panel and the frame using ETABS uniaxial hysteretic spring properties (element type PLASTIC1) to represent these energy dissipating connections. Post yield stiffness was assumed to be zero to represent elasto-plastic

behavior as in the DRAIN-2dx model. In addition, ETABS does not have the capability of representing nonlinear material behavior in beam and column elements, so only the advanced cladding connections are capable of developing hysteretic damping in the nonlinear dynamic time history analysis. Panel mass was distributed equally to the lower bearing and upper tie-back connection nodes.

The artificial Oakland ground acceleration record (Fig. 4.3) used in the DRAIN-2dx studies was also used to analyze the effect of the energy dissipating connections in the ETABS model. In addition, the1940 El Centro NS ground motion was applied as a second test case to compare the response of both the ETABS and DRAIN-2dx models of the frame. These additional studies were performed to develop a better understanding of the frame response for a ground motion with different spectral characteristics and thereby develop added confidence in the nonlinear model. They were also felt to be a useful way of calibrating the nonlinear response spectrum analysis results which provided the basis for the steel redesign studies to be presented in Sec. 4.6.

Since there was no yielding in the baseline (isolated cladding) steel frame elements due to El Centro, results of the ETABS and DRAIN-2dx analyses presented in Table 4.6 are in very good agreement. The Oakland ground motion, however, develops inelastic action in the baseline structural frame so the peak displacements from DRAIN-2dx and ETABS do not compare as well for the unclad case (Table 4.6).

Table 4.6: Comparison of ETABS and DRAIN-2dx Nominal Models without Cladding Subjected to 1940 El Centro NS (duration = 53.76 sec) and Oakland Ground Motions (duration = 59.52 sec)

	DRAIN-2dx	ETABS
	Max. Top Displ. (in.)*	Max. Top Displ. (in.)*
El Centro	13.67	13.39
Oakland	23.05	29.08

* 1 inch = 25.4 mm

Tables 4.7 and 4.8 present the results of analyses based on the DRAIN-2dx and ETABS nominal models due to the Oakland ground motion for 7 different cases. Yield force and stiffness values for the advanced connections were varied based on results of the optimization studies presented in Section 4.3. Vibration periods for modes 1 and 2 are in good agreement for both models, and maximum top story displacements from the time history analyses from the ETABS model were at most 6% different from DRAIN-2dx results for the first 6 cases (using advanced cladding connections). For the baseline (isolated cladding) case, the periods were the same. However, as noted above, the maximum displacement at the top level from ETABS was off by 26% compared to the DRAIN-2dx result due to the occurrence of yielding of beam and column elements in the unclad frame which ETABS cannot represent. In general, it can be seen that top story displacements decrease with increase in cladding connection stiffness and yield force levels, and that the effect of advanced cladding is to reduce the top story displacement by a much as 41% compared to the baseline (isolated cladding) case for this particular ground motion.

Table 4.7: Modal Periods and Top Story Displacements from DRAIN-2dx Nominal Model with Optimal Connections Subjected to Oakland Ground Motion (duration = 59.52s)

Case	Yield Force (kips)[a]	Stiffness (k/in.)[b]	Periods (sec.)		Max. Top Displ. (in.)[c]
			Mode 1	Mode 2	
1	10	103	2.025	0.702	19.58
2	10	57	2.368	0.834	20.00
3	10	34	2.626	0.938	19.90
4	20	364	1.294	0.436	13.50
5	20	198	1.632	0.557	15.28
6	20	137	1.852	0.638	16.48
Baseline	-----	-----	3.330	1.242	23.05

[a] 1 kip = 4.448 kN
[b] 1 k/in = 175.1 kN/m
[c] 1 inch = 25.4 mm

Table 4.8: Modal Periods and Top Story Displacements from ETABS Nominal Model with Optimal Connections Subjected to Oakland Ground Motion (duration = 59.52 sec)

Case	Yield Force (kips)[a]	Stiffness (k/in.)[b]	Periods (sec.)		Max. Top Displ. (in.)[c]
			Mode 1	Mode 2	
1	10	103	2.141	0.744	18.59
2	10	57	2.450	0.861	19.33
3	10	34	2.679	0.952	19.95
4	20	364	1.478	0.504	13.09
5	20	198	1.783	0.613	15.78
6	20	137	1.983	0.686	17.02
Baseline	-----	-----	3.329	1.242	29.08

[a] 1 kip = 4.448 kN
[b] 1 k/in = 175.1 kN/m
[c] 1 inch = 25.4 mm

Table 4.9 presents the variation of the maximum base shear and overturning moment for the 13 bay nominal model due to different yield force and stiffness values for the advanced cladding connections. Maximum base shear was reduced in all cases with a peak reduction of 20.8% compared to the baseline case. Maximum overturning moment was decreased significantly in cases 1-3 but increased in cases 4 and 5.

The maximum input energy and maximum hysteretic energy variations for the various cases are shown in Table 4.10. As expected, the addition of advanced cladding alters the dynamic characteristics and therefore the sensitivity of the overall structure to the specified ground motion compared to the baseline case.

Table 4.9: Base Shear and Overturning Moment from ETABS Nominal Model with Optimal Connections Subjected to Oakland Ground Motion (duration = 59.52 sec)

Case	Yield Force (kips)[a]	Stiffness (k/in.)[b]	Max. Total Base Shear (kips)[b]	Max. Total Overturning Moment (kip-feet)[c]
1	10	103	2621 (-20.8%)*	468,333 (-9.9%)*
2	10	57	2649 (-20.0%)*	459,583 (-11.6%)*
3	10	34	2836 (-14.3%)*	464,250 (-10.7%)*
4	20	364	3308 (-0.1%)*	594,750 (+14.5%)*
5	20	198	3026 (-8.6%)*	530,015 (+2.0%)*
6	20	137	2870 (-13.3%)*	514,833 (-0.9%)*
Baseline	-----	-----	3310	519,583

[a] 1 kip = 4.448 kN
[b] 1 k/in = 175.1 kN/m
[c] 1 k-ft = 1.356 kN-m
* percent change with respect to baseline (isolated cladding) case

Table 4.10: Maximum Input and Hysteretic Energy Values from ETABS Nominal Model with the Optimal Connections Subjected to Oakland Ground Motion (duration = 59.52 sec)

Case	Yield Force (kips)[a]	Stiffness (k/in.)[b]	Max. Input Energy (kip-inch)[c]	Max. Hysteretic Energy (kip-inch)
1	10	103	1.587E+05 (+0.4%)*	8.622E+04
2	10	57	1.666E+05 (+5.4%)*	8.604E+04
3	10	34	1.759E+05 (+11.3%)*	7.795E+04
4	20	364	1.269E+05 (-19.7%)*	7.611E+04
5	20	198	1.368E+05 (-13.5%)*	8.366E+04
6	20	137	1.437E+05 (-9.1%)*	8.611E+04
Baseline	-----	-----	1.581E+05	-----

[a] 1 kip = 4.448 kN
[b] 1 k/in = 175.1 kN/m
[c] 1 k-in = 0.113 kN-m
* percent change with respect to baseline (isolated cladding) case

The energy values presented in Table 4.11 show that while the maximum input energy delivered to the structure by the ground motion either increased or decreased with respect to the baseline case, the maximum kinetic energy of the clad frame was significantly reduced due the addition of advanced cladding connections. This is also reflected in the corresponding reductions in maximum interstory drift ratios (Table 4.12), story accelerations (Table 4.13), and story velocities (Table 4.14).

These results generally confirm that the DRAIN-2dx model for the nominal building, either with or without advanced cladding connectors, adequately represents the expected two dimensional behavior under the kinds of seismic loading considered in this study.

Table 4.11: Maximum Input and Kinetic Energy Values from ETABS Nominal Model with the Optimal Connections Subjected to Oakland Ground Motion (duration = 59.52 sec)

Case	Yield Force (kips)[a]	Stiffness (k/in.)[b]	Max. Input Energy (kip-inch)[c]	Max. Kinetic Energy (kip-inch)
1	10	103	1.587E+05 (+0.4%)*	2.372E+04 (-39.9%)*
2	10	57	1.666E+05 (+5.4%)*	2.527E+04 (-36.0%)*
3	10	34	1.759E+05 (+11.3%)*	2.677E+04 (-32.2%)*
4	20	364	1.269E+05 (-19.7%)*	1.404E+04 (-64.4%)*
5	20	198	1.368E+05 (-13.5%)*	1.815E+04 (-54.0%)*
6	20	137	1.437E+05 (-9.1%)*	2.137E+04 (-45.9%)*
Baseline	-----	-----	1.581E+05	3.949E+04

[a]1 kip = 4.448 kN
[b]1 k/in = 175.1 kN/m
[c] 1 k-in = 0.113 kN-m
* percent change with respect to baseline (isolated cladding) case

Table 4.12: Maximum Interstory Drift Ratios from ETABS Nominal Model with the Optimal Connections Subjected to Oakland Ground Motion (duration = 59.52 sec)

Case	Yield Force (kips)[a]	Stiffness (k/in.)[b]	Max. Interstory Drift Ratio
1	10	103	0.0080 (-34.4%)*
2	10	57	0.0082 (-32.8%)*
3	10	34	0.0083 (-32.0%)*
4	20	364	0.0064 (-47.5%)*
5	20	198	0.0072 (-41.0%)*
6	20	137	0.0073 (-40.2%)*
Baseline	-----	-----	0.0122

[a] 1 kip = 4.448 kN [b] 1 k/in = 175.1 kN/m
* percent change with respect to baseline (isolated cladding) case

Table 4.13: Maximum Roof and 10th Story Accelerations from ETABS Nominal Model with the Optimal Connections Subjected to Oakland Ground Motion (duration = 59.52 sec)

Case	Yield Force (kips)[a]	Stiffness (k/in.)[b]	Max. Story Acceleration at Roof (inch/sec)[c]	Max. Story Acceleration at 10th level (inch/sec)
1	10	103	124.9 (-27.7%)*	89.3 (-31.9%)*
2	10	57	120.0 (-30.6%)*	92.4 (-29.5%)*
3	10	34	119.7 (-30.7%)*	90.6 (-30.9%)*
4	20	364	119.6 (-30.8%)*	89.7 (-31.6%)*
5	20	198	125.3 (-27.5%)*	90.9 (-30.7%)*
6	20	137	118.2 (-31.6%)*	96.1 (-26.7%)*
Baseline	-----	-----	172.8	131.1

[a] 1 kip = 4.448 kN
[b] 1 k/in = 175.1 kN/m
[c] 1 in/sec^2 = 0.0254 m/sec^2
*percent change with respect to unclad case

Table 4.14: Maximum Roof Velocities from ETABS Nominal Model with Optimal Connections Subjected to Oakland Ground Motion (duration = 59.52 sec)

Case	Yield Force (kips)[a]	Stiffness (k/in.)[b]	Max. Story Velocity at Roof (inch/sec)[c]
1	10	103	45.08 (-30.9%)*
2	10	57	46.30 (-29.1%)*
3	10	34	49.79 (-23.7%)*
4	20	364	31.91 (-51.1%)*
5	20	198	36.31 (-44.4%)*
6	20	137	40.76 (-37.6%)*
Baseline	-----	-----	65.27

[a] 1 kip = 4.448 kN
[b] 1 k/in = 175.1 kN/m
[c] 1 in/sec = 0.0254 m/sec
* percent change with respect to unclad case

4.6 Steel Redesign

Sections 4.4 and 4.5 quantify and summarize the expected improvements in performance that might be obtained for the baseline building configuration if its conventional isolated cladding system is replaced with optimally designed advanced cladding connections. While this kind of design approach may be appropriate to increase the performance margins for essential facilities or for retrofit applications to remedy structural deficiencies with respect to contemporary code provisions, it may not be appropriate for entirely new designs. For these cases, the advanced cladding connections could be used to reduce the seismic demand on the primary structural system and thereby allow a reduction in the needed structural strengths with a commensurate

reduction in the structural weight and cost. This section presents an analysis of the study building to determine the potential reduction in structural steel that might be obtained if the objective is to maintain the same overall structural response for the baseline building in the building with optimally designed advanced cladding connectors (but with reduced primary frame properties). In other words, the design strategy is to increase hysteretic damping in the cladding connections resulting in reduced member forces for design while maintaining the overall structure response level.

4.6.1 Redesign Process

To this end, the 13 bay moment frame in the longitudinal direction was reanalyzed but this time using the structural analysis and design computer program, GTSTRUDL, in order to make use of its automated redesign capability. However, since this redesign process is based on a linear structural analysis rather than a nonlinear time history analysis as developed in Section 4.4, a novel "equivalent" linear redesign process was conceived for this purpose. In this approach, a response spectrum analysis (RSA) is used, in place of the previously employed time history nonlinear dynamic analysis, to define the maximum lateral forces to be used in the structural member selection process. In order to account for the presence of passive damping introduced by the advanced cladding connectors, the assumed modal viscous damping for the RSA is systematically adjusted to represent the effect of this added hysteretic damping. As will be argued below, this is judged to be a reasonable approximation due to the particular characteristics of the optimal cladding connectors defined by the optimization process described in Section 4.3. As for the previous studies, the same synthetic Oakland ground motion is used.

The GTSTRUDL model of the 13 bay moment frame contains 260 beam elements, 280 column elements, and 260 rectangular panel elements. The lumped mass model for the structure was computed from the self weight of the beams, columns, 4.5 inch (114.3 mm) thick precast panels and composite floor deck, and 10 psf (9.93 MPa) dead load to account for the partitions. A 100 psf (99.3 MPa) reducible live load was also used for the steel redesign sequence. Additional considerations such as P-delta effects, panel zone deformation, and soil-structure interaction were not included in the GTSTRUDL model.

By including only the first 9 modes of the structural model, 97.5% of the participating mass of the structure is included in the calculation of maximum response in the longitudinal direction. Modal results are combined using the square-root-of-the-sum-of-the-squares of individual modal maxima. In the initial response spectrum analysis based on the Oakland ground motion, 5% damping in all modes is assumed for the baseline isolated cladding case in which no damping contribution is provided by the cladding.

Figure 4.14 above outlines the full redesign process schematically starting with the baseline building model developed in the previous time history nonlinear dynamic analysis using DRAIN-2dx. This model is converted into a corresponding GTSTRUDL model with an initially assumed 5% viscous modal damping and a zero tie-back connector yield force to represent the "as-built" or baseline isolated cladding configuration. Figure 4.15 shows the beam member sizes for the longitudinal moment frame system for the baseline configuration. In the present study, the total structural weight as obtained using GTSTRUDL was 1069 kips (4757 kN). This essentially defines the design status at the point labeled START in the schematic diagram.

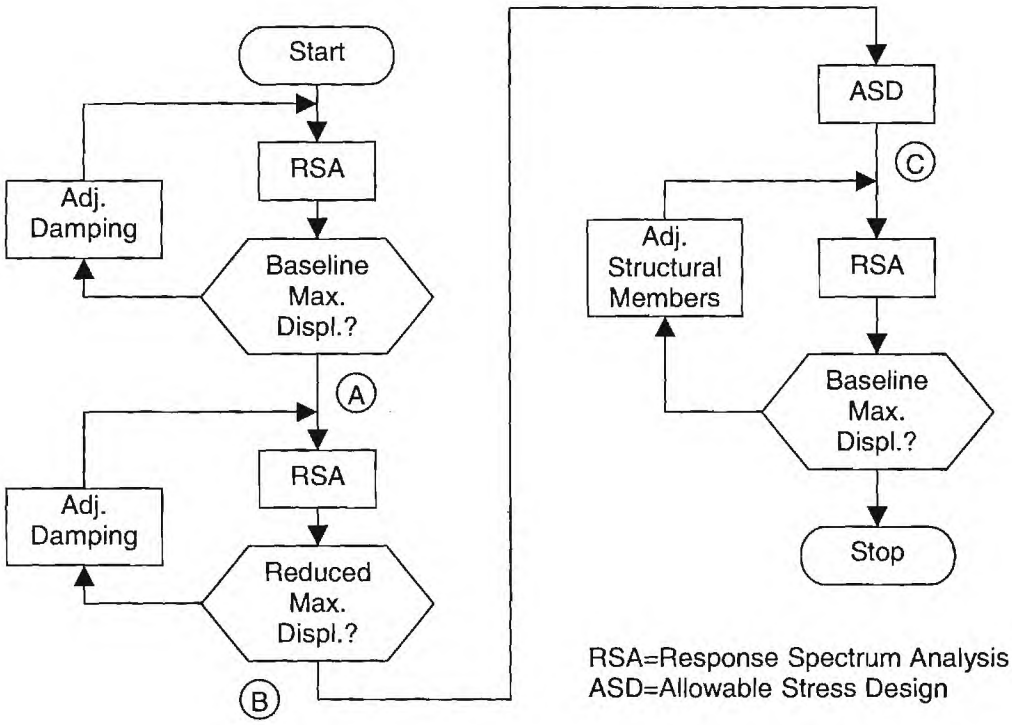

Figure 4.14 ASD Steel Redesign Procedure as Implemented Using GTSTRUDL

Next, a Response Spectrum Analysis (RSA) is used to compute an estimate of the peak displacement for the design earthquake. In the first iterative loop shown in the schematic, the resulting maximum displacement is compared to the peak displacement of the baseline building as computed using the time history nonlinear dynamic analysis using the Design Model as described in Section 4.2. This target figure is 29.68 inches (754 mm) at the roof level. To bring the peak RSA displacement value into agreement, the assumed damping in the RSA is gradually changed in successive GTSTRUDL analyses until peak displacements are found to be equal. In the present study, this resulted in a damping value of 4.9%.

Continuing from Point A in the schematic diagram, the next step in the redesign is to determine the amount of added viscous modal damping that must be added to the structure to represent the effect of the hysteretic damping provided by the optimal cladding connectors as determined by the numerical optimization design process in Section 4.3. The results in Section 4.3 and 4.4 show that the optimal connector properties define a connector with a relatively high initial elastic stiffness but a low or moderate yield force. Not surprisingly, such a connector will reach yield level displacements at small lateral response values and thus very quickly begin to develop hysteretic action. As a result, the connectors contribute essentially no additional lateral stiffness to the overall structure model, even though significant initial elastic stiffness parameter values are specified, and their sole contribution is to provide energy dissipation in the structure.

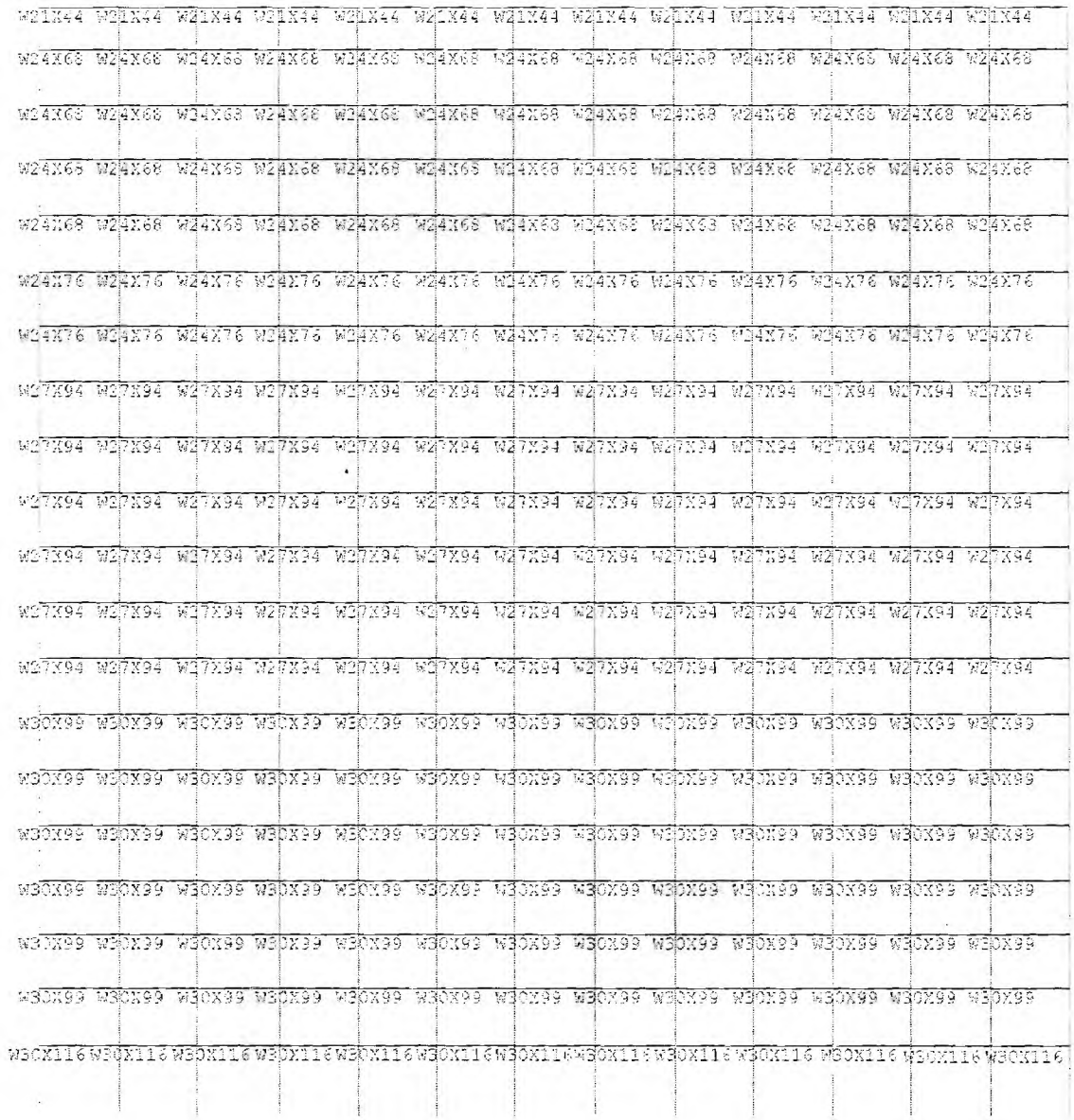

Figure 4.15 Beam Members Sizes Before Steel Redesign

To account for these effects in the structural redesign process, the cladding is assumed to provide no additional lateral stiffness and the overall modal damping of the structure is increased to represent the energy dissipative effect of the advanced connections in an approximate sense. In this case, the metric for assessing the equivalence of these two different damping processes is assumed to be the peak displacement response for the structure when subjected to the design earthquake. It should be noted that this approximation is similar to equating viscous and hysteretic work for a deformation cycle in order to define an equivalent viscous damping for simple SDOF systems with hysteretic damping.

In this case, the magnitude of the reduction in peak displacement to be achieved is defined on the basis of the peak displacement reductions determined from the time history nonlinear dynamic analysis with the optimal cladding connectors included. As noted in Table 4.5 in Section 4.4, there are several different feasible design objectives (labeled Cases a-f) depending on the overall levels of structural performance assumed for the cladding panels and the selected connectors. Response reduction ratios of from 13% to 41% can be selected from these results, and these are summarized in Table 4.14 below. The selected reduction factor is then applied to the baseline peak displacement figure of 29.68 inches (754 mm) to determine the new target peak displacement for the second iterative loop shown in the schematic diagram. The design result at Point B is a new "equivalent" value for the viscous modal damping to be used in subsequent RSA's.

Table 4.14 Peak Displacement Response Reduction Factors
for Optimal Cladding Connector Designs (from Table 4.5)

Case	Yield Force (kips)[a]	Stiffness (k/in)[b]	Max. Top Disp. (in)[c]	Disp. Reduction Factor (%)
a	20	364	13.50	41.4%
b	20	198	15.28	33.7%
c	20	137	16.48	28.5%
d	10	103	19.58	15.1%
e	10	57	20.00	13.2%
f	10	34	19.90	13.7%

[a] 1 kip = 4.448 kN
[b] 1 kip/in = 0.17512 MN/m
[c] 1 in = 25.4 mm

In the course of the above iteration loops, a family of spectral curves for modal damping values ranging from 5% to 20% are developed in GTSTRUDL for the Oakland ground motion (shown in Figure 4.3 in Section 4.2). Figure 4.16 below shows representative response spectra. The frame ductility is assumed to be 8, and this value is used to reduce the elastic response spectrum forces in GTSTRUDL to proper design levels consistent with code-level design forces. Full dead load (DL) and live load (LL) are combined with response spectrum analysis forces (RSA, acting to the right or left, + or -), which are reduced to inelastic values by dividing by the assumed ductility factor of 8 (i.e., RSA/8), to form the following load combinations for design (and redesign) of the frame:

$$[1.0\ DL + 1.0\ LL\ (+/-\ RSA)/8].$$

A representative deformed shape of the frame due to RSA is presented below in Figure 4.17.

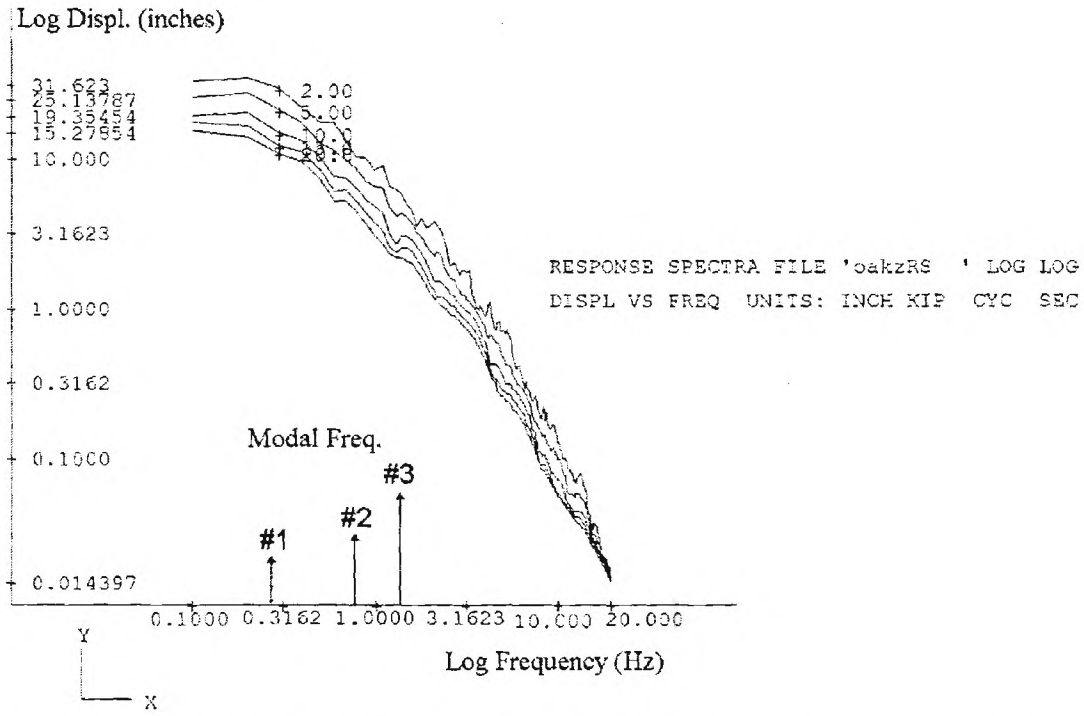

Figure 4.16 Response Spectrum Plots for Oakland Ground Motion (displacement, inches, vs frequency, Hz, for 2, 5, 10, 15, and 20% viscous damping)

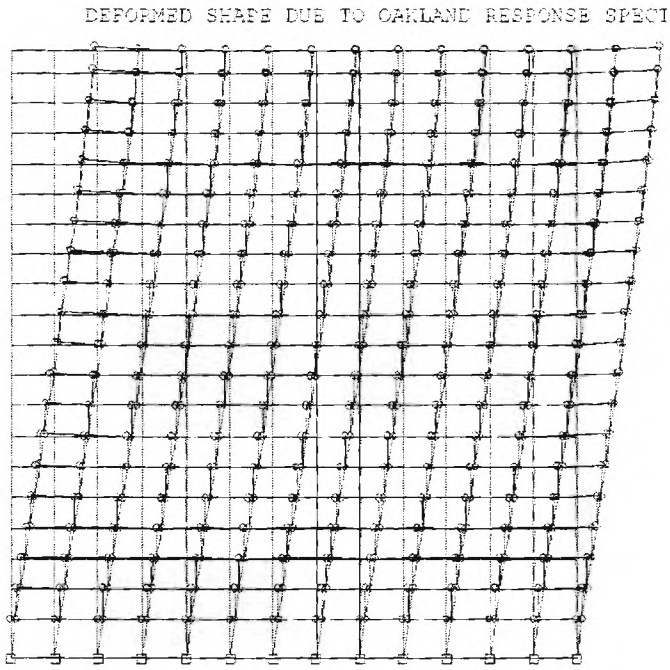

Figure 4.17 Plot of Displaced Shape of Frame Due to RSA for Oakland Ground Motion

Starting from Point B in the schematic diagram, (Fig. 4.14), the iteration loop shown on the right side of the figure represents the actual structural system redesign process to account for the presence of the advanced cladding connectors. The final RSA before Point B establishes the forces to be used in this redesign of the reference ("as-built") moment frame structure. These forces will be lower than previously used due to the added damping defined at Point B, and therefore the strength and stiffness of the structural system can be reduced by reduction in member sizes. To this end, automated member selection is performed in GTSTRUDL, and the moment frame is checked for compliance with ASD89 provisions for the load combinations specified by the previous RSA. It should be noted that ASD89 was used in the present study to more accurately approximate the original building structural design which was based on the 1982 Uniform Building Code. A36 steel was specified for beams and A572 steel for columns based on available information for the existing building. Columns were constrained to be W14 shapes in the GTSTRUDL member selection process and all columns were assumed to be braced by the composite floor deck about their minor axes. The top and bottom flanges of all beams were also assumed to be braced by the filler beams, but non-composite member properties were used for the beams in the analysis and design model. Finally, centerline dimensions were used in all calculations and shear deformations were ignored in the beams and columns.

The next step in this iteration process is to compute a new RSA for the new structural design and to compare the peak displacement response with the target value which is now taken as the original baseline value of 29.68 inches (754 mm). Using the baseline value insures that the modified structural system will be designed to the same serviceability level as the original structural system.

An iteration loop is called for only if the resulting peak response is greater than the target baseline value. In this case, it is necessary to increase the structural system member sizes in order to reduce the peak displacement to the target value, and one or more iterations may be required to accomplish this. On the other hand, if the resulting peak displacement is less than the target value, the design process is stopped. In this case it is assumed that the optimal cladding connector system is capable of a greater improvement in performance (e.g., reduction in peak displacement) than can be safely offset (e.g., within code specifications) by reductions in structural steel. As will be shown in the actual results presented below, if the optimal cladding connector design is based on the conservative selections of connector and cladding performance, more than one steel redesign iteration may be necessary to arrive at the final design. On the other hand, if the maximum levels of connector and cladding performance are assumed, the resulting peak displacement is less than the target value for a structural system that meets code provisions. This latter result implies that, in this case, the cladding system is designed to provide an excessive level of performance that may not be justified because a commensurate reduction in the structural system cannot be realized.

4.6.2 Redesign for Case F

The first redesign case considered is based on Case F in Table 4.14 and corresponds to a relatively conservative design in which the cladding is assumed to play a moderate role only (e.g., low yield force value, moderate initial stiffness). For this case, the top floor maximum displacement reduction factor was 13.7% with the advanced cladding connectors, and applying this to the baseline maximum displacement yielded a target value of 25.6 inches (651 mm). In the second iteration loop, the assumed modal damping was increased in successive iterations to

7.1% in order to achieve the reduced peak displacement target, and therefore to account for the added damping effects of the advanced cladding connectors.

Finally, the structural redesign on the right side of Figure 4.14 was executed. The beam member sizes for the redesigned configuration are shown in comparison to the as-built design in Table 4.15. In this case several iterations of the structure redesign loop on the right side of Figure 4.14 were required in order to bring the new peak displacement from 31.56 inches (802 mm) back to the baseline target value of 29.68 inches (754 mm). In order to accomplish this, the minimum member sizes for the beams had to be increased to the values as follows: (a) minimum W27 for levels 1-8; (b) minimum W24 for levels 9-18; (c) minimum W21x44 for levels 19-20. The weight of this structural frame was computed by GTSTRUDL to be 934.0 kips (4154 kN) which represents a 14.5% reduction compared to the baseline design. Table 4.16 compares the distribution of weight between the beams and the columns for this design. Table 4.17 compares the overall structural performance as measured by base shear, overturning moment and period. It is not surprising that the increased flexibility in the redesigned structural system yields lower values for the base shear and overturning moment but lengthens the fundamental period.

Table 4.15 Comparison of Steel Beam Sizes for the As-Built and Case F Redesign

Story Number	As-Built Beam Size	Case F Redesigned Beam Size
1	W30X116	W27X84
2	W30X99	W27X84
3	W30X99	W27X84
4	W30X99	W27X84
5	W30X99	W27X84
6	W30X99	W27X84
7	W30X99	W27X84
8	W27X94	W27X84
9	W27X94	W24X55
10	W27X94	W24X62
11	W27X94	W24X55
12	W27X94	W24X62
13	W27X94	W24X62
14	W24X76	W24X55
15	W24X76	W24X55
16	W24X68	W24X55
17	W24X68	W24X55
18	W24X68	W24X55
19	W24X68	W21X44
20	W21X44	W21X44

Table 4.16 Distribution of Structural Steel Weight Between Beams and Columns for the Baseline (isolated cladding) and Case F Configurations

Case	Damping (%)	Beam Weight (kips)[A]	Column Weight (kips)[A]
Baseline	4.9	402.8	666.6
Case F	7.1	308.0 (-30.8)*	626.0 (-6.5)*

[a]1 kip = 4.448 kN
* percent change with respect to baseline (as-built) case

Table 4.17 Response of GTSTRUDL Models Subjected to Oakland Response Spectra

Case	Damping	Total Base Shear (kips)[a]	Overturning Moment (kip-ft)[b]	Fundamental Period (sec)
Baseline	4.9%	3473	704,072	3.314
Case F	7.1%	2457	400,937	3.955

[a] 1 kip = 4.448 kN
[b]1 kip-ft = 1.356 kN-m

4.6.3 Redesign for Case C

A second redesign case is based on Case C in Table 4.14 and corresponds to a cladding connector system designed to achieve much higher levels of performance. In this case, the connector yield force is increased by a factor of 2 (10 kip to 20 kip) and the maximum dynamic ductility demand is maintained at a value of 50 (e.g., the connectors are assumed to have good low cycle fatigue characteristics). For this redesign case, the starting point was, again, Point A in Figure 4.14 with an assumed modal damping of 4.9% to match the baseline top floor maximum displacement. However, in the second iteration loop to adjust the damping value to account for the advanced cladding connectors, the target maximum displacement was reduced by 28.5% as indicated in Table 4.14 to a value of 21.22 inches (539 mm). The iteration loop converged with a damping value of 9.6%.

This damping value was then used in the redesign process shown on the right side of Figure 4.14 with the target peak displacement now set back to the baseline value of 29.68 inches (754 mm). In contrast to the situation for Case F above, in this case the member selection and design check (represented by the ASD block in the schematic) led to a peak displacement from the RSA that was only 27.37 inches (695 mm) which is less than the target baseline value. As a result no further steel redesign is possible since any further reduction in member sizes to achieve greater peak displacement would result in a design that fails to meet code provisions. As noted earlier, this situation indicates that the optimal cladding connectors are providing a greater reduction in the peak displacement than can be utilized to reduce structural member sizes without violating

design constraints (e.g., code provisions). The result, however, is a better design with lower peak displacement response for the design conditions.

Beam member sizes for the Case C redesigned configuration are shown in Table 4.18. The weight for this structural frame was computed by GTSTRUDL to be 889 kips (3954 kN) which represents a 20.3% reduction compared to the baseline design. Table 4.19 compares the distribution of weight between the beams and the columns for this design as well as for the Case F design considered previously. Table 4.20 compares the overall structural performance as measured by base shear, overturning moment and period for both Case F and Case C. Again, it is not surprising that the increased flexibility in the redesigned structural system yields lower values for the base shear and overturning moment but lengthens the fundamental period.

Table 4.18 Comparison of Steel Beam Sizes for the As-Built and Case C Redesign

Story Number	As-Built Beam Size	Case C Redesigned Beam Size
1	W30X116	W24X55
2	W30X99	W24X55
3	W30X99	W24X55
4	W30X99	W24X55
5	W30X99	W24X55
6	W30X99	W24X55
7	W30X99	W24X62
8	W27X94	W24X55
9	W27X94	W24X55
10	W27X94	W24X55
11	W27X94	W24X55
12	W27X94	W24X55
13	W27X94	W24X55
14	W24X76	W21X50
15	W24X76	W21X50
16	W24X68	W21X44
17	W24X68	W21X44
18	W24X68	W21X44
19	W24X68	W18X40
20	W21X44	W18X35

Table 4.19 Comparison of structural steel weight for the unclad and clad cases

Case	Damping (%)	Beam Weight (kips)[a]	Column Weight (kips)[a]	Steel Weight (kips)[a]
Baseline	4.9	403	667	1069
Case F	7.1	308 (-30.8%)*	626 (-6.5%)*	934 (-14.5%)*
Case C	9.6	238 (-69.3%)*	651 (-2.7%)*	889 (-20.3%)*

[a]1 kip = 4.448 kN
* percent change with respect to baseline (as-built) case

Table 4.20 Response of GTSTRUDL Models Subjected to Oakland Response Spectra

Case	Damping (%)	Total Base Shear (kips)[a]	Overturning Moment (kip-ft)[b]	Fundamental Period (sec)
Baseline	4.9	3473	704,072	3.314
Case F	7.1	2457	400,937	3.955
Case C	9.6	1736	276,272	4.535

[a] 1 kip = 4.448 kN
[b] 1 k-ft = 1.356 kN-m

5. Conclusions

5.1 Findings

This study has examined the application of so-called "advanced" cladding systems in building applications. This report began with a general review in Section 2 of literature related to architectural cladding and to passive energy dissipation and focused on the review of previous research by the authors and others in the particular area of passive energy dissipation using cladding. Of particular note is a doctoral study carried out by the authors' former student [Pinelli 1992] to develop an optimal design methodology for determining the design parameters for advanced cladding connectors.

On the basis of encouraging theoretical studies of systems utilizing special ductile cladding connections capable of developing passive energy dissipation for seismically induced interstory motion, an experimental study of possible advanced, ductile cladding connectors was undertaken and is described in Section 3. The present report summarizes results developed for three different kinds of advanced cladding connectors:

1. Flexural connector for tie-back applications
2. Composite (neoprene-flexure) connector for load bearing connections, and
3. Torsion connector.

The flexural connector studies were first described in an earlier Masters degree report and a Doctoral dissertation supervised by the authors, and the principal findings and results are summarized in this report. For all cases considered, very desirable and stable energy dissipation characteristics were observed for the simple tapered flexural connector designs considered. As a result, it is concluded that flexural connectors offer a viable, if not practical, approach to providing energy dissipation using the architectural cladding in a building.

The composite and torsion connector studies were carried out to explore the potential of more radical approaches. The composite connector was examined primarily for its ability to provide energy dissipation while also supporting the gravity load of a cladding panel. Several models were fabricated and tested and the results compared to simple design equations that were also developed. While it is not clear from the present study how such a connector might actually be employed in practical designs, the results strongly suggest that, if required, such a connector design is not only feasible but perhaps also practical. It might be pointed out that such connector designs might also find applications in structural designs where energy dissipation could be integrated into bearing systems (e.g., bridge designs and facilities designs).

The torsion connector concept developed in this report represents the most speculative application but it also offers the promise of a compact design and very efficient use of the working material. A detailed design model of such a connector is presented, but even though a prototype model was constructed, practical test results proved unattainable in the present study due to limitations in time and resources as well as manufacturing technology. Nonetheless, it is felt that this concept is very worthy of further investigation.

These experimental results along with the design equations for each configuration constitute an initial design resource for advanced ductile cladding connectors. While limited in the overall amount of test information, the results are broad in scope and cover a range of concepts that are thought to be viable for such applications.

Next, these results were applied, as described in Section 4, in a very practical study of how such advanced ductile cladding connectors might actually be utilized in a real building design. For this purpose, an actual 20 story steel frame structure in the US West Coast region was used. The present or baseline building design employs a traditional heavyweight cladding design using bearing connections at one end of the panels in conjunction with tie-back connections at the other to provide nearly total structural isolation of the cladding panels from the underlying structural system. In the present study, these isolating tie-back connectors were replaced with advanced ductile connectors typical of the kinds of designs studied in the laboratory testing part of the reported work. Numerical optimization methods were used to determine the design properties of these advanced connectors in order that they absorb (and dissipate) the greatest possible portion of the seismic energy input to the structure during a "design" earthquake. Practical constraints on maximum force and initial stiffness as well as on maximum dynamic ductility demand were added, the latter in order to insure a reliable service lifetime for more than one major seismic event over the building lifetime.

The design study considered two completely different (and complementary) objectives:

1. Use advanced connectors to provide an additional margin of performance (and safety) for the baseline building, and
2. Using advanced connectors to dissipate seismically induced energy and thereby to reduce structural demands, reduce the steel member sizes accordingly in order to provide essentially the same level of performance as for the baseline building, but in this case using less steel in the primary structure.

The first case is a relatively simple design problem involving addition of the advanced cladding connectors in place of the original tie-back connectors and no modifications to the baseline structure itself. For this case as described in Section 4.4, the optimally designed advanced cladding connectors provided a reduction in peak (top floor) displacements ranging from 13.2% to 41.4%, depending on the design assumptions for maximum force and maximum dynamic ductility demand in the connector.

The second design objective involves a more complex design problem as described in Section 4.6. For this case the automated design capabilities in the GTSTRUDL computer structural analysis program were used to redesign the steel frame structure in the longitudinal direction. This process utilized a response function type of analysis in which "equivalent" modal damping was added to represent the hysteretic damping provided by the advanced cladding connectors. Then the steel frame structure was redesigned to achieve comparable displacement response levels to the baseline building design but in this case using the higher modal damping equivalent to the additional passive hysteretic damping added by the optimally designed advanced connectors. Two different design cases were considered, and the overall savings in the weight of structural steel ranged from 14.5% to 20.3% compared to the baseline building design.

As a result of these studies, it is concluded that advanced ductile cladding connectors, when properly designed and applied to a suitable building, are capable of providing significant levels of performance improvement, either in terms of enhanced serviceability (e.g., reduced peak displacements) or in terms of reduced seismic demand on the primary structure (and consequent reduction in the needed structural materials).

5.2 Recommendations

The preliminary results described in this report suggest that advanced cladding systems could contribute to reduced response of actual building structures in seismic regions. While the use of architectural cladding systems to provide passive energy dissipation may not be appropriate for all building designs, the present results suggest that for those cases in which it is feasible, the performance improvement coupled with economic savings may justify its use. However, more research and study is obviously needed before this kind of a high-risk approach is actually attempted. In this connection, the following recommendations seem prudent:

1. Continue to conceive and test promising designs for advanced ductile cladding connectors in order to develop a library of feasible designs and to encourage commercial development of such devices.
2. Continue to carry out design studies involving the application of advanced ductile cladding connectors in a broader variety of building design problems.
3. Examine the design of cladding attachment systems in precast cladding panels and study how the interstory shear load introduced into the cladding panels by the action of the advanced connectors might be reliably carried.
4. Examine the feasibility of improving the interstory shear load-carrying capability of precast concrete cladding panels when specifically designed for this purpose.
5. Study the failure modes of such architectural cladding systems under extreme seismic loading and assess the implications for the present design methodology.

6.0 References

Alonso, L. J., 1989, "Mechanical Characteristics of X-Plate Energy Dissipators," CE 299 Report, University of California, Berkeley, May.

Anicic, D., Zamolo, M., and Soric, Z., 1980, "Experiments on Non-Structural Partition Walls Exposed to Seismic Forces," Proceedings, Seventh World Conference on Earthquake Engineering, Istanbul, Turkey, September 8-13, Vol. 6, pp. 144-150.

Arnold, C., Hopkins, D., and Elsesser, E., 1987, "Seismic Design of Architectural Elements," Final Report, Building Systems Development Inc., 3130 La Selva, San Mateo, California 94403, March.

Arnold, C., 1989, "Cladding Design: Recent Architectural Trends and Their Impact on Seismic Design," Proceedings, International Symposium on Architectural Precast Concrete Cladding - Its Contribution to Lateral resistance of Buildings, held in Chicago, Illinois, Nov. 8-9, pp. 14-31.

Becker, J.M., LLorente, C., and Mueller, P., 1980, "Seismic Response of Precast Concrete Walls," International Journal of Earthquake Engineering and Structural Dynamics, Vol.8, No6, November-December pp.545-564.

Bergman, D. M., and Hanson, R. D., 1988, "Characteristics of Mechanical Dampers," Proceedings, Ninth World Conference on Earthquake Engineering, Tokyo and Kyoto, Japan, August 2-9, Vol. VI, pp. 33-38.

Bergman, D. M., and Goel, S. C., 1987, "Evaluation of Cyclic Testing of Steel-Plate Devices for Added Damping and Stiffness," Report No. UCME 87-10, Department of Civil Engineering, University of Michigan, Ann Arbor, MI, November.

Blanchet, C., Craig, J. I., and Goodno, B. J., 1998, "Experimental Evaluation of Advanced Ductile Cladding Connector Designs for Passive Seismic Response Attenuation in Buildings," Proceedings, Sixth U.S. National Conference on Earthquake Engineering Research, Paper 320 on CDROM, Seattle, May 31-June 4.

Burdette, E. G., Jones, W. D. and Fricke, K. E., 1983, "Concrete Bearing Capacity around Large Inserts," Journal of Structural Engineering, Vol. 109, No. 6, June pp. 1375-1386.

Charney, F., and Harris, J. R., 1989, " The Effect of Architectural Precast Concrete Cladding on the Lateral Response of Multistory Buildings," Proceedings, International Symposium on Architectural Precast Concrete Cladding - Its Contribution to Lateral resistance of Buildings, held in Chicago, Illinois, Nov. 8-9, pp. 80-96.

Charney, F., 1996, "Nonlin Pro User Guide," Advanced Structural Concepts, 2221 East Street , Suite 204, Golden, Colorado 80401.

"Cladding Solution Sought," Engineering-News Record, Vol 220, June 23, 1988, pp. 30.

Clough, R. W., Malhas, F., and Oliva, M.G., 1989, "Seismic Behavior of Large Panel Precast Concrete Walls: Analysis and Experiment," PCI Journal, September-October, pp.42-66.

Cohen, J. M., and Powell, G. H,, 1991, "A Preliminary Study on Energy Dissipating Cladding-to-Frame Connections," Report No. UCB/EERC-91/09, EERC, University of California, Berkeley, California, September, 73 pages.

Costes, D., Jalil, W., Souloumiac, R., 1992, "Comportement des Bâtiments," Annales de l'Institut Technique du Bâtiment et des Travaux Publics, No. 502 - March-April pp. 46-48.

Craig, J. I., Leistikow, R., and Fennell, C. J., 1988, "Experimental Studies of the Performance of Precast Cladding Connections," Proceedings , Ninth World Conference on Earthquake Engineering, held in Tokyo and Kyoto, Japan on August 2-9, Vol. VI, pp. 201-206.

Craig, J.I., Goodno, B.J., Keister, M.J., and Fennell, C.J., 1986, "Hysteretic Behavior of Precast Cladding Connections," Proceedings, Third ASCE Engineering Mechanics Specialty Conference on Dynamic Response of Structures, held at UCLA on March 31-April 2, pp. 817-826.

Das, S. K., 1986 ,"A Study of Exterior facades - Problems and Solutions," Proceedings, Application and Performance of Structural Materials and Exterior Facades, edited by James W. Richardson, Jr., ASCE Convention, Boston, MA.

Dubas, P., 1972, "Interaction of Structural Elements with Cladding," Proceedings, Planning and Design of Tall Buildings, 1972 ASCE-IABSE International Conference, Vol. 2, No 17-5, ASCE, New-York, pp. 675-686.

El-Gazairly, L.F., and Goodno, B.J., 1989, "Dynamic Analysis of a Highrise Building Damaged in the Mexico Earthquake Including Cladding-Structure Interaction," Proceedings, International Symposium on Architectural Precast Concrete Cladding - Its Contribution to Lateral resistance of Buildings, held in Chicago, Illinois, Nov. 8-9, pp. 257-286.

El-Gazairly, L.F., and Goodno, B.J., and Craig, J. I., 1990, "Analytical Investigation of Advanced Connections for Precast Cladding on Buildings," Proceedings, The Fourth U.S. National Conference on Earthquake Engineering, held in Palm Springs, California, on May 20-24 Vol. 2, pp. 441-450.

El-Gazairly, L.F., and Goodno, B.J., and Craig, J. I., 1992, "Nonlinear Dynamic Analysis of RC Structures with Precast Cladding Using GT-IDARC," Proceedings, The Eighth ASCE Specialty Conference on Computing in Civil Engineering, Dallas, TX., June 7-9.

Englekirk, R., 1989, "Toward a More Effective Use of Precast Concrete Cladding," Proceedings, International Symposium on Architectural Precast Concrete Cladding - Its Contribution to Lateral resistance of Buildings, held in Chicago, Illinois, Nov. 8-9, pp. 4-13.

Elsesser, E., 1986, "A Survey of Seismic Structural Systems and Design Implications," Proceedings, Seminar and Workshop on Base Isolation and Passive Energy Dissipation, ATC, San Francisco, CA, March 12-14, pp 51-62.

"Facades: Errors Can Be Expensive," Engineering-News Record, Vol 204, No. 5, January 24, 1980, pp. 30-34.

Fintel, Mark, 1986, "Performance of Precast and Prestressed Concrete in Mexico Earthquake," PCI Journal, January-February, pp. 18-42.

Freeman, S. A., 1989, "Participation of Architectural Precast Concrete Cladding in Resisting Lateral Forces in Regions of High Seismicity," Proceedings, International Symposium on Architectural Precast Concrete Cladding - Its Contribution to Lateral resistance of Buildings, held in Chicago, Illinois, Nov. 8-9, pp. 32-35.

Freeman, S. A., 1998, personal communications.

Gaiotti, R., and Smith, B. S., 1992, "Stiffening of Moment-Resisting Frame by Precast Concrete Cladding," PCI Journal, September-October Vol. 37, no. 5, pp. 80-92.

Gjelsvik, A., 1974, "Frames and Precast Panels Walls," J. of the Struct. Div., ASCE, Vol 100, No ST2, February pp.405-426.

Glogau, O. A., 1977, "Damage Control in New Zealand Public Buildings Through Separation of Non-Structural Components," Proceedings, Sixth World Conference on Earthquake Engineering, Sarita Prakashan, Meerut, India, Vol. 5, pp.43-48.

Goodno, B.J., and Palsson, H., 1981, "Torsional Response of Partially Clad Structures," Proceedings, Conference on Earthquakes and Earthquake Engineering in the Eastern U.S., September.

Goodno, B.J., Craig, J.I., Meyyappa, M., and Palsson, H., 1983, "Cladding-Structure Interaction in Highrise Buildings," Final Report, NSF Grant No. CEE-7704269, (NTIS Report No. PB83-195891), January, 614 pages.

Goodno, B.J., Palsson, H.P., and Pless, D.G., 1984, "Localized Cladding Response and Implications for Seismic Design," Proceedings, Eighth World Conference on Earthquake Engineering, San Francisco, CA, July 21-28, Vol. V, pp. 1143-1150.

Goodno, B.J., 1986, "Cladding-Structure Interaction: The State of the Art," Invited Presentation, 1986 ASCE Structures Congress, held in New Orleans, La., Sept. 15-18, (see Structures Congress '86 Abstracts, ASCE, p. 271).

Goodno, B.J., and Palsson, H., 1986a, "Analytical Studies of Building Cladding," Journal of Structural Engineering, ASCE, Vol. 112, No. 4, Paper 20498, April pp. 665-676.

Goodno, B.J., and Pinelli, J.P., 1986b, "The Role of Cladding in Seismic Response of Lowrise Buildings in the Southeastern U.S.," Proceedings, The Third U.S. National Conference on Earthquake Engineering, held in Charleston, S.C., on August 24-28, Vol. II, pp. 883-894.

Goodno, B.J., and Naman, S.K., 1986c, "Earthquake Analysis of Lowrise Buildings in Zones of Moderate Seismicity," Proceedings, Eighth European Conference on Earthquake Engineering, held in Lisbon, Portugal, on September 7-12, Vol. 8, pp. 79-86.

Goodno, B. J., Craig, J. I., and Zeevaert-Wolff, 1987, "Behavior of Architectural Nonstructural Components in the Mexico Earthquake - First Progress Report," Proceedings, First U.S.-Mexico Workshop on 1985 Mexico Earthquake Research, held in Mexico City on November 16-18, 1986, pp. 85-90, published by Earthquake Engineering Research Institute (EERI), April.

Goodno, B. J., Craig, J. I., and Zeevaert-Wolff, 1987, "Behavior of Architectural Nonstructural Components in the Mexico Earthquake - Second Progress Report," Proceedings, 2ND U.S.-Mexico Workshop on 1985 Mexico Earthquake Research, held in Mexico City on November 5-7, 1987, 6 pages, published by Earthquake Engineering Research Institute (EERI), November.

Goodno, B. J., Craig, J. I., and Zeevaert-Wolff, 1988, "Behavior of Architectural Nonstructural Components in the Mexico Earthquake - Third Progress Report," 7 pages, Earthquake Engineering Research Institute (EERI), May.

Goodno, B. J., and Craig, J. I., 1988, "Advanced Seismic Design Methods for Precast Cladding," Report SSRP-88/08, Precast Seismic Structural Systems Workshop, Structural Systems Research

Project, Dept. of Applied Mechanics and Engineering Sciences, University of California - San Diego, ed. by M. J. N. Priestly, Nov.

Goodno, B. J., Meyyappa, M., and Nagarajaiah, S., 1988, "A Refined Model for Precast Cladding and Connections," Proceedings, Ninth World Conference on Earthquake Engineering, held in Tokyo and Kyoto, Japan on August 2-9, Vol. VI, pp. 195-200.

Goodno, B. J., Craig, J. I., and Zeevaert Wolff, A., 1989, "Behavior of Architectural Nonstructural Components in the Mexico Earthquake," Earthquake Spectra, EERI, Vol. 5, No. 1, February pp. 195-222.

Goodno, B., Craig, J., and Hsu, C-C, 1991, "Experimental Studies and Analytical Evaluation of Ductile Cladding Connections," Proceedings, Fifth South Pacific Regional Conference on Earthquake Engineering, New-Zealand, November 20-23.

Goodno, B. G., Craig, J. I. and Calise, A. J., 1992a, "Hybrid Control of Building Seismic Response Using Architectural Cladding: Overview and Preliminary Results," US/China/Japan Trilateral Seminar/Workshop on Structural Control, Shanghai, China, October 5-7

Goodno, B., Craig, J., El-Gazairly, L. and Hsu, C-C, 1992b, "Use of Advanced Cladding Systems for Passive Control of Bldg. Response in Earthquakes," Proceedings, 10th World Conference on Earthquake. Engineering, July 19-24, Madrid, Spain, vol7, pp.4195-4200.

Gram, K. G., 1976, "The Shear Effects of Precast Cladding Panels on Multistory Buildings," M.S.C.E. Special Problem Report, School of Civil Engineering, Georgia Institute of Technology, Atlanta, Georgia, June.

Grigorian, C. E., Yang, T. S., and Popov, E. P., 1987, "Slotted Bolted Connection Energy Dissipators," Earthquake Spectra, Vol. 9, No. 3, pp. 491-504.

Hegle , R. L., 1989, "Connection of Cladding to Multi-Story Structures,' Proceedings, International Symposium on Architectural Precast Concrete Cladding - Its Contribution to Lateral resistance of Buildings, held in Chicago, Illinois, Nov. 8-9, pp. 192-201.

Henry, R. M., 1980, "Cladding-Frame Interaction of a Reinforced Concrete Building," Ph.D. Thesis, Department of Civil and Urban Engineering, University of Pennsylvania, Pennsylvania.

Henry, R. M., and Roll, F., 1986, "Cladding-Frame Interaction," Journal of Structural Engineering, ASCE, Vol. 112, No. 4, Proc. Paper 20546, April pp. 815-834.

Henry, R. M., Kennedy, D., and Goodspeed, C. H., 1989, "A Simplified Box Frame Model for Structural Cladding Panels," Proceedings, International Symposium on Architectural Precast Concrete Cladding - Its Contribution to Lateral resistance of Buildings, held in Chicago, Illinois, Nov. 8-9, pp. 62-79.

Hotz, R. W., 1982, "Special Considerations in Designing Cladding Attachments," Modern Steel Construction, Third Quarter.

Hsu, C. C., 1991, "Integrated Analyses of a Cladding-Frame System with Nonlinear Panel to Structure Connections," M.S.C.E. Special Research Problem Report, School of Civil Engineering, Georgia Institute of Technology, Atlanta, Georgia, May.

Iverson, J. K., 1989, "Concrete Cladding Connections in Earthquake Country," Proceedings, International Symposium on Architectural Precast Concrete Cladding - Its Contribution to Lateral resistance of Buildings, held in Chicago, Illinois, Nov. 8-9, pp. 202-216.

Kallros, M. K., 1987, "An Experimental Investigation of the Behavior of Connections in Thin Precast Concrete Panels Under Earthquake Loading," M.S. Thesis, Department of Civil Engineering, University of British Columbia, Vancouver, Canada, April, 214 pages.

Kareem, A., 1986, "Performance of Cladding in Hurricane Alicia," Journal of Structural Engineering, ASCE, Vol. 112, No 12, Proceedings Paper 21121, December, pp. 2679-2693.

Keister, M. J., 1983, "Testing and Evaluation of Wedge-Type Precast Concrete Inserts Subjected to Pullout," M.S.C.E. Special Problem Report, School of Civil Engineering, Georgia Institute of Technology, Atlanta, Georgia, March.

Kelly, J. M., Skinner, R. I., and Heine, A. J., 1972, "Mechanisms of Energy Absorption in Special Devices for Use in Earthquake Resistant Structures," Bulletin of New Zealand Society for Earthquake Engineering, Vol.5, No 3, September.

Kemeny, Z., and Lorant, J., 1989, "Energy Dissipating Elastomeric Connections," Proceedings, International Symposium on Architectural Precast Concrete Cladding - Its Contribution to Lateral resistance of Buildings, held in Chicago, Illinois, Nov. 8-9, pp. 287-299.

Key, D. E., 1984, " The Seismic Performance of Energy Absorbing Dampers in Building Structures," Bulletin of the New Zealand National Society for Earthquake Engineering, 17 (1), March, pp. 38-46.

Khan, Z., 1997, "Analytical and Experimental Evaluation of an Advanced Cladding Connector," M.S. Special Problem Report, School of Aerospace Engineering, Georgia Institute of Technology, December.

Klingner, R. E. and Mendonca, J. A., "1982, Tensile Capacity of Short Anchor Bolts and Welded Studs: Literature Review," ACI Journal, July-August, pp. 270-279.

Klingner, R. E. and Mendonca, J. A., 1982, "Shear Capacity of Short Anchor Bolts and Welded Studs: Literature Review," ACI Journal, September-October, pp. 339-349.

Kulka, F., Lin, T. Y., and Yang, Y. C., 1975, "Prestessed Concrete Building Construction Using Precast Wall Panels," PCI Journal, Vol. 20, No. 1, January-February, pp. 62-73.

Kunnath, S., Reinhorn, A. M., 1989, "Inelastic Three-Dimensional Response Analysis of Reinforced Concrete Building Structures (IDARC-3D)," Technical Report NCEER-89-0011, State University of New York at Buffalo, April.

Le Boeuf, Pierre Marcel Serge, 1981, "Dynamic Cladding-Structure Interaction in Highrise Buildings," M.S.C.E. Thesis, School of Civil Engineering, Georgia Institute of Technology, Atlanta, Georgia, 129 pp.

Lee, D. J., 1971, "The Theory and Practice of Bearings and Expansion Joints for Bridges", Cement and Concrete Association, London.

Leistikow, R., 1988, "The Behavior of the Ductile Rod/Push-Pull Connection for Precast Cladding Panels," M.S.C.E. Special Problem Report, School of Civil Engineering, Georgia Institute of Technology, Atlanta, Georgia, March, 252 pp.

Mahmoodi, P., 1969, "Structural Dampers," Journal of Structural Engineering, ASCE, Vol. 95, No. ST8, Paper 6725, August, pp. 1661-1672.

Matthewson, C.D. , and Davey, R.A., 1979, "Design of an Earthquake Resisting Building Using Precast Concrete Cross-Braced Panels and Incorporating Energy Absorbing Devices," Bulletin of the New Zealand National Society for Earthquake Engineering, 12 (4), pp. 340-349.

McCabe, S. L., and Hall, W. J., 1989, "Assessment of Seismic Structural Damage," Journal of Structural Engineering, Vol. 115, No. 9, September, pp. 2166-2183.

McCue, G.M., 1975, "Building Enclosure and Finish Systems: Their Interaction with the Primary Structure During Seismic Action," Proceedings, U.S. National Conference on Earthquake Engineering, Ann Arbor, Michigan, June 18-20, pp. 235-244.

McCue, G.M., Skaff, A., and Boyce, J., 1978, "Architectural Design of Building Components for Earthquakes," MBT Associates, San Francisco, California.

Meyer, G., Hatfield, H., 1987, "Crossing Out Cladding Alternative. Placement of Cruciform Panels Causes Headaches for Contractors," Engineering News Record, v. 218, p. 26-27, April.

Meyyappa, M., Palsson, H., and Craig, J.I., " Modal Parameter Estimation for a Highrise Building Using Ambient Response Data Taken During Construction," Proceedings, 2nd Specialty Conference on Dynamic Response of Structures: Experimentation, Observation, Prediction, and Control, Atlanta, Georgia, January 1981, pp. 141-151.

Meyyappa, M., Goodno, B. J., and Fennell, C. J., 1988, "Modeling and Performance of Precast Cladding Connections," Proceedings, The Fifth ASCE Specialty Conference on Computing in Civil Engineering, held in Alexandria, Va., on March 29-31, pp. 209-218.

Meyyappa, M., and Craig, J. I., 1984, "Highrise Building Identification Using Transient Testing," Proceedings, Eighth World Conference on Earthquake Engineering, San Francisco, CA, July 21-28, Vol. VI, pp. 79-86.

Moor, C., 1992, "Analytical and Experimental Evaluation of Advanced Cladding Connections," M.S.C.E. Thesis, School of Civil Engineering, Georgia Institute of Technology, Atlanta, Georgia, April, 123 pp.

Morris, A.E.J., 1978, "Precast Concrete in Architecture," Whitney, New York.

Mueller, P., and Becker, J.M., 1980, "Seismic Behavior of Precast Walls Coupled Through Vertical Connections," Proceedings, Seventh World Conference on Earthquake Engineering, Istambul, Turkey, September 3-13, Vol 7, pp. 23-30.

Oliva, M. G., and Shahrooz, B. M., 1984, " Shaking Table tests of Wet Jointed Precast Panel Walls, Proceedings, Eighth World Conference on Earthquake Engineering, San Francisco, California, July 21-28.

Osborn, A. E. N., Meinhert, D. F., and Hanson, J. M., 1981, "Cyclic and Monotonic Shear Tests on Connections Between Precast Concrete Panels," WJE No. 77578, Wiss, Janey, Elstner and Associates, Inc., Northbrook, Illinois, 133pp.

Oppenheim, I.J., 1973, "Dynamic Behavior of Tall Buildings with Cladding," Proceedings, Fifth World Conference on Earthquake Engineering, Rome, Italy, June, pp. 2769-2773.

Pall, A. S., and March, C., 1980, "Optimum Seismic Resistance of Large Panel Structures Using Limited Slip Bolted Joints," Proceedings, Seventh World Conference on Earthquake Engineering, Istambul, Turkey, September 3-13, Vol 4, pp. 177-184.

Pall, A. S., 1989, "Friction Damped Connections for Precast Concrete Cladding," Proceedings, International Symposium on Architectural Precast Concrete Cladding - Its Contribution to Lateral resistance of Buildings, held in Chicago, Illinois, Nov. 8-9, pp. 300-310.

Palsson, H., and Goodno, B. J., 1982a, "A Degrading Stiffness Model for Precast Concrete Cladding," Proceedings, Seventh European Conference on Earthquake Engineering, Athens, Greece, September 20-25.

Palsson, H., 1982b, "Influence of Nonstructural Cladding on Dynamic Properties and Performance of High-rise Buildings," Ph.D. Thesis, School of Civil Engineering, Georgia Institute of Technology, Atlanta, Georgia, December, 427 pp..

Palsson, H., and Goodno, B. J., 1988, "Influence of Interstory Drift on Cladding Panels and Connections," Proceedings, 9th World Conference on Earthquake Engineering, held in Tokyo and Kyoto, Japan on August 2-9.

Palsson, H.P., Goodno, B.J., Craig, J.I., and Will, K.M., 1984, "Cladding Influence on Dynamic Response of Tall Buildings," Earthquake Engineering and Structural Dynamics Journal, Vol. 12, No. 2., March-April, pp. 215-228.

PCI Manual on Design and Typical Details of Connections for Precast and Prestressed Concrete, Second Edition, 1988, Prestressed Concrete Institute, 175 W. Jackson Blvd., Chicago, Illinois 60604.

PCI Design Handbook: Precast and Prestressed Concrete, 1985, Third Edition, Prestressed Concrete Institute, Chicago, Illinois.

Peier, Walter H., 1982, "Model for Pull-Out Strength of Anchors in Concrete," Journal of Structural Engineering, ASCE, Vol. 109, No. 5, May, pp. 1155-1173.

Pinelli, J.-P., 1984, "Seismic Behavior of Low-rise Steel Buildings," MSCE Special Problem Report, School of Civil Engineering, Georgia Institute of Technology, Atlanta, Georgia, March.

Pinelli, Jean-Paul, Craig, J. I., and Goodno, B. J., 1990, "Development of Advanced Concepts for Precast Cladding," Proceedings, ATC-29 Seminar: Seismic Design and Performance of Equipment and Nonstructural Elements in Buildings and Industrial Structures, held in Irvine, California, October 3-4, pp. 26.1-26.11.

Pinelli, J.-P., Moor, C., Craig, J. I., and Goodno, B. J., 1992, "Experimental Testing of Ductile Cladding Connections for Building Facades," International Journal of the Structural Design of Tall Buildings, John Wiley and Sons, Inc., Vol. 1, No. 1, October, pp. 57-72.

Pinelli, J. P. 1992, "Development of Energy Dissipating Cladding Connections for Passive Control of Building Seismic Response." Ph.D. dissertation, School of Civil Engineering, Georgia Institute of Technology, Atlanta, Georgia, November.

Pinelli, J. P., C. Moor, J. I. Craig, and B. J. Goodno. 1996, "Testing of Energy Dissipating Cladding Connections," Earthquake Engineering and Structural Dynamics, Vol. 25, pp. 129-147.

Pinelli, J.-P., Craig, J. I., Goodno, B. J., and Hsu, C. C., 1993, "Passive Control of Building Response Using Energy Dissipating Cladding Connections," Earthquake Spectra, Vol. 9, No. 3, pp.529-546.

Pless, D. G., 1982, "Static and Dynamic Response of Precast Cladding to Interstory Drift," MSCE Special Problem Report, School of Civil Engineering, Georgia Institute of Technology, Atlanta, Georgia, March, 259 pp.

Powell, G. H., 1973, "DRAIN-2D User's Guide," Report Number EERC 73-22, University of California, Berkeley.

Powell, G., and Schricker, V., 1977, "Ductility Demands on Joints in Large Panel Structures," Proceeding, (Meeting Preprint No 3022, 21 pp.), ASCE Fall Convention, San Francisco, October 17-21.

Prakash, V., Powell, G. H., and Campbell, S., 1993, "DRAIN-2dx Base Program Description and User Guide," Version 1.10, Dept. of Civil Engineering, University of California Berkeley, November.

Priestley, M. J. N., editor, 1988, "Precast Seismic Structural Systems Workshop," Structural Systems Research Project, Dept. of Applied Mechanics and Engineering Sciences, University of California - San Diego, Rept. SSRP-88/08, Nov.

Raths, C. H., and Mulholland, G. R., 1989, "Non-Load Bearing Precast Concrete Panel Shear Wall Type Behavior," Proceedings, International Symposium on Architectural Precast Concrete Cladding - Its Contribution to Lateral resistance of Buildings, held in Chicago, Illinois, Nov. 8-9, pp. 62-79.

Reed, D. A., 1987, "Risk Assessment for Cladding Panels: an Expert Systems Approach," Proceedings, Dynamic of Structures, Structures Congress'87, held in Orlando, Florida, pp. 556-560.

Reinhorn, A. M., Soong, T.T., Lin, R. C. and Wang, Y. P., 1989, "1/4 Scale Model Studies of Active Tendon Systems and Active Mass Dampers for Aseismic Protection", NCEER Report No. 89-0026, November.

Rihal, S. S., 1988a, "Earthquake Resistance and Behavior of Heavy Facades/Claddings and Connections in Medium-Rise Steel-Framed Buildings," Proceedings , Ninth World Conference on Earthquake Engineering, held in Tokyo and Kyoto, Japan on August 2-9, Vol. VI, pp. 207-212.

Rihal, S. S., 1988b, "Seismic Behavior and Design of precast Facades, Cladding and Connections in Low/Medium-Rise Buildings," Report ARCE R88-1, California Institute of Technology, November.

Rihal, S. S., 1989, "Earthquake Resistance and Behavior of APCC and Connections," Proceedings, International Symposium on Architectural Precast Concrete Cladding - Its Contribution to Lateral resistance of Buildings, held in Chicago, Illinois, Nov. 8-9, pp. 110-140.

Robinson, W.H., and Greenbank, L.R., 1976, "An Extrusion Energy Absorber Suitable for the Protection of Structures during an Earthquake," Earthquake Engineering and Structural Dynamics, Vol.4, pp. 251-259.

Sack, R. L. and Perry, D., 1981, "Seismic Behavior of Precast Curtain Walls in High-rise Buildings," Final Report, NSF Grant No. PFR-7720884, Department of Civil Engineering, University of Idaho, Moscow, Idaho, January, 328 pp.

Sack, R. L., Beers, R. J., Thomas, D. L., 1989, "Seismic Behavior of Architectural Precast Concrete Cladding," Proceedings, International Symposium on Architectural Precast Concrete Cladding - Its Contribution to Lateral resistance of Buildings, held in Chicago, Illinois, Nov. 8-9, pp. 141-158.

Sands, H., 1986, "Wall Systems: Analysis by Details," McGraw-Hill Book Company, New York.

Schneider, S., Lee, H. M. & Godden, W. G., 1983, "Piping Seismic Test with Energy-Absorbing Devices," Final Report, EPRI-NP-2902, Research Project 1586-1, EERC, College of Engineering, University of California, Berkeley, California, March.

Scholl, R. E., 1988, "Added Damping and Stiffness Elements for Earthquake Damage and Loss Control." Proceedings of Conference XLI: A Review of Earthquake Research Applications in the National Earthquake Hazards Reduction Program: 1877-1987, U.S. Geological Survey Open File, Report No. 88-13-A, San Diego, CA.

Shaikh, A. Fattah and Yi, Whayong, 1985, "In-Place Strength of Welded Headed Studs," PCI Journal, March-April.

Sherwood, G. C., 1975, "Effects of Precast Concrete Panels on the Stiffness of the 100 Colony Square Building," M.S.C.E. Special Problem Report, School of Civil Engineering, Georgia Institute of Technology, Atlanta, Georgia, August.

Skidmore, Owings, and Merrill, 1986, "Facades/Cladding Systems Design Data, San Francisco, California.

Skinner, R. I., Kelly, J. M., and Heine, A. J., 1973, "Energy Absorption Devices for Earthquake Resistant Structures," Proceedings, Fifth World Conference on Earthquake Engineering, Rome, Italy, June, pp. 2924-2933.

Skinner, R. I., Kelly, J. M., and Heine, A. J., 1975, "Hysteretic Dampers for Earthquake-Resistant Structures," Earthquake Engineering and Structural Dynamics, Vol.3, pp. 287-296.

Skinner, R. I., Beck, J.L., and Bycroft, G.N., 1975, "A Practical System for Isolating Structures from Earthquake Attack," Earthquake Engineering and Structural Dynamics, Vol.3, pp. 297-309.

Skinner, R. I., Heine, A. J., and Tyler, R.G., 1977, "Hysteretic Dampers to Provide Structures with Increased Earthquake Resistance," Proceedings, Sixth World Conference on Earthquake Engineering, Sarita Prakashan, Meerut, India, pp. 1319-1325.

Skinner, R. I., Tyler, R.G., Heine, A. J., and Robinson, W.H. 1980, "Hysteretic Dampers for the Protection of Structures from Earthquakes," Bulletin of the New Zealand Society for Earthquake Engineering, Vol.13, No 1, March.

Smith, B. S., and Gaiotti, R., 1989a, "Interaction of Precast Concrete Cladding with a Story-Height Frame Module," Proceedings, International Symposium on Architectural Precast Concrete Cladding - Its Contribution to Lateral resistance of Buildings, held in Chicago, Illinois, Nov. 8-9, pp. 48-61.

Smith, B. S., and Gaiotti, R., 1989b, "Effect of Precast Concrete Cladding on Static Wind Load Response of a Moment Resisting Frame Structure," Proceedings, International Symposium on Architectural Precast Concrete Cladding - Its Contribution to Lateral resistance of Buildings, Chicago, Illinois, Nov. 8-9, pp. 97-109.

Soong, T. T., Masri, S. F., and Housner, G. W., 1991, "An Overview of Active Structural Control under Seismic Loads," Earthquake Spectra, Vol. 7, No. 3, August, pp.483-505.

Spencer, R. A., 1971, "The Earthquake Response of Prestressed Concrete Structures with Nonstructural Interfloor Elements," Proceedings, First Canadian Conference on Earthquake Engineering, Vancouver, British Columbia, May, pp.354-366.

Spencer, R. A. and Neille, D. S., 1976, "Cyclic Tests of Welded Headed Stud Connections," PCI Journal, May-June, Vol. 21, No. 3, pp. 67-78.

Spronken, J. R., 1989, "Detailing of Cladding for Deformations," Proceedings, International Symposium on Architectural Precast Concrete Cladding - Its Contribution to Lateral resistance of Buildings, Chicago, Illinois, Nov. 8-9, pp. 184-191.

Stein, C., 1983, " A comparative Study of the Effects of Cladding Panel Modeling on a Structure's Static and Dynamic Behavior," Thesis, University of New Hampshire.

Stockbridge, J. G., 1984, "Experimental Methods for Evaluating the Condition of Facades to resist Seismic Forces," Proceedings, Eighth World Conference on Earthquake Engineering, San Francisco, California, July 21-28, Vol. VI, pp. 71-78.

"Symposium Tags Ignorance as Root of Facade Problems," 1980, Engineering-News Record, Vol 204, No 24, December 11, pp. 17-19.

Thiel Jr., C. C., Elsesser, E. Jones, L., Kelley, T, Bertero, V., Filippou, F., and McCann, R. , 1986, "A Seismic Energy Absorbing Cladding System: a Feasibility Study," Proceedings, Seminar and Workshop on Base Isolation and Passive Energy Dissipation, ATC, San Francisco, CA, March 12-14.

Tomasetti, R. L., Gutman, A., Lew, I. P., and Joseph, L. M., 1986, "Development of Thin Wall Cladding to Reduce Drift in High-Rise Buildings," Reports of the Working Commissions, International Association for Bridge and Structural Engineering, Vol. 49, pp. 239-246, Zurich, Switzerland.

Tyler, R.G., 1977, "Damping in Building Structures by Means of PTFE Sliding Joints," Bulletin of the New Zealand Society for Earthquake Engineering, Vol.10, No 3, September.

Tyler, R.G., 1978a, "A Tenacious Base Isolation System Using Round Steel Bars," Bulletin of the New Zealand Society for Earthquake Engineering, Vol.11, No 4, pp. 273-281,December.

Tyler, R.G., 1978b, "Tapered Steel Energy Dissipators for Earthquake Resistant Structures," Bulletin of the New Zealand Society for Earthquake Engineering, Vol.11, No 4, pp 282-294, December.

Ueda T., Kitipornchai, S., and Ling, K., 1990, " Experimental Investigation of Anchor Bolts Under Shear," Journal of Structural Engineering, ASCE, Vol. 116, No. 4, April, pp. 910-924.

Vanderplaats, G. N., 1993, DOT Users Manual, Version 4.00, VMA Engineering, Goleta, CA.

Wang, Marcy Li, 1987, "Cladding Performance on a Full Scale Test Frame," Earthquake Spectra, EERI, Vol. 3, No. 1, February, pp. 119-173.

Wang, Marcy Li, 1986, "Full Scale Test of Cladding Components," Proceedings, Third Conference on Dynamic Response of Structures, UCLA, Los Angeles, California, March 31-April 2, pp. 495-504.

Whittaker, A.S., Bertero, V.V., Thompson, C.L., and Alonso, L.J., 1991, "Seismic Testing of Steel Plate Energy Dissipation Devices," Earthquake Spectra, Vol. 7, No 4, November, pp. 563-604.

Will, K. M., Goodno, B. J., and Saurer, G., 1979, "Dynamic Analysis of Buildings with Precast Cladding," Proceedings, ASCE Seventh Conference on Electronic Computation, St Louis, Missouri, August 6-8, pp. 251-264.

Wolz, M. W., 1991a, "Nonlinear Interaction Between Building Structural Systems and Nonstructural Cladding," M.S.C.E. Master Thesis, School of Civil Engineering, Georgia Institute of Technology, Atlanta, Georgia, January, 130pp.

Wolz, M. W., Hsu, C., and Goodno, B. J., 1990, "Nonlinear Interaction Between Building Structural Systems and Nonstructural Cladding Components," Proceedings, ATC-29 Seminar: Seismic Design and Performance of Equipment and Nonstructural Elements in Buildings and Industrial Structures, held in Irvine, California, October 3-4, pp. 25.1 25.12.

Wolz, M. W., Hsu, C., El-Gazairly, L. F., Goodno, B. J., and Craig, J. I., 1991b, "Nonlinear Dynamic Analysis of Buildings with Advanced Cladding Connections, Proceedings,-ASCE Seventh Conference on Computing in Civil Engineering and Symposium on Data Bases, Washington, D. C., May 6-8, pp. 729-738.

Young, P. J., Reinhorn, A.M., and Kunnath, S.K., 1987, "IDARC: Inelastic Damage Analysis of Reinforced Concrete Frame-Shear Wall Structures," Technical Report NCEER-87-0008, State University of New York at Buffalo, July.

Zhang, R.-H., Soong, T. T., and Mahmoodi, P. , 1989, "Seismic Response of Steel Frame Structures with Added Viscoelastic Dampers," Earthquake Engineering and Structural Dynamics, Vol.18, pp. 389-396.

Appendices

A. *Listings of modified DRAIN-2dx routines*

The modifications to DRAIN-2dx (Version 1.10) were limited to subroutines that are associated with the TYPE04 element and are included in program modules: ANAL04.FOR and INEL04.FOR. Only the specific subroutines in each module that were changes are listed below and the changes are noted with the comment string: "!NIST mod" at the end of each affected line.

A.1 ANAL04 Subroutines

```
c ***********************************************************************
      SUBROUTINE ENPR04(nfoutp)                    ! NIST mods included
c ***********************************************************************
c DRAIN-2DX SIMPLE CONNECTION ELEMENT WITH ELASTIC/INELASTIC/GAP OPTIONS
c     Print result envelopes.
c -----------------------------------------------------------------------
c  DOUBLE PRECISION / LARGE
      include 'double.h'
c -----------------------------------------------------------------------
c  CALLED FROM : enprxx.
c  FILE I/O    : prints to unit nfoutp.
c -----------------------------------------------------------------------
c  ARGUMENTS
c    INPUT:
c      nfoutp = output unit for envelope values.
c -----------------------------------------------------------------------
c  LABELLED COMMONS
      include 'infel04.h'
c -----------------------------------------------------------------------

c ------------------------------------------------PRINT ENVELOPE HEADING
      if (imem.eq.1) write(nfoutp,20)
   20 format(' SIMPLE CONNECTION ELEMENTS (TYPE 04)'//
     1          '   Elem',7x,'Node',7x,'Node',2x,
     2          '   Maximum Force/Moment Values  ',1x,
     3          '   Maximum Deformation Values  ',2x,
     4         'Acc. Plastic Deformtns Elasto-Plas Load'/
     5          '    No.',7x,'  I ',7x,'  J ',2x,
     6          ' Positive  Step  Negative  Step',1x,
     7          ' Positive  Step  Negative  Step',2x,
     8          '   Positive   Negative   Energy     Revs'/)! NIST mod

c ----------------------------------------------------------ENVELOPE PRINT
      write(nfoutp,30) imem,nodi,nodj,senp,isenp,senn,isenn,venp,
     1              ivenp,venn,ivenn,vpacp,vpacn,enerel,irev  ! NIST mod
   30 format(i7,2i11,1x,4(1pe11.3,i5),2x,1p3e11.3,1x,i5)   ! NIST mod

c -----------------------------------------------------------------------
      RETURN
      END


c ***********************************************************************
      SUBROUTINE RESP04(kresis,ksave,kgem,kstep,ndof,kst,kenr,ener,
     1                  ened,enso,beto,relas,rdamp,rinit,ddise,
     2                  dise,vele)                 ! NIST mods included
c ***********************************************************************
c DRAIN-2DX SIMPLE CONNECTION ELEMENT WITH ELASTIC/INELASTIC/GAP OPTIONS
c     Element response. Update element state, form static and
```

```
c     damping resisting forces, perform energy calculations, update
c     damage measures, and put element results in /THELM/ for saving
c     or printing.
c -------------------------------------------------------------------
c  DOUBLE PRECISION / LARGE
      include 'double.h'
c -------------------------------------------------------------------
c   CALLED FROM : respxx (once for each sub-step).
c -------------------------------------------------------------------
c   INPUT
c      kresis  = indicator for calculating resisting forces
c                ( 1: static only, 2: static and damping).
c      ksave   = indicator for saving element results
c                0 : do not save results history, do not save envelopes.
c                1 : save results history, do not save envelopes.
c                2 : do not save results history, save envelopes.
c                3 : save results history, save envelopes.
c      kgem    = second order analysis code (> 0: y, 0: n)
c                (not used).
c      ndof    = no. of element DOF.
c      kenr    = energy calculation indicator
c                (2: static + dynamic, 1: static, 0: none).
c      beto    = initial stiffness damping factor.
c      ddise(ndof) = element nodal incremental displacement vector.
c      ddis(ndof)  = element total nodal displacement vector.
c      vele(ndof)  = element nodal velocity vector.
c   OUTPUT
c      ener        = change of element elasto-plastic energy.
c      ened        = change of element damping energy.
c      enso        = change of element second-order energy (=0).
c      relas(ndof) = element static resisting force vector.
c      rdamp(ndof) = element damping resisting force vector.
c      rinit(ndof) = element initial resisting force vector (=0.)
c   MODIFY
c      kstep       = step no. in this segment
c      kst         = stiffness formation code ( 1: y, 0: n).
c -------------------------------------------------------------------
c   LABELLED COMMONS
      include 'infel04.h'

      common /envelm/ enout(7),ienout(5)      ! NIST mod
      real enout
c       ienout(1) = isenp
c             (2) = isenn
c             (3) = ivenp
c             (4) = ivenn
c             (5) = irev                      ! NIST mod
c        enout(1) = senp
c             (2) = senn
c             (3) = venp
c             (4) = venn
c             (5) = vpacp
c             (6) = vpacn
c             (7) = enerel                    ! NIST mod

      common /thelm/thout(5),ithout(4)
        REAL thout
      common/tapes/inp,iou
c -------------------------------------------------------------------
c   WORK COMMON
      common /work/ dsep,fac,factor,facac,dv,dvv,pyy,dsel,dvp,std
     1             ,w(1990)
```

```
c      dsel = change in force for elastic (E) component.
c      dsep = change in forec for elasto-plastic (E-P) component.
c      dv = deformation increment.
c      dvv = velocity increment.
c      dvp = plastic deformation increment.
c      fac,factor,facac = used to trace out non-linear path.
c      st = static force/moment
c      std = damping force/moment
c ---------------------------------------------------------------------
c   ARGUMENT DECLARATIONS
      dimension relas(ndof),rdamp(ndof),rinit(ndof),ddise(ndof),
     1          dise(ndof),vele(ndof)
c ---------------------------------------------------------------------

c ------------------------------------------------DEFORMATION INCREMENT
      dv = ddise(2)-ddise(1)


c -------------------RESET ENVELOPE STEP VALUES FOR NEW ANALYSIS SEGMENT
      if(kstep.eq.-1)then
        isenn=0
        isenp=0
        ivenn=0
        ivenp=0
        kstep=1
         irev=0                              ! NIST mod
         dvold=dv                            ! NIST mod
         enerel=0.d0                         ! NIST mod
      end if

c--------------------------ACCUMULATE DISPLACEMENT REVERSALS (NIST mod)
      if(dv*dvold.LT.0.d0) then
           irev=irev+1
           dvold=dv
       end if

c ---------------------------------------------------------------------
c --------------------TRACE NON-LINEAR PATH FOR ELASTO-PLASTIC COMPONENT
c ---------------------------------------------------------------------
      facac=0.d0

   20 factor=1.d0-facac

c ------------------------------------------------CURRENTLY ELASTIC
        if(kody.eq.0)then
          iev=0
          dsep=ealep*dv

c---negative deformation
          if (dsep.lt.0.d0)then

c---yielding or elastic type
            if(kelas.ne.2) then
              fac=(pyn-sep)/dsep
              if (fac.lt.factor)then
                iev=1
                pyy=pyn
              end if
c---gap type
            else
              if(nogap.ne.0 .and. vtot.ge.vgmax) then
                fac=-sep/dsep
                if (fac.lt.factor)then
```

```
                  iev=2
                  pyy=0.d0
                end if
              else
                fac=(pyn-sep)/dsep
                if (fac.lt.factor)then
                  iev=1
                  pyy=pyn
                end if
              end if
            end if

c---positive deformation
          else if(dsep.gt.0.d0)then

c---yielding or elastic type
            if(kelas.ne.2) then
              fac=(pyp-sep)/dsep
              if (fac.lt.factor)then
                iev=1
                pyy=pyp
              end if
c---gap type
            else
              if(nogap.ne.0 .and. vtot.le.vgmin) then
                fac=-sep/dsep
                if (fac.lt.factor)then
                  iev=2
                  pyy=0.d0
                end if
              else
                fac=(pyp-sep)/dsep
                if (fac.lt.factor)then
                  iev=1
                  pyy=pyp
                end if
              end if
            end if

          end if

c---new yield or gap opening
          if(iev.ne.0)then
            if(kenr.gt.0) ener=ener+(sep+pyy)*0.5*factor*dv
            sep=pyy
            kody=iev
            if(kody.eq.2) nogap=1
c---remains elastic
          else
            if(kenr.gt.0) ener=ener+(sep+0.5*factor*dsep)*factor*dv
            sep=sep+factor*dsep
          end if

c ------------------------------------------------------CURRENTLY YIELDING
        else if(kody.eq.1) then

c---reverses
          if (sep*dv.lt.0.d0)then
           irev=irev+1                                  ! NIST mod

c---unloads inelastically
            if (kelas.eq.0) then
              factor=0.d0
```

```
              kody=0
            else if (kelas.eq.2) then
              factor=0.d0
              kody=0
              if(dv.lt.0.d0) then
                vgmax=vtot-pyp/ealep
              else
                vgmin=vtot-pyn/ealep
              end if

c---reverses elastically (kelas=1)
            else
              if (dv.lt.0.d0) then
                fac=(pyp/ealep-vtot)/dv
                if (fac.lt.factor) then
                  factor=fac
                  kody=0
                end if
              else if (dv.gt.0.d0) then
                fac=(pyn/ealep-vtot)/dv
                if (fac.lt.factor) then
                  factor=fac
                  kody=0
                end if
              end if
              if (kenr.gt.0) ener=ener+sep*factor*dv
            end if

c---continues to yield
          else
            dvp=factor*dv
            if(dvp.gt.0.d0) then
              vpacp=vpacp+dvp
             else
              vpacn=vpacn+dvp
            end if
            if(kenr.gt.0) ener=ener+sep*dvp
            if(kelas.eq.2) nogap=1
          end if

c ------------------------------------------------CURRENTLY HAS OPEN GAP
        else
          if(dv.lt.0.d0) then
            fac=(vgmin-vtot)/dv
          else if(dv.gt.0.d0)then
            fac=(vgmax-vtot)/dv
          end if
          if (fac.lt.factor) then
            factor=fac
            kody=0
          end if

        end if

c ---------------------------------------CHECK FOR COMPLETION OF CYCLE
      facac=facac+factor
      if (facac.lt.0.99999d0) go to 20

c ---------------------------------------------------------------------
c ------------------------------------------------------TRACING COMPLETE
c ---------------------------------------------------------------------

c ---------------------------------------------UPDATE TOTAL DEFORMATION
```

```
      vtot=vtot+dv

c ----------------------------UPDATE ELASTIC COMPONENT FORCE AND ENERGY
      dsel=eale*dv
      sel=sel+dsel

      if(kenr.gt.0)then
        ener=ener+(sel-dsel*0.5)*dv
         enerel=enerel+ener                    ! NIST mod (with elastic)
        enso = 0.d0
      end if

c ------------------------------------------------STATIC RESISTING FORCES
      st = sel+sep
      relas(2)=st
      relas(1)=-st

c ------------------------------------------------INITIAL RESISTING FORCES
c --no element loads for this element type
      rinit(1)=0.
      rinit(2)=0.

c ------------------------------------------------DAMPING FORCES AND ENERGY

      if(kresis.eq.2) then
        dvv=vele(2)-vele(1)
        std=(ealep+eale)*dvv*beto
        if (kenr.eq.2) ened=ened+(std+stdp)*dv*0.5
        stdp=std
        rdamp(2)=std
        rdamp(1)=-std
      else
        std=0.
        if (kenr.eq.2) ened=ened+(std+stdp)*dv*0.5
        stdp=0.
        rdamp(1)=0.
        rdamp(2)=0.
      end if

c ------------------------------------------------UPDATE ENVELOPE VALUES

c --max force
      stt=st+std
      if (stt.gt.senp) then
        senp=stt
        isenp=kstep
      else if(stt.lt.senn)then
        senn=stt
        isenn=kstep
      endif

c --max deformation
      if (vtot.gt.venp) then
        venp=vtot
        ivenp=kstep
      else if (vtot.lt.venn)then
        venn=vtot
        ivenn=kstep
      endif

c ------------------------------------------------SAVE RESULT HISTORIES
      if (ksave .eq. 1 .or. ksave .eq. 3) then
        ithout(1)=nodi
```

```
        ithout(2)=nodj
        ithout(3)=krotr
        ithout(4)=kody
        thout(1)=st
        thout(2)=std
        thout(3)=vtot
        thout(4)=vpacp
        thout(5)=vpacn
      end if
c -------------------------------------------------------------SET /ENVELM/
      if (ksave .eq. 2 .or. ksave .eq. 3) then
        ienout(1) = isenp
        ienout(2) = isenn
        ienout(3) = ivenp
        ienout(4) = ivenn
        ienout(5) = irev                          ! NIST mod
        enout(1) = senp
        enout(2) = senn
        enout(3) = venp
        enout(4) = venn
        enout(5) = vpacp
        enout(6) = vpacn
         enout(7) = enerel                         ! NIST mod
      end if

c -----------------------------------SET INDICATOR FOR STIFFNESS CHANGE
      if(kodyx.ne.kody) kst=1

c ---------------------------------------------------------------------
      return
      end
```

A.2 INEL04 Subroutines

```
c *********************************************************************
      SUBROUTINE INEL04(kdata)                    ! NIST mods added
c *********************************************************************
c DRAIN-2DX SIMPLE CONNECTION ELEMENT WITH ELASTIC/INELASTIC/GAP OPTIONS
c     Data input,initialization etc.
c     Set up /infel04/ blocks for all elements in a group.
c ---------------------------------------------------------------------
c  DOUBLE PRECISION / LARGE
      include 'double.h'
c ---------------------------------------------------------------------
c  CALLED FROM : inelxx
c  FILE I/O    : read element data from inp.
c                print element data to iou.
c ---------------------------------------------------------------------
c  ARGUMENTS
c    MODIFY:
c     kdata = error counter, add 1 for each error
c ---------------------------------------------------------------------
c   RESTRICTIONS
c     Max. 40 stiffness types.
c ---------------------------------------------------------------------
c  LABELLED COMMONS
      include 'infel04.h'
      include 'cline.h'
      include 'ptop.h'
      common/tapes/inp,iou
c ---------------------------------------------------------------------
```

```
c  WORK COMMON
      common /work/ftyp(40,5),iftyp(40,2),psh,ppsh,xyi(2),xyj(2),
     1             nmbt,inel,inodi,inodj,inc,iinc,imbt,iimbt,ier,
     2             kkn,kkd,kkie,kkre,kkig,kkrg,kkl,kkon,kkol,w(1745)

c       ftyp(40,5)  = type properties (5 properties, up to 40 types)
c                     1 = stiffness
c                     2 = hardening ratio
c                     3 = positive yield strength
c                     4 = negative yield strength
c                     5 = overshoot tolerance
c       iftyp(40,2) = property codes
c                     1 = direction code (1=X, 2=Y, 3=R)
c                     2 = elasticity code
c                         0 = basic inelastic
c                         1 = elastic
c                         2 = inelastic with gap
c       psh         = strain hardening ratio.
c       ppsh        = 1-psh
c       xyi,j(2)    = node i,j coordinates
c       nmbt        = no. of property types.
c       inel        = input element no.
c       inodi       = input node i
c       inodj       = input node j
c       inc,iinc    = node no. increment
c       imbt,iimbt  = property type no.
c       ier         = error code
c -------------------------------------------------------------------
c  LOCAL DECLARATIONS
      character*1 iast(2),iastt
c -------------------------------------------------------------------

c ---------------------------------------------------------CONSTANTS
c --asterisk for generation
      iast(1)=' '
      iast(2)='*'
c --small number
      small=1.e-10

c ------------------------------------------------GROUP CONTROL VARIABLES
c --  no. of element nodes = 2
c --  no. of element dofs = 2
c --  code for zeroing /infel/ = 1 (zero)
c --  no. of 1-byte variables in /infel/ = 0
c --  no. of 2-byte variables in /infel/ = 0
c --  no. of 4-byte variables in /infel/ = 14          ! NIST mod
c --  no. of 8-byte variables in /infel/ = 20          ! NIST mod
c --  no. of 16-byte variables in /infel/ = 0
c --  code for zeroing /infgr/ = 0 (do not zero)
c --  no. of 1-byte variables in /infgr/ = 0
c --  no. of 2-byte variables in /infgr/ = 0
c --  no. of 4-byte variables in /infgr/ = 0
c --  no. of 8-byte variables in /infgr/ = 0
c --  no. of 16-byte variables in /infgr/ = 0
c --  no. of words per element load set = 0
c --  no. of nonlinear output items per element = 9
c --  no. of linear output items per element = 2
c --  no. of 4-byte units required for element envelopes = 12 ! NIST mod

      call econtr(2,2,1,0,0,14,20,0,0,0,0,0,0,0,9,2,12)     ! NIST mod

c ---------------------------------------------CONTROL INFORMATION
      call getlin
```

```
      read(xxline,10) nmbt
   10 format(i5)

      write(iou,20) nmbt
   20 format(//' SIMPLE CONNECTION ELEMENTS (TYPE 04) VERSION 1.10'//
     1         ' Control Information '//
     2         '   No. of property types = ',i4)

      if(nmbt.le.0 .or. nmbt.gt.40) then
        write(iou,*) ' ***ERROR - no. of prop types'
        kdata=kdata+1
        nmbt=1
      end if

c -----------------------------------------HEADING FOR PROPERTY TYPES
      write(iou,30)
   30 format(/' Property Types '//
     1        '   Type',4x,'  Elastic',4x,'Hardening',
     2        3x,'Pos. Yield',3x,'Neg. Yield',4x,'Overshoot',
     3        2x,'Dirn',2x,'Elas'/
     4        '    No.',4x,'Stiffness',4x,'  Ratio  ',
     5        3x,' Strength ',3x,' Strength ',4x,'Tolerance',
     6        2x,'Code',2x,'Code'/)

c ---------------------------------------------------------PROPERTY TYPES
      do 60 it=1,nmbt

        call getlin
        read(xxline,40) i,(ftyp(it,j),j=1,5),(iftyp(it,j),j=1,2)
   40   format (i5,5f10.0,2i5)

        if(ftyp(it,2).eq.0.d0) ftyp(it,2)=0.00001

        write(iou,50) i,(ftyp(it,j),j=1,5),(iftyp(it,j),j=1,2)
   50   format (i7,1p5e13.4,2i6)

        if (i.ne.it) then
          write(iou,*) ' ***ERROR - types not in sequence'
          kdata=kdata+1
        end if
        if(ftyp(it,2).gt.0.9999999) then
          write(iou,*) ' ***ERROR - strn hard ratio too big'
          kdata=kdata+1
        end if
        if(ftyp(it,5).lt.small) then
          write(iou,*) ' ***ERROR - overshoot too small'
          kdata=kdata+1
        end if
        if (iftyp(it,1).lt.1 .or. iftyp(it,1).gt.3) then
          write(iou,*) ' ***ERROR - dirn code not 1,2 or 3'
          kdata=kdata+1
          imem=inel
        end if
        if (iftyp(it,2).lt.0 .or. iftyp(it,2).gt.2) then
          write(iou,*) ' ***ERROR - elas code not 0,1 or 2'
          kdata=kdata+1
          imem=inel
        end if

   60 continue

c ------------------------------------------------HEADING FOR ELEMENTS
      write (iou,70)
```

```
   70 format(/' Element Generation Commands'//
     1        '    Elem',7x,'Node',7x,'Node',7x,'Node',4x,'Prop'/
     2        '     No.',7x,'  I ',7x,'  J ',7x,'Diff',4x,'Type'/)

c ------------------------------------------------------ELEMENT GENERATION
c --blank line or "*' line for last element

      imem=0

   80 call getlin
      if(xxline(1:1).eq.'*') then
        inel=0
      else
        read(xxline,100) inel,inodi,inodj,iinc,iimbt
  100   format(i5,3i10,i5)
      end if

      if(inel.gt.0) then

  110   imem=imem+1

        if(imem.lt.inel .and. imem.ne.1) then
          nodi=nodi+inc
          nodj=nodj+inc
          iastt=iast(2)
        else
          nodi=inodi
          nodj=inodj
          inc=iinc
          if (inc.eq.0) inc=1
          if(iimbt.ne.0) imbt=iimbt
          iastt=iast(1)
        end if

c ------------------------------------------------------PRINT ELEMENT DATA
        write(iou,130) iastt,imem,nodi,nodj,inc,imbt
  130   format (3x,a1,i4,3i11,i8)

c ------------------------------------------------------CHECK FOR ERRORS
        if(imem.eq.1.and.inel.ne.1) then
          write(iou,*) ' ***ERROR - must start with elem 1'
          kdata=kdata+1
          imem=inel
        end if
        if (inel.lt.imem) then
          write(iou,*) ' ***ERROR - elem out of sequence'
          kdata=kdata+1
          imem=inel
        end if
        if (imbt.le.0 .or. imbt.gt.nmbt) then
          write(iou,*) ' ***ERROR - no such prop type'
          kdata=kdata+1
          imbt=1
        end if

        call coords(nodi,0,xyi,ier)
        if(ier.ne.0) then
          write(iou,140) nodi
  140     format(' ***ERROR - no such node:',i10)
          kdata=kdata+1
        end if
        call coords(nodj,0,xyj,ier)
        if(ier.ne.0) then
```

```
          write(iou,140) nodj
          kdata=kdata+1
        end if

        if(abs(xyi(1)-xyj(1))+abs(xyi(2)-xyj(2)).gt.1.d-3) then
          write(iou,*) ' ***WARNING - node coords not same'
        end if

c -------------------------------------------------SET ELEMENT PROPERTIES
        rstif=ftyp(imbt,1)
        psh=ftyp(imbt,2)
        ppsh=1.d0-psh
        ealep=rstif*ppsh
        eale=rstif*psh
        pyp=ftyp(imbt,3)*ppsh
        pyn=(-dabs(ftyp(imbt,4)))*ppsh
        ovtol=ftyp(imbt,5)
        krotr=iftyp(imbt,1)
        kelas=iftyp(imbt,2)

c ---------------------------------------------------------INITIALIZE STATE
c --done by zeroing /infel/

c ---------------------------------------------------------SEND ELEMENT NODES
        call elnode(nodi,ier1)
        call elnode(nodj,ier2)
        if(ier1+ier2.ne.0) then
          write(iou,*) ' ***ERROR - elnode'
          kdata=kdata+1
        end if

c ------------------------------------------------------FORM LOCATION MATRIX
        if(kdata.gt.0) krotr=1

        call locmat(nodi,0,krotr,ier1)
        call locmat(nodj,0,krotr,ier2)

        if(ier1+ier2.ne.0) then
          write(iou,*) ' ***ERROR - locmat'
          kdata=kdata+1
        end if

c ---------------------------------------------STORE ELEMENT INFEL BLOCK
c --also saves /infgr/ if first element, counts elements in group
c --and sets stiffness matrix profile.

        call finish

c ---------------------------------------------GENERATE MISSING ELEMENTS
        if(imem.lt.inel) then
          go to 110
        else
          go to 80
        end if

c ------------------------------------------------------------LAST ELEMENT
      end if

      if(imem.eq.0) then
        write(iou,*) ' ***ERROR - no elements in group'
        kdata=kdata+1
      end if
```

```
C ***********************************************************************
      RETURN
      END
C ***********************************************************************
```

B. Optimization program listings

This appendix includes listings of all of the programs used to implement the numerical optimization used to define the optimal values for the cladding connector properties. The programs are all written in Fortran77 and were compiled using Digital Visual Fortran 5 on an Intel Pentium II 266 MHz system running Windows NT 4.0.

The Main program controls all operations and calls several subprograms. The optimization is carried out using DOT (Ver 4) which is implemented as a subroutine call. The DOT code is provided by VMA Engineering in source form and must be compiled into the main numerical optimization code. The objective function is evaluated by executing DRAIN-2dx to compute the building performance, the energy dissipation figures, and the connector dynamic ductility. This is accomplished by first creating a new DRAIN input file (drain.inp) and then making a system call to execute DRAIN-2dx. Additional subroutines are used to post-process the DRAIN-2dx output files to extract the needed information in order to evaluate the objective function and constraint(s).

The Main program and all subroutines, including DOT, are compiled, linked and executed as a single program (.exe file). DRAIN-2dx is compiled separately and is executed independently of the Main program (which waits for DRAIN to complete).

B.1 Main Program

```
c**********************************************************************
      PROGRAM main
c**********************************************************************
c Program to carry out numerical optimization of a NIST building design
c using the DOT numerical optimization code with DRAIN2dx.  NIST will
c do the following:
c
c   1. Open 'nist.inp' and read initialization paramters (see below).
c   2. Initialize DOT parameters and make initial DOT call.
c   3. Call UPDATE to create a new 'drain.inp' input file by reading
c        a template file called 'drain.txt' and writing 'drain.inp'.
c        (See UPDATE for how to structure template file.)
c   4. Execute DRAIN2dx using WinNT SYSTEM call to command shell.
c      NOTE: must hardcode name of DRAIN (currently: d2dx1m)
c   5. Call EXTRACTout to extract the max ductility demand and elasto-
c      plastic (hyst.) work done by Type04 from DRAIN .OUT file.
c   6. Call EXTRACTslo to extract the total external work from the
c      DRAIN .SLO file.
c   7. Compute the objective function value and the constraint value
c      from the above information.
c   8. Call DOT.
c   9. If not converged (INFO#0) loop from #3 above with new params.
c----------------------------------------------------------------------
c NOTES:
c   a. All data files, nist.exe and d2dx1m.exe must be in same
c      directory and must be executed from Command Prompt window.
c   b. All data is passed by file I/O and Fortran File I/O calls are
c      used to handle the file processing.
c   c. File errors are reported by the individual subroutines and
c      program execution is halted.
c----------------------------------------------------------------------
c Input files:
c   1.'drain.txt' input file template with string '![PAR04]' used
c      used to identify following line as parameters to be changed
c      when preparing new 'drain.inp' file.
```

```
c   2.'nist.inp' input file as follows:
c      Line #1 contains the name of the DRAIN Problem Name.  It is
c        used to form the .OUT and .SLO file names.
c      Line #2 contains initial ekc & fc values.
c      Line #3 contains upper limits for ekc & fc and the max ductility.
c      Line #4 contains DOT method ID (see below for key values).
c      All data are in free field format with comma delimiters.
c      Max ductility will be used to define the constraint.
c Output file:
c   1. DOT will write an output file called 'nist.out' that contains
c      the results of the numerical optimization. Design variable #1
c      corresponds to ekc and #2 corresponds to fc.
c   2. DRAIN2dx will write several different output files.  Only the
c      .out and .slo files are used (all are over-written for each
c      successive execution of DRAIN during the optimization).
c-----------------------------------------------------------------------
c VERSION 1.1, j.craig, 8/98
c     1.0 Initial effort with accum. plastic defor. as ductility
c     1.1 Use dynamic ductility (requires modified Drain2dx)
c-----------------------------------------------------------------------
c
c  Use DVF library containing SYSTEM() routine to run DRAIN2dx
      USE DFPORT
c  Data arrays needed by main & DOT (parameters define problem size)
      LOGICAL present
      CHARACTER fname*31
      PARAMETER(nrwk=1000,nriwk=300,ndx=2,ncon=1)
      DIMENSION x(ndx),xl(ndx),xu(ndx),g(ncon),wk(nrwk),iwk(nriwk),
     1 rprm(20),iprm(20)
      DIMENSION enerel(20),irevs(20)
      DATA iprm,rprm/20*0,20*0.0/
c-----------------------------------------------------------------------
c  DOT parameter definitions
c  info:       0=done; 1=continue
c  method:     0/1=MFD; 2=SLP; 3=SQP
c  iprint:     output; 0..7 (see doc)
c  ndx:        # design variables
c  ncon:       # constraints in G
c  x(ndx):     design vector
c  xl(ndx):    x lower bound
c  xu(ndx):    x upper bound
c  obj:        objective function
c  minmax:     0,-1=min; 1=max
c  g(ncon):    inequality constraints (g<0)
c  rprm(20):   control params (0=use default values)
c  iprm(20):   control params (0=use default values)
c  wk(nrwk):   work array (real)
c  nrwk:       1000+ for small problems
c  iwk(nriwk): work array (integer)
c  nriwk:      300+ for small problems
c-----------------------------------------------------------------------
c
c Get initial conditions from FILE=nist.inp:
      open(unit=10,file='nist.inp',err=9000)
      read(10,*,err=9100) fname
      read(10,*,err=9110) ekc,fc
      read(10,*,err=9130) ekcmax,fcmax,ductmax
      read(10,*,err=9130) method
      close(unit=10)
      PRINT*,'Initial conditions:'
      PRINT*,fname
     PRINT*,ekc,fc
     PRINT*,ekcmax,fcmax,ductmax
```

```
      PRINT*,method
       x(1)=ekc
       x(2)=fc
       xl(1)=0.0
       xl(2)=0.0
       xu(1)=ekcmax
       xu(2)=fcmax
c Other DOT parameters:
       iprint=3     ! Print out results at each iteration
       minmax=1     ! Find maximum
       info=0
c Now set up an output file for DOT to write into:
c First see if 'dot.out' already exists and if so delete it:
       inquire(file='dot.out',exist=present)
       if (present) then
              open(unit=112,file='dot.out')
              close(unit=112,status='DELETE')
       end if
c Create new 'dot.out':
       open(unit=112,file='dot.out',status='NEW')
c Now set IPRM(5)=112 so DOT will have I/O unit number:
       IPRM(5)=112
c      IPRM(13)=112
c Optimization loop - initialization
      PRINT*,'Starting DOT.'
       call DOT(info,method,iprint,ndx,ncon,x,xl,xu,obj,minmax,g,
     1 rprm,iprm,wk,nrwk,iwk,nriwk)
       iter=0
c
       do while (info.NE.0)
           iter=iter+1
           PRINT*,'Function Call #:',iter
           PRINT*,'Updating drain.inp'
              call update(x(1),x(2))
           PRINT*,'Run DRAIN'
           ier=SYSTEM('nist')     ! Hard coded DRAIN2dx name
           if (ier.EQ.-1) then
                  iernum=ierrno()
               PRINT*,'ERROR: System call failed; ier=',iernum
               stop
           endif
           PRINT*,'Extract results'
              call extractout(fname,enerh,enerel,irevs,20)
           call extractslo(fname,enerext)
c          Compute objective and ductility constraint:
              obj=enerh/enerext
           duct=0.0
           do iflor=1,20
               ductflor=enerel(iflor)*x(1)/x(2)/x(2)/(irevs(iflor)**0.4)
               if(ductflor.GT.duct) duct=ductflor
           end do
              g(1)=duct/ductmax-1.0      ! g<0 to satisfy constraint
              call DOT(info,method,iprint,ndx,ncon,x,xl,xu,obj,minmax,g,
     1   rprm,iprm,wk,nrwk,iwk,nriwk)
           PRINT*,'-------------------------------'
       end do
       close(unit=112)
       stop
c-----------------------------------------------------------------------
9000   PRINT*,'NIST: Cannot open nist.inp for initial values.'
       stop
9100   PRINT*,'NIST: Cannot read line #1 of nist.inp.'
       stop
```

```
9110   PRINT*,'NIST: Cannot read line #2 of nist.inp.'
       stop
9120   PRINT*,'NIST: Cannot read line #3 of nist.inp.'
       stop
9130   PRINT*,'NIST: Cannot read line #4 of nist.inp.'
       stop
c-----------------------------------------------------------------------
       end
```

B.2 Subroutines (excluding DOT)

```
c***********************************************************************
       subroutine update(ekelnew,fynew)
c***********************************************************************
c Routine to read a reference DRAIN input file (drain.txt) and
c produce an updated version (drain.inp). If 'drain.inp' already
c exists, it will be deleted first. Update will search 'drain.txt' for
c a comment line with string '[PAR04]' in positions 2:8 and it will
c then update the line that follows.  This line should be the line
c in *PARAMETERS that specifies the Type04 element k1 & fy properties.
c-----------------------------------------------------------------------
c ARGUMENTS
c  ekelnew = new TYPE04 element initial stiffness
c  fynew   = new TYPE04 element yield (+/- are symmetric)
c
c Note: Assume all other parameters in the line are unchanged.
c-----------------------------------------------------------------------
c Input:  file 'drain.txt' which is template for creating 'drain.inp'.
c Output: file 'drain.inp' which is used by DRAIN2dx.
c-----------------------------------------------------------------------
c VERSION 1.0, j.craig, 7/98
c-----------------------------------------------------------------------
       LOGICAL present,done,found
       CHARACTER line*80,endline*20
c
c Open reference drain input file (source for drain.inp):
       open(unit=10,file='drain.txt',status='OLD',iostat=ier,err=9000)
c Now delete old 'drain.inp' if it exists:
       inquire(file='drain.inp',exist=present)
       if (present) then
              open(unit=12,file='drain.inp')
              close(unit=12,status='DELETE')
       end if
c Create new 'drain.inp':
       open(unit=12,file='drain.inp',status='NEW')
c
c Read and copy reference file until marker record:
       found=.FALSE.
       done=.FALSE.
       read(10,1000,end=9100) line
       do while (.NOT.done)
              write(12,1000) line
              if (line(2:8).EQ.'[PAR04]') then
                     found=.TRUE.
                     read(10,1100) ktype,ekel,ekhard,fy1,fy2,endline
                     ekel=ekelnew
                     fy=fynew
                     write(12,1100) ktype,ekel,ekhard,fy,fy,endline
              end if
```

```
            read(10,1000,iostat=ier10) line
            if (ier10.EQ.-1) done=.TRUE.
      end do
      close(unit=12)
      close(unit=10)
      if (.NOT.found) then
            PRINT*,'UPDATE: Unexpected EOF before key in reference file.'
            PRINT*,'        Output file (drain.inp) was not changed.'
      end if
      return
c-----------------------------------------------------------------------
1000  FORMAT(A)
1100  FORMAT(I5,4F10.2,A20)
9000  PRINT*,'UPDATE: Unable to open reference DRAIN file (drain.txt).'
      stop
9100  PRINT*,'UPDATE: Unexpected EOF at start of reference file.'
      stop
      end

c***********************************************************************
      subroutine extractout(fname,enerh,enerel,irevs,iflors)
c***********************************************************************
c Subroutine to process DRAIN2dx output file with only envelopes
c printed and extract the hysteretic (elasto-plastic) work in
c connections (enerh) and a measure of the connector ductility.
c-----------------------------------------------------------------------
c Version
c     1.0 Base using max total inelastic deformation in + or - dir
c         as measure of ductility in connectors
c     1.1 Use modified DRAIN2dx which lists Elasto-Plastic work for
c         each element in a group along with number of reversals.
c         This allows main pgm to compute dynamic ductility.
c     1.2 Modified for 1 bay bldg model and group #5 connectors.
c-----------------------------------------------------------------------
c Input:  fname = name of DRAIN output file WITHOUT the .OUT extension.
c Output: enerh = hysteretic energy ("elasto-plastic work" for Type04
c                 elements in Group 5 written to .OUT file). User must
c                 make sure Group 5 is used to designate this group.
c         enerel= Elasto-Plastic work in connector for each floor.
c         irevs = Number of reversals for connectors in each floor
c         iflors= Number of floors (also dimension of enerel & irevs)
c         duct  = Used in Ver 1.0; ductility demand for single Type04
c                 (The max abs(accumulated plastic deformation)
c-----------------------------------------------------------------------
      CHARACTER*(*) fname
      CHARACTER ffname*31,line*132
      DIMENSION enerel(iflors),irevs(iflors)
      LOGICAL done,done2
c-----------------------------------------------------------------------
c Open and read TYPE04 max ductility and total elasto-plastic work
c from file specified as 'fname.out'; read first line:
      ffname=TRIM(fname)//'.out'  ! remove trailing blanks & concatenate
      open(unit=10,file=ffname,status='OLD',err=9000)
c
      done=.FALSE.
      done2=.FALSE.
      read(10,1000,err=9100) line
      do while (.NOT.done)
            if (line(2:10).EQ.'ENVELOPES'.AND.line(32:32).EQ.'5') then
                  do 10 i=1,6         ! Position to start of ductility data
                        read(10,1000,err=9100) line
10                  continue
                    do 30 i=1,20 ! Read dyn ductility data;
```

```
                        read(10,1100,err=9200) enerel(i),irevs(i)
30                   continue
                  do while (.NOT.done2) ! Position to elasto-plastic work
                      read(10,1000,err=9100) line
                      if (line(2:10).EQ.'WORK DONE') then
                               do 50 i=1,8
                                      read(10,1000,err=9100) line
50                             continue
                               read(10,1200,end=9300) enerh
                               close(unit=10)
                               return
                      end if
                   end do
                  end if
                  read(10,1000,end=9400) line
       end do
       PRINT*,'EXTRACTout: Unexpected EOF.'
       stop
c-----------------------------------------------------------------------
1000   FORMAT(A)
1100   FORMAT(1x,29x,4(16x),2x,22x,E11.3,I6)
1200   FORMAT(1x,8x,E13.5)
c-----------------------------------------------------------------------
9000   PRINT*,'EXTRACTout: Cannot open nist.out.'
       stop
9100   PRINT*,'EXTRACTout: Error reading to position in file.'
       stop
9200   PRINT*,'EXTRACTout: Error reading ductility data.'
       stop
9300   PRINT*,'EXTRACTout: Error reading elasto-plastic work data.'
       stop
9400   PRINT*,'EXTRACTout: Unexpected EOF.'
       stop
       end

c**********************************************************************
       subroutine extractslo(fname,enerext)
c**********************************************************************
c Subroutine to process DRAIN2dx .SLO file which contains energy
c quantities and unbalance information.  The file name WITHOUT the
c .SLO extension must be provided in the fname input argument.  The
c routine extracts and returns the total external work a the end
c of the DRAIN run.
c
c The routine will position to the EOF and backup 2 records in order
c to read the last output line and extract the total external work.
c All other information in the file is ignored.
c
c Note: it is essential that there are no extra lines after the last
c data line in the .SLO file!
c-----------------------------------------------------------------------
       CHARACTER*(*) fname
       CHARACTER ffname*31,line*132
       LOGICAL filend
c-----------------------------------------------------------------------
c Open and read total external energy from 'fname.out':
       ffname=TRIM(fname)//'.slo'
       open(unit=10,file=ffname,status='OLD',err=9000)
c
       filend=.FALSE.
       do while (.NOT.filend)
           read(10,1000,iostat=ier) line
              if (ier.EQ.-1) filend=.TRUE.
```

```
      end do
      backspace(unit=10)
      backspace(unit=10)
      read(10,1100) enerext
      close(unit=10)
      return
c-----------------------------------------------------------------------
1000   FORMAT(A)
1100  FORMAT(1x,4x,10x,4(11x),E11.3)
c-----------------------------------------------------------------------
9000   PRINT*,'EXTRACTslo: Cannot open specified .SLO file:',ffname
      stop
      end
```

C. Nominal building model input file for DRAIN-2dx

```
! NOMINAL MODEL
! LONGITUDINAL MOMENT FRAME WITH CLADDING STIFFNESS
!
!UNITS L IN F K
*STARTXX
  long7-08          0 1 0 1    B           (LONGITUDINAL)  20-STORY FRAME
!
*NODECOORDS
! 13 BAY EXTERIOR MOMENT FRAME WITHOUT CLADDING STIFFNESS NODE GENERATION
C         1        0.0        0.0
C        14     2769.0        0.0
C        15        0.0      192.0
C        16      213.0      192.0
C        17      426.0      192.0
C        18      639.0      192.0
C        19      852.0      192.0
C        20     1065.0      192.0
C        21     1278.0      192.0
C        22     1491.0      192.0
C        23     1704.0      192.0
C        24     1917.0      192.0
C        25     2130.0      192.0
C        26     2343.0      192.0
C        27     2556.0      192.0
C        28     2769.0      192.0
C        29        0.0      342.0
C        43        0.0      492.0
C        57        0.0      642.0
C        71        0.0      792.0
C        85        0.0      942.0
C        99        0.0     1092.0
C       113        0.0     1242.0
C       127        0.0     1392.0
C       141        0.0     1542.0
C       155        0.0     1692.0
C       169        0.0     1842.0
C       183        0.0     1992.0
C       197        0.0     2142.0
C       211        0.0     2292.0
C       225        0.0     2442.0
C       239        0.0     2592.0
C       253        0.0     2742.0
C       267        0.0     2892.0
C       281        0.0     3006.0
C       294     2769.0     3006.0
L         1         14          1   12          0
F        15         28          1       267         14
L       281        294          1   12          0
! 13 BAY EXTERIOR MOMENT FRAME CLADDING STIFFNESS NODE GENERATION
C       295        0.0        0.0
C       308     2769.0        0.0
C       309        0.0      192.0
C       310      213.0      192.0
C       311      426.0      192.0
C       312      639.0      192.0
C       313      852.0      192.0
C       314     1065.0      192.0
C       315     1278.0      192.0
C       316     1491.0      192.0
C       317     1704.0      192.0
C       318     1917.0      192.0
C       319     2130.0      192.0
C       320     2343.0      192.0
C       321     2556.0      192.0
C       322     2769.0      192.0
C       323        0.0      342.0
C       337        0.0      492.0
C       351        0.0      642.0
```

```
C      365       0.0     792.0
C      379       0.0     942.0
C      393       0.0    1092.0
C      407       0.0    1242.0
C      421       0.0    1392.0
C      435       0.0    1542.0
C      449       0.0    1692.0
C      463       0.0    1842.0
C      477       0.0    1992.0
C      491       0.0    2142.0
C      505       0.0    2292.0
C      519       0.0    2442.0
C      533       0.0    2592.0
C      547       0.0    2742.0
C      561       0.0    2892.0
C      575       0.0    3006.0
C      588    2769.0    3006.0
L      295       308          1   12          0
F      309       322          1       561          14
L      575       588          1   12          0
!
C      589       0.0       0.0
C      602    2769.0       0.0
C      603       0.0     192.0
C      604     213.0     192.0
C      605     426.0     192.0
C      606     639.0     192.0
C      607     852.0     192.0
C      608    1065.0     192.0
C      609    1278.0     192.0
C      610    1491.0     192.0
C      611    1704.0     192.0
C      612    1917.0     192.0
C      613    2130.0     192.0
C      614    2343.0     192.0
C      615    2556.0     192.0
C      616    2769.0     192.0
C      617       0.0     342.0
C      631       0.0     492.0
C      645       0.0     642.0
C      659       0.0     792.0
C      673       0.0     942.0
C      687       0.0    1092.0
C      701       0.0    1242.0
C      715       0.0    1392.0
C      729       0.0    1542.0
C      743       0.0    1692.0
C      757       0.0    1842.0
C      771       0.0    1992.0
C      785       0.0    2142.0
C      799       0.0    2292.0
C      813       0.0    2442.0
C      827       0.0    2592.0
C      841       0.0    2742.0
C      855       0.0    2892.0
C      869       0.0    3006.0
C      882    2769.0    3006.0
L      589       602          1   12          0
F      603       616          1       855          14
L      869       882          1   12          0
!
C      883       0.0       0.0
C      896    2769.0       0.0
C      897       0.0     192.0
C      898     213.0     192.0
C      899     426.0     192.0
C      900     639.0     192.0
C      901     852.0     192.0
C      902    1065.0     192.0
C      903    1278.0     192.0
C      904    1491.0     192.0
```

```
C      905    1704.0     192.0
C      906    1917.0     192.0
C      907    2130.0     192.0
C      908    2343.0     192.0
C      909    2556.0     192.0
C      910    2769.0     192.0
C      911       0.0     342.0
C      925       0.0     492.0
C      939       0.0     642.0
C      953       0.0     792.0
C      967       0.0     942.0
C      981       0.0    1092.0
C      995       0.0    1242.0
C     1009       0.0    1392.0
C     1023       0.0    1542.0
C     1037       0.0    1692.0
C     1051       0.0    1842.0
C     1065       0.0    1992.0
C     1079       0.0    2142.0
C     1093       0.0    2292.0
C     1107       0.0    2442.0
C     1121       0.0    2592.0
C     1135       0.0    2742.0
C     1149       0.0    2892.0
C     1163       0.0    3006.0
C     1176    2769.0    3006.0
L      883       896          1   12          0
F      897       910          1      1149         14
L     1163      1176          1   12          0
!
C     1177       0.0       0.0
C     1190    2769.0       0.0
C     1191       0.0     192.0
C     1192     213.0     192.0
C     1193     426.0     192.0
C     1194     639.0     192.0
C     1195     852.0     192.0
C     1196    1065.0     192.0
C     1197    1278.0     192.0
C     1198    1491.0     192.0
C     1199    1704.0     192.0
C     1200    1917.0     192.0
C     1201    2130.0     192.0
C     1202    2343.0     192.0
C     1203    2556.0     192.0
C     1204    2769.0     192.0
C     1205       0.0     342.0
C     1219       0.0     492.0
C     1233       0.0     642.0
C     1247       0.0     792.0
C     1261       0.0     942.0
C     1275       0.0    1092.0
C     1289       0.0    1242.0
C     1303       0.0    1392.0
C     1317       0.0    1542.0
C     1331       0.0    1692.0
C     1345       0.0    1842.0
C     1359       0.0    1992.0
C     1373       0.0    2142.0
C     1387       0.0    2292.0
C     1401       0.0    2442.0
C     1415       0.0    2592.0
C     1429       0.0    2742.0
C     1443       0.0    2892.0
C     1457       0.0    3006.0
C     1470    2769.0    3006.0
L     1177      1190          1   12          0
F     1191      1204          1      1443         14
L     1457      1470          1   12          0
*RESTRAINTS
S 111          1        14          1
```

```
!
S 001       295      1470         1
S 111       295       575        14
S 111       883      1163        14
S 111       296       308         1
S 111       589       601         1
S 111      1457      1470         1
S 111      1163      1176         1
S 111       602       882        14
S 111      1190      1470        14
!
*SLAVING
S 100        21        15        20         1
S 100        21        22        28         1
S 100        35        29        34         1
S 100        35        36        42         1
S 100        49        43        48         1
S 100        49        50        56         1
S 100        63        57        62         1
S 100        63        64        70         1
S 100        77        71        76         1
S 100        77        78        84         1
S 100        91        85        90         1
S 100        91        92        98         1
S 100       105        99       104         1
S 100       105       106       112         1
S 100       119       113       118         1
S 100       119       120       126         1
S 100       133       127       132         1
S 100       133       134       140         1
S 100       147       141       146         1
S 100       147       148       154         1
S 100       161       155       160         1
S 100       161       162       168         1
S 100       175       169       174         1
S 100       175       176       182         1
S 100       189       183       188         1
S 100       189       190       196         1
S 100       203       197       202         1
S 100       203       204       210         1
S 100       217       211       216         1
S 100       217       218       224         1
S 100       231       225       230         1
S 100       231       232       238         1
S 100       245       239       244         1
S 100       245       246       252         1
S 100       259       253       258         1
S 100       259       260       266         1
S 100       273       267       272         1
S 100       273       274       280         1
S 100       287       281       286         1
S 100       287       288       294         1
! PANELS DEFORM IN SHEAR MODE ONLY
S 100       603       310
S 100       604       311
S 100       605       312
S 100       606       313
S 100       607       314
S 100       608       315
S 100       609       316
S 100       610       317
S 100       611       318
S 100       612       319
S 100       613       320
S 100       614       321
S 100       615       322
!
S 100       617       324
S 100       618       325
S 100       619       326
S 100       620       327
```

```
S 100       621       328
S 100       622       329
S 100       623       330
S 100       624       331
S 100       625       332
S 100       626       333
S 100       627       334
S 100       628       335
S 100       629       336
!
S 100       631       338
S 100       632       339
S 100       633       340
S 100       634       341
S 100       635       342
S 100       636       343
S 100       637       344
S 100       638       345
S 100       639       346
S 100       640       347
S 100       641       348
S 100       642       349
S 100       643       350
!
S 100       645       352
S 100       646       353
S 100       647       354
S 100       648       355
S 100       649       356
S 100       650       357
S 100       651       358
S 100       652       359
S 100       653       360
S 100       654       361
S 100       655       362
S 100       656       363
S 100       657       364
!
S 100       659       366
S 100       660       367
S 100       661       368
S 100       662       369
S 100       663       370
S 100       664       371
S 100       665       372
S 100       666       373
S 100       667       374
S 100       668       375
S 100       669       376
S 100       670       377
S 100       671       378
!
S 100       673       380
S 100       674       381
S 100       675       382
S 100       676       383
S 100       677       384
S 100       678       385
S 100       679       386
S 100       680       387
S 100       681       388
S 100       682       389
S 100       683       390
S 100       684       391
S 100       685       392
!
S 100       687       394
S 100       688       395
S 100       689       396
S 100       690       397
S 100       691       398
```

```
S 100       692       399
S 100       693       400
S 100       694       401
S 100       695       402
S 100       696       403
S 100       697       404
S 100       698       405
S 100       699       406
!
S 100       701       408
S 100       702       409
S 100       703       410
S 100       704       411
S 100       705       412
S 100       706       413
S 100       707       414
S 100       708       415
S 100       709       416
S 100       710       417
S 100       711       418
S 100       712       419
S 100       713       420
!
S 100       715       422
S 100       716       423
S 100       717       424
S 100       718       425
S 100       719       426
S 100       720       427
S 100       721       428
S 100       722       429
S 100       723       430
S 100       724       431
S 100       725       432
S 100       726       433
S 100       727       434
!
S 100       729       436
S 100       730       437
S 100       731       438
S 100       732       439
S 100       733       440
S 100       734       441
S 100       735       442
S 100       736       443
S 100       737       444
S 100       738       445
S 100       739       446
S 100       740       447
S 100       741       448
!
S 100       743       450
S 100       744       451
S 100       745       452
S 100       746       453
S 100       747       454
S 100       748       455
S 100       749       456
S 100       750       457
S 100       751       458
S 100       752       459
S 100       753       460
S 100       754       461
S 100       755       462
!
S 100       757       464
S 100       758       465
S 100       759       466
S 100       760       467
S 100       761       468
S 100       762       469
```

```
S 100       763       470
S 100       764       471
S 100       765       472
S 100       766       473
S 100       767       474
S 100       768       475
S 100       769       476
!
S 100       771       478
S 100       772       479
S 100       773       480
S 100       774       481
S 100       775       482
S 100       776       483
S 100       777       484
S 100       778       485
S 100       779       486
S 100       780       487
S 100       781       488
S 100       782       489
S 100       783       490
!
S 100       785       492
S 100       786       493
S 100       787       494
S 100       788       495
S 100       789       496
S 100       790       497
S 100       791       498
S 100       792       499
S 100       793       500
S 100       794       501
S 100       795       502
S 100       796       503
S 100       797       504
!
S 100       799       506
S 100       800       507
S 100       801       508
S 100       802       509
S 100       803       510
S 100       804       511
S 100       805       512
S 100       806       513
S 100       807       514
S 100       808       515
S 100       809       516
S 100       810       517
S 100       811       518
!
S 100       813       520
S 100       814       521
S 100       815       522
S 100       816       523
S 100       817       524
S 100       818       525
S 100       819       526
S 100       820       527
S 100       821       528
S 100       822       529
S 100       823       530
S 100       824       531
S 100       825       532
!
S 100       827       534
S 100       828       535
S 100       829       536
S 100       830       537
S 100       831       538
S 100       832       539
S 100       833       540
```

```
S 100       834       541
S 100       835       542
S 100       836       543
S 100       837       544
S 100       838       545
S 100       839       546
!
S 100       841       548
S 100       842       549
S 100       843       550
S 100       844       551
S 100       845       552
S 100       846       553
S 100       847       554
S 100       848       555
S 100       849       556
S 100       850       557
S 100       851       558
S 100       852       559
S 100       853       560
!
S 100       855       562
S 100       856       563
S 100       857       564
S 100       858       565
S 100       859       566
S 100       860       567
S 100       861       568
S 100       862       569
S 100       863       570
S 100       864       571
S 100       865       572
S 100       866       573
S 100       867       574
!
S 100       869       576
S 100       870       577
S 100       871       578
S 100       872       579
S 100       873       580
S 100       874       581
S 100       875       582
S 100       876       583
S 100       877       584
S 100       878       585
S 100       879       586
S 100       880       587
S 100       881       588
!
S 100      1177       884
S 100      1178       885
S 100      1179       886
S 100      1180       887
S 100      1181       888
S 100      1182       889
S 100      1183       890
S 100      1184       891
S 100      1185       892
S 100      1186       893
S 100      1187       894
S 100      1188       895
S 100      1189       896
!
S 100      1191       898
S 100      1192       899
S 100      1193       900
S 100      1194       901
S 100      1195       902
S 100      1196       903
S 100      1197       904
S 100      1198       905
```

```
S 100       1199        906
S 100       1200        907
S 100       1201        908
S 100       1202        909
S 100       1203        910
!
S 100       1205        912
S 100       1206        913
S 100       1207        914
S 100       1208        915
S 100       1209        916
S 100       1210        917
S 100       1211        918
S 100       1212        919
S 100       1213        920
S 100       1214        921
S 100       1215        922
S 100       1216        923
S 100       1217        924
!
S 100       1219        926
S 100       1220        927
S 100       1221        928
S 100       1222        929
S 100       1223        930
S 100       1224        931
S 100       1225        932
S 100       1226        933
S 100       1227        934
S 100       1228        935
S 100       1229        936
S 100       1230        937
S 100       1231        938
!
S 100       1233        940
S 100       1234        941
S 100       1235        942
S 100       1236        943
S 100       1237        944
S 100       1238        945
S 100       1239        946
S 100       1240        947
S 100       1241        948
S 100       1242        949
S 100       1243        950
S 100       1244        951
S 100       1245        952
!
S 100       1247        954
S 100       1248        955
S 100       1249        956
S 100       1250        957
S 100       1251        958
S 100       1252        959
S 100       1253        960
S 100       1254        961
S 100       1255        962
S 100       1256        963
S 100       1257        964
S 100       1258        965
S 100       1259        966
!
S 100       1261        968
S 100       1262        969
S 100       1263        970
S 100       1264        971
S 100       1265        972
S 100       1266        973
S 100       1267        974
S 100       1268        975
S 100       1269        976
```

```
S 100       1270        977
S 100       1271        978
S 100       1272        979
S 100       1273        980
!
S 100       1275        982
S 100       1276        983
S 100       1277        984
S 100       1278        985
S 100       1279        986
S 100       1280        987
S 100       1281        988
S 100       1282        989
S 100       1283        990
S 100       1284        991
S 100       1285        992
S 100       1286        993
S 100       1287        994
!
S 100       1289        996
S 100       1290        997
S 100       1291        998
S 100       1292        999
S 100       1293       1000
S 100       1294       1001
S 100       1295       1002
S 100       1296       1003
S 100       1297       1004
S 100       1298       1005
S 100       1299       1006
S 100       1300       1007
S 100       1301       1008
!
S 100       1303       1010
S 100       1304       1011
S 100       1305       1012
S 100       1306       1013
S 100       1307       1014
S 100       1308       1015
S 100       1309       1016
S 100       1310       1017
S 100       1311       1018
S 100       1312       1019
S 100       1313       1020
S 100       1314       1021
S 100       1315       1022
!
S 100       1317       1024
S 100       1318       1025
S 100       1319       1026
S 100       1320       1027
S 100       1321       1028
S 100       1322       1029
S 100       1323       1030
S 100       1324       1031
S 100       1325       1032
S 100       1326       1033
S 100       1327       1034
S 100       1328       1035
S 100       1329       1036
!
S 100       1331       1038
S 100       1332       1039
S 100       1333       1040
S 100       1334       1041
S 100       1335       1042
S 100       1336       1043
S 100       1337       1044
S 100       1338       1045
S 100       1339       1046
S 100       1340       1047
```

```
S 100       1341       1048
S 100       1342       1049
S 100       1343       1050
!
S 100       1345       1052
S 100       1346       1053
S 100       1347       1054
S 100       1348       1055
S 100       1349       1056
S 100       1350       1057
S 100       1351       1058
S 100       1352       1059
S 100       1353       1060
S 100       1354       1061
S 100       1355       1062
S 100       1356       1063
S 100       1357       1064
!
S 100       1359       1066
S 100       1360       1067
S 100       1361       1068
S 100       1362       1069
S 100       1363       1070
S 100       1364       1071
S 100       1365       1072
S 100       1366       1073
S 100       1367       1074
S 100       1368       1075
S 100       1369       1076
S 100       1370       1077
S 100       1371       1078
!
S 100       1373       1080
S 100       1374       1081
S 100       1375       1082
S 100       1376       1083
S 100       1377       1084
S 100       1378       1085
S 100       1379       1086
S 100       1380       1087
S 100       1381       1088
S 100       1382       1089
S 100       1383       1090
S 100       1384       1091
S 100       1385       1092
!
S 100       1387       1094
S 100       1388       1095
S 100       1389       1096
S 100       1390       1097
S 100       1391       1098
S 100       1392       1099
S 100       1393       1100
S 100       1394       1101
S 100       1395       1102
S 100       1396       1103
S 100       1397       1104
S 100       1398       1105
S 100       1399       1106
!
S 100       1401       1108
S 100       1402       1109
S 100       1403       1110
S 100       1404       1111
S 100       1405       1112
S 100       1406       1113
S 100       1407       1114
S 100       1408       1115
S 100       1409       1116
S 100       1410       1117
S 100       1411       1118
```

```
S 100       1412       1119
S 100       1413       1120
!
S 100       1415       1122
S 100       1416       1123
S 100       1417       1124
S 100       1418       1125
S 100       1419       1126
S 100       1420       1127
S 100       1421       1128
S 100       1422       1129
S 100       1423       1130
S 100       1424       1131
S 100       1425       1132
S 100       1426       1133
S 100       1427       1134
!
S 100       1429       1136
S 100       1430       1137
S 100       1431       1138
S 100       1432       1139
S 100       1433       1140
S 100       1434       1141
S 100       1435       1142
S 100       1436       1143
S 100       1437       1144
S 100       1438       1145
S 100       1439       1146
S 100       1440       1147
S 100       1441       1148
!
S 100       1443       1150
S 100       1444       1151
S 100       1445       1152
S 100       1446       1153
S 100       1447       1154
S 100       1448       1155
S 100       1449       1156
S 100       1450       1157
S 100       1451       1158
S 100       1452       1159
S 100       1453       1160
S 100       1454       1161
S 100       1455       1162
!
S 010        603       1177
S 010        604       1178
S 010        605       1179
S 010        606       1180
S 010        607       1181
S 010        608       1182
S 010        609       1183
S 010        610       1184
S 010        611       1185
S 010        612       1186
S 010        613       1187
S 010        614       1188
S 010        615       1189
!
S 010        617       1191
S 010        618       1192
S 010        619       1193
S 010        620       1194
S 010        621       1195
S 010        622       1196
S 010        623       1197
S 010        624       1198
S 010        625       1199
S 010        626       1200
S 010        627       1201
S 010        628       1202
```

```
S 010       629       1203
!
S 010       631       1205
S 010       632       1206
S 010       633       1207
S 010       634       1208
S 010       635       1209
S 010       636       1210
S 010       637       1211
S 010       638       1212
S 010       639       1213
S 010       640       1214
S 010       641       1215
S 010       642       1216
S 010       643       1217
!
S 010       645       1219
S 010       646       1220
S 010       647       1221
S 010       648       1222
S 010       649       1223
S 010       650       1224
S 010       651       1225
S 010       652       1226
S 010       653       1227
S 010       654       1228
S 010       655       1229
S 010       656       1230
S 010       657       1231
!
S 010       659       1233
S 010       660       1234
S 010       661       1235
S 010       662       1236
S 010       663       1237
S 010       664       1238
S 010       665       1239
S 010       666       1240
S 010       667       1241
S 010       668       1242
S 010       669       1243
S 010       670       1244
S 010       671       1245
!
S 010       673       1247
S 010       674       1248
S 010       675       1249
S 010       676       1250
S 010       677       1251
S 010       678       1252
S 010       679       1253
S 010       680       1254
S 010       681       1255
S 010       682       1256
S 010       683       1257
S 010       684       1258
S 010       685       1259
!
S 010       687       1261
S 010       688       1262
S 010       689       1263
S 010       690       1264
S 010       691       1265
S 010       692       1266
S 010       693       1267
S 010       694       1268
S 010       695       1269
S 010       696       1270
S 010       697       1271
S 010       698       1272
S 010       699       1273
```

```
!
S 010       701       1275
S 010       702       1276
S 010       703       1277
S 010       704       1278
S 010       705       1279
S 010       706       1280
S 010       707       1281
S 010       708       1282
S 010       709       1283
S 010       710       1284
S 010       711       1285
S 010       712       1286
S 010       713       1287
!
S 010       715       1289
S 010       716       1290
S 010       717       1291
S 010       718       1292
S 010       719       1293
S 010       720       1294
S 010       721       1295
S 010       722       1296
S 010       723       1297
S 010       724       1298
S 010       725       1299
S 010       726       1300
S 010       727       1301
!
S 010       729       1303
S 010       730       1304
S 010       731       1305
S 010       732       1306
S 010       733       1307
S 010       734       1308
S 010       735       1309
S 010       736       1310
S 010       737       1311
S 010       738       1312
S 010       739       1313
S 010       740       1314
S 010       741       1315
!
S 010       743       1317
S 010       744       1318
S 010       745       1319
S 010       746       1320
S 010       747       1321
S 010       748       1322
S 010       749       1323
S 010       750       1324
S 010       751       1325
S 010       752       1326
S 010       753       1327
S 010       754       1328
S 010       755       1329
!
S 010       757       1331
S 010       758       1332
S 010       759       1333
S 010       760       1334
S 010       761       1335
S 010       762       1336
S 010       763       1337
S 010       764       1338
S 010       765       1339
S 010       766       1340
S 010       767       1341
S 010       768       1342
S 010       769       1343
!
```

```
S 010       771       1345
S 010       772       1346
S 010       773       1347
S 010       774       1348
S 010       775       1349
S 010       776       1350
S 010       777       1351
S 010       778       1352
S 010       779       1353
S 010       780       1354
S 010       781       1355
S 010       782       1356
S 010       783       1357
!
S 010       785       1359
S 010       786       1360
S 010       787       1361
S 010       788       1362
S 010       789       1363
S 010       790       1364
S 010       791       1365
S 010       792       1366
S 010       793       1367
S 010       794       1368
S 010       795       1369
S 010       796       1370
S 010       797       1371
!
S 010       799       1373
S 010       788       1374
S 010       789       1375
S 010       790       1376
S 010       791       1377
S 010       792       1378
S 010       793       1379
S 010       794       1380
S 010       795       1381
S 010       796       1382
S 010       797       1383
S 010       798       1384
S 010       799       1385
!
S 010       813       1387
S 010       814       1388
S 010       815       1389
S 010       816       1390
S 010       817       1391
S 010       818       1392
S 010       819       1393
S 010       820       1394
S 010       821       1395
S 010       822       1396
S 010       823       1397
S 010       824       1398
S 010       825       1399
!
S 010       827       1401
S 010       828       1402
S 010       829       1403
S 010       830       1404
S 010       831       1405
S 010       832       1406
S 010       833       1407
S 010       834       1408
S 010       835       1409
S 010       836       1410
S 010       837       1411
S 010       838       1412
S 010       839       1413
!
S 010       841       1415
```

```
S 010       842       1416
S 010       843       1417
S 010       844       1418
S 010       845       1419
S 010       846       1420
S 010       847       1421
S 010       848       1422
S 010       849       1423
S 010       850       1424
S 010       851       1425
S 010       852       1426
S 010       853       1427
!
S 010       855       1429
S 010       856       1430
S 010       857       1431
S 010       858       1432
S 010       859       1433
S 010       860       1434
S 010       861       1435
S 010       862       1436
S 010       863       1437
S 010       864       1438
S 010       865       1439
S 010       866       1440
S 010       867       1441
!
S 010       869       1443
S 010       870       1444
S 010       871       1445
S 010       872       1446
S 010       873       1447
S 010       874       1448
S 010       875       1449
S 010       876       1450
S 010       877       1451
S 010       878       1452
S 010       879       1453
S 010       880       1454
S 010       881       1455
!
S 010       310        884
S 010       311        885
S 010       312        886
S 010       313        887
S 010       314        888
S 010       315        889
S 010       316        890
S 010       317        891
S 010       318        892
S 010       319        893
S 010       320        894
S 010       321        895
S 010       322        896
!
S 010       324        898
S 010       325        899
S 010       326        900
S 010       327        901
S 010       328        902
S 010       329        903
S 010       330        904
S 010       331        905
S 010       332        906
S 010       333        907
S 010       334        908
S 010       335        909
S 010       336        910
!
S 010       338        912
S 010       339        913
```

```
S 010       340       914
S 010       341       915
S 010       342       916
S 010       343       917
S 010       344       918
S 010       345       919
S 010       346       920
S 010       347       921
S 010       348       922
S 010       349       923
S 010       350       924
!
S 010       352       926
S 010       353       927
S 010       354       928
S 010       355       929
S 010       356       930
S 010       357       931
S 010       358       932
S 010       359       933
S 010       360       934
S 010       361       935
S 010       362       936
S 010       363       937
S 010       364       938
!
S 010       366       940
S 010       367       941
S 010       368       942
S 010       369       943
S 010       370       944
S 010       371       945
S 010       372       946
S 010       373       947
S 010       374       948
S 010       375       949
S 010       376       950
S 010       377       951
S 010       378       952
!
S 010       380       954
S 010       381       955
S 010       382       956
S 010       383       957
S 010       384       958
S 010       385       959
S 010       386       960
S 010       387       961
S 010       388       962
S 010       389       963
S 010       390       964
S 010       391       965
S 010       392       966
!
S 010       394       968
S 010       395       969
S 010       396       970
S 010       397       971
S 010       398       972
S 010       399       973
S 010       400       974
S 010       401       975
S 010       402       976
S 010       403       977
S 010       404       978
S 010       405       979
S 010       406       980
!
S 010       408       982
S 010       409       983
S 010       410       984
```

```
S 010        411        985
S 010        412        986
S 010        413        987
S 010        414        988
S 010        415        989
S 010        416        990
S 010        417        991
S 010        418        992
S 010        419        993
S 010        420        994
!
S 010        422        996
S 010        423        997
S 010        424        998
S 010        425        999
S 010        426       1000
S 010        427       1001
S 010        428       1002
S 010        429       1003
S 010        430       1004
S 010        431       1005
S 010        432       1006
S 010        433       1007
S 010        434       1008
!
S 010        436       1010
S 010        437       1011
S 010        438       1012
S 010        439       1013
S 010        440       1014
S 010        441       1015
S 010        442       1016
S 010        443       1017
S 010        444       1018
S 010        445       1019
S 010        446       1020
S 010        447       1021
S 010        448       1022
!
S 010        450       1024
S 010        451       1025
S 010        452       1026
S 010        453       1027
S 010        454       1028
S 010        455       1029
S 010        456       1030
S 010        457       1031
S 010        458       1032
S 010        459       1033
S 010        460       1034
S 010        461       1035
S 010        462       1036
!
S 010        464       1038
S 010        465       1039
S 010        466       1040
S 010        467       1041
S 010        468       1042
S 010        469       1043
S 010        470       1044
S 010        471       1045
S 010        472       1046
S 010        473       1047
S 010        474       1048
S 010        475       1049
S 010        476       1050
!
S 010        478       1052
S 010        479       1053
S 010        480       1054
S 010        481       1055
```

```
S 010       482       1056
S 010       483       1057
S 010       484       1058
S 010       485       1059
S 010       486       1060
S 010       487       1061
S 010       488       1062
S 000       489       1063
S 000       490       1064
!
S 010       492       1066
S 010       493       1067
S 010       494       1068
S 010       495       1069
S 010       496       1070
S 010       497       1071
S 010       498       1072
S 010       499       1073
S 010       500       1074
S 010       501       1075
S 010       502       1076
S 010       503       1077
S 010       504       1078
!
S 010       506       1080
S 010       507       1081
S 010       508       1082
S 010       509       1083
S 010       510       1084
S 010       511       1085
S 010       512       1086
S 010       513       1087
S 010       514       1088
S 010       515       1089
S 010       516       1090
S 010       517       1091
S 010       518       1092
!
S 010       520       1094
S 010       521       1095
S 010       522       1096
S 010       523       1097
S 010       524       1098
S 010       525       1099
S 010       526       1100
S 010       527       1101
S 010       528       1102
S 010       529       1103
S 010       530       1104
S 010       531       1105
S 010       532       1106
!
S 010       534       1108
S 010       535       1109
S 010       536       1110
S 010       537       1111
S 010       538       1112
S 010       539       1113
S 010       540       1114
S 010       541       1115
S 010       542       1116
S 010       543       1117
S 010       544       1118
S 010       545       1119
S 010       546       1120
!
S 010       548       1122
S 010       549       1123
S 010       550       1124
S 010       551       1125
S 010       552       1126
```

```
S 010        553       1127
S 010        554       1128
S 010        555       1129
S 010        556       1130
S 010        557       1131
S 010        558       1132
S 010        559       1133
S 010        560       1134
!
S 010        562       1136
S 010        563       1137
S 010        564       1138
S 010        565       1139
S 010        566       1140
S 010        567       1141
S 010        568       1142
S 010        569       1143
S 010        570       1144
S 010        571       1145
S 010        572       1146
S 010        573       1147
S 010        574       1148
!
S 010        576       1150
S 010        577       1151
S 010        578       1152
S 010        579       1153
S 010        580       1154
S 010        581       1155
S 010        582       1156
S 010        583       1157
S 010        584       1158
S 010        585       1159
S 010        586       1160
S 010        587       1161
S 010        588       1162
!
*MASSES
! NODAL MASS GENERATION FOR 13 BAY EXTERIOR MOMENT FRAME
S 100    2.21894        15        28         1                    14.0  0.137450
S 100    2.29273        29        42         1                    14.0  0.137450
S 100    2.28756        43        56         1                    14.0  0.137450
S 100    2.27979        57        70         1                    14.0  0.137450
S 100    2.27202        71        84         1                    14.0  0.137450
S 100    2.26684        85        98         1                    14.0  0.137450
S 100    2.25907        99       112         1                    14.0  0.137450
S 100    2.24872       113       126         1                    14.0  0.137450
S 100    2.24483       127       140         1                    14.0  0.137450
S 100    2.24095       141       154         1                    14.0  0.137450
S 100    2.23318       155       168         1                    14.0  0.137450
S 100    2.16586       169       182         1                    14.0  0.137450
S 100    2.15810       183       196         1                    14.0  0.137450
S 100    2.15033       197       210         1                    14.0  0.137450
S 100    2.13997       211       224         1                    14.0  0.137450
S 100    2.12832       225       238         1                    14.0  0.137450
S 100    2.12055       239       252         1                    14.0  0.137450
S 100    2.11667       253       266         1                    14.0  0.137450
S 100    2.11667       267       280         1                    14.0  0.137450
S 100    2.09596       281       294         1                    14.0  0.137450
! NODAL MASS GENERATION FOR CLADDING CONNECTIONS
S 100   0.041429      1177      1189         1                     4.0  0.137450
S 100   0.041429       884       896         1                     4.0  0.137450
S 100   0.041429       603       615         1                     4.0  0.137450
S 100   0.041429       310       322         1                     4.0  0.137450
S 100   0.032367      1191      1203         1                     4.0  0.137450
S 100   0.032367      1205      1217         1                     4.0  0.137450
S 100   0.032367      1219      1231         1                     4.0  0.137450
S 100   0.032367      1233      1245         1                     4.0  0.137450
S 100   0.032367      1247      1259         1                     4.0  0.137450
S 100   0.032367      1261      1273         1                     4.0  0.137450
S 100   0.032367      1275      1287         1                     4.0  0.137450
```

```
S 100  0.032367      1289      1301         1                    4.0  0.137450
S 100  0.032367      1303      1315         1                    4.0  0.137450
S 100  0.032367      1317      1329         1                    4.0  0.137450
S 100  0.032367      1331      1343         1                    4.0  0.137450
S 100  0.032367      1345      1357         1                    4.0  0.137450
S 100  0.032367      1359      1371         1                    4.0  0.137450
S 100  0.032367      1373      1385         1                    4.0  0.137450
S 100  0.032367      1387      1399         1                    4.0  0.137450
S 100  0.032367      1401      1413         1                    4.0  0.137450
S 100  0.032367      1415      1427         1                    4.0  0.137450
S 100  0.032367      1429      1441         1                    4.0  0.137450
S 100  0.024599      1443      1455         1                    4.0  0.137450
S 100  0.032367       324       336         1                    4.0  0.137450
S 100  0.032367       338       350         1                    4.0  0.137450
S 100  0.032367       352       364         1                    4.0  0.137450
S 100  0.032367       366       378         1                    4.0  0.137450
S 100  0.032367       380       392         1                    4.0  0.137450
S 100  0.032367       394       406         1                    4.0  0.137450
S 100  0.032367       408       420         1                    4.0  0.137450
S 100  0.032367       422       434         1                    4.0  0.137450
S 100  0.032367       436       448         1                    4.0  0.137450
S 100  0.032367       450       462         1                    4.0  0.137450
S 100  0.032367       464       476         1                    4.0  0.137450
S 100  0.032367       478       490         1                    4.0  0.137450
S 100  0.032367       492       504         1                    4.0  0.137450
S 100  0.032367       506       518         1                    4.0  0.137450
S 100  0.032367       520       532         1                    4.0  0.137450
S 100  0.032367       534       546         1                    4.0  0.137450
S 100  0.032367       548       560         1                    4.0  0.137450
S 100  0.032367       562       574         1                    4.0  0.137450
S 100  0.024599       576       588         1                    4.0  0.137450
S 100  0.032367       617       629         1                    4.0  0.137450
S 100  0.032367       631       643         1                    4.0  0.137450
S 100  0.032367       645       657         1                    4.0  0.137450
S 100  0.032367       659       671         1                    4.0  0.137450
S 100  0.032367       673       685         1                    4.0  0.137450
S 100  0.032367       687       699         1                    4.0  0.137450
S 100  0.032367       701       713         1                    4.0  0.137450
S 100  0.032367       715       727         1                    4.0  0.137450
S 100  0.032367       729       741         1                    4.0  0.137450
S 100  0.032367       743       755         1                    4.0  0.137450
S 100  0.032367       757       769         1                    4.0  0.137450
S 100  0.032367       771       783         1                    4.0  0.137450
S 100  0.032367       785       797         1                    4.0  0.137450
S 100  0.032367       799       811         1                    4.0  0.137450
S 100  0.032367       813       825         1                    4.0  0.137450
S 100  0.032367       827       839         1                    4.0  0.137450
S 100  0.032367       841       853         1                    4.0  0.137450
S 100  0.032367       855       867         1                    4.0  0.137450
S 100  0.024599       869       881         1                    4.0  0.137450
S 100  0.032367       898       910         1                    4.0  0.137450
S 100  0.032367       912       924         1                    4.0  0.137450
S 100  0.032367       926       938         1                    4.0  0.137450
S 100  0.032367       940       952         1                    4.0  0.137450
S 100  0.032367       954       966         1                    4.0  0.137450
S 100  0.032367       968       980         1                    4.0  0.137450
S 100  0.032367       982       994         1                    4.0  0.137450
S 100  0.032367       996      1008         1                    4.0  0.137450
S 100  0.032367      1010      1022         1                    4.0  0.137450
S 100  0.032367      1024      1036         1                    4.0  0.137450
S 100  0.032367      1038      1050         1                    4.0  0.137450
S 100  0.032367      1052      1064         1                    4.0  0.137450
S 100  0.032367      1066      1078         1                    4.0  0.137450
S 100  0.032367      1080      1092         1                    4.0  0.137450
S 100  0.032367      1094      1106         1                    4.0  0.137450
S 100  0.032367      1108      1120         1                    4.0  0.137450
S 100  0.032367      1122      1134         1                    4.0  0.137450
S 100  0.032367      1136      1148         1                    4.0  0.137450
S 100  0.024599      1150      1162         1                    4.0  0.137450
*ELEMENTGROUP
    2    1    0       0.014394                    COLUMNS AND BEAMS
```

```
 28    0   28
  1   29000.0        0.1       34.2     4930.0   4.0   4.0   2.0
  2   29000.0        0.1       29.1     3990.0   4.0   4.0   2.0
  3   29000.0        0.1       27.7     3270.0   4.0   4.0   2.0
  4   29000.0        0.1       22.4     2100.0   4.0   4.0   2.0
  5   29000.0        0.1       20.1     1830.0   4.0   4.0   2.0
  6   29000.0        0.1       13.0      843.0   4.0   4.0   2.0
  7   29000.0        0.1       75.6     3400.0   4.0   4.0   2.0
  8   29000.0        0.1       62.0     2660.0   4.0   4.0   2.0
  9   29000.0        0.1       56.8     2400.0   4.0   4.0   2.0
 10   29000.0        0.1       46.7     1900.0   4.0   4.0   2.0
 11   29000.0        0.1       42.7     1710.0   4.0   4.0   2.0
 12   29000.0        0.1       38.8     1530.0   4.0   4.0   2.0
 13   29000.0        0.1       32.0     1240.0   4.0   4.0   2.0
 14   29000.0        0.1       29.1     1110.0   4.0   4.0   2.0
 15   29000.0        0.1       21.8      796.0   4.0   4.0   2.0
 16   29000.0        0.1       20.0      723.0   4.0   4.0   2.0
 17   29000.0        0.1       15.6      541.0   4.0   4.0   2.0
 18   29000.0        0.1       91.4     4330.0   4.0   4.0   2.0
 19   29000.0        0.1       68.5     3010.0   4.0   4.0   2.0
 20   29000.0        0.1       26.5      999.0   4.0   4.0   2.0
 21   29000.0        0.1      125.0     2360.0   4.0   4.0   2.0
 22   29000.0        0.1      101.0     1810.0   4.0   4.0   2.0
 23   29000.0        0.1       91.4     1610.0   4.0   4.0   2.0
 24   29000.0        0.1       75.6     1290.0   4.0   4.0   2.0
 25   29000.0        0.1       68.5     1150.0   4.0   4.0   2.0
 26   29000.0        0.1       56.8      931.0   4.0   4.0   2.0
 27   29000.0        0.1       46.7      748.0   4.0   4.0   2.0
 28   29000.0        0.1       42.7      677.0   4.0   4.0   2.0
  1    1     13608     13608
  2    1     11232     11232
  3    1     10008     10008
  4    1      7200      7200
  5    1      6372      6372
  6    1      5184      5184
  7    2     24350     24350      3780      3780  1.0 0.15   1 0.15
  8    2     19500     19500      3100      3100  1.0 0.15   1 0.15
  9    2     17750     17750      2840      2840  1.0 0.15   1 0.15
 10    2     14350     14350      2335      2335  1.0 0.15   1 0.15
 11    2     13000     13000      2135      2135  1.0 0.15   1 0.15
 12    2     11700     11700      1940      1940  1.0 0.15   1 0.15
 13    2      9600      9600      1600      1600  1.0 0.15   1 0.15
 14    2      8650      8650      1455      1455  1.0 0.15   1 0.15
 15    2      6300      6300      1090      1090  1.0 0.15   1 0.15
 16    2      5750      5750      1000      1000  1.0 0.15   1 0.15
 17    2      4355      4355       780       780  1.0 0.15   1 0.15
 18    2     30150     30150      4570      4570  1.0 0.15   1 0.15
 19    2     21800     21800      3425      3425  1.0 0.15   1 0.15
 20    2      7850      7850      1325      1325  1.0 0.15   1 0.15
 21    2     21700     21700      6250      6250  1.0 0.15   1 0.15
 22    2     16900     16900      5050      5050  1.0 0.15   1 0.15
 23    2     15200     15200      4570      4570  1.0 0.15   1 0.15
 24    2     12300     12300      3780      3780  1.0 0.15   1 0.15
 25    2     11050     11050      3425      3425  1.0 0.15   1 0.15
 26    2      9000      9000      2840      2840  1.0 0.15   1 0.15
 27    2      7300      7300      2335      2335  1.0 0.15   1 0.15
 28    2      6650      6650      2135      2135  1.0 0.15   1 0.15
!   BEAMS
  1        15        16        1    1    0    1    1
 14        29        30        1    2    0    2    2
 27        43        44        1    2    0    2    2
 40        57        58        1    2    0    2    2
 53        71        72        1    2    0    2    2
 66        85        86        1    2    0    2    2
 79        99       100        1    2    0    2    2
 92       113       114        1    3    0    3    3
105       127       128        1    3    0    3    3
118       141       142        1    3    0    3    3
131       155       156        1    3    0    3    3
144       169       170        1    3    0    3    3
157       183       184        1    3    0    3    3
```

```
  170       197       198         1    4    0    4    4
  183       211       212         1    4    0    4    4
  196       225       226         1    5    0    5    5
  209       239       240         1    5    0    5    5
  222       253       254         1    5    0    5    5
  235       267       268         1    5    0    5    5
  248       281       282         1    6    0    6    6
  260       293       294         1    6    0    6    6
! COLUMNS H-2,H-15 EXTERIOR COLUMNS
  261         1        15         0    7    0    7    7
  262        15        29        14    8    0    8    8
  264        43        57        14    9    0    9    9
  266        71        85        14   10    0   10   10
  268        99       113        14   11    0   11   11
  270       127       141        14   12    0   12   12
  272       155       169        14   13    0   13   13
  274       183       197        14   14    0   14   14
  276       211       225        14   15    0   15   15
  278       239       253        14   16    0   16   16
  280       267       281         0   17    0   17   17
  281        14        28         0    7    0    7    7
  282        28        42        14    8    0    8    8
  284        56        70        14    9    0    9    9
  286        84        98        14   10    0   10   10
  288       112       126        14   11    0   11   11
  290       140       154        14   12    0   12   12
  292       168       182        14   13    0   13   13
  294       196       210        14   14    0   14   14
  296       224       238        14   15    0   15   15
  298       252       266        14   16    0   16   16
  300       280       294         0   17    0   17   17
! COLUMNS H-3,H-4,H-5,H-6,H-8,H-9,H-11,H-12,H-13,H-14   INTERIOR COLUMNS
  301         2        16         1   18    0   18   18
  305         7        21         1   18    0   18   18
  307        10        24         1   18    0   18   18
  310        13        27         0   18    0   18   18
  311        16        30         1    7    0    7    7
  315        21        35         1    7    0    7    7
  317        24        38         1    7    0    7    7
  320        27        41         0    7    0    7    7
  321        30        44         1    7    0    7    7
  325        35        49         1    7    0    7    7
  327        38        52         1    7    0    7    7
  330        41        55         0    7    0    7    7
  331        44        58         1   19    0   19   19
  335        49        63         1   19    0   19   19
  337        52        66         1   19    0   19   19
  340        55        69         0   19    0   19   19
  341        58        72         1   19    0   19   19
  345        63        77         1   19    0   19   19
  347        66        80         1   19    0   19   19
  350        69        83         0   19    0   19   19
  351        72        86         1    8    0    8    8
  355        77        91         1    8    0    8    8
  357        80        94         1    8    0    8    8
  360        83        97         0    8    0    8    8
  361        86       100         1    8    0    8    8
  365        91       105         1    8    0    8    8
  367        94       108         1    8    0    8    8
  370        97       111         0    8    0    8    8
  371       100       114         1    8    0    8    8
  375       105       119         1    8    0    8    8
  377       108       122         1    8    0    8    8
  380       111       125         0    8    0    8    8
  381       114       128         1    8    0    8    8
  385       119       133         1    8    0    8    8
  387       122       136         1    8    0    8    8
  390       125       139         0    8    0    8    8
  391       128       142         1    9    0    9    9
  395       133       147         1    9    0    9    9
  397       136       150         1    9    0    9    9
```

```
  400       139       153         0    9    0    9    9
  401       142       156         1    9    0    9    9
  405       147       161         1    9    0    9    9
  407       150       164         1    9    0    9    9
  410       153       167         0    9    0    9    9
  411       156       170         1   10    0   10   10
  415       161       175         1   10    0   10   10
  417       164       178         1   10    0   10   10
  420       167       181         0   10    0   10   10
  421       170       184         1   10    0   10   10
  425       175       189         1   10    0   10   10
  427       178       192         1   10    0   10   10
  430       181       195         0   10    0   10   10
  431       184       198         1   11    0   11   11
  435       189       203         1   11    0   11   11
  437       192       206         1   11    0   11   11
  440       195       209         0   11    0   11   11
  441       198       212         1   11    0   11   11
  445       203       217         1   11    0   11   11
  447       206       220         1   11    0   11   11
  450       209       223         0   11    0   11   11
  451       212       226         1   11    0   11   11
  455       217       231         1   11    0   11   11
  457       220       234         1   11    0   11   11
  460       223       237         0   11    0   11   11
  461       226       240         1   11    0   11   11
  465       231       245         1   11    0   11   11
  467       234       248         1   11    0   11   11
  470       237       251         0   11    0   11   11
  471       240       254         1   20    0   20   20
  475       245       259         1   20    0   20   20
  477       248       262         1   20    0   20   20
  480       251       265         0   20    0   20   20
  481       254       268         1   20    0   20   20
  485       259       273         1   20    0   20   20
  487       262       276         1   20    0   20   20
  490       265       279         0   20    0   20   20
  491       268       282         1   20    0   20   20
  495       273       287         1   20    0   20   20
  497       276       290         1   20    0   20   20
  500       279       293         0   20    0   20   20
!   COLUMNS  H-7,H-10  INTERIOR COLUMNS
  501         6         20        0   21    0   21   21
  502        20         34       14   22    0   22   22
  504        48         62       14   23    0   23   23
  508       104        118       14   24    0   24   24
  512       160        174       14   25    0   25   25
  514       188        202       14   26    0   26   26
  516       216        230       14   27    0   27   27
  520       272        286        0   28    0   28   28
  521         9         23        0   21    0   21   21
  522        23         37       14   22    0   22   22
  524        51         65       14   23    0   23   23
  528       107        121       14   24    0   24   24
  532       163        177       14   25    0   25   25
  534       191        205       14   26    0   26   26
  536       219        233       14   27    0   27   27
  540       275        289        0   28    0   28   28
*ELEMENTGROUP
    6    1    0                              CLADDING PANELS
    1
    1   1000000 100000000   1000000 100000000   1000000
    1       603       310      1177       884        14    1
   21       604       311      1178       885        14    1
   41       605       312      1179       886        14    1
   61       606       313      1180       887        14    1
   81       607       314      1181       888        14    1
  101       608       315      1182       889        14    1
  121       609       316      1183       890        14    1
  141       610       317      1184       891        14    1
  161       611       318      1185       892        14    1
```

```
  181        612        319       1186        893         14     1
  201        613        320       1187        894         14     1
  221        614        321       1188        895         14     1
  241        615        322       1189        896         14     1
  260        881        588       1455       1162          0     1
*ELEMENTGROUP
    4     1     0                                BEARING CLADDING CONN. (X)
    1
    1   1000000          0      10000      10000       0.01     1     1
    1          1       1177         14     1
   21          2        884         14     1
   41          2       1178         14     1
   61          3        885         14     1
   81          3       1179         14     1
  101          4        886         14     1
  121          4       1180         14     1
  141          5        887         14     1
  161          5       1181         14     1
  181          6        888         14     1
  201          6       1182         14     1
  221          7        889         14     1
  241          7       1183         14     1
  261          8        890         14     1
  281          8       1184         14     1
  301          9        891         14     1
  321          9       1185         14     1
  341         10        892         14     1
  361         10       1186         14     1
  381         11        893         14     1
  401         11       1187         14     1
  421         12        894         14     1
  441         12       1188         14     1
  461         13        895         14     1
  481         13       1189         14     1
  501         14        896         14     1
  520        280       1162          0     1
*ELEMENTGROUP
    4     1     0                                BEARING CLADDING CONN. (Y)
    1
    1   1000000          0      10000      10000       0.01     2     1
    1          1       1177         14     1
   21          2        884         14     1
   41          2       1178         14     1
   61          3        885         14     1
   81          3       1179         14     1
  101          4        886         14     1
  121          4       1180         14     1
  141          5        887         14     1
  161          5       1181         14     1
  181          6        888         14     1
  201          6       1182         14     1
  221          7        889         14     1
  241          7       1183         14     1
  261          8        890         14     1
  281          8       1184         14     1
  301          9        891         14     1
  321          9       1185         14     1
  341         10        892         14     1
  361         10       1186         14     1
  381         11        893         14     1
  401         11       1187         14     1
  421         12        894         14     1
  441         12       1188         14     1
  461         13        895         14     1
  481         13       1189         14     1
  501         14        896         14     1
  520        280       1162          0     1
*ELEMENTGROUP
    4     1     0                             TIE-BACK GROUND-FIFTH (X)
    1
    1        103          0         10         10       0.01     1     0
```

```
     1         15        603          1     1
    14         16        310          1     1
    27         29        617          1     1
    40         30        324          1     1
    53         43        631          1     1
    66         44        338          1     1
    79         57        645          1     1
    92         58        352          1     1
   104         70        364          0     1
*ELEMENTGROUP
     4     1     0                          TIE-BACK FIFTH-NINTH (X)
     1
     1       103          0         10          10       0.01     1     0
     1         71        659          1     1
    14         72        366          1     1
    27         85        673          1     1
    40         86        380          1     1
    53         99        687          1     1
    66        100        394          1     1
    79        113        701          1     1
    92        114        408          1     1
   104        126        420          0     1
*ELEMENTGROUP
     4     1     0                          TIE-BACK NINTH-THIRTEENTH (X)
     1
     1       103          0         10          10       0.01     1     0
     1        127        715          1     1
    14        128        422          1     1
    27        141        729          1     1
    40        142        436          1     1
    53        155        743          1     1
    66        156        450          1     1
    79        169        757          1     1
    92        170        464          1     1
   104        182        476          0     1
*ELEMENTGROUP
     4     1     0                          TIE-BACK THIRTEENTH-SEVENTEENTH (X)
     1
     1       103          0         10          10       0.01     1     0
     1        183        771          1     1
    14        184        478          1     1
    27        197        785          1     1
    40        198        492          1     1
    53        211        799          1     1
    66        212        506          1     1
    79        225        813          1     1
    92        226        520          1     1
   104        238        532          0     1
*ELEMENTGROUP
     4     1     0                          TIE-BACK SEVENTEENTH-ROOF (X)
     1
     1       103          0         10          10       0.01     1     0
     1        239        827          1     1
    14        240        534          1     1
    27        253        841          1     1
    40        254        548          1     1
    53        267        855          1     1
    66        268        562          1     1
    79        281        869          1     1
    92        282        576          1     1
   104        294        588          0     1
*ELEMENTGROUP
     4     1     0                          TIE-BACK (Y)
     1
     1       100          0      10000       10000       0.01     2     1
     1         15        603          1     1
    14         16        310          1     1
    27         29        617          1     1
    40         30        324          1     1
    53         43        631          1     1
    66         44        338          1     1
```

```
   79        57        645         1    1
   92        58        352         1    1
  104        70        364         0    1
!
  105        71        659         1    1
  118        72        366         1    1
  131        85        673         1    1
  144        86        380         1    1
  157        99        687         1    1
  170       100        394         1    1
  183       113        701         1    1
  206       114        408         1    1
  208       126        420         0    1
!
  209       127        715         1    1
  222       128        422         1    1
  235       141        729         1    1
  248       142        436         1    1
  261       155        743         1    1
  274       156        450         1    1
  287       169        757         1    1
  300       170        464         1    1
  312       182        476         0    1
!
  313       183        771         1    1
  326       184        478         1    1
  339       197        785         1    1
  352       198        492         1    1
  365       211        799         1    1
  378       212        506         1    1
  391       225        813         1    1
  404       226        520         1    1
  416       238        532         0    1
!
  417       239        827         1    1
  430       240        534         1    1
  443       253        841         1    1
  456       254        548         1    1
  469       267        855         1    1
  482       268        562         1    1
  495       281        869         1    1
  508       282        576         1    1
  520       294        588         0    1
*RESULTS
NSD     111          1      1470          1
E       111     1    1  540     1
E       111     2    1  260     1
E       111     3    1  520     1
E       111     4    1  520     1
E       111     5    1  104     1
E       111     6    1  104     1
E       111     7    1  104     1
E       111     8    1  104     1
E       111     9    1  104     1
E       111    10    1  520     1
!
*ACCNREC      ![Inserted by NONLIN-Pro]
 oak1   oakz_475.acc          (8F10.0)  OAKLAND EQ - 475 YR - Z DIRECTION
2976     8    0    0       1.0    386.22       .02       0.0
!
*PARAMETERS
! Dynamic control: use events but no accel or vel corrections
DC  1    0    0
! Dynamic time step specification
DT    0.01
! Dynamic output = 0.1sec
!     Sstp      Stim Rstp      Rtim Ostp      Otim Estp      Etim Ostp      Otim
OD       0       0.0    0       0.0    0       0.0    0       0.0    0      20.0
!
*MODE                                   MODAL ANALYSIS
    3      0.10    0    0    0
```

```
*ACCN                                   OAKLAND EQ - 475 YR - Z DIRECTION
      50.0 5000     1
1     oak1        1.0         1.0
!
*STOP
```

D. Design building model input file for DRAIN-2dx

```
! DESIGN MODEL
! 1-BAY-20-STORY FRAME REPRESENTING THE LONGIT FRAME (WITH CLADDING)
!
!UNITS L IN F K
*STARTXX
    1bay-A          0 1 0 1    B          20-STORY-1-BAY FRAME WITH CLADDING CONN
!
*NODECOORDS
! 1 BAY MOMENT FRAME WITHOUT CLADDING STIFFNESS NODE GENERATION
C         1        0.0        0.0
C         2        0.0      192.0
C         3        0.0      342.0
C         4        0.0      492.0
C         5        0.0      642.0
C         6        0.0      792.0
C         7        0.0      942.0
C         8        0.0     1092.0
C         9        0.0     1242.0
C        10        0.0     1392.0
C        11        0.0     1542.0
C        12        0.0     1692.0
C        13        0.0     1842.0
C        14        0.0     1992.0
C        15        0.0     2142.0
C        16        0.0     2292.0
C        17        0.0     2442.0
C        18        0.0     2592.0
C        19        0.0     2742.0
C        20        0.0     2892.0
C        21        0.0     3006.0
C        22      213.0        0.0
C        23      213.0      192.0
C        24      213.0      342.0
C        25      213.0      492.0
C        26      213.0      642.0
C        27      213.0      792.0
C        28      213.0      942.0
C        29      213.0     1092.0
C        30      213.0     1242.0
C        31      213.0     1392.0
C        32      213.0     1542.0
C        33      213.0     1692.0
C        34      213.0     1842.0
C        35      213.0     1992.0
C        36      213.0     2142.0
C        37      213.0     2292.0
C        38      213.0     2442.0
C        39      213.0     2592.0
C        40      213.0     2742.0
C        41      213.0     2892.0
C        42      213.0     3006.0
! CLADDING CONNECTIONS NODE GENERATION
C        43        0.0        0.0
C        44        0.0      192.0
C        45        0.0      342.0
C        46        0.0      492.0
C        47        0.0      642.0
C        48        0.0      792.0
C        49        0.0      942.0
C        50        0.0     1092.0
C        51        0.0     1242.0
C        52        0.0     1392.0
C        53        0.0     1542.0
C        54        0.0     1692.0
C        55        0.0     1842.0
C        56        0.0     1992.0
C        57        0.0     2142.0
C        58        0.0     2292.0
```

```
C       59        0.0    2442.0
C       60        0.0    2592.0
C       61        0.0    2742.0
C       62        0.0    2892.0
C       63        0.0    3006.0
!
C       64        0.0       0.0
C       65        0.0     192.0
C       66        0.0     342.0
C       67        0.0     492.0
C       68        0.0     642.0
C       69        0.0     792.0
C       70        0.0     942.0
C       71        0.0    1092.0
C       72        0.0    1242.0
C       73        0.0    1392.0
C       74        0.0    1542.0
C       75        0.0    1692.0
C       76        0.0    1842.0
C       77        0.0    1992.0
C       78        0.0    2142.0
C       79        0.0    2292.0
C       80        0.0    2442.0
C       81        0.0    2592.0
C       82        0.0    2742.0
C       83        0.0    2892.0
C       84        0.0    3006.0
!
C       85      213.0       0.0
C       86      213.0     192.0
C       87      213.0     342.0
C       88      213.0     492.0
C       89      213.0     642.0
C       90      213.0     792.0
C       91      213.0     942.0
C       92      213.0    1092.0
C       93      213.0    1242.0
C       94      213.0    1392.0
C       95      213.0    1542.0
C       96      213.0    1692.0
C       97      213.0    1842.0
C       98      213.0    1992.0
C       99      213.0    2142.0
C      100      213.0    2292.0
C      101      213.0    2442.0
C      102      213.0    2592.0
C      103      213.0    2742.0
C      104      213.0    2892.0
C      105      213.0    3006.0
!
C      106      213.0       0.0
C      107      213.0     192.0
C      108      213.0     342.0
C      109      213.0     492.0
C      110      213.0     642.0
C      111      213.0     792.0
C      112      213.0     942.0
C      113      213.0    1092.0
C      114      213.0    1242.0
C      115      213.0    1392.0
C      116      213.0    1542.0
C      117      213.0    1692.0
C      118      213.0    1842.0
C      119      213.0    1992.0
C      120      213.0    2142.0
C      121      213.0    2292.0
C      122      213.0    2442.0
C      123      213.0    2592.0
C      124      213.0    2742.0
C      125      213.0    2892.0
C      126      213.0    3006.0
```

```
!
*RESTRAINTS
S 111          1         22         21
S 001         43        126          1
! REDUNDANT NODES
S 111         43         43          0
S 111         84         84          0
S 111         85         85          0
S 111        126        126          0
!
*SLAVING
! PANELS DEFORM IN SHEAR MODE ONLY
S 100         44         86
S 100         45         87
S 100         46         88
S 100         47         89
S 100         48         90
S 100         49         91
S 100         50         92
S 100         51         93
S 100         52         94
S 100         53         95
S 100         54         96
S 100         55         97
S 100         56         98
S 100         57         99
S 100         58        100
S 100         59        101
S 100         60        102
S 100         61        103
S 100         62        104
S 100         63        105
S 100         64        106
S 100         65        107
S 100         66        108
S 100         67        109
S 100         68        110
S 100         69        111
S 100         70        112
S 100         71        113
S 100         72        114
S 100         73        115
S 100         74        116
S 100         75        117
S 100         76        118
S 100         77        119
S 100         78        120
S 100         79        121
S 100         80        122
S 100         81        123
S 100         82        124
S 100         83        125
!
S 010         44         64
S 010         45         65
S 010         46         66
S 010         47         67
S 010         48         68
S 010         49         69
S 010         50         70
S 010         51         71
S 010         52         72
S 010         53         73
S 010         54         74
S 010         55         75
S 010         56         76
S 010         57         77
S 010         58         78
S 010         59         79
S 010         60         80
S 010         61         81
```

```
S 010        62        82
S 010        63        83
S 010        86       106
S 010        87       107
S 010        88       108
S 010        89       109
S 010        90       110
S 010        91       111
S 010        92       112
S 010        93       113
S 010        94       114
S 010        95       115
S 010        96       116
S 010        97       117
S 010        98       118
S 010        99       119
S 010       100       120
S 010       101       121
S 010       102       122
S 010       103       123
S 010       104       124
S 010       105       125
!
*MASSES
! NODAL MASS GENERATION FOR FRAME NODES
S 100   2.21894         2        23        21                    2.0  0.137450
S 100   2.29273         3        24        21                    2.0  0.137450
S 100   2.28756         4        25        21                    2.0  0.137450
S 100   2.27979         5        26        21                    2.0  0.137450
S 100   2.27202         6        27        21                    2.0  0.137450
S 100   2.26684         7        28        21                    2.0  0.137450
S 100   2.25907         8        29        21                    2.0  0.137450
S 100   2.24872         9        30        21                    2.0  0.137450
S 100   2.24483        10        31        21                    2.0  0.137450
S 100   2.24095        11        32        21                    2.0  0.137450
S 100   2.23318        12        33        21                    2.0  0.137450
S 100   2.16586        13        34        21                    2.0  0.137450
S 100   2.15810        14        35        21                    2.0  0.137450
S 100   2.15033        15        36        21                    2.0  0.137450
S 100   2.13997        16        37        21                    2.0  0.137450
S 100   2.12832        17        38        21                    2.0  0.137450
S 100   2.12055        18        39        21                    2.0  0.137450
S 100   2.11667        19        40        21                    2.0  0.137450
S 100   2.11667        20        41        21                    2.0  0.137450
S 100   2.09596        21        42        21                    2.0  0.137450
! NODAL MASS GENERATION FOR CLADDING NODES
S 100  0.538577        44        64        20                    4.0  0.137450
S 100  0.538577        86       106        20                    4.0  0.137450
S 100  0.420771        45        62         1                    4.0  0.137450
S 100  0.420771        65        82         1                    4.0  0.137450
S 100  0.420771        87       104         1                    4.0  0.137450
S 100  0.420771       107       124         1                    4.0  0.137450
S 100  0.319787        63        83        20                    4.0  0.137450
S 100  0.319787       105       125        20                    4.0  0.137450
!
! GROUP#1
*ELEMENTGROUP
    2    1    0       0.014394                      COLUMNS AND BEAMS
   17    0    2
! Cross-section area of columns are calculated using the method of first moment
    1   29000.0       0.1    8548.8   27440.0  4.0  4.0  2.0
    2   29000.0       0.1    7033.0   21490.0  4.0  4.0  2.0
    3   29000.0       0.1    6379.1   19040.0  4.0  4.0  2.0
    4   29000.0       0.1    5825.3   16800.0  4.0  4.0  2.0
    5   29000.0       0.1    5567.9   16310.0  4.0  4.0  2.0
    6   29000.0       0.1    5179.2   14840.0  4.0  4.0  2.0
    7   29000.0       0.1    4342.0   11900.0  4.0  4.0  2.0
    8   29000.0       0.1    3892.2   10570.0  4.0  4.0  2.0
    9   29000.0       0.1    3666.0   10080.0  4.0  4.0  2.0
   10   29000.0       0.1    2589.6    6468.0  4.0  4.0  2.0
   11   29000.0       0.1    2480.4    6261.0  4.0  4.0  2.0
```

```
   12   29000.0        0.1       34.2   69020.0  4.0  4.0  2.0
   13   29000.0        0.1       29.1   55860.0  4.0  4.0  2.0
   14   29000.0        0.1       27.7   45780.0  4.0  4.0  2.0
   15   29000.0        0.1       22.4   29400.0  4.0  4.0  2.0
   16   29000.0        0.1       20.1   25620.0  4.0  4.0  2.0
   17   29000.0        0.1       13.0   11802.0  4.0  4.0  2.0
    1    2    10E+10     10E+10     10E+10     10E+10   1.0 0.15  1.0 0.15
    2    1    10E+10     10E+10
! BEAMS
    1          2         23          0   12     0    2    2
    2          3         24          1   13     0    2    2
    8          9         30          1   14     0    2    2
   14         15         36          1   15     0    2    2
   16         17         38          1   16     0    2    2
   20         21         42          0   17     0    2    2
! COLUMNS (LEFT)
   21          1          2          0    1     0    1    1
   22          2          3          1    2     0    1    1
   24          4          5          1    3     0    1    1
   26          6          7          1    4     0    1    1
   28          8          9          1    5     0    1    1
   30         10         11          1    6     0    1    1
   32         12         13          1    7     0    1    1
   34         14         15          1    8     0    1    1
   36         16         17          1    9     0    1    1
   38         18         19          1   10     0    1    1
   40         20         21          0   11     0    1    1
! COLUMNS (RIGHT)
   41         22         23          0    1     0    1    1
   42         23         24          1    2     0    1    1
   44         25         26          1    3     0    1    1
   46         27         28          1    4     0    1    1
   48         29         30          1    5     0    1    1
   50         31         32          1    6     0    1    1
   52         33         34          1    7     0    1    1
   54         35         36          1    8     0    1    1
   56         37         38          1    9     0    1    1
   58         39         40          1   10     0    1    1
   60         41         42          0   11     0    1    1
!
! GROUP#2
*ELEMENTGROUP
    6    1    0                              CLADDING PANELS
    1
    1   1000000 100000000   1000000 100000000   1000000
    1         44         86         64        106         1    1
   20         63        105         83        125         0    1
!
! GROUP#3
*ELEMENTGROUP
    4    1    0                              BEARING CLADDING CONN. (X)
    1
    1   1000000          0      10000      10000      0.01    1    1
    1          1         64          1    1
   20         20         83          0    1
   21         22        106          1    1
   40         41        125          0    1
!
! GROUP#4
*ELEMENTGROUP
    4    1    0                              BEARING CLADDING CONN. (Y)
    1
    1   1000000          0      10000      10000      0.01    2    1
    1          1         64          1    1
   20         20         83          0    1
   21         22        106          1    1
   40         41        125          0    1
!
! GROUP#5
*ELEMENTGROUP
    4    1    0                              TIE-BACK CONN. (X)
```

```
    1
    1       6375          0        260        260       0.01    1    0
    1          2         44          1    1
   20         21         63          0    1
   21         23         86          1    1
   40         42        105          0    1
!
! GROUP#6
*ELEMENTGROUP
    4    1    0                            TIE-BACK CONN. (Y)
    1
    1       1300          0      10000      10000       0.01    2    1
    1          2         44          1    1
   20         21         63          0    1
   21         23         86          1    1
   40         42        105          0    1
!
*RESULTS
NSD    111         21         21         1
!E      111
!
*ACCNREC      ![Inserted by NONLIN-Pro]
 oak1   oakz_475.acc          (8F10.0)  OAKLAND EQ - 475 YR - Z DIRECTION
2976     8    0    0       1.0    386.22        .02        0.0
!
*PARAMETERS
! Dynamic control: use events but no accel or vel corrections
DC  1    0    0
! Dynamic time step specification
DT    0.01
! Dynamic output = 0.1sec
!     Sstp       Stim Rstp       Rtim Ostp       Otim Estp       Etim Ostp       Otim
OD       0        0.0    0        0.0    0       0.01    0        0.0    0        0.0
!
*MODE                                    MODAL ANALYSIS
    3      0.50    0    0    0
*ACCN                                    OAKLAND EQ - 475 YR - Z DIRECTION
      50.0 5000    1
1     oak1        1.0        1.0
!
*STOP
```

E. Baseline building model input file for GTSTRUDL

```
STRUDL ' 13 BAY LONGITIDUNAL FRAME WITH CLADDING STIFFNESS '
UNITS INCHES KIPS CYCLES
$ GENERATE ALL JOINTS
GENERATE 14 JOINTS ID 1 1 X 0.0 DIFF 0,13 AT 213.0
REPEAT 20 ID 14 Y DIFF 192.0, 18 AT 150.0, 114.0
GENERATE 13 JOINTS ID 1001 1 X 0.0 DIFF 1 ,12 AT 213.0 Y=192
REPEAT 19 ID 100 Y DIFF  18 AT 150.0, 114.0
GENERATE 13 JOINTS ID 1014 1 X 0.0 DIFF 212.0 ,12 AT 213.0 Y=192
REPEAT 19 ID 100 Y DIFF  18 AT 150.0, 114.0
STATUS SUPPORT JOINTS 1 TO 14
TYPE PLANE FRAME
$ GENERATE ALL BEAMS
MEMBER INCIDENCES
GENERATE 13 MEMBERS ID 101 1 F 15 1 T 16 1
REPEAT 19 ID 100 F 14 T 14
$ GENERATE ALL COLUMNS
GENERATE 20 MEMBERS ID 10001 1 F 1 14 T 15 14
REPEAT 13 ID 10000 F 1 T 1
TYPE PLANE STRESS $ cladding panels
GENERATE 13 ELEMENTS ID 'PANEL1' 1 FROM 1 1 TO 2 1 TO 1014 1 TO 1001 1
REPEAT 19 TIMES ID 13 FROM 14 TO 14 TO 100 TO 100
ELEMENT PROPERTIES
'PANEL1' TO 'PANEL260' TYPE 'PSHQ' THICKNESS 4.5
TYPE PLANE TRUSS $ upper tie-back cladding connectors
$ horizontal connectors, kx = 80 kips/inch
GENERATE 13 MEMBERS ID 'CONN1' 1 FROM 15 1 TO 1001 1
REPEAT 19 TIMES ID 13 FROM 14 TO 100
GENERATE 13 MEMBERS ID 'CONN261' 1 FROM 16 1 TO 1014 1
REPEAT 19 TIMES ID 13 FROM 14 TO 100
type plane frame
$ vertical connectors, ky = 100 kips/inch
GENERATE 13 MEMBERS ID 'CONN521' 1 FROM 15 1 TO 1001 1
REPEAT 19 TIMES ID 13 FROM 14 TO 100
GENERATE 13 MEMBERS ID 'CONN781' 1 FROM 16 1 TO 1014 1
REPEAT 19 TIMES ID 13 FROM 14 TO 100
member release
'CONN521' to 'CONN1040' end force x $ modified cantilever elem for ky springs
$
material steel all
CONSTANTS
 E 29000 ALL MEMBERS
 E 3600 ELEMENTS 'PANEL1' TO 'PANEL260'
 POISSON 0.2 ELEMENTS 'PANEL1' TO 'PANEL260'
 BETA 90.0 MEMBERS 60001 TO 60020 90001 TO 90020
MEMBER PROPERTIES
$ BEAMS
101 TO 113 AX 34.2 IZ 4930.0
201 TO 213 AX 29.1 IZ 3990.0
301 TO 313 AX 29.1 IZ 3990.0
401 TO 413 AX 29.1 IZ 3990.0
501 TO 513 AX 29.1 IZ 3990.0
601 TO 613 AX 29.1 IZ 3990.0
701 TO 713 AX 29.1 IZ 3990.0
801 TO 813 AX 27.7 IZ 3270.0
901 TO 913 AX 27.7 IZ 3270.0
1001 TO 1013 AX 27.7 IZ 3270.0
1101 TO 1113 AX 27.7 IZ 3270.0
1201 TO 1213 AX 27.7 IZ 3270.0
1301 TO 1313 AX 27.7 IZ 3270.0
1401 TO 1413 AX 22.4 IZ 2100.0
```

```
1501 TO 1513 AX 22.4 IZ 2100.0
1601 TO 1613 AX 20.1 IZ 1830.0
1701 TO 1713 AX 20.1 IZ 1830.0
1801 TO 1813 AX 20.1 IZ 1830.0
1901 TO 1913 AX 20.1 IZ 1830.0
2001 TO 2013 AX 13.0 IZ  843.0
$ COLUMNS AT COLUMN LINES 1,14 STRONG AXIS
10001 140001 AX 75.6 IZ 3400.0
10002 10003 140002 140003 AX 62.0 IZ 2660.0
10004 10005 140004 140005 AX 56.8 IZ 2400.0
10006 10007 140006 140007 AX 46.7 IZ 1900.0
10008 10009 140008 140009 AX 42.7 IZ 1710.0
10010 10011 140010 140011 AX 38.8 IZ 1530.0
10012 10013 140012 140013 AX 32.0 IZ 1240.0
10014 10015 140014 140015 AX 29.1 IZ 1110.0
10016 10017 140016 140017 AX 21.8 IZ  796.0
10018 10019 140018 140019 AX 20.0 IZ  723.0
10020 140020 AX 35.0 IZ 2300.0
$ COLUMNS AT COLUMN LINES 2-5,7,8,10-13 STRONG AXIS
20001 TO 50001 BY 10000 70001 80001 100001 TO 130001 BY 10000 AX 91.4 IZ 4330.0
20002 TO 50002 BY 10000 70002 80002 100002 TO 130002 BY 10000 AX 75.6 IZ 3400.0
20003 TO 50003 BY 10000 70003 80003 100003 TO 130003 BY 10000 AX 75.6 IZ 3400.0
20004 TO 50004 BY 10000 70004 80004 100004 TO 130004 BY 10000 AX 68.5 IZ 3010.0
20005 TO 50005 BY 10000 70005 80005 100005 TO 130005 BY 10000 AX 68.5 IZ 3010.0
20006 TO 50006 BY 10000 70006 80006 100006 TO 130006 BY 10000 AX 62.0 IZ 2660.0
20007 TO 50007 BY 10000 70007 80007 100007 TO 130007 BY 10000 AX 62.0 IZ 2660.0
20008 TO 50008 BY 10000 70008 80008 100008 TO 130008 BY 10000 AX 62.0 IZ 2660.0
20009 TO 50009 BY 10000 70009 80009 100009 TO 130009 BY 10000 AX 62.0 IZ 2660.0
20010 TO 50010 BY 10000 70010 80010 100010 TO 130010 BY 10000 AX 56.8 IZ 2400.0
20011 TO 50011 BY 10000 70011 80011 100011 TO 130011 BY 10000 AX 56.8 IZ 2400.0
20012 TO 50012 BY 10000 70012 80012 100012 TO 130012 BY 10000 AX 46.7 IZ 1900.0
20013 TO 50013 BY 10000 70013 80013 100013 TO 130013 BY 10000 AX 46.7 IZ 1900.0
20014 TO 50014 BY 10000 70014 80014 100014 TO 130014 BY 10000 AX 42.7 IZ 1710.0
20015 TO 50015 BY 10000 70015 80015 100015 TO 130015 BY 10000 AX 42.7 IZ 1710.0
20016 TO 50016 BY 10000 70016 80016 100016 TO 130016 BY 10000 AX 42.7 IZ 1710.0
20017 TO 50017 BY 10000 70017 80017 100017 TO 130017 BY 10000 AX 42.7 IZ 1710.0
20018 TO 50018 BY 10000 70018 80018 100018 TO 130018 BY 10000 AX 26.5 IZ  999.0
20019 TO 50019 BY 10000 70019 80019 100019 TO 130019 BY 10000 AX 26.5 IZ  999.0
20020 TO 50020 BY 10000 70020 80020 100020 TO 130020 BY 10000 AX 26.5 IZ  999.0
$ COLUMNS AT COLUMN LINES 6,9 WEAK AXIS
60001 90001 AX 125.0 IZ 2360.0
60002 60003 90002 90003 AX 101.0 IZ 1810.0
60004 TO 60007 BY 1 90004 TO 90007 BY AX 91.4 IZ 1610.0
60008 TO 60011 BY 1 90008 TO 90011 BY AX 75.6 IZ 1290.0
60012 60013 90012 90013 AX 68.5 IZ 1150.0
60014 60015 90014 90015 AX 56.8 IZ  931.0
60016 TO 60019 BY 1 90016 TO 90019 BY AX 46.7 IZ  748.0
60020 90020 AX 42.7 IZ  677.0
$ 1 INCH TIE-BACK CONNECTIONS IN X DIRECTION (truss bars)
$ 'CONN1' TO 'CONN520' AX 0.00275862 $ kx = 80 kips/inch = EA/L, L=1 inch
$ but use kx=0 in new steel re-design procedure in which cladding has very little
effect
$    on overall bldg lateral stiffness (due to low yield force & very small lateral
displ.
$    at which connectors yield) BUT increases equivalent viscous damping through
$    hysteretic damping of advanced connectors > so account for advanced cladding
$    connectors through damping ratios below
'CONN1' TO 'CONN520' AX 1.e-6 $ alternatively, kx = approx zero for isolating cladding
case
$ 1 INCH TIE-BACK CONNECTIONS IN Y DIRECTION (cantilevers with axial & moment
releases)
'CONN521' to 'CONN1040' ax 1. iz 0.001149425 $ ky = 100 kips/inch = 3EI/L^3
INERTIA OF JOINTS WEIGHT $ includes both frame & other tributary DL
```

```
  EXISTING 15 28 TRANSLATION ALL 72.0714
  EXISTING 29 42 TRANSLATION ALL 71.7321
  EXISTING 43 56 TRANSLATION ALL 71.5892
  EXISTING 57 70 TRANSLATION ALL 71.3750
  EXISTING 71 84 TRANSLATION ALL 71.1607
  EXISTING 85 98 TRANSLATION ALL 71.0178
  EXISTING  99 112 TRANSLATION ALL 70.8035
  EXISTING 113 126 TRANSLATION ALL 70.5178
  EXISTING 127 140 TRANSLATION ALL 70.4107
  EXISTING 141 154 TRANSLATION ALL 70.3035
  EXISTING 155 168 TRANSLATION ALL 70.0892
  EXISTING 169 182 TRANSLATION ALL 68.2321
  EXISTING 183 196 TRANSLATION ALL 68.0178
  EXISTING 197 210 TRANSLATION ALL 67.8035
  EXISTING 211 224 TRANSLATION ALL 67.5178
  EXISTING 225 238 TRANSLATION ALL 67.1964
  EXISTING 239 252 TRANSLATION ALL 66.9821
  EXISTING 253 266 267 280 TRANSLATION ALL 66.875
  EXISTING 281 294 TRANSLATION ALL 64.2678
  EXISTING 16 TO 27 TRANSLATION ALL 68.0714
  EXISTING 30 TO 41 TRANSLATION ALL 68.6071
  EXISTING 44 TO 55 TRANSLATION ALL 68.4642
  EXISTING 58 TO 69 TRANSLATION ALL 68.2500
  EXISTING 72 TO 83 TRANSLATION ALL 68.0357
  EXISTING 86 TO 97 TRANSLATION ALL 67.8928
  EXISTING 100 TO 111 TRANSLATION ALL 67.6785
  EXISTING 114 TO 125 TRANSLATION ALL 67.3928
  EXISTING 128 TO 139 TRANSLATION ALL 67.2857
  EXISTING 142 TO 153 TRANSLATION ALL 67.1785
  EXISTING 156 TO 167 TRANSLATION ALL 66.9642
  EXISTING 170 TO 181 TRANSLATION ALL 65.1071
  EXISTING 184 TO 195 TRANSLATION ALL 64.8928
  EXISTING 198 TO 209 TRANSLATION ALL 64.6785
  EXISTING 212 TO 223 TRANSLATION ALL 64.3928
  EXISTING 226 TO 237 TRANSLATION ALL 64.0714
  EXISTING 240 TO 251 TRANSLATION ALL 63.8571
  EXISTING 254 TO 265 268 TO 279 TRANSLATION ALL 63.750
  EXISTING 282 TO 293 TRANSLATION ALL 61.8928
  EXISTING 1001 TO 1026 TRANSLATION ALL 4.0
  EXISTING 1101 TO 2900 TRANSLATION ALL 3.125
  EXISTING 2901 TO 2926 TRANSLATION ALL 2.375
$ DL COMMANDS
LOADING 'totalDL' 'Cladding & frame DEAD LOAD'
$ values taken from inertia of jts weight above
JOINT LOADS
15 28 FORCE Y -72.0714
29 42 FORCE Y -71.7321
43 56 FORCE Y -71.5892
57 70 FORCE Y -71.3750
71 84 FORCE Y -71.1607
85 98 FORCE Y -71.0178
99 112 FORCE Y -70.8035
113 126 FORCE Y -70.5178
127 140 FORCE Y -70.4107
141 154 FORCE Y -70.3035
155 168 FORCE Y -70.0892
169 182 FORCE Y -68.2321
183 196 FORCE Y -68.0178
197 210 FORCE Y -67.8035
211 224 FORCE Y -67.5178
225 238 FORCE Y -67.1964
239 252 FORCE Y -66.9821
253 266 267 280 FORCE Y -66.875
```

```
281 294 FORCE Y -64.2678
16 TO 27 FORCE Y -68.0714
30 TO 41 FORCE Y -68.6071
44 TO 55 FORCE Y -68.4642
58 TO 69 FORCE Y -68.2500
72 TO 83 FORCE Y -68.0357
86 TO 97 FORCE Y -67.8928
100 TO 111 FORCE Y -67.6785
114 TO 125 FORCE Y -67.3928
128 TO 139 FORCE Y -67.2857
142 TO 153 FORCE Y -67.1785
156 TO 167 FORCE Y -66.9642
170 TO 181 FORCE Y -65.1071
184 TO 195 FORCE Y -64.8928
198 TO 209 FORCE Y -64.6785
212 TO 223 FORCE Y -64.3928
226 TO 237 FORCE Y -64.0714
240 TO 251 FORCE Y -63.8571
254 TO 265 268 TO 279 FORCE Y -63.750
282 TO 293 FORCE Y -61.8928
1001 TO 1026 FORCE Y -4.0
1101 TO 1126 1201 TO 1226 1301 TO 1326 FORCE Y -3.125
1401 TO 1426 1501 TO 1526 1601 TO 1626 FORCE Y -3.125
1701 TO 1726 1801 TO 1826 1901 TO 1926 FORCE Y -3.125
2001 TO 2026 2101 TO 2126 2201 TO 2226 FORCE Y -3.125
2301 TO 2326 2401 TO 2426 2501 TO 2526 FORCE Y -3.125
2601 TO 2626 2701 TO 2726 2801 TO 2826 FORCE Y -3.125
2901 TO 2926 FORCE Y -2.375
$ LL COMMANDS
LOADING 'LL' '100 psf LIVE LOAD'
JOINT LOADS
15 TO 280 FORCE Y -14.0
281 TO 294 FORCE Y -4.5
MEMBER LOADS
101 TO 1901 BY 100 FORCE Y CONC FRACT P -14.0 L 0.5
102 TO 1902 BY 100 FORCE Y CONC FRACT P -14.0 L 0.5
103 TO 1903 BY 100 FORCE Y CONC FRACT P -14.0 L 0.5
104 TO 1904 BY 100 FORCE Y CONC FRACT P -14.0 L 0.5
105 TO 1905 BY 100 FORCE Y CONC FRACT P -14.0 L 0.5
106 TO 1906 BY 100 FORCE Y CONC FRACT P -14.0 L 0.5
107 TO 1907 BY 100 FORCE Y CONC FRACT P -14.0 L 0.5
108 TO 1908 BY 100 FORCE Y CONC FRACT P -14.0 L 0.5
109 TO 1909 BY 100 FORCE Y CONC FRACT P -14.0 L 0.5
110 TO 1910 BY 100 FORCE Y CONC FRACT P -14.0 L 0.5
111 TO 1911 BY 100 FORCE Y CONC FRACT P -14.0 L 0.5
112 TO 1912 BY 100 FORCE Y CONC FRACT P -14.0 L 0.5
113 TO 1913 BY 100 FORCE Y CONC FRACT P -14.0 L 0.5
2001 TO 2013 FORCE Y CONC FRACT P -4.5 L 0.5
$
 EIGEN PARAMETERS
   SOLVE USING GTLANCZOS
   NUMBER OF MODES 9
   PRINT MAX
 END OF EIGEN PARAMETERS
$ ADJUST THE DAMPING RATIO TO ACCOUNT FOR EFFECT OF ADVANCED CLADDING CONN HYSTERESIS
damping ratios 0.071 9 $ ASSUMED DAMPING FOR ADVANCED CLADDING CASE
bypass $ >>>>>>>>>>> response spectrum file 'oakzRS' already exists in user data set
$                    file 'nist.ds'
cinput $ create response spectra follows
create response spectra displ vs freq file 'oakzRS'
units cycles seconds
freq range from 0.1 to 20. at 0.1
damping ratio 0.02 0.05 0.10 0.15 0.20
```

```
include natural struc freq
use accel time hist file 'oakz4751'
end of create r s
bypass $ <<< resp spectrum file 'oakzRS' already exists in 'nist.ds'
cinput $ RSA follows
respons spec loading 'l-eq' 'longitudinal EQ - x direction'
support accel
transl x 1.0 file 'oakzRS'
end of respons spectr load
$
output decimal 3
dynamic analy modal
cinput standard $ dynamic list follows
list dynam partic fact
list resp spectr spec accel
$
compute respons spec displ force reac modal comb rms
creat pseudo static loadin 'oakzEQx1' 'rms of loading L-EQ' from rms of load 'l-eq'
$
cinput $ transient EQ analysis follows (but bypass this part)
bypass $ transient analysis >>
$ add time-history for comparison
transient load 'oakzTH'
support accel
trans x file 'oakz4751'
integrate from 0. to 58. at 0.02 $ record length is 59.52 seconds
end of transient load
perform transient analysis
list trans displ joint 294 2926
bypass $ transient analysis <<<
$
$ >>> DL analysis & combination with pseudo-static load results
$ combine frame & cladding DL with 'oakzEQx1' results
load combination 1 specs 'totalDL' 1.0 'LL' 1.0 'oakzEQx1' 0.125 $ use 1/(ductility=8)
for oakzEQx
load combination 2 specs 'totalDL' 1.0 'LL' 1.0 'oakzEQx1' -0.125
bypass $ >>> define static lateral load 'UBC82' from x-dir ELFP design calcs
load 'UBC82' 'lateral loads from UBC82 ELFP, base shear = 1464k/2'
joint loads
15 FORCE X 3.34
29 FORCE X 6.29
43 FORCE X 9.05
57 FORCE X 11.81
71 FORCE X 14.57
85 FORCE X 17.33
99 FORCE X 20.09
113 FORCE X 22.85
127 FORCE X 25.61
141 FORCE X 28.37
155 FORCE X 31.13
169 FORCE X 33.87
183 FORCE X 36.65
197 FORCE X 39.41
211 FORCE X 42.17
225 FORCE X 44.92
239 FORCE X 47.68
253 FORCE X 50.44
267 FORCE X 53.20
281 FORCE X 193.32
load combination 3 specs 'totalDL' 1.0 'LL' 1.0 'UBC82' 1.0 $ use full 'UBC82' right
load combination 4 specs 'totalDL' 1.0 'LL' 1.0 'UBC82' -1.0 $ use full 'UBC82' left
bypass $ <<<< UBC82 design forces & load combos are listed above
cinput $ stiffness analysis for frame (DL & LL), cladding DL & x-dir EQ follows
```

```
steel takeoff
steel takeoff members 10001 to 10020 20001 to 20020 30001 to 30020 -
40001 to 40020 50001 to 50020 60001 to 60020 70001 to 70020 80001 to 80020 -
90001 to 90020 100001 to 100020 110001 to 110020 120001 to 120020 -
130001 to 130020 140001 to 140020
STIFFNESS ANALYSIS
load list 1 2
cinput $ now redesign frame based on load combinations 1 & 2 (all DL plus +-EQ)
$ steel design commands here > A572 steel for columns, A36 for beams
parameters
code ASD9 all members $ allowable stress design, 1989 AISC code
TBLNAM WBEAM9 members 101 to 113 201 to 213 301 to 313 401 to 413 501 to 513
TBLNAM WBEAM9 members 601 to 613 701 to 713 801 to 813 901 to 913 1001 to 1013
TBLNAM WBEAM9 members 1101 to 1113 1201 to 1213 1301 to 1313 1401 to 1413
TBLNAM WBEAM9 members 1501 to 1513 1601 to 1613 1701 to 1713 1801 to 1813
TBLNAM WBEAM9 members 1901 to 1913 2001 to 2013
TBLNAM WCOLUMN9 members 10001 to 10020 20001 to 20020 30001 to 30020
TBLNAM WCOLUMN9 members 40001 to 40020 50001 to 50020 60001 to 60020
TBLNAM WCOLUMN9 members 70001 to 70020 80001 to 80020 90001 to 90020
TBLNAM WCOLUMN9 members 100001 to 100020 110001 to 110020
TBLNAM WCOLUMN9 members 120001 to 120020 130001 to 130020 140001 to 140020
$ beams
steelgrd A36 members 101 to 113 201 to 213 301 to 313 401 to 413 501 to 513
steelgrd A36 members 601 to 613 701 to 713 801 to 813 901 to 913 1001 to 1013
steelgrd A36 members 1101 to 1113 1201 to 1213 1301 to 1313 1401 to 1413
steelgrd A36 members 1501 to 1513 1601 to 1613 1701 to 1713 1801 to 1813
steelgrd A36 members 1901 to 1913 2001 to 2013
$ columns
steelgrd A572-G50 members 10001 to 10020 20001 to 20020 30001 to 30020
steelgrd A572-G50 members 40001 to 40020 50001 to 50020 60001 to 60020
steelgrd A572-G50 members 70001 to 70020 80001 to 80020 90001 to 90020
steelgrd A572-G50 members 100001 to 100020 110001 to 110020
steelgrd A572-G50 members 120001 to 120020 130001 to 130020 140001 to 140020
$ maximum unbraced length of compression flange
frunlcf 0.333 mem 101 to 113 201 to 213 301 to 313 401 to 413 501 to 513
frunlcf 0.333 mem 601 to 613 701 to 713 801 to 813 901 to 913 1001 to 1013
frunlcf 0.333 mem 1101 to 1113 1201 to 1213 1301 to 1313 1401 to 1413
frunlcf 0.333 mem 1501 to 1513 1601 to 1613 1701 to 1713 1801 to 1813
frunlcf 0.333 mem 1901 to 1913 2001 to 2013
$ compute kz for columns except column lines at 6 and 9
compk kz mem 10001 to 10020 20001 to 20020 30001 to 30020
compk kz mem 40001 to 40020 50001 to 50020 70001 to 70020 80001 to 80020
compk kz mem 100001 to 100020 110001 to 110020 120001 to 120020
compk kz mem 130001 to 130020 140001 to 140020
$ compute ky for columns (column lines at 6 and 9)
compk ky mem 60001 to 60020 90001 to 90020
$ column sidesway uninhibited in plane of the frame
sdswayz yes mem 10001 to 10020 20001 to 20020 30001 to 30020
sdswayz yes mem 40001 to 40020 50001 to 50020 70001 to 70020 80001 to 80020
sdswayz yes mem 100001 to 100020 110001 to 110020 120001 to 120020
sdswayz yes mem 130001 to 130020 140001 to 140020
sdswayy yes mem 60001 to 60020 90001 to 90020
$ column sidesway inhibited normal to the plane of the frame
sdswayy no mem 10001 to 10020 20001 to 20020 30001 to 30020
sdswayy no mem 40001 to 40020 50001 to 50020 70001 to 70020 80001 to 80020
sdswayy no mem 100001 to 100020 110001 to 110020 120001 to 120020
sdswayy no mem 130001 to 130020 140001 to 140020
sdswayz no mem 60001 to 60020 90001 to 90020
$ specify ky as 1.0 for all columns except (column lines at 6 and 9)
ky 1.0 mem 10001 to 10020 20001 to 20020 30001 to 30020
ky 1.0 mem 40001 to 40020 50001 to 50020 70001 to 70020 80001 to 80020
ky 1.0 mem 100001 to 100020 110001 to 110020 120001 to 120020
ky 1.0 mem 130001 to 130020 140001 to 140020
```

```
$ specify kz as 1.0 for columns (column lines at 6 and 9)
kz 1.0 mem 60001 to 60020 90001 to 90020
$ define column lines for automatic k-factor computation
column line 1 members 10001 to 10020
column line 2 members 20001 to 20020
column line 3 members 30001 to 30020
column line 4 members 40001 to 40020
column line 5 members 50001 to 50020
column line 6 members 60001 to 60020
column line 7 members 70001 to 70020
column line 8 members 80001 to 80020
column line 9 members 90001 to 90020
column line 10 members 100001 to 100020
column line 11 members 110001 to 110020
column line 12 members 120001 to 120020
column line 13 members 130001 to 130020
column line 14 members 140001 to 140020
$ all columns to be selected only W14 shapes
units inch
member constraints
10001 to 10020 20001 to 20020 30001 to 30020 constrain 'ND' eq 14.0
40001 to 40020 50001 to 50020 60001 to 60020 constrain 'ND' eq 14.0
70001 to 70020 80001 to 80020 90001 to 90020 constrain 'ND' eq 14.0
100001 to 100020 110001 to 110020 constrain 'ND' eq 14.0
120001 to 120020 130001 to 130020 140001 to 140020 constrain 'ND' eq 14.0
$
101 to 113 201 to 213 301 to 313 401 to 413 501 to 513 constrain 'ND' ge 27.0
601 to 613 701 to 713 801 to 813 constrain 'ND' ge 27.0
901 to 913 1001 to 1013  constrain 'ND' ge 24.0
1101 to 1113 1201 to 1213 1301 to 1313 1401 to 1413  constrain 'ND' ge 24.0
1501 to 1513 1601 to 1613 1701 to 1713 1801 to 1813  constrain 'ND' ge 24.0
1901 to 1913 2001 to 2013  constrain 'ND' ge 21.0
$ BEAMS
section fract ns 5 0.0 0.25 0.5 0.75 1.0 mem 101 to 113 201 to 213 301 to 313
section fract ns 5 0.0 0.25 0.5 0.75 1.0 mem 401 to 413 501 to 513 601 to 613
section fract ns 5 0.0 0.25 0.5 0.75 1.0 mem 701 to 713 801 to 813 901 to 913
section fract ns 5 0.0 0.25 0.5 0.75 1.0 mem 1001 to 1013 1101 to 1113
section fract ns 5 0.0 0.25 0.5 0.75 1.0 mem 1201 to 1213 1301 to 1313
section fract ns 5 0.0 0.25 0.5 0.75 1.0 mem 1401 to 1413 1501 to 1513
section fract ns 5 0.0 0.25 0.5 0.75 1.0 mem 1601 to 1613 1701 to 1713
section fract ns 5 0.0 0.25 0.5 0.75 1.0 mem 1801 to 1813 1901 to 1913
section fract ns 5 0.0 0.25 0.5 0.75 1.0 mem 2001 to 2013
select members 101 to 113 201 to 213 301 to 313 401 to 413 501 to 513
select members 601 to 613 701 to 713 801 to 813 901 to 913 1001 to 1013
select members 1101 to 1113 1201 to 1213 1301 to 1313 1401 to 1413
select members 1501 to 1513 1601 to 1613 1701 to 1713 1801 to 1813
select members 1901 to 1913 2001 to 2013
$ columns
select members 10001 to 10020 20001 to 20020 30001 to 30020 as column
select members 40001 to 40020 50001 to 50020 60001 to 60020 as column
select members 70001 to 70020 80001 to 80020 90001 to 90020 as column
select members 100001 to 100020 110001 to 110020 as column
select members 120001 to 120020 130001 to 130020 140001 to 140020 as column
steel takeoff
take members 101 to 113 as largest 'SZ' of members 101 to 113
take members 201 to 213 as largest 'SZ' of members 201 to 213
take members 301 to 313 as largest 'SZ' of members 301 to 313
take members 401 to 413 as largest 'SZ' of members 401 to 413
take members 501 to 513 as largest 'SZ' of members 501 to 513
take members 601 to 613 as largest 'SZ' of members 601 to 613
take members 701 to 713 as largest 'SZ' of members 701 to 713
take members 801 to 813 as largest 'SZ' of members 801 to 813
take members 901 to 913 as largest 'SZ' of members 901 to 913
```

```
take members 1001 to 1013 as largest 'SZ' of members 1001 to 1013
take members 1101 to 1113 as largest 'SZ' of members 1101 to 1113
take members 1201 to 1213 as largest 'SZ' of members 1201 to 1213
take members 1301 to 1313 as largest 'SZ' of members 1301 to 1313
take members 1401 to 1413 as largest 'SZ' of members 1401 to 1413
take members 1501 to 1513 as largest 'SZ' of members 1501 to 1513
take members 1601 to 1613 as largest 'SZ' of members 1601 to 1613
take members 1701 to 1713 as largest 'SZ' of members 1701 to 1713
take members 1801 to 1813 as largest 'SZ' of members 1801 to 1813
take members 1901 to 1913 as largest 'SZ' of members 1901 to 1913
take members 2001 to 2013 as largest 'SZ' of members 2001 to 2013
steel takeoff
steel takeoff members 10001 to 10020 20001 to 20020 30001 to 30020 -
40001 to 40020 50001 to 50020 60001 to 60020 70001 to 70020 80001 to 80020 -
90001 to 90020 100001 to 100020 110001 to 110020 120001 to 120020 -
130001 to 130020 140001 to 140020
steel takeoff members 101 to 113
steel takeoff members 201 to 213
steel takeoff members 301 to 313
steel takeoff members 401 to 413
steel takeoff members 501 to 513
steel takeoff members 601 to 613
steel takeoff members 701 to 713
steel takeoff members 801 to 813
steel takeoff members 901 to 913
steel takeoff members 1001 to 1013
steel takeoff members 1101 to 1113
steel takeoff members 1201 to 1213
steel takeoff members 1301 to 1313
steel takeoff members 1401 to 1413
steel takeoff members 1501 to 1513
steel takeoff members 1601 to 1613
steel takeoff members 1701 to 1713
steel takeoff members 1801 to 1813
steel takeoff members 1901 to 1913
steel takeoff members 2001 to 2013
cinput $ now redo RSA for redesigned frame then another stiffness analysis
load list all
damping ratios 0.071 9 $ ASSUMED DAMPING FOR ADVANCED CLADDING CASE
dynamic analy modal
compute respons spec displ force reac modal comb rms
creat pseudo static loadin 'oakzEQx2' 'rms of loading L-EQ' from rms of load '1-eq'
load combination 3 specs 'totalDL' 1.0 'LL' 1.0 'oakzEQx2' 0.125 $ use 1/(ductility=8)
for oakzEQx
load combination 4 specs 'totalDL' 1.0 'LL' 1.0 'oakzEQx2' -0.125 $ use
1/(ductility=8) for oakzEQx
STIFFNESS ANALYSIS
cinput
load list all
damping ratios 0.071 9 $ ASSUMED DAMPING FOR ADVANCED CLADDING CASE
dynamic analy modal
compute respons spec displ force reac modal comb rms
creat pseudo static loadin 'oakzEQx3' 'rms of loading L-EQ' from rms of load '1-eq'
STIFFNESS ANALYSIS
list disp joints 294
list sum reactions
load list 3 4
check code members 101 to 113 201 to 213 301 to 313 401 to 413 501 to 513
check code members 601 to 613 701 to 713 801 to 813 901 to 913 1001 to 1013
check code members 1101 to 1113 1201 to 1213 1301 to 1313 1401 to 1413
check code members 1501 to 1513 1601 to 1613 1701 to 1713 1801 to 1813
check code members 1901 to 1913 2001 to 2013
check code members 10001 to 10020 20001 to 20020 30001 to 30020
```

```
check code members 40001 to 40020 50001 to 50020 60001 to 60020
check code members 70001 to 70020 80001 to 80020 90001 to 90020
check code members 100001 to 100020 110001 to 110020
check code members 120001 to 120020 130001 to 130020 140001 to 140020
cinput
$FINISH
```

To: thelma.woods@oca.gatech.edu, wanda.simon@oca.gatech.edu,
kamie.cunningham@oca.gatech.edu
Subject: Research Report Approval Sheet

Below is the result of your feedback form. It was submitted by
Barry Goodno (bgoodno@ce.gatech.edu) on Thursday, October 8, 1998 at 16:37:34

Period_Covered: July 1995 to Sept. 1998

Author: James I. Craig (AE) & Barry J. Goodno (CE)

Date_Mailed1: PDF file to OCA

Deliverable: 37486

Due_Date: Sept. 1, 1998

Final_Report: on

Lab_Dist: on

Lab_School_Center: CEE

None: on

Phone: 894-2227

Project_Num: E20-W95

Report_Title: DUCTILE CLADDING CONNECTION SYSTEMS FOR SEISMIC DESIGN

Restrictions_No: on

Unclassified: on
